Novel manufacturing methods to realise electronic textiles: Modular systems and stretchable, helical electronics

Jessica Stanley

December 2023

Abstract

In electronic textiles (e-textiles), electronic parts are embedded in clothing and other textiles. This work addressed two key e-textile manufacturing challenges: reliable connections between e-textile parts, and manufacturing methods for stretchable e-textiles. Key developments include a novel 'interposer' for detachable connections in modular e-textiles, and new method for stretchable e-textiles using flexible electronic strips wound into a helical structure.

A modular temperature sensing garment was created, with sensors located on the thigh, scapula, lower back and chest. Sensors on the thigh were the most accurate, which has implications for future e-textile temperature sensing applications. An interposer – a bridge between dissimilar parts in a circuit – was developed, using two small connectors not previously used in e-textiles. These were incorporated in an updated sensing garment, which survived 1000 cycles of stretching and bending, showing that modular e-textiles are a viable alternative to permanently connected parts.

Stretchable 'helical e-strips' were developed by winding strips of flexible circuitry around stretchable rubber cord. Helical e-strips were able to stretch by over 100% before breaking, survived up to 10 washing machine cycles, and over 3000 cycles of stretching by 30% or 40%, depending on the materials used. These results compare well with existing (planar) stretchable electronics technologies, and as helical e-strips are only at the early stages of development, this indicates that with further development they could outperform the current standards.

A new flexible electronics fabrication method was also developed, using the vinyl cutter, a widely available machine. Features as small as 100 μm were successfully fabricated, and this method has potential to make flexible electronics prototyping faster, and accessible outside specialised labs.

In conclusion, this work contributes to the advancement of e-textiles by presenting solutions that enhance modularity and stretchability, paving the way for stretchable e-textiles designed for easy disassembly and reduced waste.

Table of Contents

List of Figures

List of Tables

List of Abbreviations

ACA   Anisotropic Conductive Adhesive

AWG   American Wire Gauge

DAQ   Data Acquisition (Device)

EPDM   Ethylene Propylene Diene Monomer

FFC   Flexible Flat Cable

FPC   Flexible Printed Circuit

FR4   A type of flame retardant fiberglass-reinforced epoxy resin material

IC   Integrated Circuit

ICA   Isotropic Conductive Adhesive

LED   Light Emitting Diode

NCA   Non-Conductive Adhesive

NTC   Negative Temperature Coefficient

PCB   Printed Circuit Board

PDMS   Polydimethylsiloxane

PET   Polyethylene Terephthalate

PEN   Polyethylene Naphthalate

PI   Polyimide

PU   Polyurethane

RPM   Rotations Per Minute

SMD   Surface Mounted Device

TPU   Thermoplastic Polyurethane

UV   Ultraviolet

ZIF   Zero Insertion Force

Acknowledgements

It is a widely acknowledged fact that although a PhD is individual work, it is not possible to get through one alone (or at least not with sanity intact). I am grateful to my supervisor Yang Wei, as his knowledge of electronics, and enthusiasm for research and e-textile innovation, are immense. And my other supervisors, John Hunt and Phil Kunovski, for their support and advice, and to Nottingham Trent University and Kymira for funding this work. Thanks also to the students who supported this work: Jasmyn Cliff-Patel, Danielle Lawson, Eleanor Martin, Ines Pinho Bastos Dos Reis Guerreiro, Mariana Ventura Martins, Shrilakshmi Baby-Sankar, Arif Nazir, Oliver Handford, Khaled Hamed, and Daniel Ogden. And Toju Raine at Kymira.

I want to thank the NTU Engineering Technical Team, who are a wonderful bunch of people and without whose support this thesis would not exist. And my fellow PhD students and colleagues, whose support has been invaluable. I am particularly grateful to four of these people: Jarede Mayers, Hannah Manley, Wendy Balestri and Nikki Sizer, for their friendship and support. Thanks also to the other members of the Smart Wearable Research Group, and my colleague and collaborator Katy Griggs.

I also want to acknowledge several friends, particularly Miriam, Niamh, Sarah, and Tom, for their support, and their ongoing patience with my inability to respond to messages within a reasonable timeframe. And my family: my brother Ieuan and sister-in-law Abi, and my niece and nephews, Matilda, Alexander and Brannoc. Also my stepdad John, and my step-nieces Lola and Juno. And above all, my mum Amanda, who has been my biggest supporter from day 1 (literally), and whose love of art and science fiction has been a major influence in my career and life in general. There are also several people who are no longer here but who continue to have an impact on me: my grandparents, particularly my granny Noeline Scales. My dad Seán Stanley, whose interest in taking apart computers might have come in useful in the past four years. And Danijela Kulezić-Wilson, who I am grateful to have known.

Over 10 years ago I stumbled across the emerging field of e-textiles. A video by Becky Stern, on sewing conductive thread circuits, and a tutorial by Leah Buechley, on a turn signal bike jacket, sparked an interest in electronics that I didn't know I had. It ended up being a gateway to a lot of things, this PhD included, and I owe my gratitude to the people who shared their knowledge freely online. And Cecilia Raspanti and Anastasia Pistofidou of Fabricademy, my stepping stone from e-textiles as a hobby to a career, and whose infectious enthusiasm for collaboration and sustainable textile innovation I hope to pass on to others.

Chapter 1 Introduction

1.1 The potential of e-textiles

Textiles are deeply embedded in our lives, and the same could increasingly be said of electronic devices. These two fields are normally seen as very much separate, yet in reality their histories are interwoven, as there are many examples of electronics and computing borrowing and adapting textile techniques. The Analytical Engine, which was never built but was the first design for a computer, used a punch-card system inspired by those used in Jacquard looms to weave patterns in fabric. In the words of Ada Lovelace, who conceived of the Analytical Engine with Charles Babbage in the 19th Century, 'the Analytical Engine weaves algebraic patterns, just as the Jacquard loom weaves flowers and leaves' [1]. In the 1960s, women with textile skills were employed to weave core memory out of fine wires and magnetic rings, nicknamed 'little old lady memory', for NASA space missions [2]. And screen printing, which may have origins as far back as the 9th Century in China, was developed to print patterns on textiles, but has been adapted by the electronics industry to create printed circuit boards, as well as individual components.

But it is only in the past few decades that electronics technology has advanced to the point where a new combination of the two fields has emerged: electronic textiles, normally abbreviated to e-textiles. In e-textiles, electronic circuitry and components are embedded in textiles (primarily clothing, but also upholstery and other textiles used in interior architecture). This allows clothing to become sensors, measuring physiological signals such as heart rate and temperature, or tracking the position or movement of the body. It enables garments to deliver medical treatment, such as soft electrodes that deliver electrical stimulation, for patients receiving rehabilitation therapy after suffering a stroke. It embeds new functions in the textiles that already surround us, and has creative applications as well: clothing that can light up, display digital images, or play sound.

In short, e-textiles promise a future of soft, flexible, stretchable electronic devices. Rigid wearables replaced with textile alternatives, that are comfortable to wear. An e-textile future means freedom from being hooked up to uncomfortable, immobile medical equipment that requires a visit to a hospital or GP surgery. And a future where embedding electronics in textiles allows for new ways for us to interact with our electronic devices.

While there are a handful of e-textile products already on the market, these are not yet mainstream, and most contain a significant number of rigid parts. To realise the full potential of e-textiles, and commercial success, several technical and production challenges need to be overcome. These include a lack of standards for materials and manufacturing methods. E-textiles can be constructed by various methods, including the use of textile techniques (e.g. weaving circuits with conductive threads), or electronics techniques (embedding flexible circuitry on plastic films inside textiles).

Conductive textiles or printed conductive patterns can be used to make simple flexible sensors or actuators, and innovations in ultra-thin wafer technology have led to flexible silicon chips [3], but most components cannot yet be made in flexible format, and conventional (and rigid) electronic components are still needed. Durability and washability are other areas which are under active investigation: e-textiles, specifically those worn on the body, need to be washable, and not break when the body moves and stretches. While there are standards in development to help assess the durability of e-textiles, there is limited data available on what tests can properly mimic the stresses exerted on e-textile circuitry when worn on the body.

This thesis presents research on two key issues: firstly, determining reliable interfaces between materials with dissimilar mechanical properties; a critical requirement for durable e-textiles. That is, reliable connectors and joining technologies are needed to connect rigid components or circuit modules to flexible or stretchable interconnects. This is particularly important for modular systems, which consist of discrete parts which need to be easily connected and disconnected. Modular systems have been recommended in the design of sustainable e-textiles, as they support easier repair, re-configuration, or recycling of parts than systems where everything is permanently fused together, and textile and electronic parts can't be separated for recycling.

Secondly, finding and defining new stretchable electronics technology for stretch e-textile garments. Major breakthroughs have been achieved in the creation of flexible electronics, with flexible cables being commonly used inside digital cameras and smartphones, to connect displays to other circuitry or save space due to their ability to fold. But achieving stretch is more difficult. As the invention of spandex and other elastic fibres has gradually led to stretch garments being very common, e-textiles that can only bend, and not stretch, will have limited applications. Stretchable electronics technologies exist, but as will be discussed further in Chapter 2, these all have limitations. An alternative approach is

researched and evidenced in this thesis. First, flexible 'e-strips', being long strips of flexible circuitry, are fabricated. Then, they are wound around, and bonded to, a stretchable rubber cord. This creates a spring, or helix structure, transforming the flexible e-strip to a flexible and stretchable helical e-strip. While not the first time helical geometry has been used in electronics, it is the first time a full circuit has been made in helical form, rather than a single component, or a stretchable interconnect containing no components. The resulting structure is shown to be stretchable, and both LED lighting and temperature sensing helical e-strips are demonstrated as possible applications, alongside mechanical and wash durability testing to validate the concept.

1.2 Motivation

This project was part funded by Kymira Ltd, a UK company active in smart garment innovation, developing products primarily aimed at sports and medical markets. This is the link with e-textile manufacturing, which is mentioned in the title of this thesis. The goals of the project were therefore guided by manufacturing needs identified by Kymira who were (at the time the project started) expanding their manufacturing capabilities into e-textiles.

The aim of the project can be summarised as follows:

To design and fabricate novel e-strips for e-textiles, using printed and flexible electronics techniques to achieve stretchable, helical geometry capable of at least 30% linear strain, and develop detachable interfaces for e-strips to enhance reparability and reusability of smart garments through modular design.

1.3 Research objectives

The following objectives were identified to achieve the project's aim:

1. Design and fabricate novel e-strip geometries, including helical structures, to achieve at least 30% linear strain, for incorporation into stretch garments.

2. Evaluate and compare printed and flexible electronics fabrication methods, specifically dispenser printing, screen printing and etching techniques, to manufacture e-strips with as small as 0201 (0.6 mm x 0.3 mm) components and 100 µm pitch features.

3. Identify at least two electronic connectors with small footprint (≤ 1 mm pitch) with potential for use in interconnecting e-strips to other parts of an e-textile circuit, and use these connectors to construct a modular e-textile system aimed at increasing smart garment sustainability by promoting reparability and reconfiguration.

4. Assess and quantify reliability of e-strips and connectors, through tensile texting, bend testing, and wash cycle testing.

1.4 Structure of the thesis

The thesis is structured as follows:

Chapter 2 is a literature review, detailing the background to the work, and state of the art. This covers fabrication methods for e-textiles, with specific attention to the methods used in this work. It also explores the role of modular design and connectors in e-textiles, and existing solutions for stretchable electronics, using both planar and helical geometries.

Chapter 3 covers the materials and methods used in the project, including printed and flexible electronics techniques, and various test methods employed to evaluate prototypes produced during the project.

Chapter 4 explains how methods to create conductive tracks on flexible substrates were evaluated, in order to pick one to use for the rest of the work. Dispenser printing on polyimide film is covered, as well as methods to etch copper-plated polyimide film. A novel method for flexible electronics prototyping using adhesive vinyl and a vinyl cutter arose from this.

Chapter 5 explores modular design in e-textiles, through creating a prototype modular e-textile system to measure skin temperature during cycling. It then documents the development of an interposer for better interconnections in modular systems, and an updated version of the modular skin temperature sensing system.

Chapter 6 covers the design and fabrication of helical e-strips, stretchable structures made from a thin strip of flexible circuitry wrapped around and elastic core. It then showcases applications of this technology, specifically helical LED and temperature sensing e-strips.

Chapters 7 concludes the thesis as a whole and discusses future work.

Several students and colleagues at NTU Engineering have collaborated on this work. In particular, summer student Jasmyn Cliff-Patel designed mechanical testing accessories, and helped build a twist testing machine, described in Chapter 3. Arif Nazir and Khaled Hamed printed some of the circuits, and performed some of the measurements, in Chapter 4, as part of their undergraduate dissertation projects. Danielle Lawson ran the human participant trials in Chapter 5 as part of her undergraduate dissertation project, and Inês Guerreiro and Eleanor Martin contributed to that project as well as summer students. The cycling garments

covered in Chapter 5 were a collaboration with sports engineer Dr Katy Griggs. Dr Philippa Jobling provided fabrics used in Chapter 5. And MSc student Shrilakshmi Baby Sankar assisted with some of the mechanical testing in Chapter 6. Senior technician Damien Goy advised on mechanical testing, and Technical Specialist Iain Mitchell fabricated aluminium parts used for mechanical testing. Senior Technicians Esme Butcher and Xzara Foster laser cut and 3D printed mechanical testing accessories.

Kymira part funded this project and provided guidance on the direction of the project as well as advice and feedback on the work produced, but apart from the contributions listed above, the writer of this thesis performed all of the work presented herein.

1.5 Statement of novelty

The following novel developments are covered by this thesis:

Flexible and printed electronics prototyping

A flexible electronics prototyping process using a vinyl cutter to cut flexible circuit modules and create a mask for etching copper-coated polymer films, with features as small as 100 µm. The vinyl cutter replaces several pieces of equipment used in standard flexible electronics fabrication methods and reduces the number of processing steps. This method also allows for the mask and the flexible circuit substrate to be cut at the same time, eliminating alignment errors between mask and substrate. As this machine is commonly owned by hobbyists or available in fablabs and makerspaces around the world, this process has the potential to broaden access to flexible electronics fabrication outside specialised labs and manufacturing facilities.

Interconnection methods for e-textiles

A novel interposer that enables detachable connections between dissimilar materials in e-textiles, e.g. allowing a flexible sensor to be connected to stitched conductive thread tracks, using small footprint flexible electronics connectors not previously used in e-textiles. While there are existing examples of detachable interposers and flexible interposers in e-textiles, the only examples that are both flexible and detachable use snap fasteners as connectors, with ≥10 mm pitch, compared to the ≤1 mm pitch demonstrated in this work.

Helical e-strips: 3D structure for stretchable electronics

A fabrication process to realise helical e-strips, consisting of a long, thin strip of flexible circuitry wrapped around a stretchable rubber cord core. While helical geometry has been used in e-textiles before, only helical interconnects or very simple single components have

been demonstrated, i.e. a single conductive track formed into a helix. The helical e-strips demonstrated in this work also contain small surface mount components within their structure, which is a significant advancement from previous work. This is demonstrated through LED and temperature sensing helical e-strips as narrow as 2 mm in diameter, with the ability to survive 3000 cycles of 30%-40% stretch, and 10 washing machine cycles. These results are comparable to existing stretchable electronics technologies, but further development of the technology beyond the prototypes presented in this thesis could see helical e-strips outperforming current technologies.

1.6 Publications arising from this thesis

1. J. Stanley, J. A. Hunt, P. Kunovski, and Y. Wei, "Novel Interposer for Modular Electronic Textiles: Enabling Detachable Connections Between Flexible Electronics and Conductive Textiles," IEEE Sensors Lett., vol. 6, no. 6, pp. 1–4, May 2022, doi: 10.1109/LSENS.2022.3176726.

2. J. Stanley, K. Griggs, O. Handford, J. A. Hunt, P. Kunovski, and Y. Wei, "Modular E-Textile Platform for Real-Time Sensing," Proc. - Int. Symp. Wearable Comput. ISWC, pp. 131–135, Sep. 2022, doi: 10.1145/3544794.3560293.

3. J. Stanley, J. A. Hunt, P. Kunovski, and Y. Wei, "A review of connectors and joining technologies for electronic textiles," Eng. Reports, p. e12491, Dec. 2021, doi: 10.1002/ENG2.12491.

4. J. Stanley, P. Kunovski, J. A. Hunt, Y. Wei, "Stretchable electronic strips for electronic textiles enabled by 3D helical structure," Sci Rep 14, 11065 (2024). https://doi.org/10.1038/s41598-024-61406-7

Other publications not included in the thesis:

1. Y. ElSaboni, J. A. Hunt, J. Stanley, C. Moffatt, and Y. Wei, "Development of a textile based protein sensor for monitoring the healing progress of a wound," *Sci. Reports 2022 121*, vol. 12, no. 1, pp. 1–12, May 2022, doi: 10.1038/s41598-022-11982-

2. S. Kumar, R. Singh, A. P. Singh, J. Stanley, and Y. Wei, "On comparison of sensing capabilities of three-dimensional printed wearable sensors," https://doi.org/10.1177/14644207231198708, Sep. 2023, doi: 10.1177/14644207231198708.

Patents arising from this thesis:

1. P. Kunovski, Y. Wei, J. Stanley, 'Electronic unit for a textile', UK patent application No. GB2618195A, 2023.

Chapter 2 Literature Review

To create stretchable, helical circuits, understanding of how planar, flexible circuits are fabricated is essential, as these are one of the building blocks of the helical structure that was developed in Chapter 6. A secondary investigation into connectors for e-textiles, and collaboration with colleagues interested in skin temperature measurement for sports, developed into an exploration of modular e-textile systems, and an interposer device to aid in the development of such systems. In other words, there are several topics to cover.

This literature review is split into three parts, covering:

1. E-textile definitions and fabrication methods
2. Connectors and modular systems
3. Stretchable electronics state of the art

A substantial proportion of the first two sections is adapted from the review article written during this project, which is listed in Chapter 1, Section 1.6 .

Temperature sensors were also produced during this project, to demonstrate potential applications of the technology developed. As this was not the main focus of the project, a review of e-textile temperature sensors is not included in this chapter. This is instead included in Chapter 5, which covers temperature sensor applications in more detail.

2.1   E-textile fabrication methods

This section focuses on e-textile fabrication methods and is structured as follows:

- First, a brief overview of the current state of the art of e-textiles, including commercial products currently available.
- Then, an overview of e-textile construction techniques, as these are many and varied, as well as some definitions of terminology. Flexible and printed electronics fabrication techniques are covered in more detail than other techniques, as these were used in this work.
- Finally, a discussion of the techniques selected for evaluation in this work, and the equipment required.

Resistance is measured by applying a small current between two points, and measuring the resulting voltage drop between those points. However, in a 2-wire measurement, the resistance measured will also include the resistance of the probes used to connect the multimeter (or other measuring device) to the sample under test. These usually have quite low resistance, but as the prototypes tested in this work typically have a resistance of < 1 Ω, including the resistance of the probes introduces error into the measurement. A 4-wire resistance measurement, by comparison, uses one set of probes to supply the current, and another set to measure the voltage drop. This removes the resistance of the probes themselves from the measurement, increasing the accuracy.

2.1.1 E-textiles overview and definitions

Though the embedding of electronics in clothing began as early as the beginning of the 20th Century [4], it is only in the past two decades that advances in material and manufacturing techniques have made the production of commercial e-textile products possible. Products, such as those for tracking physical activity and sports performance [5], have not yet seen widespread adoption, but are growing in number. Some forecasters predict that the e-textile market will grow to above USD$700 million by 2033 [6]. Early e-textile innovator Leah Buechley notes in her 2007 PhD thesis that materials for e-textiles were scarcely available at that time [7], whereas now there are many suppliers selling conductive thread sewing kits and sewable components, and microcontroller boards designed for stitching onto fabric (the first of which, the Lilypad Arduino, was developed by Buechley herself [8]). Examples of e-textile commercial products and research prototypes are shown in Figure 2-1.
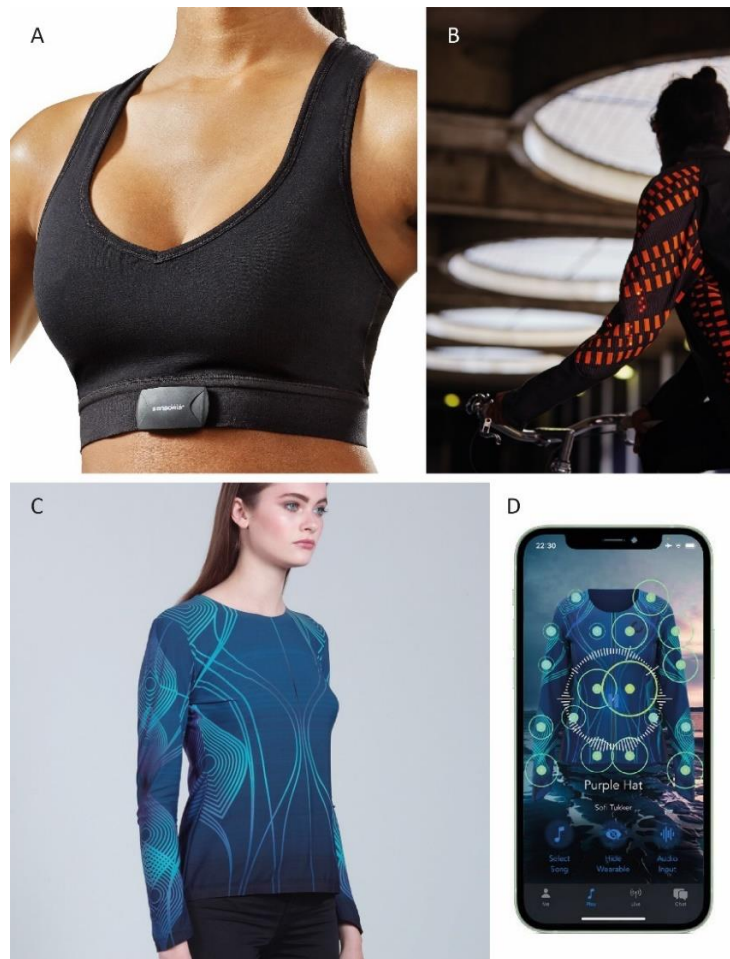
Figure 2-1. Examples of e-textile applications.

A) Sensoria Fitness sports bra featuring a heart rate monitor. [9] Copyright Sensoria Inc. Reproduced with permission; B) Illuminated cycling jacket containing LED yarns. Reproduced under the terms of the CC-BY license. [10] Copyright 2019, the authors, published by MDPI. C) SoundShirt by CuteCircuit with embedded haptic actuators that respond to sound. D) SoundShirt mobile app. [11] Copyright CuteCircuit, reproduced with permission.

A 2020 review of e-textile products shows that the two leading categories of commercially available e-textiles are those aimed at sports and healthcare [12]. Embedding sensors in garments can enable data collection on sports performance, for example monitoring heart rate [9], which can give insight into fitness and performance. In healthcare, e-textile medical devices can use similar sensors to perform electrocardiography [13] or deliver various forms of treatment [14,15]. Or rehabilitation, e.g. electrical stimulation to aid in recovery from stroke [15].

Beyond sports and medical applications, other products provide new ways to interact with technology, e.g. by turning a jacket sleeve into an interface for controlling a smartphone [16]. Others seek to augment human sensory ability, such as CuteCircuit's SoundShirt [11], which uses embedded haptic actuators to allow the wearer to feel music instead of, or as well as, hearing it. Garments with embedded LEDs for lighting or wearable displays are another

application category, and electroluminescent fabrics have been realized through printing with functional inks [17,18], weaving with luminescent fibres [19], or embedding LEDs inside yarns [10]. These can be used for aesthetic or artistic purposes, or for safety, for example to make pedestrians and cyclists visible to motorists on dark roads. Heated clothing is another area of interest [20], with applications in protective clothing and winter sports.

Do-It-Yourself (DIY) kits and tools also enable e-textiles to be created outside specialized labs, including the Lilypad Arduino, similar sewable microcontrollers by Adafruit [21], Loomia Packs & Parts prototyping modules [22], and extensive documentation on e-textile construction methods by Kobakant [23].

As an emerging field, there is not yet a consensus on e-textile terminology. Other terms that describe, or overlap with, e-textiles include smart garments, smart fabrics, intelligent textiles, wearable electronics, textronics, and electro-textiles. BSI Technical Report ISO/TR 23383:2020 recommends standard definitions and categorizations for this field [24], and based on this advice the following definitions are used:

- E-textile: A garment or other textile product that contains embedded electronics, whether the circuitry is made of textile components or more conventional electronic circuitry.
- Electrically conductive textiles: textiles that either contain conductive fibres or are coated with metal or a conductive polymer, out of which e-textile circuits may be constructed. Also referred to in this thesis as just "conductive textiles".
- Resistance is measured by applying a small current between two points, and measuring the resulting voltage drop between those points. However, in a 2-wire measurement, the resistance measured will also include the resistance of the probes used to connect the multimeter (or other measuring device) to the sample under test. These usually have quite low resistance, but as the prototypes tested in this work typically have a resistance of < 1 Ω, including the resistance of the probes introduces error into the measurement. A 4-wire resistance measurement, by comparison, uses one set of probes to supply the current, and another set to measure the voltage drop. This removes the resistance of the probes themselves from the measurement, increasing the accuracy.

2.1.2 Fabrication methods overview

The field of e-textiles is interdisciplinary, with researchers and practitioners from electronic engineering, fashion, textile design, chemical engineering, nanotechnology, and human

computer interaction, among others, all active in the field. This diversity is reflected in the variety of approaches that have been taken to creating e-textiles, which are covered in detail in several reviews [25,26]. Excluding early wearable electronics projects which consisted of conventional electronics - bulky rigid circuit boards connected by wires - stitched onto clothing or inserted into pockets, e-textile construction techniques can be loosely divided into three categories, examples of which are depicted in Figure 2-2. These are:

a) Textile as electronics
b) Disappearing electronics in textiles
c) Printed electronics on textiles and new conductive materials
d) Hybrid e-textiles, being a combination of two or more of the above categories
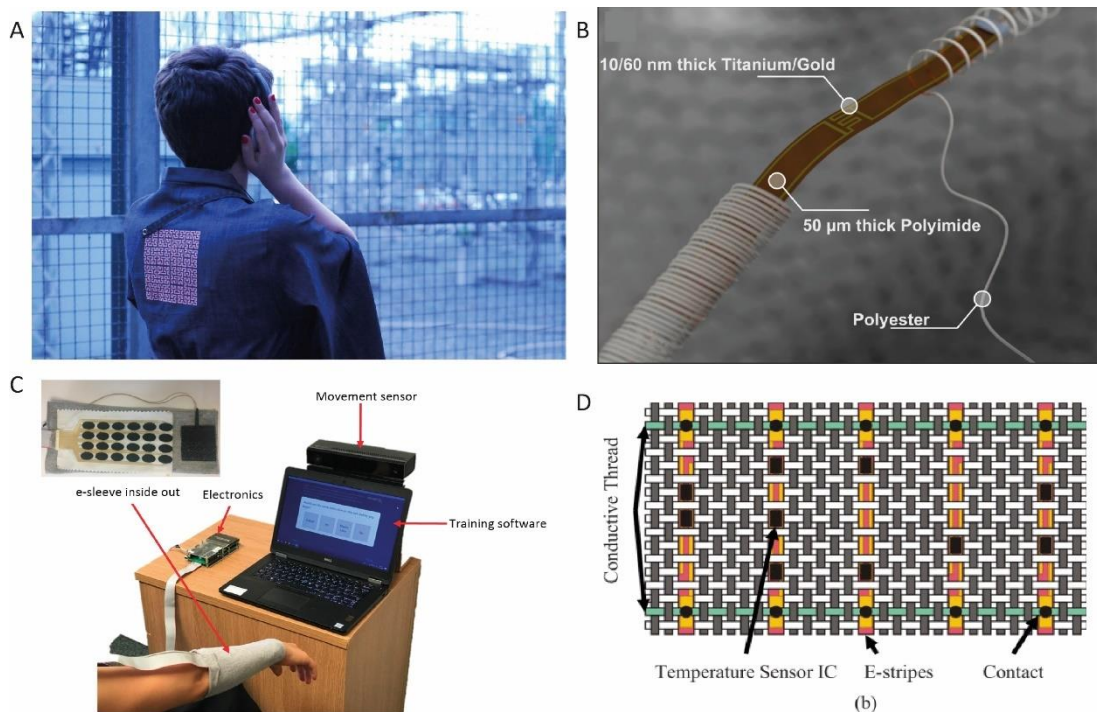
Figure 2-2. Examples of e-textile construction methods.

A) Textiles as electronics: Fractal Antennae by Afroditi Psarra, featuring an antenna laser cut from copper fabric adhered to textile. Reproduced with permission.[27] Copyright Afroditi Psarra. B) Disappearing electronics in textiles: Flexible temperature sensor strip embedded in a yarn. Reproduced under the terms of the CC-BY license.[28]; C) New flexible materials for electronics: screen printed electrode sleeve for stroke rehabilitation therapy. Reproduced under the terms of the CC-BY license.[15] Copyright 2018, the authors, published by MDPI. D) Hybrid approaches: Flexible temperature strips woven into conductive fabric with conductive thread bus bars. Reproduced with permission.[29] Copyright 2018, IEEE.

2.1.3 Textile as electronics

This approach replaces traditional electronic circuitry with textile alternatives. Wires or printed circuit boards (PCBs) are replaced by conductive threads or fabrics, made from thin

metal fibres, or coated with metallic or conductive polymer layers. These materials can then be used in place of normal textiles in standard textile manufacturing processes. As shown in Figure 2-3, conductive threads can be woven or knitted into fabric, or stitched onto it, to form conductive tracks. Conductive tracks can also be made from strips of conductive fabric, cut by hand or by machine, and then stitched or bonded to fabric. Electronic components can then be stitched, soldered, or otherwise connected to the conductive textile tracks to form a circuit. Circuits can be crafted by hand or use textile manufacturing processes such as weaving [30], knitting [31] or machine embroidery [32] to incorporate conductive tracks into fabric during or after fabric creation.
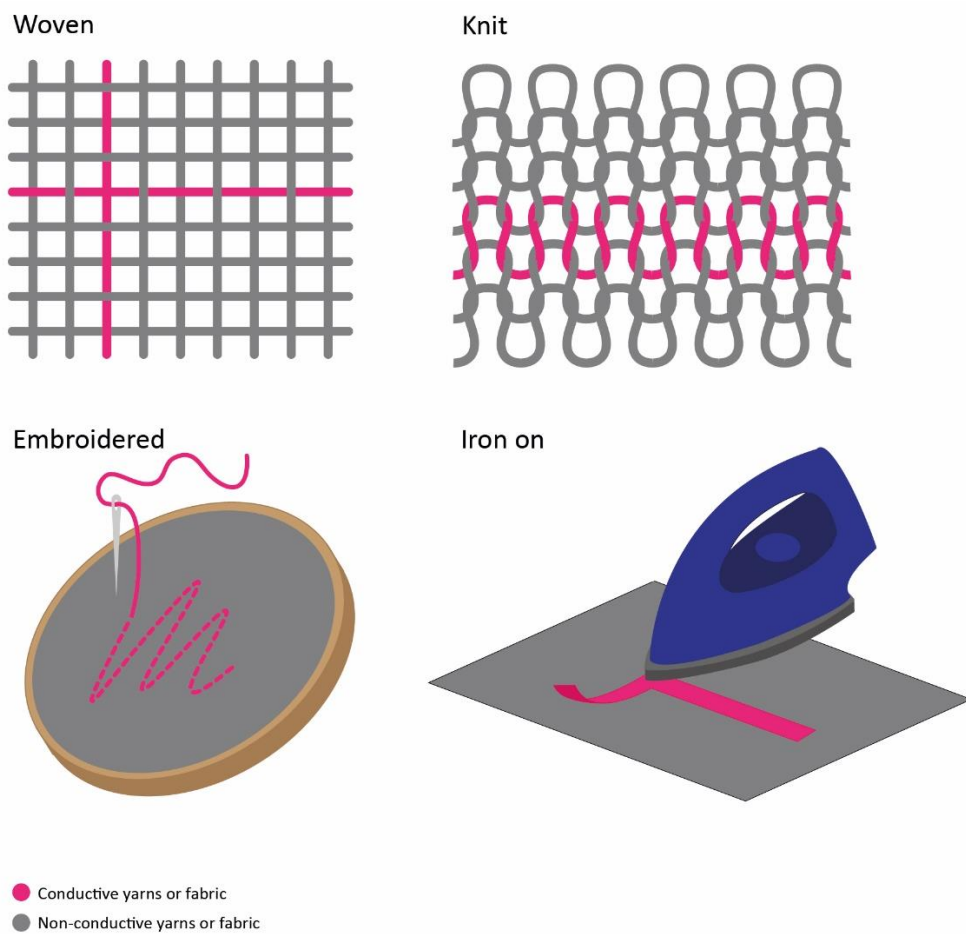
Figure 2-3. Textile construction methods for e-textiles.

Woven: weaving conductive fibres into fabric; Knit: knitting conductive fibres into fabric; Embroidered: embroidering conductive thread onto fabric; Iron on: Ironing or heat pressing strips of conductive fabric onto non-conductive fabric.

A further step is to make all components of an e-textile circuit out of textiles, ultimately replacing all rigid components with textile alternatives. Fully textile sensors have been demonstrated, including bend and strain sensors [33],[34]. However, it is not (or not yet) possible

to make all components required for an e-textile circuit out of textiles. This means that conductive textiles can't be used to make fully textile smart garments, and instead need to be used in conjunction with other electronics technologies.

While this approach is appealing because it means that e-textile garments can be made from textile parts, direct connection of components (for example resistors, LEDs, integrated circuit (IC) chips) to conductive threads often is much more challenging than attaching them to rigid or flexible PCBs [35,36]. As a result, conductive textiles are most often used as interconnects between rigid or flexible circuit modules. Manufacturing processes to construct e-textiles in this manner include specialised embroidery machines by ZSK Gmbh, which can embroider small PCB modules directly onto textiles [37]. And the Fraunhofer Institute for Reliability and Microintegration have developed custom machinery to laminate PCB modules onto stitched conductive tracks [38]. However, these are not yet well-established manufacturing processes. And though textiles are washable, conductive coatings on threads and fabrics can flake off after multiple washes, unless insulated [39].

2.1.4   Disappearing electronics in textiles

The diameter of the threads used to create textiles sets a lower limit to the size of the circuitry that can be constructed from textile parts. This ranges from 100 μm for thin sewing threads, up to 15 mm for chunky wool yarns, with conductive threads used in e-textiles typically being 1-3 mm thick. But existing electronics fabrication methods can create flexible circuits at least an order of magnitude smaller, using, for example, microfabrication processes, which are used to create smartphones and other devices. Thus another approach to e-textile construction is to fabricate electronics on flexible substrates, which is what the term 'flexible electronics' normally refers to, rather than being an umbrella term for all flexible circuitry, including conductive textiles.

Flexible electronic modules can be embedded inside textiles, whether in the seams, in pockets or channels [40,41], or inside yarns themselves [42]. This method uses the textile as a carrier for the electronics, not an integral part of the circuitry itself, which means that the manufacturing of textile and electronic parts can be kept mostly separate until the final assembly stages. This may have the advantage of making electronic parts easier to separate from the textile at the product's end of life, and minimise the need for custom machinery and interdisciplinary textile and electronics knowledge during the manufacturing process.

As flexible electronics fabrication methods are used in this work, a more detailed look at standard processes is required. This includes printing techniques, which can be used to

deposit conductive inks on polymer substrates. But as these processes can also be performed directly on textiles, they are discussed in the next section.

A standard fabrication method for this approach involves the etching of a thin copper film (typically 18-35 μm thick) laminated to a flexible plastic substrate (typically 25 −125 μm thick). Polyimide (PI), often known by the brand name Kapton™, is the most common substrate, as its flexibility, combined with a high melting point of 375-401 °C [43], makes it compatible with soldering and other high temperature processes in electronics fabrication. Polyethylene Terephthalate (PET) and Polyethylene Naphthalate (PEN) are also common: these are transparent, and therefore useful in applications where PI's amber colour is unsuitable. However, both have lower temperature resistance than PI, with PET films having a maximum working temperature of around 150 °C, and PEN around 235 °C [44]. This is a limitation of PET and PEN relative to PI. PET, for example, is often seen in printed sensors such as piezoresistive strain and pressure sensors that use crimped connectors to interface with other components, and don't contain any soldered parts [45]. Thermoplastic polyurethane (TPU) is also used as a print substrate, either for flexible or stretchable electronic devices. It also has a lower melting temperature than PI, at around 150 °C [46].

To etch copper-plated film a mask must first be applied, covering the areas that are needed to make the circuit. There are several options for fabricating this mask, of which the industry standard is photolithography [47], used for both rigid and flexible PCB fabrication. This involves laminating a photosensitive polymer film to the copper-plated film, and selectively exposing it to UV light to harden the film in specific areas. This can be achieved with a printed mask on transparent film, placed between the photosensitive film and the UV light source (this process is illustrated in Figure 2-4). Or with a photoplotter, where a moving UV light source creates the mask [47]. Other methods to create the mask include iron-on transfers using printer toner to create the mask [48], or more DIY methods using spray paint and a laser engraver to selectively remove the spray paint from the copper-plated film [49]. And for clarity, what is referred to as the 'mask' in this work is sometimes referred to as the 'resist'.

The masked film is then etched, typically in a ferric chloride or sodium persulphate solution. Chemical reactions between these compounds and copper etch the exposed copper, dissolving it into the etching solution and leaving only the areas covered by the mask intact. This method can be used to make flexible flat cables (flexible interconnects), or the etched substrate can be populated with surface mount components to create flexible PCBs.
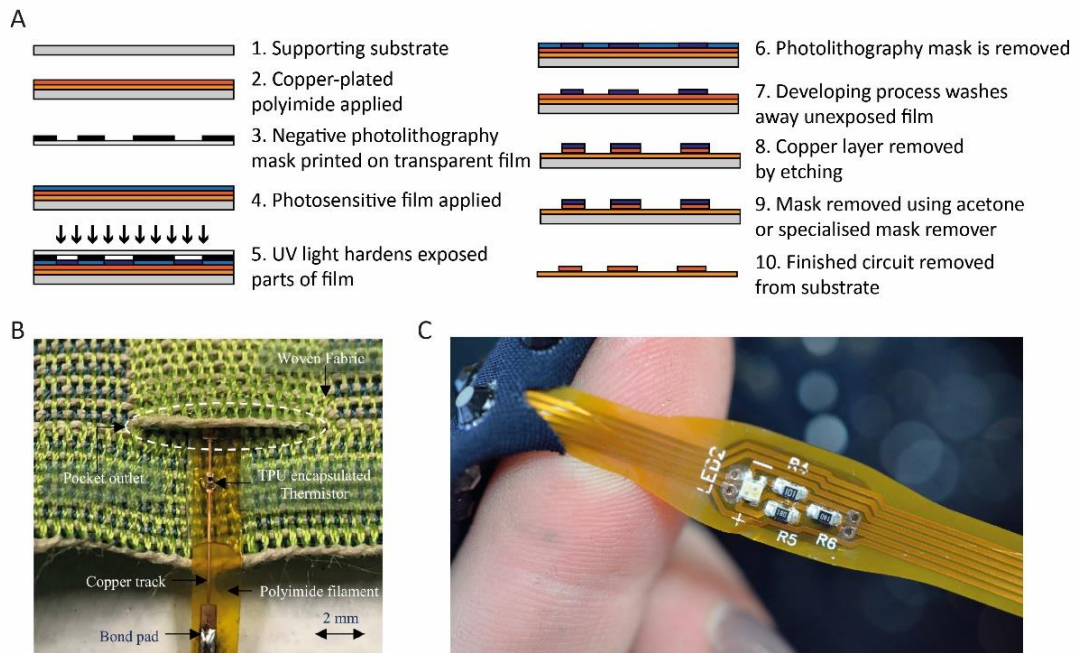
Figure 2-4. Flexible electronics fabrication.

A) Dry film photolithography process; B) Etched flexible temperature sensing circuit embedded in textile [50]; C) Flexible LED circuit module embedded in a light-up garment by Cute Circuit. Photo by Becky Stern, reproduced under the terms of the CC-BY license [51].

2.1.5   Printed electronics on textiles and new conductive materials

Printing techniques including screen, dispenser and inkjet printing have been used in the textile and electronic industries for a long time but have recently been adapted to print directly onto fabrics using functional inks [14,15]. As fabric is usually knit or woven from yarns (natural or synthetic fibres spun into long strands) or threads (thin yarns), it has high surface roughness and is porous. This makes it breathable, but can also negatively affect print quality. Therefore it is common to print on coated fabrics [52], or to print a dielectric 'interface' layer first, creating a smooth surface on which to print functional inks [53]. Laminating printed electronics onto garments, for later separation of electronics and textiles, has been suggested as a more sustainable alternative to printing directly on fabric, as highlighted by Dutch fashion tech designers Marina Toeters [54] and Pauline van Dongen [55].

While it is not currently possible to print all components, printed electroluminescent (light emitting) structures [17], transistors and logic gates[56], and passive components [57] have all been created to date. New research in nanotechnology and flexible electronics may eliminate the need for traditional components, and rigid PCBs, e.g. with the development of inherently flexible ultra-thin devices [58]. Nanomaterials such as MXene [59] and carbon nanotubes [60], as

well as transparent conducting polymers such as PEDOT:PSS [61], can be combined with textiles to create new e-textile possibilities.

It is also possible to solder components to printed conductive ink using low temperature solder, so it is possible to use this method to make printed circuits on some types of textile. In terms of limitations, printed tracks and other materials used to laminate and encapsulate printed parts on textiles are not breathable, which can impact the comfort and wearability of a smart garment if large areas of the textile are covered with printed electronics.

2.1.5.1   Screen printing

Screen printing and dispenser printing will now be discussed in more depth, as these were both considered for use in this work. More detailed information on inkjet printing and other techniques can be found in a review by Khan et al [62], and at the end of this section.

Screen printing is a technique that has long been used in the garment industry, and more recently in electronics, for the production of PCBs. The 'screen' is a mesh held taut by a frame. The mesh can be made from polymer fibres such as polyester, or fine metal wire, and the frame can be made from a variety of materials, including aluminium.

To form a pattern on the screen, it is covered with a photosensitive emulsion, and then a mask is placed on top, blocking the areas that are needed for the print pattern and forming a stencil on top of the mesh. Exposure to UV light hardens the emulsion, and then undeveloped emulsion is washed away. This effectively forms a flexible stencil, as illustrated in Figure 2-5A.

Once the screen has been manufactured, the screen printing process illustrated in Figure 2-5A can be performed. A squeegee spreads ink across the screen, filling the mesh with conductive ink. This process is called flooding. Next, the squeegee moves back across the screen, pressing it down onto the substrate. As the screen is flexible, it snaps back off the substrate after the squeegee has passed, depositing the ink onto the substrate. The squeegee pressure is pneumatically controlled, and the speed of the squeegee's movement, and the gap between the substrate and the screen, are all adjustable. Finding the right combination for the particular ink, substrate, and screen in use is critical to achieve a good quality print.
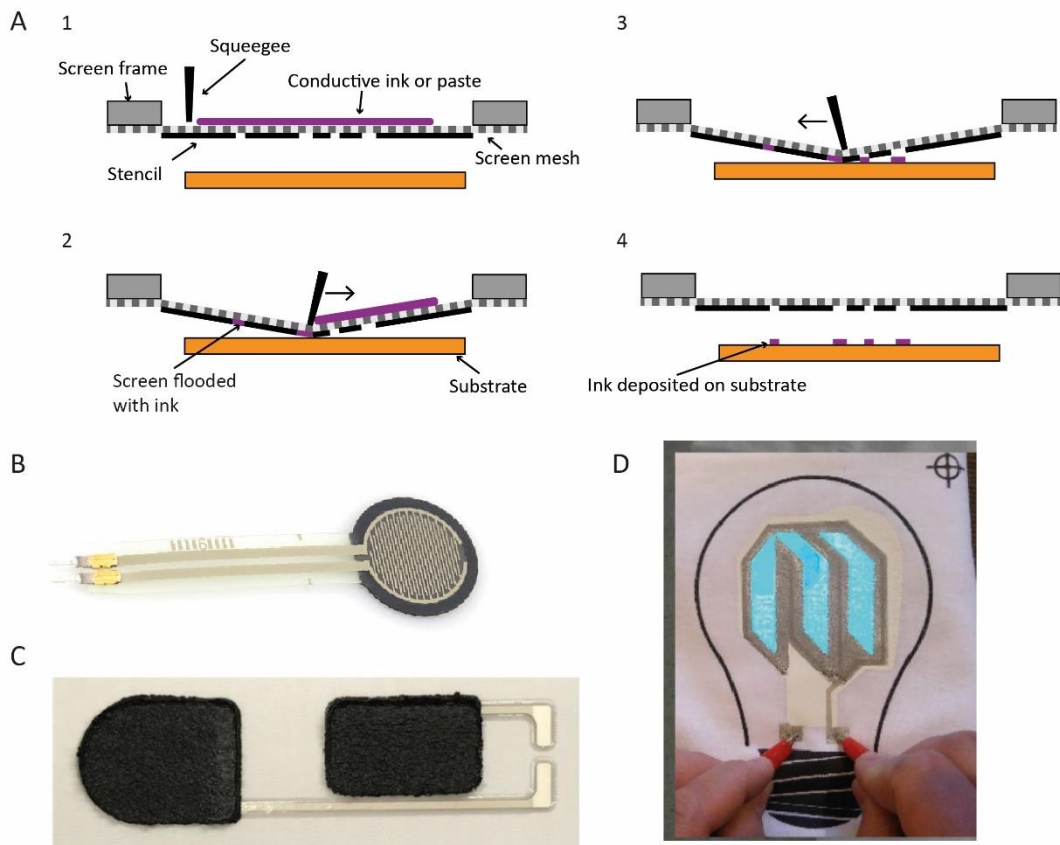
Figure 2-5. Screen printing: method and examples.

A) Illustration of the screen printing process, where ink is spread across a screen and allowed to fall through the screen onto the substrate in a defined pattern; B) Screen printed force sensitive resistor. Image copyright of Sparkfun Ltd, reproduced under the terms of the CC-BY license; C) Screen printed carbon electrodes and silver tracks on textile for electrical stimulation [14]© 2019 IEEE, reproduced with permission ; D) screen printed electroluminescent structure on textiles [18]. Reproduced under the terms of the CC-BY license.

Screen printing is an established manufacturing process used in the production of both rigid and flexible PCBs. But it is also used to print electronics on textiles. This includes printed electrodes for stroke rehabilitation [15] and electrical stimulation for lymphatic flow [14]. And more complex printed structures, such as flexible electroluminescent devices realised through multi-layer printing of conductive, dielectric and electroluminescent inks [18,63].

2.1.5.2 Dispenser printing

In dispenser printing, a cartridge of ink is attached to a gantry that allows the cartridge to move freely in the x-y plane, tracing out a pre-defined pattern and dispensing ink out of a nozzle to print circuit traces (Figure 2-6A). Similar to how a 3D printer operates, except that generally one layer of ink is printed, instead of many stacked layers of 3D printing filament.
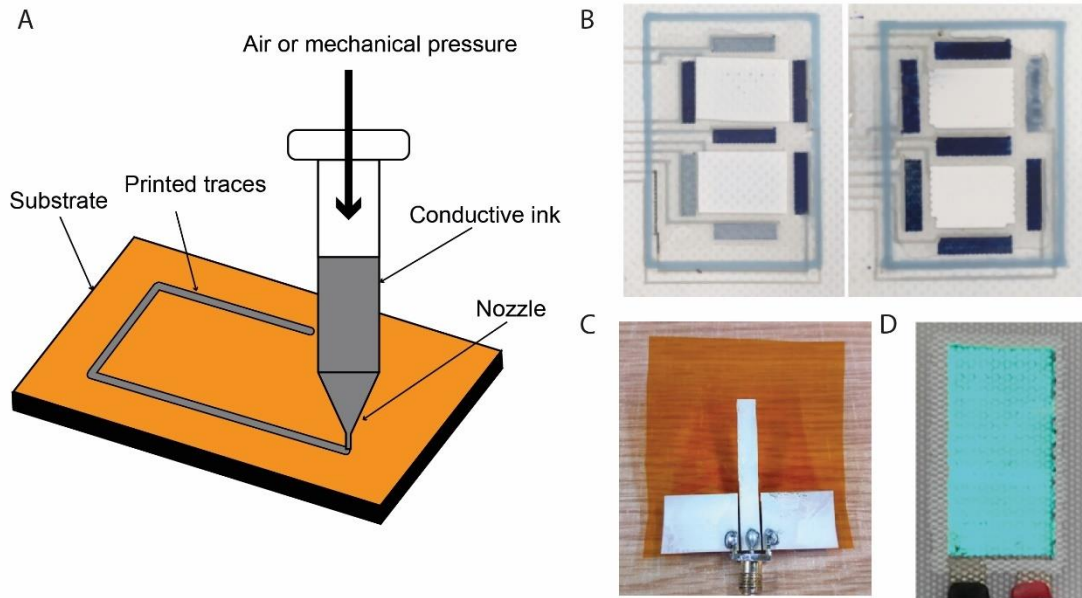
Figure 2-6. Dispenser printing: Method and examples.

A) illustration of the process. A cartridge of conductive ink is moved around an x-y plane, dispensing conductive ink in a defined pattern; B) Electrochromic display on textiles fabricated using dispenser printing [64] © 2017 IET, reproduced with permission.; C) Dispenser printed antenna on PI using silver ink [65]. © 2020 IEEE, reproduced with permission D) Dispenser printed electroluminescent pattern on textiles [17]. © 2016 Institute of Physics, reproduced with permission.

Inks used for screen printing can also be used in dispenser printing, which allows both methods to realise the same applications. As shown in Figure 2-6, this includes electrochromic displays, antennae, and electroluminescent structures. However, it is worth noting that dispenser printing is less efficient in terms of time and other resources (i.e. scalable) than screen printing as a high-volume manufacturing process. With screen printing, many copies of one design can be fit on one screen, allowing multiple copies to be printed in one go. With dispenser printing, the print head must trace out each part of each design individually, which means that total print duration increases with the number and complexity of prints.

2.1.5.3 Other printing processes

Alongside screen printing and dispenser printing, it is worth mentioning other techniques and briefly discussing how they compare. These include:

- Inkjet: Small ink droplets are propelled from a print head onto a print substrate. This technique uses lower viscosity inks than screen and dispenser printing.
- Reverse offset: Ink is applied to a roller, which is then rolled across a surface with raised areas in the shape of the desired pattern (relief plate or roller). The rolling

process transfers ink only onto these raised parts. The print substrate is then rolled across the surface, selectively transferring ink onto the substrate in the desired pattern.

- Gravure / gravure offset: Similar to offset printing, except that ink is deposited into recessed parts of a surface, using a blade, instead of onto raised parts.
- Flexographic: Another similar technique to offset printing, except that where offset printing normally uses a rigid (metal) relief plate or roller, in flexography this is a flexible material.
- Slot die coater: A method to create coatings or films on a substrate. A metal 'die', similar to a screen printing squeegee except rigid and usually metal, is moved across the substrate at a fixed height above it, spreading ink into an even film.
- Rotary screen: A form of screen printing using rollers instead of flat surfaces.

Figure 2-7A is a graphic produced by Hu et al [66] comparing the resolution and throughput (related to speed, a measure of a technique's production efficiency) of several of these techniques. Dispenser printing is not covered in this figure, but as mentioned in the previous sections, it has relatively low throughput as each design has to be traced out individually by the print nozzle. Figure 2-7B shows another comparison by Matsui et al [67], this time comparing resolution to the thickness of the printed patterns produced. It is clear from this that printing processes are many and varied, but with some overlap between their specifications, so that several processes could be used to produce the same circuit.
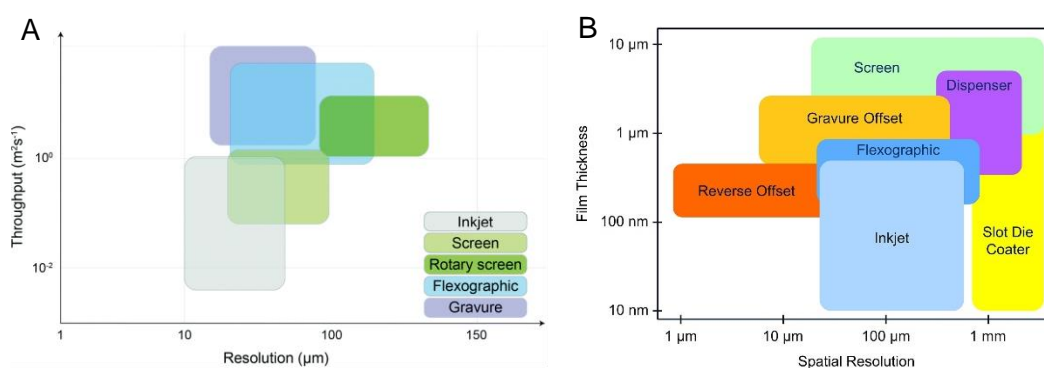
Figure 2-7. Comparison of printing techniques.

A) Printing techniques organised by resolution and throughput, which is a measure of production efficiency and is related to its speed. Dispenser printing is not listed here, but would rank relatively low in terms of throughput as it cannot produce multiple samples at once, unlike screen printing and other techniques. Reproduced from Hu et al [66] © 2018 Royal Society of Chemistry. Reproduced with permission; B) Comparison in terms of spatial resolution and film thickness, reproduced from Matsui et al [67]. Reproduced under the terms of the CC-BY license.

2.1.6 Hybrid e-textiles

In practice, many e-textiles are constructed from a mix of the above techniques. Some elements of a circuit, e.g. a sensor, may be constructed entirely from conductive textiles, while other parts of the circuit are built into a rigid module that attaches to the garment. Other examples include using conductive textiles as interconnects between circuit modules, e.g. using embroidered conductive thread traces to interconnect flexible PCBs [68].

Another method uses fine enamelled (Litz) wire, which is flexible and insulated, with electronic components soldered directly to the wire. Components are encapsulated in resin after soldering, and then the entire structure is wrapped in yarn using braiding machinery. The resulting 'e-yarn' can then be integrated into a garment [69]. This approach works well for simple circuits requiring two or three wires to interconnect components such as LEDs. But for more complex circuits, for example using motion sensing ICs, the wires currently have to be soldered by hand, which is labour intensive and time consuming [70].

Other hybrid examples include work by Zysset et al [29] consisting of flexible circuit modules with conductive thread bus bars, and *Closed-Loop Athleisure Fashion* [54], where a rigid control module interfaces with printed sensors laminated onto the garment. This is an example of a pattern many e-textiles follow: flexible sensors are embedded into a garment, and a removable rigid module houses the battery and control circuitry. This means that to create e-textiles it is necessary to have reliable ways to connect parts of a circuit together, whether attaching rigid components to flexible substrates, joining a rigid module to a flexible interconnect, or joining flexible conductors of the same type, e.g. conductive thread tracks.

2.1.7 Summary of fabrication techniques

The foregoing sections have shown that there are many and varied approaches to creating e-textiles. Some adapt textile manufacturing techniques to create e-textiles, while others do the opposite and adapt electronics manufacturing methods to work with textiles.

The development of new conductive materials, as mentioned in Section 2.1.5, are likely to revolutionise the e-textiles industry in the future. However, this work is focused on how e-textiles can be realised in the short term, not in the coming decades. It is thus advantageous to make use of established manufacturing processes and materials, or those that can be easily scaled up. This means using printed and flexible electronics processes, which are the most mature of the technologies for e-textile fabrication. Using stitched conductive threads is also a viable option, but only to create interconnects between flexible circuit modules, as the attachment of components to conductive threads is not a standardised process.

2.2 Connectors and modular systems

This section focuses on the use of modular systems in e-textiles, covering the following topics:

- First, a review of connectors and modular systems for e-textiles, highlighting the lack of connectors designed specifically for e-textiles.
- Then, an overview of what 'modular' means, and the different degrees to which modular design can be employed in electronics, textiles, and e-textiles. And the important role connectors play in the development of modular e-textiles designed to prioritise repair and recycling.

As stated at the start of the chapter, much of the content of this section is adapted from 'A review of connectors and joining technologies for electronic textiles', which is included in the list of publications in Chapter 1, Section 1.6 .

2.2.1 Connectors and modular e-textile systems

Though they are a critical part of e-textile construction, durable and reliable connections between different materials in an e-textile circuit remain a challenge. In the classic electronics text "The Art of Electronics", Horowitz and Hill describe the connector as "An essential ingredient (and usually the most unreliable part) of any piece of electronic equipment" [71]. This is especially the case for e-textiles, where electronic parts must be flexible, and comfortable to wear. Connectors and joining technologies are a central part of this, as connecting e-textile parts in a way that is electrically reliable and durable, without negatively impacting the form and function of a garment, has proven challenging to date.

This section reviews key joining technologies used in e-textiles, demonstrating that few solutions have been specifically developed for e-textile applications. Existing solutions are mostly connectors designed for use in rigid electronics, or textile closure mechanisms adapted to work with e-textiles. A need for development of new joining technologies for e-textiles, as well as further research into the performance of existing methods, is highlighted.

The term "joining technologies" will refer to all methods and materials used to make contact between parts of a circuit. These have been divided into two categories: a) detachable joining technologies, usually called connectors: these are typically electromechanical components such as snap fasteners or USB connectors, used for functions such as attaching a power source to an e-textile garment; and b) fixed joining technologies such as stitching or soldering, used for example to attach electronic components to flexible substrates. Fixed in

this context means that the connection isn't easily detached and reattached, not that it's physically impossible to remove the connection. A solder joint can be reworked, for example, and stitches can be undone, but not with the same speed or ease that a snap fastener or USB cable can be connected and disconnected.

Figure 2-8 shows examples of two different joining technologies used in e-textiles and highlights common joining terminology, also described in Table 2-1. There are many more ways to characterize joining technologies, but these are the most relevant to e-textile applications which are usually battery powered and involve low voltages.

Table 2-1. Explanations of common joining terminology

Characteristic	Description
Number of contacts	Contacts are the parts, usually metal, of a connector that form an electrical connection when brought into physical contact. They can range in numbers from 1 to several hundred in a single connector.
Pitch	Distance between the centres of two adjacent contacts. Pitch can range from less than 1 mm up to several cm depending on the application, and standardized pitch values allow interchangeable use of electronic parts.
Gender	Connectors often come in two varieties which 'mate' to connect, traditionally called 'male' and 'female' but more recently the terms 'plug' and 'receptacle' have been adopted.
Mating cycles	How many times a connector can be connected and re-connected, ranging from one mating cycle up to tens of thousands, depending on the connection mechanism.
Contact resistance	Resistance introduced into a circuit by the interface between contacts, which is influenced by several variables including the force applied to the contacts, the materials they are made from, and their surface roughness.

Figure 2-8 also illustrates the fact that most, if not all, connectors are only detachable at one end: one end attaches permanently to a wire, fabric, or other conductive interconnect, and the other is detachable and may be connected and disconnected repeatedly. Thus any connector, which is detachable, also needs a fixed joining technology such as soldering or crimping to fix it in place at one end.
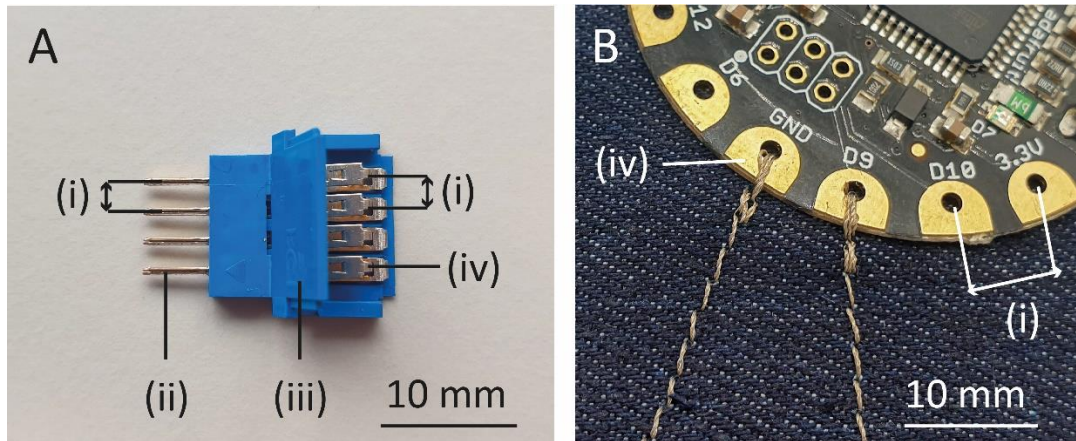
Figure 2-8. Joining technology terminology.

A) (i) Pitch, (ii) Detachable contact, (iii) Connector housing, (iv) Fixed contact. a) An Amphenol FCI Clincher connector, featuring detachable pin contacts at one end, and 'clincher' crimp connectors designed to make permanent contact with a flexible flat cable or flexible printed cable at the other end. b) a stitched connection to sewable contact pads on an Adafruit Flora microcontroller, an example of a fixed joining technology.

Despite the vast number of joining technologies in existence, very few have been developed specifically for e-textiles. A few companies have produced connectors for 'wearable' applications, but most focus more on non-textile wearable applications such as smart watches or other wrist-worn wearables, and very few are available for purchase off the shelf. Joining technologies for e-textiles also appear rarely within the literature on e-textiles, with many focusing on the development of novel textile sensors or actuators, or flexible conductive materials, rather than the business of bringing a system-level solution together.

2.2.1.1   Fixed joining technologies

Among fixed joining technologies (Figure 2-9, Table 2-2), a common method is soldering, where a metal alloy is melted and used to attach components to conductive substrates, and sometimes to join circuit modules to interconnects [35,41,69]. Soldering has high compatibility with rigid and flexible circuit boards, but there are only a few conductive threads and textiles that can survive the high temperatures involved (typically >200 °C, but low temperature solder with working temperatures around 150 °C exists). Several adhesives have been used as alternatives. These include a) non-conductive adhesive bonding (NCA), b) isotropic electrically conductive adhesives (ICA), and c) anisotropic conductive adhesives (ACA).
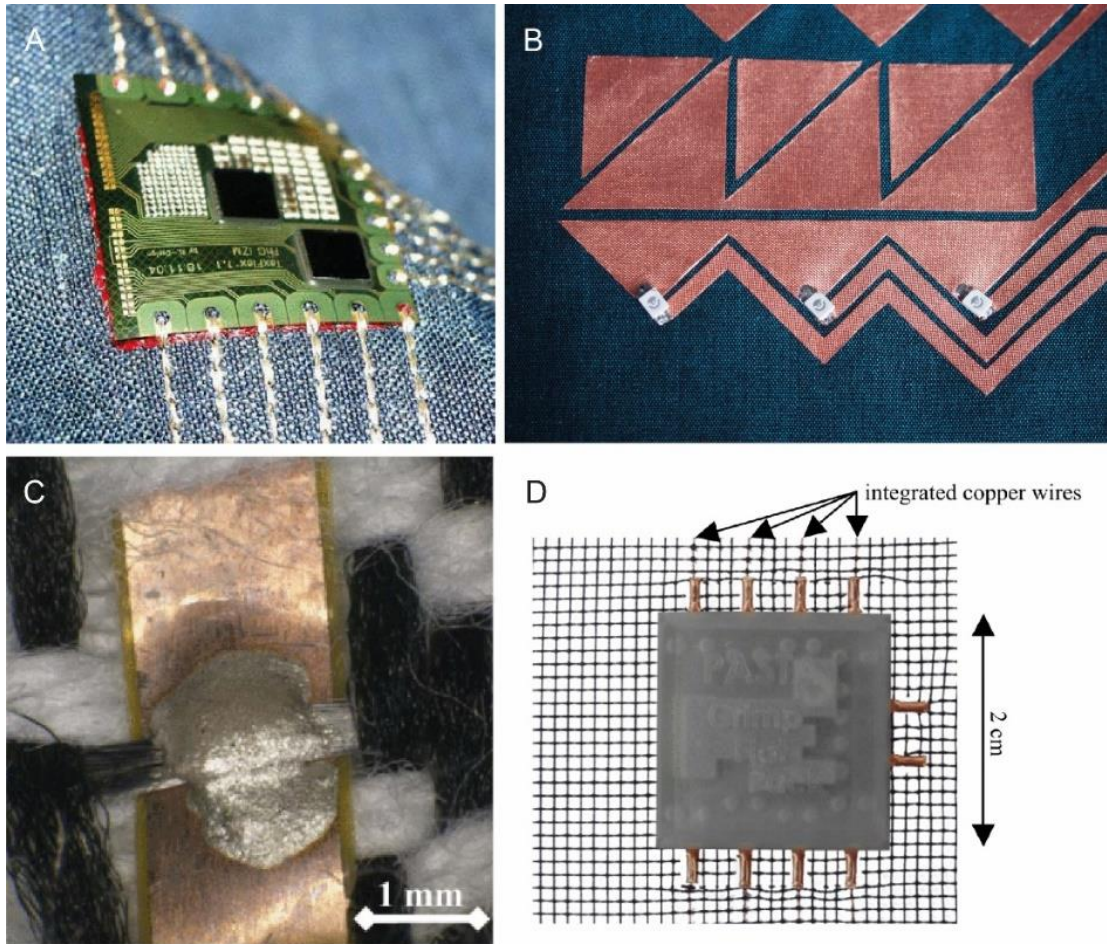
Figure 2-9. Fixed joining technologies used in e-textiles.

A) embroidered contacts to a flexible PCB. [72] © 2005 IEEE. Reproduced with permission; B) LEDs soldered to copper conductive fabric. Copyright Liza Stark, reproduced with permission; C) Isotropic conductive adhesive (ICA) used to bond conductive thread to a flexible filament. [29] © 2012, IEEE, reproduced with permission; D) Prototype of an e-textile module crimped to copper wires in fabric. [73] © 2012, IEEE, reproduced with permission.

Adhesive bonding has the advantage of lower curing temperatures than soldering requires, making it suitable for a wider range of fabric applications. Conductive adhesives also have the potential to replace (often lead-based) solder with more environmentally friendly alternatives. The trade-off is that these typically have higher contact resistance and lower mechanical strength than soldered connections, but future developments in material science may change this. The working principles of adhesive bonding methods are illustrated in Figure 2-10.

NCA bonding, used in flip-chip assembly, has been adapted by Fraunhofer IZM to contact rigid circuit modules with conductive textile interconnects [38,74,75]. A thermoplastic film is sandwiched between a rigid PCB module and conductive threads coated with thermoplastic. Under force and heat, contact is made between the PCB contact pads and the conductive

cores of the yarns, and curing the adhesive maintains pressure on this connection. The method has been refined and a custom textile bonding machine has been developed.

ICA bonding involves adding a conductive filler to an adhesive material, e.g. silver flakes added to epoxy [29,76,77]. ACA is similar, except that the concentration of conductive filler is much lower. This means that when ACA is sandwiched between two contacts stacked on top of each other, ACA conducts electricity only in direction that force is applied, commonly the vertical (z-) direction, as the concentration of conductive particles isn't high enough to conduct in the x-y plane [41,78,79]. This makes it suitable for fine-pitch connectors, and means it is sometimes called z-axis tape/film, but also means it has higher contact resistance than ICA. These conductive adhesives are reviewed in more depth by Aradhana et al [77].
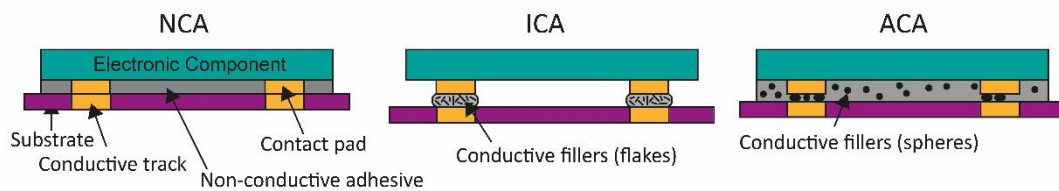
Figure 2-10. Illustration of NCA (non-conductive adhesive), ICA and ACA adhesive bonding processes.

It is also possible to stitch connections with conductive thread, either by hand or using a sewing or embroidery machine[32,80]. However, work by Linz et al has shown that without additional reinforcement, embroidered contacts tend to relax (and therefore suffer an increase in contact resistance) over time [68,80]. Welding [32,81,82] and crimping [83–85] (also referred to as cold welding) are also possible but less commonly used.

Table 2-2 Comparison of fixed joining technologies

Name	Method of attachment	Compatible with	Durability	Advantages	Disadvantages	Ref
Machine embroidered conductive thread	Embroidery machine. For some conductive threads, or more complex designs, specialist machinery required.	• Textile • Rigid PCB with sewable pads • Flexible PCB • Wire	• Can be damaged by temperature (contact resistance) • Conductive coating can flake off during washing	• Compatible with most textiles • Scalable with right equipment • Flexible • Looks and feels like textile	• Durability is not well studied • Temperature and washing can relax connection • Specialized machinery • Not suitable for joining discrete electronic components directly • Some conductive threads not compatible with standard embroidery machines	32,72,80
Hand stitched conductive thread	Hand sewing tools (needle and conductive thread)	• Textile • Rigid or flexible PCB with sewable pads • Wire	• Preliminary washing tests show continued function after washing at 20 °C	• Doesn't require specialized equipment or technical knowledge	• Reliability not well documented, but expected to be lower than machine stitching • Time consuming, therefore not scalable	86
Soldering	Soldering equipment, heat. Typically above 250 °C, low temperature options still require >150 °C	• Rigid PCB • Metal wire • Limited textiles • Some conductive inks • Standard components	• Strong electrical connection • Not flexible, requires protection against breakage at interfaces	• Compatible with standard electronics processes • High availability • Adaptable to both high and low volume	• High application temperature even with low temperature solder paste • Not compatible with many conductive textiles • Not flexible	35,41,69
Welding	Heat (produced as a by-product) Welding equipment.	• Some conductive textiles • Metal wires	• Contact resistance <1 Ohm • Requires encapsulation to survive washing	• Compatible with wider range of conductive threads than soldering (e.g. stainless steel thread)	• High temperature can damage delicate textiles and some printed conductive tracks on textiles	32,81,82
Crimping and rivets	Crimping tool (manually operated or automated)	Depending on product: • Textiles • Rigid and PCBs • Wires	• Preliminary evidence of washability • Supports repeated connection/disconnection	• Room temperature application • Compatible with both high and low volume production	• Not compatible with all types of e-textile material • Some types of crimp connector do not survive washing	83–85
Adhesives: NCA	Heat and pressure, supplied by die bonder or custom equipment.	• Bonding rigid modules or components to conductive tracks	• Resistant to temperature and humidity cycling	• Demonstrated to work with 1.27mm pitch components	• Requires die bonder or custom equipment • High bonding temperature (197 °C)	38,74,75
Adhesives: ICA	Some variants are heat curable; others cure at room temperature. Dispensed manually or by machine.	• Textiles • Rigid PCBs • Flexible PCBs • Standard components	• Encapsulation is required to prevent breaking	• Lower curing temperature than soldering • Compatible with printed conductive tracks	• More mechanically brittle than soldering • Higher contact resistance than soldering • Absorbs moisture if not encapsulated	29,76,77
Adhesives: ACA	Can be cured at room temperature. Heat or pressure reduce cure time. Applied manually or dispensed by machine.	• Textiles • Rigid PCBs • Flexible PCBs • Surface mount components	• Mechanically strong but electrical connection unreliable under strain	• Suitable for components with very fine pitch • Low curing temperature	• High contact resistance relative to ICA or soldering • Inconsistent contact resistance under strain	41,78,79

Table 2-3: Comparison of detachable joining technologies (connectors)

Name	Method of attachment	Compatible materials	Durability	Advantages	Disadvantages	Ref
Snap fasteners	Sew, crimp or solder, depending on variant.	• Textiles • Rigid PCBs • Flexible PCBs • Wires	• Produced as a long-lasting garment fastener. Electrical durability not tested.	• Widely availability • Mechanical durability • Protective enclosure not needed • Attachment can be done by hand or automated	• Relatively large footprint (typically 10mm diameter per contact) • Electrical characteristics not well studied	32,87
Pogo pins	Solder to rigid PCB	• Rigid PCBs	• 10,000 mating cycles • Contact resistance 20 mΩ	• Small footprint • Low contact resistance when properly mated.	• Require sturdy housing to maintain contact which can be bulky.	88
Magnets	Conductive adhesive	• Textiles • Rigid PCBs • Wires	Not defined	• Contact maintained without additional mechanical support	• Limited data on suitability as an electronic connector	89,90
Conductive hook and loop	Sewing or adhesive	• Textiles	• 10,000 mating cycles • Contact resistance unclear	• Possible inconsistent contact resistance	• Not extensively studied • Large footprint • Stability of contact resistance unclear	91–93
Zipper	Sewing	• Textiles	Not defined	• Looks like clothing rather than electronic component	• Electrical properties not tested	94–96
Button	Sewing	• Textiles	Not defined	• Looks like clothing rather than electronic component	• Not robust enough for use as a proper joining technology	97
Pin header	Soldering	• Some textiles • Rigid PCBs • Wires	• 50-300 mating cycles depending on metal used to plate contacts	• High availability • Standard pitch compatible with other components • high mating cycles	• May disconnect easily inside clothing (not tested) • Not tested for use in textiles	86,98,99
Amphenol FCI clincher	Crimping	• Flexible PCBs • Some conductive textiles	• 100 mating cycles • Mating / unmating force 300 g / contact • Contact resistance 20 mΩ • Preliminary evidence suggests ability to survive 50 wash cycles	• 2.54mm pitch compatible with standard components • Compatible with both low and high volume production • Low contact resistance	• Not designed for use in e-textiles, may disconnect easily inside clothing • Not compatible with all e-textile interconnect materials	83,100–103
Wireless	Stitched or printed onto fabric	• Textile • Rigid PCB • Flexible PCB	• Preliminary evidence of washability • Highly flexible	• No physical connection required • Flexibility	• Signal loss/lag • Inductive coupling requires AC signal and additional electronics	104–107
Alligator clips	Not applicable	• Textiles • Rigid PCBs	• Can be attached/removed repeatedly • Contact with very thin or delicate materials can be unstable	• Availability • Quick to attach and remove • Useful for prototyping and testing of connections	• Relatively bulky • Jaws can cause damage to textiles • Not suitable beyond prototyping stage	108
E-textile prototyping connectors	Not applicable	• Textiles	Not tested	• High compatibility with textiles • Useful for prototyping	• Not commercially available, must be custom made • Durability not tested	108,109

2.2.1.2 Detachable joining technologies

Of the connector options (Figure 2-11, Table 2-1), snap fasteners, also called gripper snaps, press studs, poppers, or press fasteners, are by far the most used connector in e-textiles [32,87]. Despite their popularity, limited research has been carried out on the suitability of snap fasteners as electronic connectors. One study reported preliminary positive results on the use of snap fasteners as connectors for low and medium bandwidth signal transmission along conductive textile transmission lines [87]. And standards do exist for snap fasteners, but only on their mechanical resistance when used a garment fastener [110]. Standards and further research are required to assess, for example, the number of mating cycles they can survive as an electronic connector.
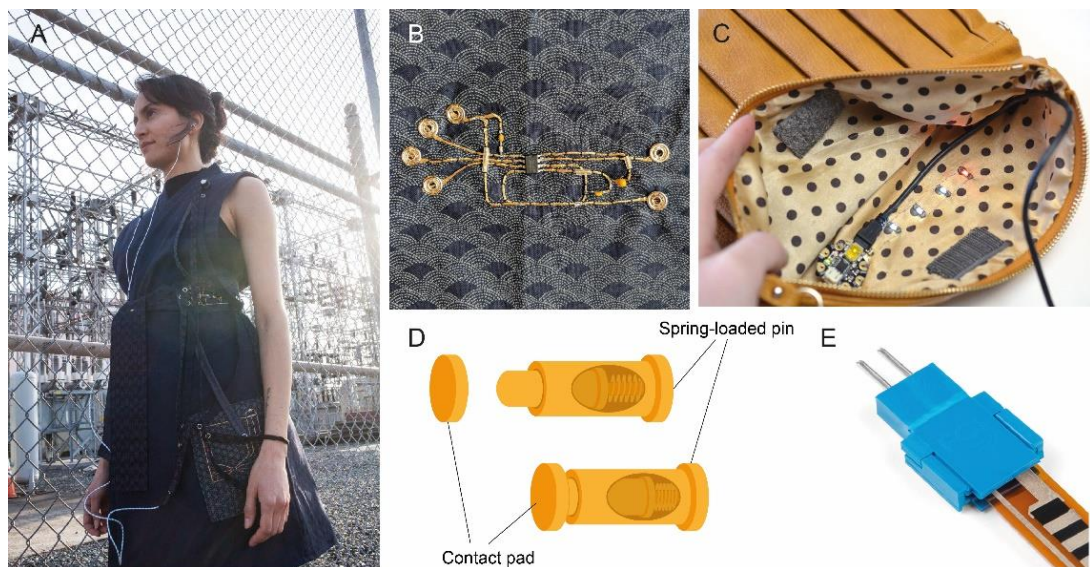
Figure 2-11. Connectors used in e-textiles.

A)-B) Snap fasteners used as modular connectors in Embodied RF Ecologies by Afroditi Psarra. Copyright Afroditi Psarra. Reproduced with permission; C) Conductive hook-and-loop used as a switch for a bag with embedded LEDs. Copyright Becky Stern. Reproduced with permission; D) Illustration of pogo pin, showing spring mechanism of the pin and flat contact pad when separated (top) and in contact (bottom); E) Two terminal Amphenol FCI Clincher connector, used with a flexible sensor printed on PI. Copyright Sparkfun, reproduced under the terms of the CC-BY license.

Other textile closure mechanisms such as metal zippers [94–96] and buttons [97] have been adapted into e-textile connectors. Similarly, conductive hook-and-loop (Velcro) can be coated with silver and used as a connector [91–93]. However, it's unclear whether any of these can provide consistent, reliable connections for anything except very simple circuits. Other connectors in this category are mostly electronics connectors: pin headers [86,98,99], pogo pins [88], and connectors for flexible electronics, for example Amphenol FCI clincher connectors, which have pin headers at one end, and crimp contacts to connect to flexible circuits (or

conductive thread tracks) at the other [83,100–103]. Wireless connection through NFC or RFID, using printed or embroidered coils, has also been investigated, but mostly to transmit power rather than signals [104–107].

The need for rapid prototyping and testing tools for e-textiles has led to the creation of several e-textile kits and prototyping connectors. Standard electronics prototyping processes, such as using a solderless breadboard and jumper wires, have limited compatibility with e-textiles. Sewing a prototype with conductive thread is time-consuming and doesn't support quick design changes, and conductive thread or other flexible interconnect materials often have significantly higher resistance than breadboard jumper cables.

Alligator clips are commonly used for e-textile prototyping, and many e-textile products such as the Adafruit Flora feature large contact pads which are designed for attaching alligator clips before sewing or soldering a fixed connection, as shown in Figure 2-12A. However, alligator clips and other standard tools such as multimeter probes and grabbers or spring hook clips, can be difficult to attach to e-textiles, and can also cause damage to delicate fabrics.
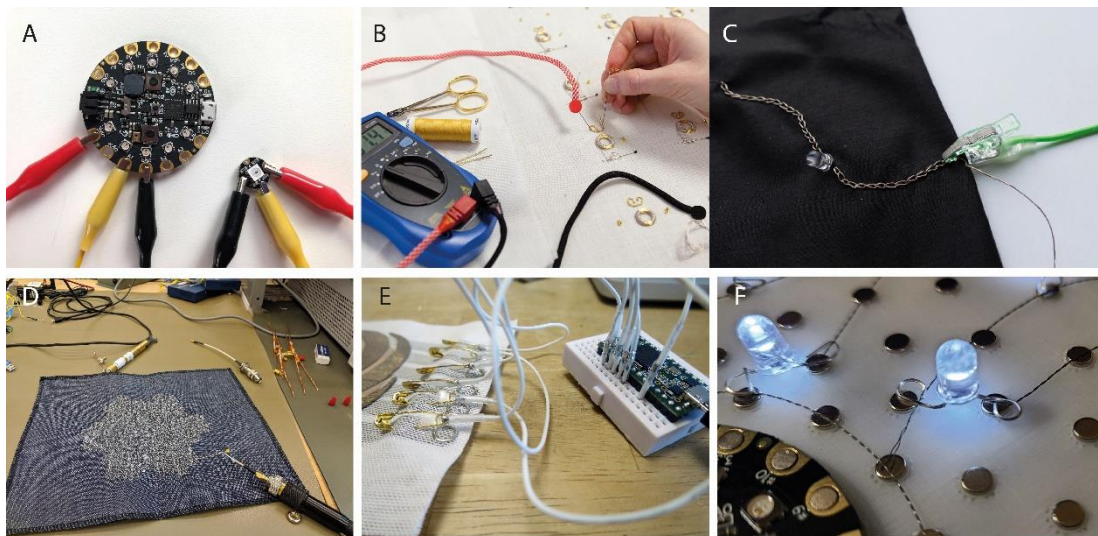
Figure 2-12. E-textile prototyping connectors.

a) Alligator clips. Reproduced with permission. Copyright Becky Stern. b) Pin probes by Irene Posch. Reproduced with permission. Copyright Irene Posch. c) Fabric pinch clip by Irene Posch. Reproduced with permission.[108]. Copyright Irene Posch. d) Pin coaxial connector by Afroditi Psarra (for an antenna). Reproduced with permission. Copyright Afroditi Psarra. e) Safety pin crocodile clips by Rachel Freire. Reproduced with permission.[111] Copyright Rachel Freire. f) Threadboard prototyping kit[90]. Reproduced with permission. Copyright Chris Hill.

Posch et al explored these issues in depth and proposed designs for new tools that merge standard electronics tools with textile tools such as pins[108]. One of these is the Pin Probe, which combines a 4 mm banana plug, paracord, conductive thread, a pin and 3D printed parts to create a connector which can be inserted into a multimeter at one end, and pinned into the fabric at the other, creating a useful tool for probing connections on fabric circuits. Similarly, the Fabric Pinch Clip adds conductive tape to a plastic sewing clip to create a fabric-compatible cable. These connectors are shown in Figure 2-12B and Figure 2-12C.

Building on this work, safety pin crocodile clips by Rachel Freire [109], shown in Figure 2-12E provide another way to interface between traditional electronics prototyping tools and fabric circuitry. Pins have also been used by Afroditi Psarra to make custom connectors to test an e-textile antenna, as depicted in Figure 2-12D. The Tools We Want project [112] proposes additional tools for e-textiles that merge electronics and textile practice.

Threadboard [90], shown in Figure 2-12F, is an e-textile prototyping platform that takes a different approach, using a grid of magnets to route conductive thread and connect it to components. This is suitable for prototyping e-textile projects using conductive thread, and facilitates prototyping using the same materials as will be used in the finished product. Conductive fabric tape, usually conductive fabric with a conductive adhesive backing, can also be used to create rapid e-textile prototypes[113]. A novel connector demonstrated by Li et al, and designed for use with standard through-hole components, consists of a coil of conductive thread encased in resin [114]. It is proposed that this connector allows components to be removed for washing, as components can be inserted and removed as needed. This could be useful as a kind of fabric breadboard, but for use in a commercial product would be inconvenient for a user to remove all components and then replace them on every wash.

Some e-textile kits provide for the need for different joining technologies at the prototyping stage compared a finished product. Prototyping parts by Loomia [22] have breadboard-compatible contacts that can be used for prototyping, and then cut off so that fixed connections can be made to a separate set of contacts by soldering. Textile Prototyping Lab's e-textile kit takes a slightly different approach, consisting of rigid PCB modules with sewable contacts for making garment prototypes. For higher volume production, these contacts can be removed, reducing the overall size of the module, and components connected to conductive thread interconnects using NCA bonding instead [75].

There seems to be an opportunity for a new category of connection that falls in between fixed and detachable. As an emerging technology, e-textiles should be constructed in a

manner that facilitates repair and recycling, in order to limit waste, and avoid the creation of a new, unrecyclable, waste stream [115]. Intentionally designing for disassembly has been proposed as a partial solution for reducing the environmental impact of e-textiles, including unravelling an e-textile to recover materials for reuse [116], or using a modular design [117]. For this to be achieved, suitable connectors will need to be identified. One option for this is to look at small connectors designed for flexible electronics. A few of these have been investigated for e-textile use, such as the Amphenol FCI Clincher connector mentioned earlier in this chapter. But there are many that have not yet been evaluated.

2.2.2 Motivation for modular design

Seamless integration of electronics into textiles is often cited as the ultimate goal of e-textiles, i.e. garments where the electronic circuitry is completely undetectable by the user. However, realizing this goal may have negative consequences for sustainability, as it makes repair or recycling of an e-textile product more difficult. Köhler [118] points out that when e-textiles break through to mass markets, this will create a new waste stream of products that can't be recycled in either textile or Waste Electrical and Electronic Equipment (WEEE) recycling.

If e-textiles must, at present, contain environmentally harmful materials, then we can at least facilitate easy repair, and try to reuse components and materials as much as possible. Design for recycling guidelines generally recommend minimising the number of materials used in a garment, to minimise the need for separation of materials for recycling. E-textiles typically contain textiles, electronic components, either conductive yarns, fabric with printed conductive tracks, or plastics with metallic tracks. A garment containing all of these cannot be recycled using either textile or electronics recycling, so if e-textiles are to contribute a circular economy, the different parts of the garment must be separable, and there is a need for proper end-of-life solutions specifically for e-textiles [119,120]. Furthermore, the development of 'right to repair' legislation is something that should be considered. This gives consumers the right to request replacement parts and repair information for devices and equipment. It currently only applies to large appliances like washing machines, and varies from country to country. But this may well grow in popularity and extend to other types of devices in the future, potentially including e-textiles. A modular design may make repair easier to facilitate, as a system where individual parts can be replaced is inherently more repairable than one in which a fault in one part means the entire system is defunct.

Another aspect of sustainability is ensuring that a product remains in use for as long as possible, i.e. maximising its lifetime before it enters a recycling process, or landfill. As pointed out by Hardy et al, there may be a significant mismatch between the expected lifetime of a garment and its embedded electronics [117]. They give the example of an e-textile denim jacket which the manufacturers guarantee to be washable 10 times. But a denim jacket would be expected to last 5 years, which means there is a significant mismatch between the expected lifetimes of electronics and textiles. If this is the case, then such a garment must be repairable, with electronic parts accessible for repair or updating until the garment has worn out. Or conversely, if the electronic parts in an e-textile garment last longer than the textile, it should be possible to remove and transfer them to a new garment.

Others have suggested business models for e-textiles that are based on leasing garments rather than selling them [119], so that manufacturers can use their specialist knowledge to repair and reuse e-textile circuitry.

In addition to sustainability considerations, keeping the electronic and textile parts separate has also been highlighted as a means for easier manufacturing, as it allows for the textile and electronic parts to be manufactured separately and assembled at the end of garment production, which could minimise the need for specialised e-textile knowledge in the manufacturing process.

2.2.3 Modular design in electronics, textiles, and e-textiles

2.2.3.1 Modularity in rigid electronics

There are many examples of modular design in conventional (i.e. rigid) electronics. Most computers are manufactured in a modular format that allows modification after manufacturing. For example, additional memory can be added by slotting in an additional circuit board, and graphics cards can be removed and replaced to perform upgrades or repairs. Development boards like Arduino and Raspberry Pi can be connected to additional boards (Arduino 'shields', Raspberry Pi 'hats' or Adafruit Feather 'wings', for example) that slot on top of (or otherwise connect to) the main board, as depicted in Figure 2-13.

And in the realm of electronic music, the modular synthesizer has been in existence since the mid-20th Century. Oscillator modules generate waveforms with varying shapes (and therefore varying sounds), and other modules can be slotted into the system to alter the waveform, or create sequences of notes to play repeatedly. Kosmodular, an example of such a system by UK musician and unconventional electronic instrument builder LOOK MUM NO COMPUTER, is shown in Figure 2-13.
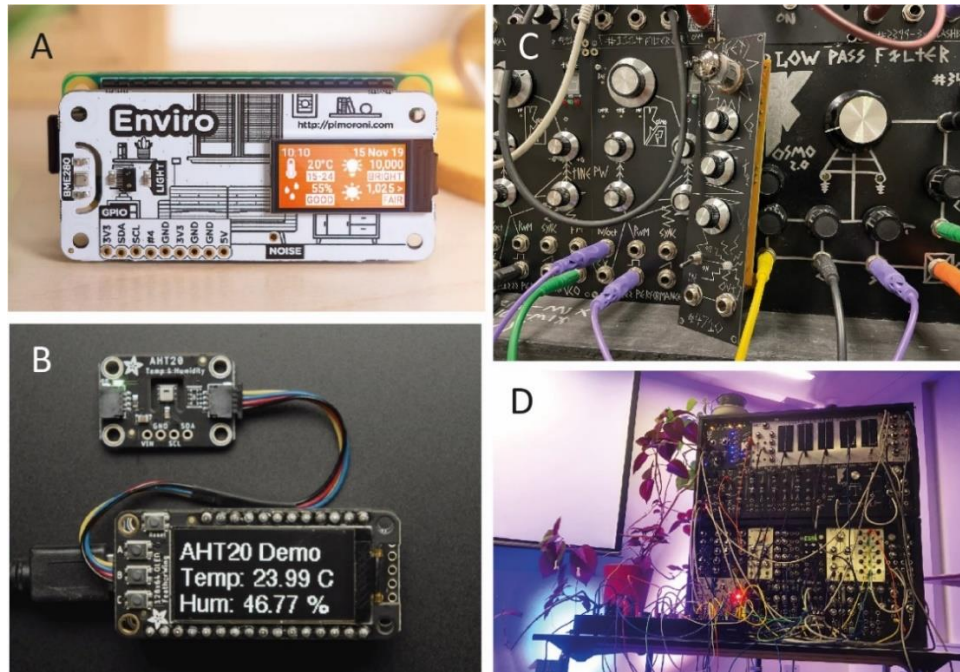
Figure 2-13. Examples of modular design in electronics.

A) Raspberry Pi 'Enviro hat' to measure environmental conditions with Raspberry Pi, by Pimoroni. © Pimoroni, reproduced with permission; B) Adafruit Feather equipped with LCD screen 'wing', connected to a temperature and humidity module. Photo by Kattni Rembor, reproduced under open source license terms (CC BY-SA 3.0); C) Modular synthesiser module by LOOK MUM NO COMPUTER; D) Full modular synthesiser setup by LOOK MUM NO COMPUTER. Reproduced with permission.

2.2.3.2 Modular design in fashion

In the 21st Century, we have a vast array of clothing options available to us. Much of this is cheap, fast fashion, an industry defined by Niinimaki et al as "a business model based on offering consumers frequent novelty in the form of low-priced, trend-led products" [121]. However, they and many others have pointed out that there are huge ethical issues around fast fashion. Its low cost is made possible by cheap labour, where cost saving for consumers is prioritised over safe working conditions and fair pay for workers. The quality is also low: a t-shirt may be much cheaper than in years gone by, but the quality of the fabric, its construction, and its expected lifetime have also reduced.

Sustainability is a multi-faceted issue, and there are many variables to consider in addressing the clothing industry's sustainability problems. One approach to improving sustainability is to promote reuse and repair of a garment rather than focusing on recycling. The vast majority of discarded clothing ends up in landfill or is incinerated, and significant portion of clothing sent for recycling ends also ends up in landfill [122]. Recycling is preferable to incineration of landfill, but it makes sense to focus on keeping a garment in use for as long as possible.
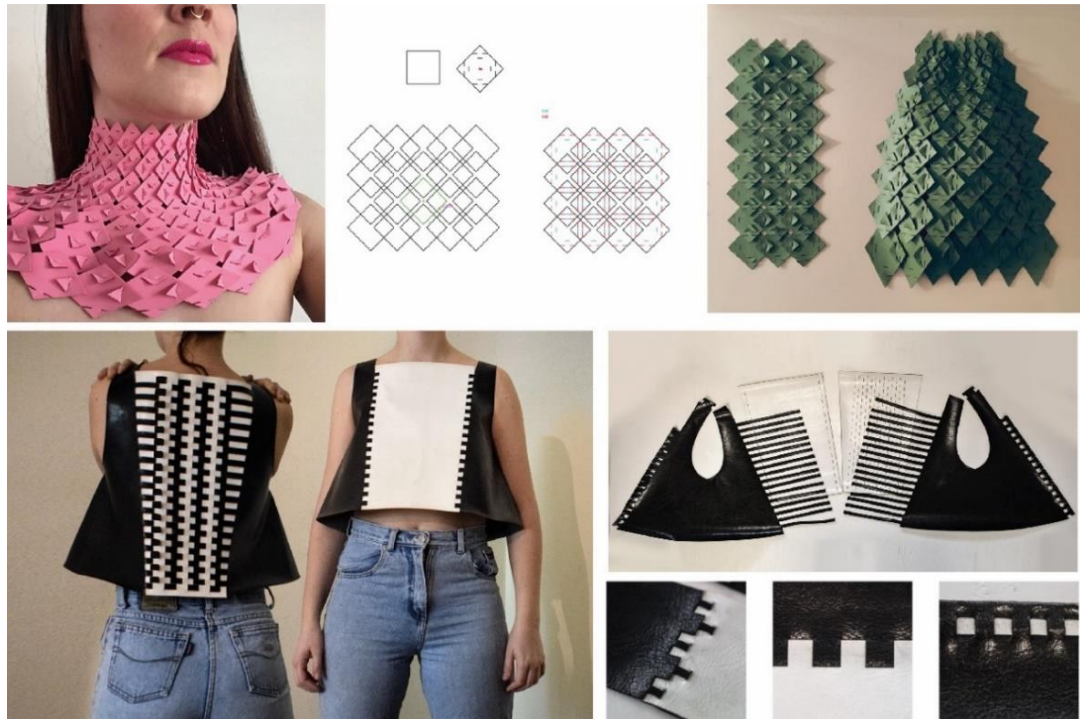
Figure 2-14. Examples of modular design in fashion.

Small modules, as demonstrated by 'Modular increase and decrease' by Loes Bogers [123] (top row) allow for a wide range of structures to be created from simple modules. Or larger modules can be used to create seamless garments, as seen in 'Seamless weaved garment' by Maite Sosa Methol (bottom row) [124]. Both works were produced as part of Fabricademy, a distributed textile education programme supporting innovation in textiles, sustainability, and technology. Images reproduced under the terms of the CC-BY open source licenses.

One way to tackle this issue is modular design, which has been adopted by several designers and fashion collectives. Small interlocking fabric modules can be used to construct garments, with the possibility to disassemble and re-build in another form (satisfying consumer desire for new clothes without discarding old clothes and buying new ones). Or larger interlocking modules can be used to make seamless garments. Examples of both are shown in Figure 2-14, with work by Loes Bogers and Maita Sosa Methol. Both were created during Fabricademy, a textile and technology education programme with a sustainability focus (of which the writer of this thesis is also a graduate). These designs are also documented in an open source repository [125].

2.2.3.3   Modular e-textiles: state of the art

A modular system is one composed of discrete modules which are joined to form a complete system, and there are many examples of modular e-textiles, particularly in the form of e-textile toolkits [126–128]. While some use connectors or interconnects which support reconfiguration [129], many use snaps, which have a relatively large footprint. Others use stitched connections to conductive thread interconnects [72].
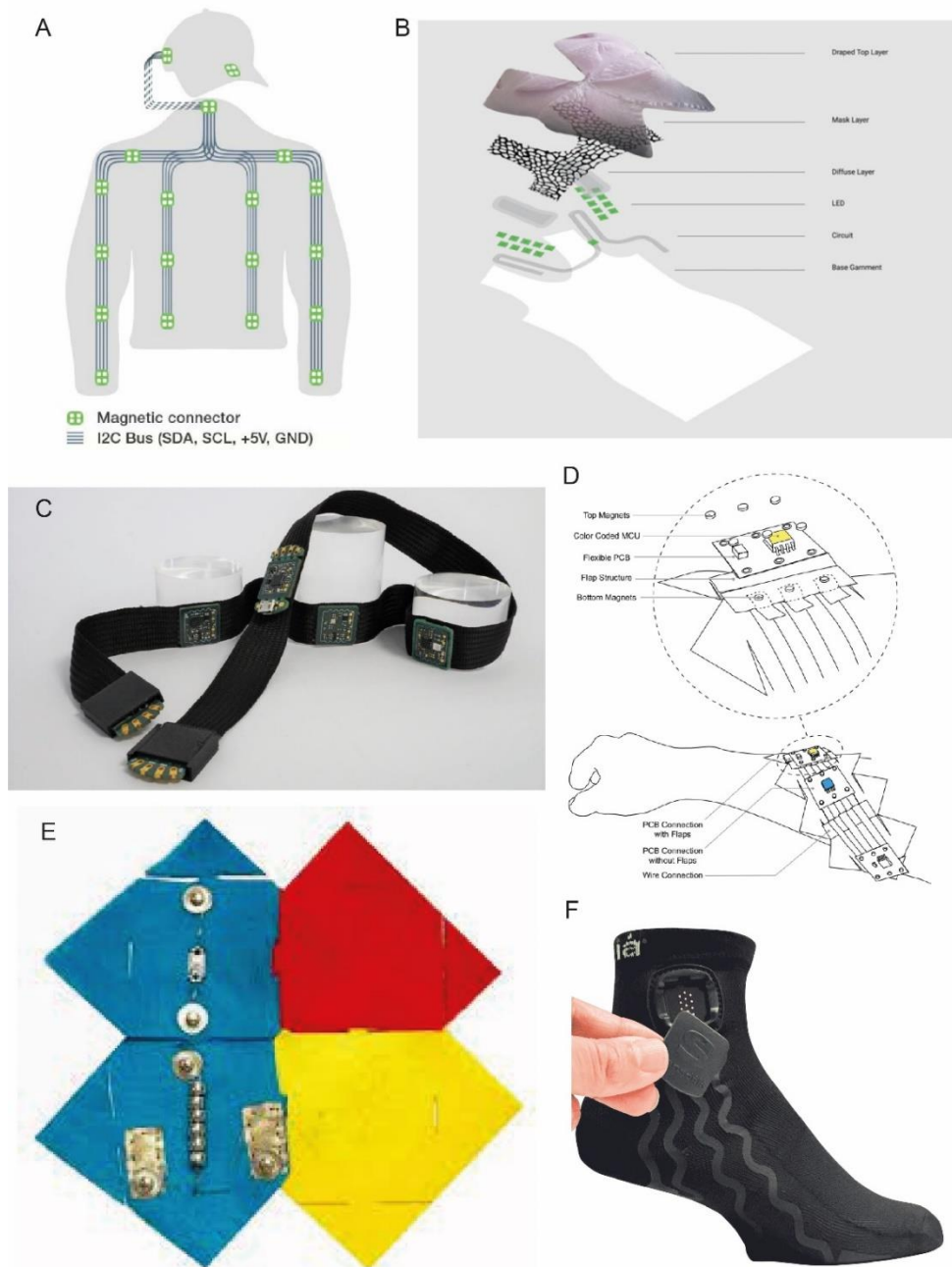
Figure 2-15. Examples of modular e-textile systems.

A) E-textile garment concept where I2C-enabled sensors are attached to conductive tracks in the garment with magnets [89] © 2010 IEEE, reproduced with permission; B) 'Second skin' modular garment with multiple layers making up the garment [130] Reproduced under the terms of the CC-BY license.; C) Textile Prototyping Lab e-textile toolkit, where circuit modules can be stitched or laminated onto textiles [75] Reproduced under the terms of the CC-BY license; D) SkinKit prototyping toolkit for building circuits on the skin [129] © 2021 ACM, reproduced with permission; E) Wearable, modular electronic patches for e-textile prototyping [131]. Reproduced with permission; F) Sensoria Smart Sock, exhibiting the most common implementation of modular design in e-textiles, where a detachable rigid control module connects to flexible sensors embedded in the garment [132]. Reproduced with permission.

There is some variability in the definition of 'modular', as evidenced by Figure 2-15. In some cases, like the Textile Prototyping Lab toolkit, circuit modules are attached to conductive textile interconnects, but are permanently joined and not able to be repeatedly attached and detached [75]. In other cases, disconnection for reconfiguration is prioritised, such as in the modular system by Righetti et al where flexible sensor modules are attached to conductive tracks in a garment using magnets as connectors [89]. Similarly, SkinKit [129] and Swatch-bits [131] feature circuit modules that can be easily assembled or disassembled, as they are designed for prototyping. And Second Skins by Malou Beemer uses another interpretation of modularity, where an e-textile garment is constructed from several separate layers, but with all circuitry included on one layer [130]. Finally, the most common type of modular design in e-textiles is that where a detachable rigid control module connects to flexible or textile sensors embedded in a garment, usually using snap fasteners or pogo pins to connect rigid modules to soft and flexible embedded parts.

2.2.3.4 Can e-textiles be 'more modular'?

Most e-textile garments currently employ a modular system, to a degree: the current standard in commercial e-textile garments is that sensors are embedded in the garment, and a rigid control module attaches to the garment (usually via snap fasteners or pogo pins) but is detachable for washing. A question asked in this thesis is: can we go a step further with this, making e-textiles 'more modular', to better support repair and recycling? Instead of the standard situation where the only detachable part is the control module, what if we also place detachable connections inside the garment? A power supply might still need to be attached on the outside of a garment and be removed for washing, but modular parts inside the garment would only need to be disconnected and reconnected intermittently, when the garment is undergoing repairs, receiving an update, or being disassembled at end of life.

One concern might be that including more connectors in garments would add bulk and make the garment less wearable. But given the number of small connectors that have been developed for flexible electronics and smartphones, it may be possible to use connectors that would take up less space than rigid parts that commonly appear in garments, such as buttons, zippers, and similar fasteners. Although the issue of sustainability in e-textiles is much more than recycling and reuse [133], prioritising modular design means that connectors have an important role to play in the sustainability of e-textiles. An area that has not yet been thoroughly explored is the potential for using modular design inside garments to connect circuit modules to conductive interconnects. As mentioned in the previous section, evaluation of small connectors for flexible electronics could lead to new ways to join

electronic parts in e-textiles. These would fall in between fully integrated and fully modular: circuits designed to be disassembled and reassembled not hundreds or thousands of times, but maybe up to ten times, when a garment needs to be updated, repaired, or recycled.

2.3   Stretchable electronics

The final section of this literature review covers technologies that enable stretchable electronics, for embedding in stretch fabrics. Specifically:

- State of the art technologies for stretchable electronics, covering both planar devices as well as helical and other 3D geometries, are reviewed, highlighting the potential for stretchable e-textiles using fully helical circuit modules.
- Finally, there is a short discussion of how the research questions identified in this chapter impact the choice of fabrication methods used to investigate them.

A significant portion of this section was included in "Stretchable electronic strips for electronic textiles enabled by 3D helical structure", which is included in the list of publications in Section 1.6.

2.3.1   Introduction and motivation

The term flexible electronics normally refers to circuits formed on thin, flexible polymer films. These include laminated or printed flexible flat cables (FFC) used to interconnect rigid circuit modules, but can also incorporate surface mount (SMD) components to create flexible printed circuit boards (Flex PCBs). These are commonly used in devices such as cameras and wireless earphones, to reduce weight and allow circuit boards to fold or roll up to fit into small spaces. They are also used in laptops and smartphones to connect displays to other circuitry. These are just a few example applications, and as mentioned in Section 2.1.4, flex PCBs have also been incorporated into e-textiles.

However, many textiles are stretchable as well as flexible. While there are many items of clothing that are minimally stretchable – denim jeans, wool coats, formal shirts and suits – stretch fabrics have steadily risen in popularity since the invention of stretchable synthetic fibres such as spandex in the mid-20th century. For example, clothing designed for sports (sportswear) must allow the body to move freely. As an athlete runs or jumps, for example, they must not be constricted by either textile or embedded electronic parts. Or consider compression garments, used for both sports and medical applications, where tight-fitting stretch fabric is used to create compression, for example on a limb that is swollen, or needs support after injury [134]. In many medical and sports applications, such as temperature

sensing, heart rate measurement, or electrical stimulation, sensors or electrodes in e-textile garments need to be in contact with the body, rather than merely close to it. A tight fit is therefore needed, and this is most often achieved with stretch fabrics. And as the medical and sport markets are two key areas of development for e-textiles [5,135], there is a need for reliable, stretchable e-textiles.

More broadly, stretch fabrics are also commonly used in everyday garments. This is reflected by the growing 'athleisure' trend, where items of clothing traditionally only worn for athletic activities (for example, leggings or Lycra shorts) are worn day to day, or even chosen for their aesthetic [136]. And the recent Covid-19 lockdowns seem to have caused a lasting shift in clothing choice towards comfortable clothing [137], and an increase in online shopping for garments, where garments that can "stretch to fit" can be bought online without having to be tried on in a physical shop [138].

2.3.2 Stretchable electronics state-of-the-art

There are several existing methods to fabricate stretchable electronics [139], but none has yet reached widespread commercial adoption. In many cases this is due to incompatibility between stretchable materials and standard electronics manufacturing processes. For clarity, the term "stretchable electronics" may describe a) a system of rigid or flexible modules joined by stretchable interconnects, b) an individual stretchable component, for example a sensor or electrode. The remainder of this chapter describes and compares different methods to realise stretchable electronics, which can be loosely organised into two categories:

a) Using inherently stretchable materials, e.g., stretchable conductive inks, nanomaterial-enabled stretchable polymers, or stretchable substrates for electronics such as TPU or silicone.

b) Engineering the geometry of flexible materials to make them stretchable. This includes using serpentine (wavy) or zigzag patterns, as well as helices.

c) A combination of both, for example serpentine metallic tracks laminated to an elastomer substrate.

Much of the work covered in this section is related to e-textiles, but there are also many examples of stretchable electronics for on-skin applications, where the device is adhered to the skin rather than embedded in a garment. As these are subject to many of the same constraints as e-textiles (must stretch and bend with the body, must be washable, unless disposable) some of these are included here.

At this point it is important to quantify the "stretch" that is referred to when discussing stretch fabrics. Depending on the yarns used to construct the fabric (e.g. wool or Spandex), and the method by which it is constructed (e.g. knitting or weaving), such a fabric may stretch by anywhere from 18% to over 100% with respect to its original dimensions [140]. As will be seen later in this section, there isn't a clear benchmark for stretchable electronics devices in terms of how much they should stretch. And while fabrics used for sportswear may be highly stretchable, the seams in a garment, and other elements such as zippers, are less so, so it is not necessarily required that all electronic parts in a Spandex garment much stretch by 100%. In consultation with Kymira, and aligning with existing work on stretch e-textile garments[141], a benchmark of 30% stretch (i.e. linear strain) was chosen for this work.

2.3.3 Knitting and stitching with conductive threads and yarns

Sewing techniques used to make seams in stretch garments use zigzag or other looping stitches that extend as the garment stretches, and these have been used to stitch stretchable conductive tracks on fabric with conductive threads [142]. Knitting conductive yarns into the structure of fabric can create the same effect, as knit fabrics are typically stretchable. Examples of stretchable electronics using knit or stitched conductive threads are shown in Figure 2-16.
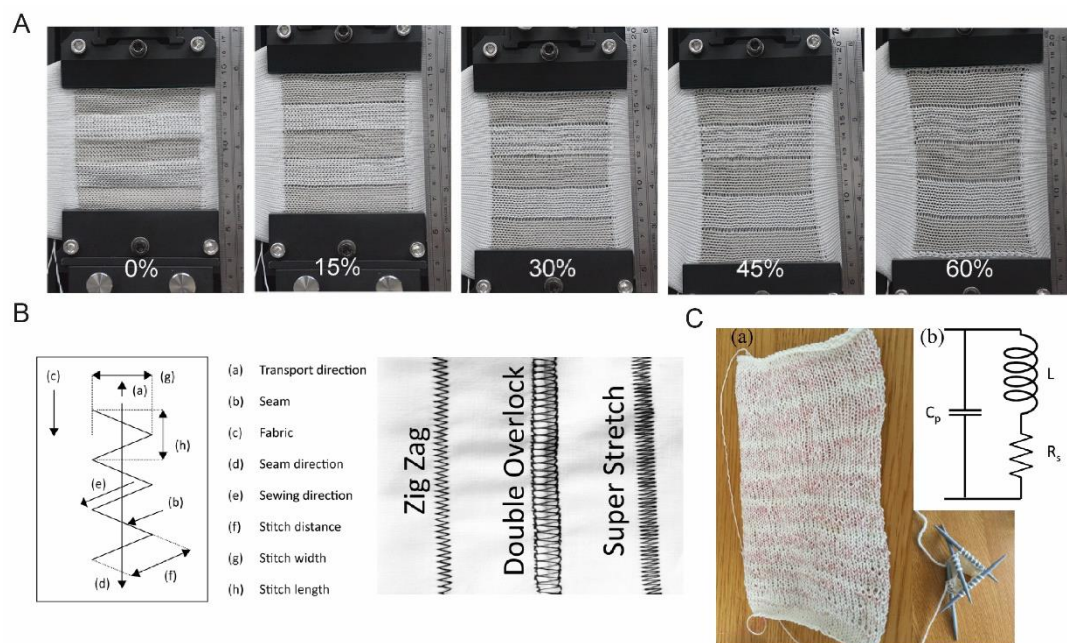
Figure 2-16. Stretchable electronics enabled by stitched or knitted conductive threads.

A) Stretchable knit fabric incorporating conductive threads[143] © 2020 Elsevier, reproduced with permission; B) Stretchable conductive thread pattern used as a strain sensor [144] © 2020 ACM, reproduced with permission; C) a) knitted inductor formed by incorporating conductive threads into fabric as it is knitted, and b) equivalent circuit [145]. © 2019 IEEE, reproduced with permission.

However, while it is possible to attach components directly to conductive threads, this is challenging [35], and conductive threads are primarily used as interconnects between rigid circuit modules [32,75,146] and flexible circuit modules [72,147] or to construct textile sensors [33,144,148], including knitted inductors[145].

Conductive threads are breathable and conform well to fabric, but have limited washability[149], and it is difficult to connect electronic components directly to them in a reliable manner, as most are not compatible with soldering. Stretchable conductive thread assemblies are also more commonly used as strain sensors, as their resistance can change significantly when stretched [33,144].

2.3.4 Serpentine geometries on flexible and stretchable substrates

Similarly, flexible electronic circuits ("flex circuits") may be formed or printed in serpentine / horseshoe shapes. In some cases, a PI substrate is also cut in a serpentine geometry, allowing the whole assembly to stretch[40], and in others feature serpentine metal tracks on a stretchable substrate such as thermoplastic polyurethane (TPU), polydimethylsiloxane (PDMS), or other elastomers [150,151]. Examples of serpentine structures used in e-textiles can be seen in Figure 2-17.

However, these materials have limited compatibility with many standard electronics manufacturing processes, for example needing to be placed on a non-elastic carrier film for roll-to-roll manufacturing [152], or deforming when exposed to the high (>200 °C) temperatures normally required for soldering, the most common and durable method to attach components to circuits.

The main disadvantage of serpentine tracks is that stress concentrates in certain areas (Figure 2-17D), at the parts of the structure with highest curvature [153–155], which can ultimately lead to failure caused by cracks in the metal tracks. Their shape also means that a strip of circuitry with serpentine traces is significantly wider than one with straight traces.
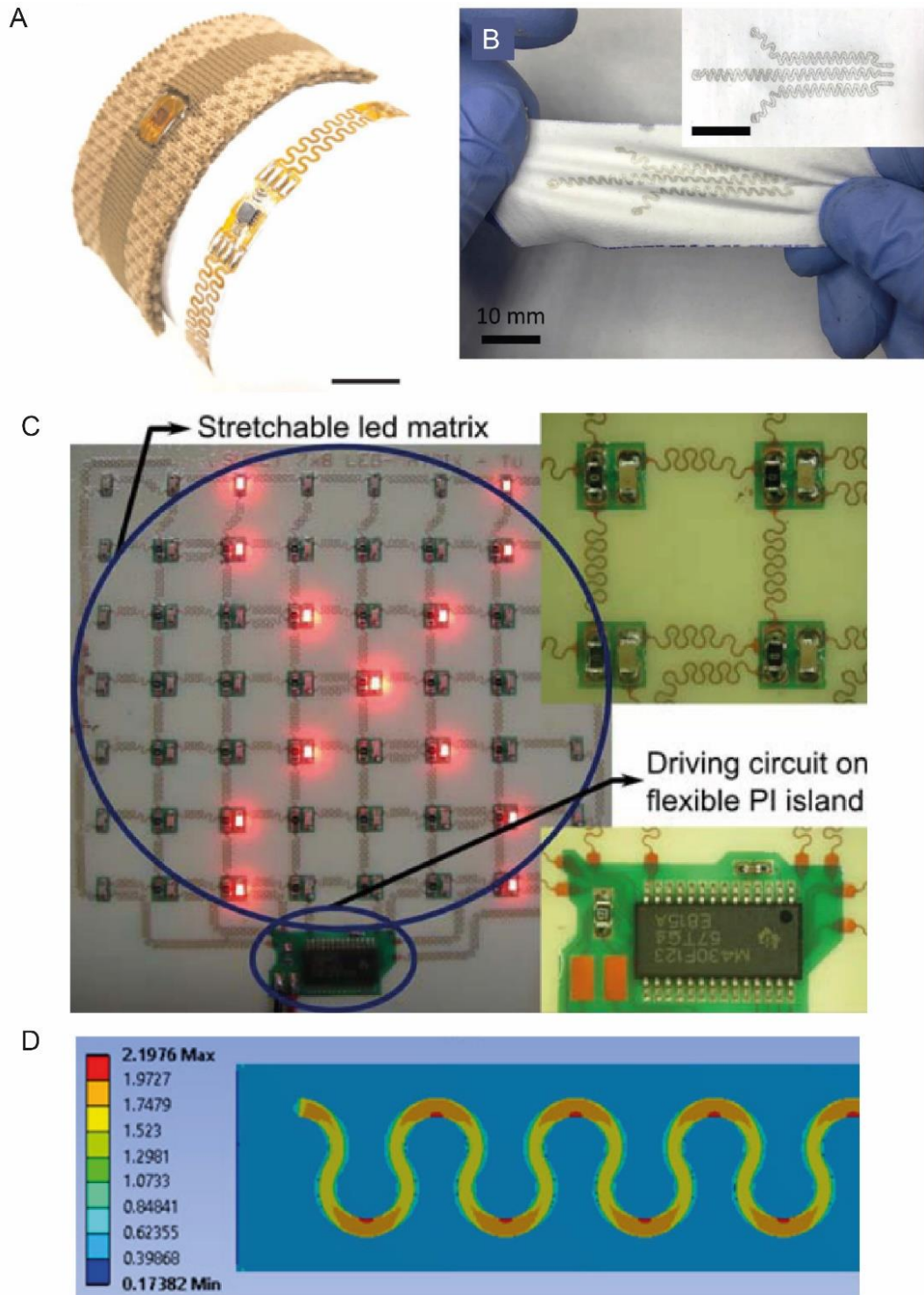
Figure 2-17. Serpentine traces on various substrates.

A) Copper-plated PI cut into stretchable serpentine geometry, for integration into a stretchable knit garment [40].

Reproduced under the terms of the CC-BY license; B) Printed stretchable serpentine traces on fabric, encapsulated

with PDMS [156]. ©2018 Wiley, reproduced with permission; C) Stretchable LED matrix with serpentine metal traces

on an inherently stretchable elastomer substrate [151]; © 2012 Taylor & Francis, reproduced with permission; D)

Simulation of serpentine structure showing concentration of stress (orange areas) [155]. © 2017 Elsevier,

reproduced with permission.

2.3.5 Alternative geometries with out-of-plane deformation

While it is most common to see in-plane serpentine structures (that is, where the serpentine shape is parallel to the plane of the textile and lies flat on its surface) there have also been demonstrations of out of plane serpentine structures. Some of these utilise controlled buckling as a means to enable stretch [157].

Another, less common, approach borrows from the Japanese paper art of kirigami, creating conductive textiles by inkjet printing silver inks onto woven fabric, and enabling stretch by strategically placing cuts in the fabric [158]. Other examples include kirigami-inspired nanomaterials [159]. Another example combines an origami structure – the Miura Ori pattern, which uses a specific folded structure to enable stretch – with kirigami elements to create a stretchable structure [160].

Figure 2-18 shows examples of these. To use these methods in e-textiles, it would be necessary to embed them in stretchable encapsulation, to prevent the structures from being crushed when worn on the body. In the case of the Miura-Ori circuit board (Figure 2-18C), the authors embed the stretchable circuit board in an elastomer, which is 5 mm thick (much thicker than most textiles). A similar approach would need to be taken with serpentine structures created using controlled bucking (Figure 2-18A).
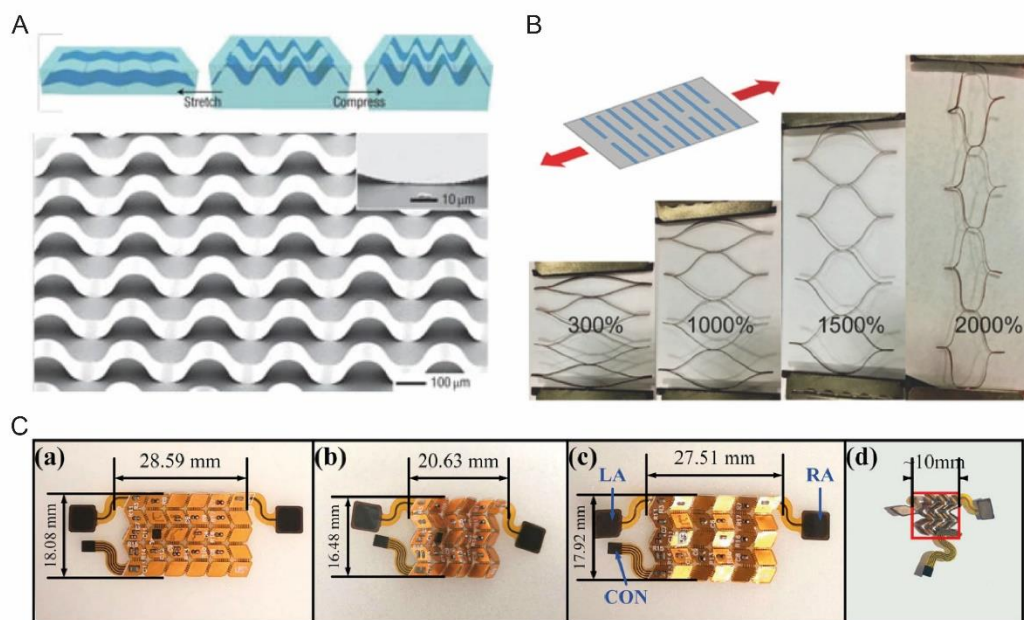
Figure 2-18. Alternative geometries for stretch.

A) Controlled buckling of semiconductor ribbons on a pre-stretched PDMS substrate [161] © 2007 Springer Nature, reproduced with permission; B) Kirigami inspired nanomaterial stretchable interconnect [162] © 2018 Wiley, reproduced with permission; C) Miura-Ori inspired stretchable circuit board, a) unfolded, b) folded, c) unfolded again, and d) compressed [160]. Reproduced under the terms of the CC-BY license.

This is a disadvantage relative to the planar serpentine structures discussed in the previous section, which are up to two orders of magnitude thinner and will conform better to the textile in which they are embedded. The kirigami structure shown in Figure 2-18B could also be easily damaged by washing in a domestic washing machine (for example, becoming knotted or entangled with other items) unless securely attached to, or encapsulated by, a supporting material.

2.3.6 Inherently stretchable conductors and stretchable components

Stretchable printed electronics can also be fabricated using liquid metal, i.e. metals or metal alloys which typically have gel-like consistency at room temperature [163,164]. An appealing feature of liquid metal is that it can self-heal, which has clear potential for use in e-textiles. However, it exhibits significant change in resistance when stretched. It is therefore most often used to measure strain, e.g. strain gauges made by the US company Liquid Wire [165]. Similarly, there are stretchable conductive inks, but these tend to exhibit the same relationship between resistance and strain [166]. Stretchable optic fibres, made from silicone-coated urethane fibre, have also been stitched onto textiles and used as strain sensors [167].

If, in the future, all electronic components can be made stretchable, their stretchability could be matched to the textile in which they are to be embedded. This would solve much of the issues experienced today, where failures in flexible and stretchable circuits often occur at interfaces between rigid components and flexible or stretchable parts. However, this would require a significant change in electronic device packaging. Though flexible components have been achieved, these are at the research stage of development and not yet commercially available [168]. Almost all electronic components are produced in a rectangular plastic enclosure with metal contacts designed for attachment to a PCB, and a total packaging redesign would be required to create flexible packaging and flexible contacts.

In the meantime, current e-textiles rely on the use of some rigid components. These components – usually mounted on flexible or rigid PCB modules – must be connected to the stretchable interconnects. And there are, at the moment, fewer solutions for connecting inherently stretchable materials like liquid metal to PCBs than there are for more conventional interconnect materials such as copper.

2.3.7 Helical geometry

Helical geometry was first employed in textiles centuries ago. Metallic threads used for decorative garments and tapestries can be formed by wrapping thin strips of metal around a core yarn, typically silk. This has been documented in Asia, in Indonesian [169] and Indian textiles [170], and in European Renaissance tapestries [171], and is still used today. In an early paper on e-textiles, Orth and Post used silk organza fabric made from silver wrapped yarn as a conductive substrate for e-textiles [172]. Examples of these yarns are shown in Figure 2-19.

Figure 2-19. Decorative wrapped yarns with helical structure.

A) The helical structure of metal-wrapped silk threads in silk organza is visible in this microscope image [172] © 1997 IEEE, reproduced with permission; B)-C) Microscope images of a silver-wrapped silk yarn with a triple layer helical structure in a Renaissance tapestry [171]. © National Museum of Australia.

Though they have a helical structure, the metal fibres are wrapped around non-stretchable core materials, such as silk. The overall structure is therefore not stretchable, and the purpose is purely decorative. Another example of helical structure in textiles is the helical auxetic yarn (HAY), where a thin thread is wrapped around a thicker one, and stretching this structure leads to a rippling effect, causing the yarn to increase in thickness as it is stretched (auxetic behaviour) [173].

Helical geometry has also been used in electronics, but existing work has focused on helical interconnects joining planar circuit modules, rather than entire helical circuits. A selection of these is shown in Figure 2-20. This includes helical polyurethane (PU) and copper fibres [174], helical conductive yarn [175], helical copper interconnects embedded in silicone [176], and helical interconnects for epidermal electronics [177]. Individual helical components have also been created, including, helical 'fibre pumps' [178] and printed transistors on PEN film wrapped around a PU fibre [179].
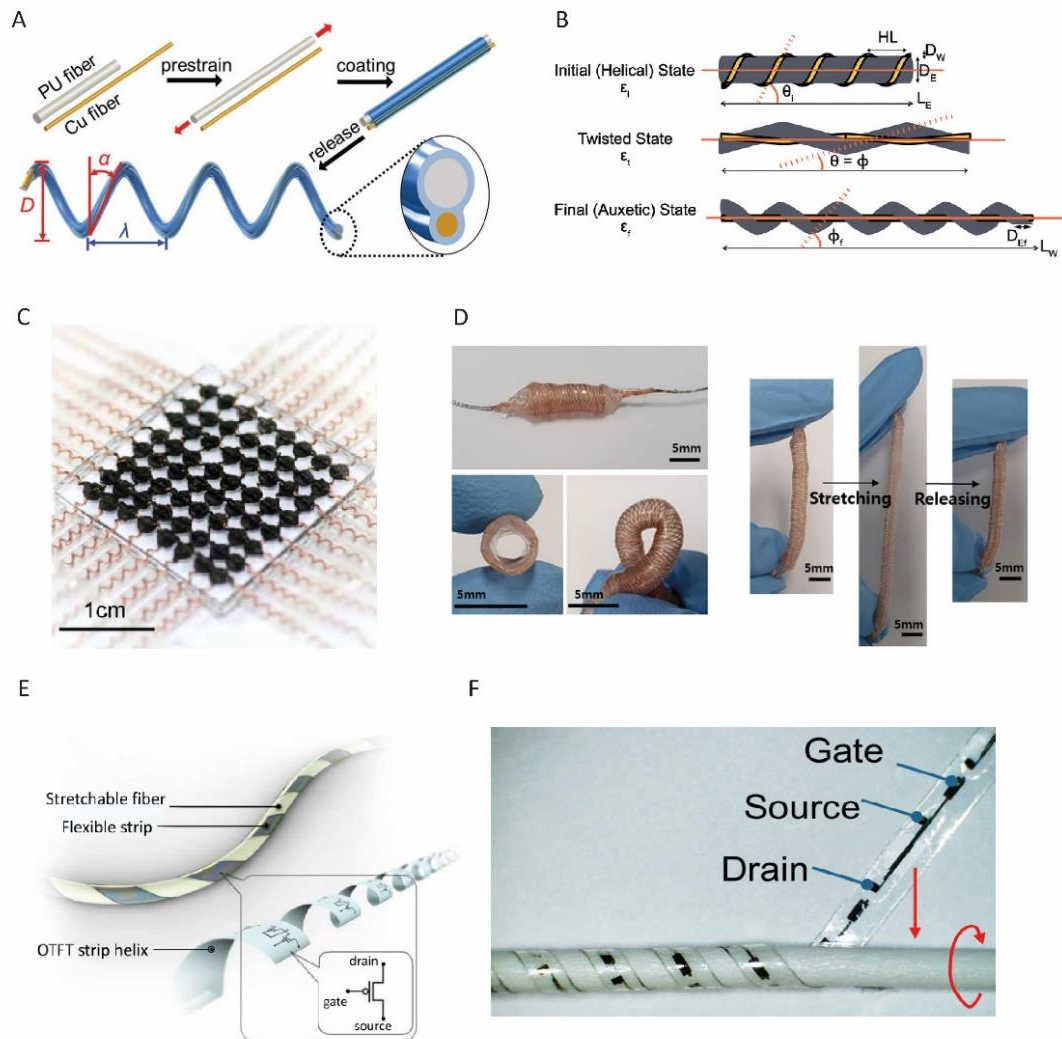
Figure 2-20. Examples of helical geometry in electronics.

A) Helical fibres composed from copper and PU fibres [174]. © 2020 Wiley, reproduced with permission; B) Helical auxetic yarn capacitive strain sensor, where a copper wire is wrapped around a stretchable core yarn [180]. © 2023 Wiley, reproduced with permission; C) Helical electrodes embedded in a stretchable elastomer to realise a stretchable sensor array for robotic skin [181]. © 2017 Elsevier, reproduced with permission; D) Braided stretchable interconnects, where multiple helices of fine copper wire are embedded in silicone [182]. Reproduced under the terms of the CC-BY license; E)-F) Printed transistor on PEN film wrapped around a stretchable fibre [179]. © 2021 IEEE, reproduced with permission.

Helical electrodes formed from copper wire wrapped around a nylon core have also been developed for use in robotic skin [181], as well as helical energy harvesting devices to power pacemakers [183], and flexible lithium-ion batteries using helical electrodes [184]. The HAY structure mentioned above has also been utilised in e-textiles as a strain sensor.

The majority of the above are constructed from a cylindrical fibre (a wire or thread) wound into a helix, and most feature an elastic core material that supports the structure. There are

also a number of patents which have mentioned helical structure in e-textiles [185–187]. Of these, none mentions using conventional SMD components, and the focus of all is on helical interconnects. This existing work has demonstrated the potential of helical geometry for stretchable electronics, but fully helical circuits using components have not yet been explored. This is perhaps surprising, as when a helix extends, it distributes stress evenly along its structure, which could be highly beneficial for preventing failures in stretchable electronics.

2.3.8 Comparison between stretchable electronics technologies

Table 2-4 provides a comparison between selected works on stretchable electronics, with a focus on helical geometries. One thing is immediately apparent: there is a lack of consensus about how stretchable electronic devices should be evaluated. Some studies perform wash testing, others do not. Some focus on cyclic testing at moderate (30-40%) stretch, while others focus on demonstrating the ability to achieve extreme (500%) strain before breaking, but do not show how the device performs under repeated stretching. In e-textiles, many cycles of low to moderate strain can be expected as the body moves, so cyclic testing is important. Wash testing is also key, as a stretchable device that cannot survive a domestic washing machine wash cycle will have limited practical use. Or will need to be disposable, which is wasteful and not environmentally friendly.

As stated in the previous chapter, new stretchable materials hold promise for the future of stretchable electronics, but it is unclear how long it will take for these to become readily commercially available. That is, to achieve compatibility with existing electronics manufacturing processes, or for the widespread adoption of new processes that can achieve stretchable electronics. Given this, what can we achieve now, using already established manufacturing processes? Helical geometry seems under-explored with existing research focusing on interconnects and simple components. There is an opportunity to explore helical circuits, formed by winding thin strips of flexible circuitry (containing SMD components) into helical geometry. The development of fully helical circuits ("helical e-strips") was explored in this work and is covered in Chapter 6.

Table 2-4. Comparison between stretchable electronics technologies

Description	Type of circuit	Materials	Maximum stretch	Cyclic tests	Wash tests	Comments	Ref
Conductive textiles							
StretchEBand: embroidered conductive thread sensor	Strain sensor	Silver-plated nylon thread stitched onto stretch fabric (polyester blended with elastodiene)	240%	Not performed	Not performed	Functionality of strain sensor demonstrated, but durability was not assessed	144
Knitted conductive textiles	Textile triboelectric nanogenerator	Silver conductive yarns formed into a knit fabric	60%	6000 cycles of 45% stretch	Not performed	Would need to be subjected to wash testing to assess durability	143
Knitted inductors	Single component: inductor	Copper wires knit into fabric structure	Not determined	Not performed	Not performed	Demonstrates functionality as an inductor, but durability is not investigated	145
Serpentine structure							
Tailored e-textile sensing garment	Flexible PCB modules joined by serpentine interconnects	Copper tracks on PI film, and flexible PI modules containing SMD components. Wires also used to join modules	79-88%	1000 cycles at 30% strain	Able to survive 10 wash cycles	Demonstrates resistance to cyclic stretching and washing, but this is only preliminary data	40
Copper and printed silver serpentine tracks	Interconnect	Copper foil embedded in PU and PDMS. Silver ink printed on non-woven fabric	Not determined. Study focuses on cyclic durability	Up to 100,000 cycles of 20% strain	Not performed	Comprehensive study on cyclic durability of serpentine interconnects at low to moderate (20%) stretch. Higher levels of strain are not explored	188
Stretchable LED matrix	Stretchable interconnect, and flexible / stretchable LED matrix	Etched copper serpentine interconnects embedded in PDMS, used to join flexible circuit 'islands'	Not determined	Not performed	Encapsulated LED modules were able to survive 5-10 wash cycles at 40 °C and 60 °C. Full stretchable LED matrix was not washed	Demonstrates successful fabrication of fully stretchable circuit, but lacks tensile testing data, focusing only on wash testing	151
Origami, kirigami							
Miura-ori enabled stretchable circuit board	ECG monitoring system	Copper tracks and SMD components on PI, embedded in silicone	Not determined. Tested up to 40% strain	All samples survived 3000 cycles of approx. 24% stretch	Not performed	Full circuit, but it's unclear how it would be incorporated into textiles	160
Kirigami-inspired textile electronics	Interconnect	Silver conductive ink, inkjet printed onto woven PET fabric, then laser cut into kirigami structure	Approximately 600%	1000 cycles of 100% strain, with 20-30% increase in resistance after testing	Not performed	There is a change in resistance between unstretched and stretched states, which may be an issue for some applications	189

Serpentine geometry formed by controlled buckling	Interconnect	Gallium Arsenide ribbons coated with silicone dioxide, on a PDMS substrate	Not determined. Stretched up to 51%	Not performed	Not performed	Demonstrates proof of concept, but at an early stage not suitable for integration in e-textiles	157
Stretchable conductors							
Conductive ink printed on TPU substrate	Interconnect	Silver conductive ink screen printed on TPU film	Half of the samples broke before 74% strain	Resistance increased from approximately 1.5 Ω to 5 Ω after 1000 cycles of 20% stretch	Not performed	Resistance varies with tensile strain, making this suitable for strain sensing, but possibly not as an interconnect	166
Liquid metal	Strain sensor	Liquid metal paste made from GAInSn and Ni nanoparticles, printed and then encapsulated in silicone	Not determined	10,000 cycles of 50% strain with stable resistance	Not performed	Exhibits good stability under many thousands of tensile strain cycles, but is just a series of printed lines, rather than a full circuit	164
Helical structures							
3D helical fibre	Interconnect, used to make LED circuit with through hole LEDs	Copper wire bonded PU fibre with cyanoacrylate coating	At 300% strain helical structure is lost	30% strain, 300 cycles per hour, for 10,000 cycles. No damage reported	Samples survived ultrasonic washing at 20, 30 and 55 °C for 100 min, both with and without detergent	Interconnect only. Wash test does not simulate textile washing procedure, so is not a realistic assessment of washability	174
Hierarchically interlocked helical conductive yarn	Conductive yarn	Conductive yarn made from silver nanowires, MXene, and TPU	1000%	3500 cycles at 200% strain	Not performed	Highly stretchable conductor, unclear if useful for building fully stretchable circuits with other components	175
Braided textile-based interconnection	Interconnect	Multiple copper wires braided to form a multiple helix structure, embedded in silicone	762%	500 cycles at 500% stretch	Not performed	Interconnect only, 3 mm – 5 mm in diameter, most of which may be too thick for textile integration	176
Helical printed transistor	Single component: transistor	Organic thin film transistor on PEN substrate	50% (theoretically determined)	Not performed	Not performed	Only one component, not a full circuit. Lacks information on washability	179
Lantern-inspired on-skin helical interconnects	Interconnect	Helical copper wire embedded in PU / PDMS fibre solution	Approximately 175%	3000 cycles at 50% strain	Not performed	Interconnect only, not designed for e-textile integration	177

2.4 Summary

This chapter began with a review of e-textile fabrication techniques. Then, connectors and joining methods for e-textiles were reviewed. Most, if not all, are solutions designed either for electronics or textiles and have been adapted for use in e-textiles. The potential benefits of using modular design in e-textiles have been discussed, as well as the central role that connectors need to play in achieving modular e-textiles. There is still the opportunity and need for e-textiles to be made 'more modular' with the use of smaller footprint connectors than commonly used connectors such as snap fasteners.

On the subject of stretchable electronics technologies, from reviewing the various methods – serpentine geometries, stretchable conductors and substrates, origami and kirigami patterns and helical geometry – helical geometry in particular appears to be under-explored. While there are several examples of helical interconnects, and a few cases of single components being made in helical form, fully helical circuits do not appear to have been demonstrated. That is, a thin strip of flexible circuitry, using small footprint SMD components (1 mm x 2 mm or smaller) could be wound into a helix and become stretchable.

Referring to Section 2.1, which fabrication methods should be used to investigate a) making 'more modular' e-textile systems, and b) helical circuits? One of the conclusions of that section was that printed and flexible electronics processes should be used, with stitched conductive tracks being used only as interconnects between flexible modules. In practical terms, the readily available printed and flexible electronics fabrication processes for this project were:

- Screen printing, using a TWS SR2700 semi-automatic screen printer.
- Dispenser printing, using a Voltera V-One dispenser printer.
- Etching copper-plated flexible plastic films, using a sodium persulphate bubble etch tank, and several different tools and materials to make etch masks.

Screen printing can be ruled out at this point. Though it is a well-established manufacturing method, with good repeatability and reliability, it has one major disadvantage for this work. To investigate modular and helical electronics, it is important to be able to easily alter the design of printed and flexible circuit modules. For example, after fabricating a prototype, it may become apparent that its design needs to be changed. This might mean making it longer, shorter, adding or removing components, or changing the layout of components, or the width of traces. In screen printing, once a screen is manufactured to print a specific

design, it cannot be changed. This means that if the design turns out to be flawed, the screen is now redundant.

In dispenser printing, changing the design is as simple as uploading the new design to the printer software. Conductive inks used in screen printing can also be used in dispenser printing, so a design prototyped using dispenser printing could be scaled up and manufactured using screen printing, using the same materials. Etching processes can also facilitate simple design changes, by altering the etch mask that protects the parts of the copper that are required for the circuit. As described in Section 2.1, etch masks can be printed directly onto the copper, or printed on PET film using an inkjet printer, neither of which is time-consuming or costly.

Both dispenser printing and etching processes were therefore selected for further evaluation.

Chapter 3   Materials and Methods

This is a thesis heavily focused on fabrication. All of the e-textile devices presented in it were made and tested by the author, rather than designed and or manufactured elsewhere. As a consequence, there is some overlap between methods and results. In some cases, the distinction is clear: an existing fabrication technique is used to create a prototype of a novel device, and that device is the result. But in other cases, existing techniques were adapted in the process of making prototypes, and the fabrication techniques themselves become results. To keep things clear, this chapter gives an overview of all fabrication and test methods used – as they were many and varied – explaining what they are and why they were chosen.

In many cases, methods and materials were changed or enhanced over the course of the project, and this progression is documented in this chapter. For example, the method used to cut flexible circuit modules out of a larger sheet of material evolved from simple and approximate (using scissors or craft knife) to precise (using a vinyl cutter). This was motivated by a need to cut more precise, complex outlines as the work progressed. Where there were novel adaptations to techniques, or in-depth evaluations that constitute experimental results, these are discussed in brief, but proper discussion and evaluation of them is left to later chapters.

In terms of overall methodology, there were a few options which were considered at the start of the project, in consultation with Kymira. These included:

1. Simulate, then fabricate: Simulation of circuit designs using software such as Ansys or COMSOL, to evaluate the mechanical stresses on various parts of a circuit when subjected to bending or stretching, and only fabricating the circuit after optimising the design.

2. Outsource manufacturing: This would mean coming up with general circuit designs and then sending them to Kymira to turn into a manufacturable design, and then sending the design to a flexible PCB manufacturer for fabrication.

3. In-house prototyping: Designing and fabricating all prototypes at Nottingham Trent University using available lab equipment, for rapid production and iteration of designs, and the ability to produce new prototypes outside the normal specifications of a PCB manufacturer.

Simulation is a valuable tool, but it was agreed that making and testing several iterations of prototypes would be equally as efficient, and more closely aligned with the experience and background of the writer of this thesis. And although outsourcing fabrication to a manufacturer could also have been an effective way to run the project, this was not chosen for the following reason: when designing new devices, errors often occur, and these often don't become apparent until after the device has been made. If fabrication is done in house, a small number of samples can be made, errors quickly spotted, and the design updated, with fewer delays and expenditure than if it is outsourced to a manufacturer. Most of the work covered in this thesis is about producing prototypes of new configurations of flexible and stretchable electronics and proving their viability. If, in future, these move forward to more extensive testing, or to production, then establishing a manufacturing process with an external company will be explored at that point.

3.1   Fabricating flexible and printed electronics

The following sections outline printed and flexible electronics fabrication methods which were used during the project. The processes follow the same general format:

1.   Design of the circuit schematic and layout.
2.   Creation of conductive tracks on a flexible substrate to form circuit traces.
3.   Attachment of components, usually by soldering.
4.   Encapsulation of components and conductive tracks, i.e., coating them with dielectric materials for mechanical support and electrical insulation.

In many cases, the process also involved cutting out the outlines of the circuit. This was performed at different stages in the process, as will be explained in later sections.

3.1.1   Circuit Design

The two main tools used for circuit design were: a) Autodesk Eagle, a PCB design software, and b) Adobe Illustrator, which is a versatile tool for 2D drawing. Circuit schematics and layouts were mainly created in Eagle, but outlines (i.e. the shape of an individual circuit module), and details such as stitching holes, were created in Illustrator. As has been highlighted by Tools We Want, a collaborative project by e-textile researchers and designers Irene Posch, Ebru Kurbak, Hannah-Perner Wilson and Mika Satomi, a tool combining the capabilities of these two software packages would be very useful for e-textile design [190].
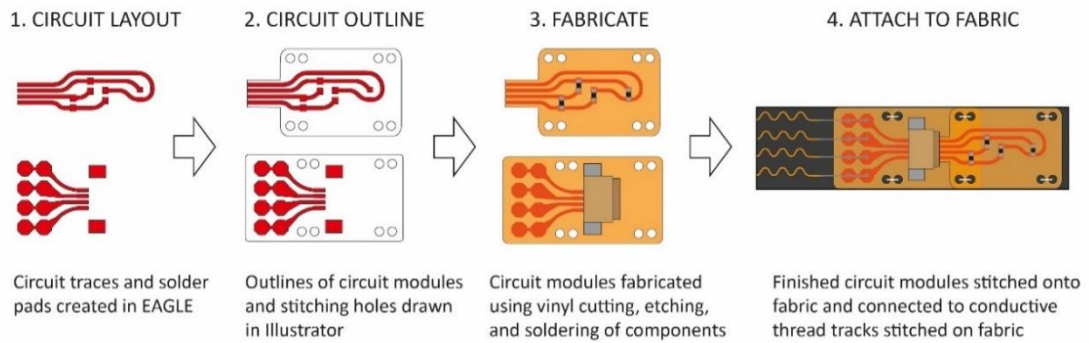
Figure 3-1. Overview of the circuit design process used in this project.

1) Circuit schematic and layout created in Autodesk EAGLE; 2) Design is imported into Adobe Illustrator to create outlines and stitching holes for the circuit module; 3) circuit modules are fabricated on copper-plated polyimide film; 4) circuit modules are attached to fabric and joined to conductive thread interconnects..

An example of the process is shown in Figure 3-1, using the example of temperature sensor and interposer circuit modules which will be covered in Chapter 5. Illustrator was also used to design solder paste stencils, coverlay (flexible encapsulation for conductive tracks in flexible electronics), photolithography masks, and any other part that needed to be cut using a vinyl cutter, a machine which served many purposes in this project. In some cases, Illustrator was also used to modify or create very simple circuit layouts instead of using Eagle.

3.1.2 Methods to create conductive tracks

To create conductive tracks on polymer films or on textiles, two methods were used: a) dispenser printing conductive inks, and b) etching copper-plated PI film. As mentioned in the previous two chapters, printed and flexible electronics fabrication methods were chosen because they can be scaled up using established manufacturing processes. And as set out at the end of the previous chapter, screen printing was also evaluated, but ultimately not used because it is less suited to rapid iteration of designs than dispenser printing or etching processes.

3.1.2.1 Dispenser printing

A Voltera V-One dispenser printer was used in this work. The printer is shown in Figure 3-2, along with the relevant parts and materials involved in printing on flexible substrates. This is a commercially available dispenser printer, controlled by a companion computer application. Voltera supply their own inks, but as they are based in Canada and this work was carried out in the United Kingdom, it was more convenient to use inks from UK suppliers. Flexible silver conductive ink from Engineered Conductive Materials (product no. CI-1036, total solids content 66%, viscosity 25,000 cps) was used. Empty nozzles, pistons and other printing

consumables were obtained from Intertronics Ltd, and cartridges to fit the V-One were obtained from Nordson Ltd. These are shown in Figure 3-2C and D. The process of calibrating the V-One for new inks is covered in the next chapter.

Figure 3-2. Dispenser printing.

A) illustration of the process. A cartridge of conductive ink is moved around an x-y plane, dispensing conductive ink in a defined pattern; B) the Voltera V-One printer used in this work, printing conductive tracks to create a flexible circuit; C) Parts: the cartridge is filled with silver ink, and then a piston is inserted to seal the ink inside. The tip cap and end cap are placed on the cartridge when not in use, to keep the ink fresh and prevent spills; D) cartridge filled with ink, equipped with piston and nozzle before printing.

3.1.2.1.1 Ink preparation

Before printing, cartridges of ink needed to be prepared. This involved a) mixing the tub of ink by hand, using a spatula; b) pouring a small quantity of ink into a smaller container, and mixing in a Thinky ARE-250 speed mixer (a centrifugal mixing machine which ensures smooth consistency of ink and removes bubbles from the mixture); c) using a syringe to fill a cartridge with mixed ink. A nozzle can then be attached for printing (Figure 3-2D).

3.1.2.1.2 Printing process for flexible substrates

The general process for dispenser printing is set out below. This is adapted from Voltera's standard process for printing on rigid substrates, as documented on their website [191].

- A cartridge of ink was prepared as described in the previous section, or a prepared cartridge was removed from a refrigerator and left to rest for 30 minutes to come to room temperature.
- A piece of PI film was cut and prepared by wiping with isopropyl alcohol (IPA) to clean the surface of oils and dust.
- Spray adhesive (3M Adhesive Spray Mount, 3M LTD) was used to attach the substrate to a rigid backing material. The V-One comes with a kit including small FR4 boards (50 mm x 76 mm and 101 mm x 127 mm) which were used for this.
- The substrate was clamped on the V-One's print bed, and the print file was loaded using the V-One software.
- The substrate was probed so that the correct print height could be determined, and to detect any irregularities in the surface of the substrate that might cause issues. This process was performed by the V-One, using a probe attachment that moves around the substrate and measures the height at different points.
- A print nozzle was attached to the cartridge of ink, which was then attached to the V-One, and a calibration pattern was printed to test the print settings.
- Settings were adjusted if needed, such as the ink pressure and print height, until good printing quality was achieved. These settings are documented further in the next chapter.
- The full pattern was then printed.
- The print was heat cured using the V-One's heated bed at 140 °C for 20 minutes, in line with curing settings provided by the ink manufacturer.

3.1.2.2   Etching copper-plated PI

As outlined in Chapter 2, conductive tracks can be formed by etching metal-plated films, the most common of which is copper-plated PI. Several films with 18 μm copper thickness, and PI thicknesses of 25 μm, 50 μm and 75 μm were obtained from GTS Flexible LTD.

To etch circuit traces on copper-plated PI film, an etch mask must be applied to the copper to protect the parts that are needed for the circuit. Three different etch masks were used in this work. As detailed further in the next chapter, each of these has advantages and disadvantages, and is suitable for different applications and levels of production. The third method, using adhesive vinyl and a vinyl cutter to make the etch mask, was developed during this PhD project. Figure 3-3 illustrates the different methods by which a mask can be made, which were all used at different stages of this work. They are as follows:

1.   Toner transfer (Figure 3-3A): The mask was printed on a coated paper using a laser printer. The coating prevents the printer toner from sinking into the paper, so it remains on the surface. The paper was then laminated to copper-plated PI using an ordinary laminator, which transfers the toner from paper to copper. A 'green film' was then laminated on. This is a special film provided with the kit, which sticks to the toner and makes the mask more opaque.

2.   Dry film photolithography (Figure 3-3B): A photosensitive dry film was laminated to copper-plated PI. Separately, a negative UV mask was created by printing the inverse of the circuit pattern on a transparent film*. This was placed on top of the photosensitive film in a UV exposure box, allowing UV light to cross-link and harden exposed photosensitive film. A developing process then washed away unexposed film.

3.   Adhesive vinyl mask (Figure 3-3C): This is a method that was developed in the course of this work. Adhesive vinyl, a material commonly used to make signs and stickers, is applied to the copper-plated PI. A vinyl cutter then cuts out the circuit pattern, and tweezers are used to remove excess vinyl.

* This is the standard method to fabricate the UV mask, but it was discovered during this project that it can also be made by cutting heat transfer vinyl, a material used to make graphics on garments. This method is further discussed in the next chapter.
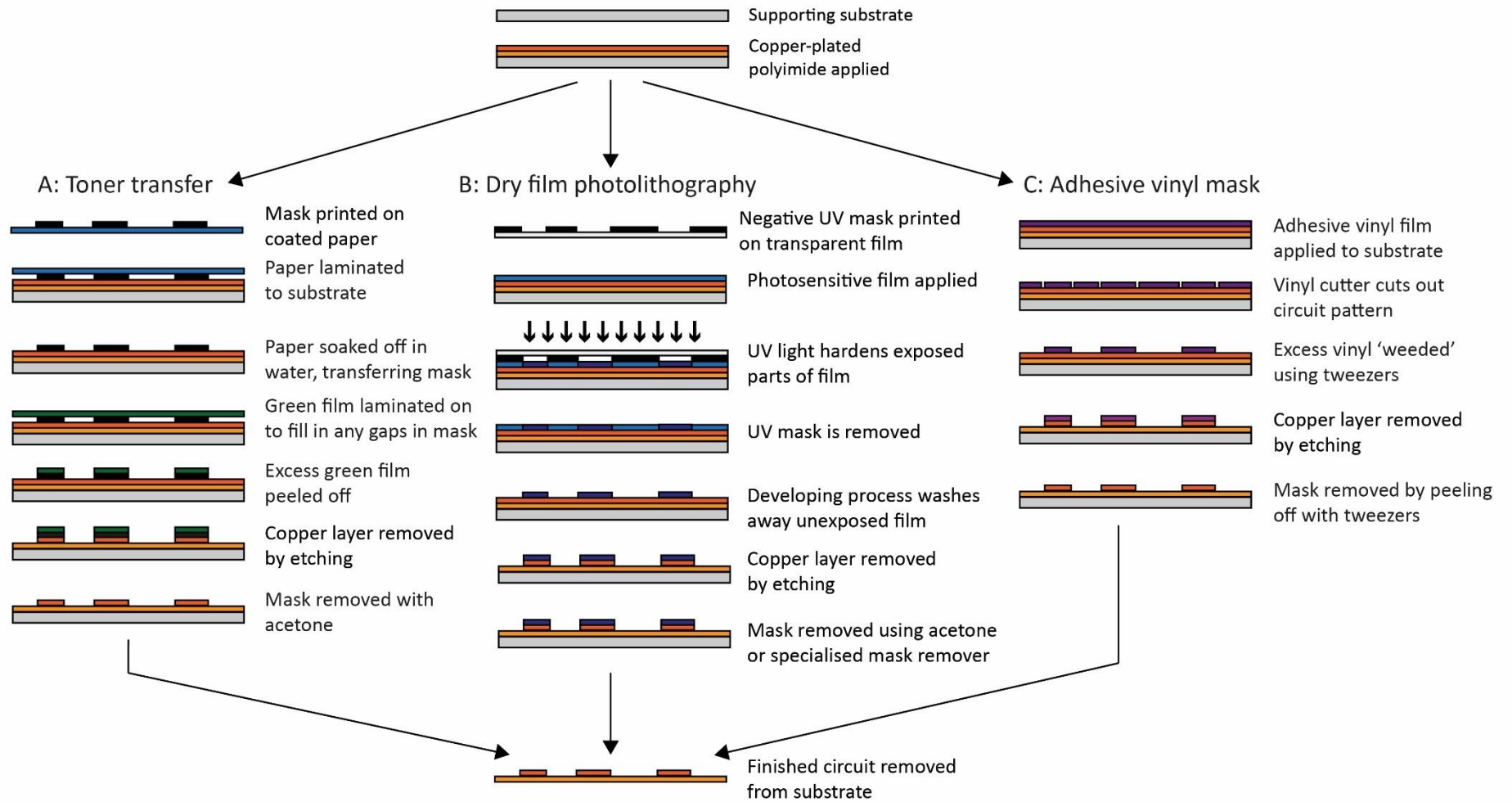
Figure 3-3. Different methods to create masks for etching copper-plated polymer films.

A) Toner transfer method prints the mask on a coated paper, which is later transferred to the flexible substrate; B) Dry film photolithography involves lamination of a photosensitive film to the substrate, and exposing specific areas to UV light to harden the film, creating the mask; C) Adhesive vinyl is applied to the substrate, then a vinyl cutter cuts out the circuit pattern, and excess vinyl is removed using tweezers. This method was developed as part of this project.

Two different etch tanks were used in this project. A Fortex bubble etch tank (Chapter 5 and part of Chapter 4) and a Mega Electronics PA210 bubble etch tank (Chapter 6 and part of Chapter 4). The Fortex tank was used in the first half of the project, but then developed a fault and was replaced by the Mega Electronics tank. In all cases, the etchant was made from 1 kg of fine sodium persulphate crystals (Fortex Engineering Ltd, Lincoln, UK) mixed with 5L of water and heated to approximately 45 °C by the etch tank.

3.1.2.3 Stitched conductive tracks

In Chapter 5, conductive threads were also used to create conductive tracks. This method was used only to create stretchable interconnects connecting flexible circuit modules to each other; components were not attached directly to conductive threads. A Brother Innovis sewing machine was used for this.

Machine stitching normally uses two threads: a top thread which is threaded through the needle, and a bottom (bobbin) thread on a small spool, located in a rotating case called a bobbin, underneath the needle. The fabric to be stitched is placed below the needle, but above the bobbin, and each time the needle pierces through the fabric, the bobbin rotates, and the top thread and bobbin thread interlace to form a stitch.

When sewing with conductive thread, using a regular (i.e. non-conductive) thread as the top thread, and the conductive thread as the bobbin thread, is usually the best course of action. This is because conductive threads are usually thicker and rougher than regular sewing thread [192,193]. And as the top thread takes a route with several twists and turns, passing through different parts of the sewing machine before arriving at the needle, most conductive threads are likely to break or become jammed when used as the top thread in a standard sewing machine.

The conductive thread used in this work was a solderable thread (insulated conductive thread, SewIY Ltd) which consists of fine enamelled copper wires braided with a Kevlar supporting thread. It was exclusively used as the bobbin thread, and the bobbin tension needed to be adjusted so that smooth, good quality stitches were achieved. The tension of both top and bobbin threads is generally adjustable in sewing machines, as different types and weights of thread, stitched onto different types of fabric, need to be held at different levels of tension to feed through the machine smoothly and produce good quality stitches.

3.1.3 Cutting circuit outlines, coverlay and stencils

Flexible circuit material was cut from large rolls of PI, or copper-plated PI. At the start of the project, circuit outlines were cut by hand using a scissors or craft knife, after circuit traces had been made by etching or printing. This is fine for simple, rectangular designs, but as more complex shapes needed to be realised, a precise method for cutting outlines was needed. Figure 3-4 illustrates the progression in circuit outline complexity during the project. Luckily, there is a machine that can perform this task easily: the vinyl cutter. This is a computer-controlled cutter designed for cutting thin films (vinyl) to make signs, and graphics for laminating onto garments, but it can cut many other types of film for other uses, and some can also cut rubber or textiles. Featuring a fine, swivelling blade, vinyl cutters can achieve fine resolution: the Roland GS-24 model used in this project was used to cut features as small as 100 μm.
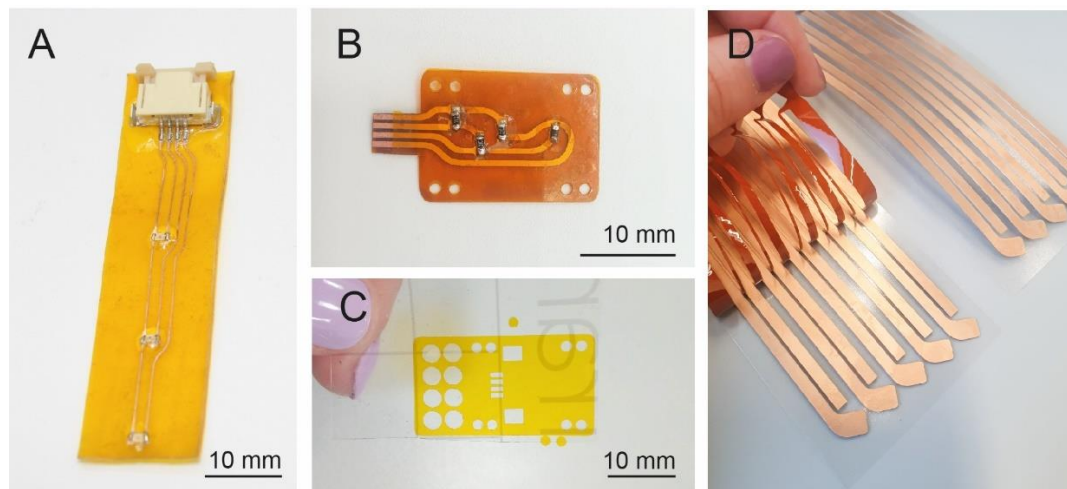
Figure 3-4. Examples of methods to cut circuit outlines.

A) An LED circuit on PI film, cut by hand using a craft knife; B) Temperature sensor module, with more complex shape and small cutout holes for stitching onto fabric, which would have been challenging to cut by hand/ C) coverlay film for another circuit module, cut from 250 μm thick PI, including features as fine as 1 mm pitch; D) copper-plated PI film outlines for helical e-strips in Chapter 6, whose ends need to be precisely angled.

Two approaches to cutting flexible circuit outlines with the vinyl cutter were evaluated: a) etching (or printing) first, then cutting, and b) cutting first, then creating the conductive tracks. As etching rather than printing was used for circuits needing precise outlines (as will be explained in the next chapter), the remainder of this section will describe the process for cutting outlines for etched circuits only. However, the same process applies to printed circuits, except that the material to be cut is PI film, rather than copper-plated PI film.

The Roland GS-24 (hereafter referred to as just 'the vinyl cutter') has an alignment feature that can align with existing features. This is designed for printable vinyl, where a design is printed on clear or white vinyl, and then its outline is cut out. This method works by including black circular crop marks at the edges of the design, which the machine scans for and detects using an optical sensor. It has a margin of error of 1 mm, which is acceptable for many applications, but for many of the devices fabricated in this work, this can cause issues with misalignment. For example, some of the flexible circuits produced in Chapter 6 were 1.5 – 3 mm wide, meaning that a 1 mm error in alignment causes significant errors.

The first approach to cutting after etching was to etch the crop marks, i.e. including them in the etch mask. However, the copper crop marks are quite close in colour to the PI film substrate, which made it impossible for the optical sensor to detect them. Colouring the crop marks in with a black marker made it possible for the vinyl cutter to detect them, but only partially improved the results (as seen in Figure 3-5A, B and C). Alternatively, the circuit pattern can be printed in black and white on paper, which is used to align the vinyl cutter. Then, spray adhesive can be used to attach the PI with printed or etched metal tracks on top for cutting out. As can be seen in Figure 3-5E and F, alignment errors of 1-2 mm remained.
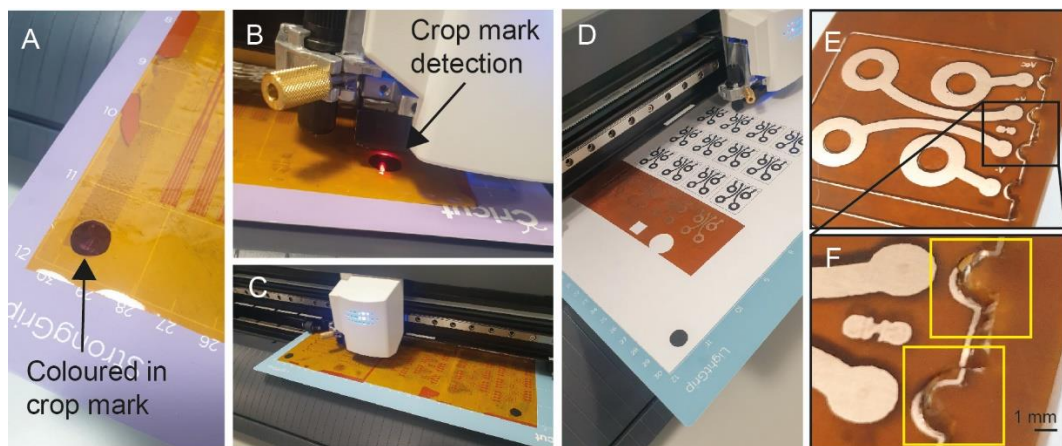
Figure 3-5. Creating conductive tracks, then cutting outlines using the vinyl cutter

A) Crop mark on PI, coloured in so that the vinyl cutter's optical sensor could detect it; B) Optical sensor detecting a crop mark; C) Cutting the outlines, showing multiple crop marks; D) Alternative method, printing the circuit patterns on paper and aligning the patterned PI on top to cut outlines; E) Close-up of previous image; F) Close-up showing cutting misalignment, highlighted by yellow boxes.

The other option is to cut the outlines first, then create the conductive tracks. After evaluating the different options, this was chosen as the preferred method. As it is usually more efficient to print or etch multiple circuits at once, a method is therefore needed to

keep all of the circuits aligned in a fixed pattern, e.g. for aligning a photolithography mask later on. Alignment becomes more critical during that stage of the process when the outlines are cut first.

To achieve this, the following process was developed, using transfer tape obtained from Grafityp LTD (UK). This is also shown in Figure 3-6. Transfer tape is a clear tape designed to keep disconnected parts of a vinyl design aligned when applying it to a surface: it sticks well to PI to keep it in place temporarily, but can also be peeled off easily. It was used as follows:

1. Transfer tape was applied to the PI, or to the non-conductive side of the copper-plated PI (double-sided copper-plated PI is available but was not used in this work).
2. The circuit outlines were cut on the vinyl cutter. The force that the knife applies to the cutting material is adjustable, so it can be adjusted to cut only through the PI material, not the transfer tape.
3. Excess material was weeded (removed), leaving the circuit outlines adhered to the transfer tape.
4. Circuit traces were etched or printed, and components were attached to the circuit.
5. Each individual circuit was then able to be gently peeled off the transfer tape. Acetone can be used to dissolve the adhesive if needed.
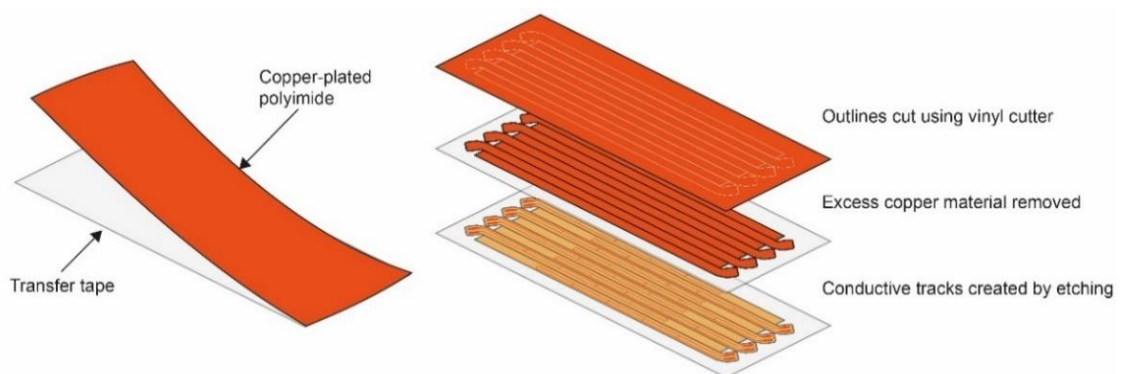
Figure 3-6. Cutting flexible circuit outlines before etching.

Copper-plated PI is applied to clear transfer tape (left), and then the outlines are cut using the vinyl cutter, excess material removed, and conductive tracks etched (right).

3.1.4 Encapsulation

Electronic components and conductive traces in circuits need to be encapsulated, i.e. covered with a dielectric material. This serves two purposes: a) protecting the circuit from damage, and b) providing electrical insulation to prevent accidental short circuiting. This is particularly important for e-textiles, where uninsulated flexible circuitry may accidentally short circuit when the fabric folds, or from moisture when the user sweats.

Several different encapsulation materials and methods were used during the project. These can be split into two categories:

1. glob top encapsulation, which is dispensed onto components to form a protective dome around them.
2. Encapsulation of conductive traces, which was done by applying a thin layer of adhesive, or a thin PI film (coverlay film).

For glob-top encapsulation, the following materials, shown in Figure 3-7, were used:

- Plasti-dip: this is a non-toxic, clear rubber material that cures with exposure to air. It was dispensed onto components using a syringe. It was used for early prototypes and in Chapter 5, but the results were irregular in shape. This is not desirable.

- UV curable medical adhesives from Dymax Ltd: As a more professional alternative to Plasti-dip, flexible medical adhesives were used. These were selected in consultation with Intertronics LTD, who specialise in adhesives for the electronics industry. The adhesives are certified safe for medical use and produced a cleaner, more reproducible result. As well as being curable by UV light, they have a secondary heat curing mechanism designed to cure parts that might be blocked from light.

In both cases, glob top encapsulation was applied with a syringe.
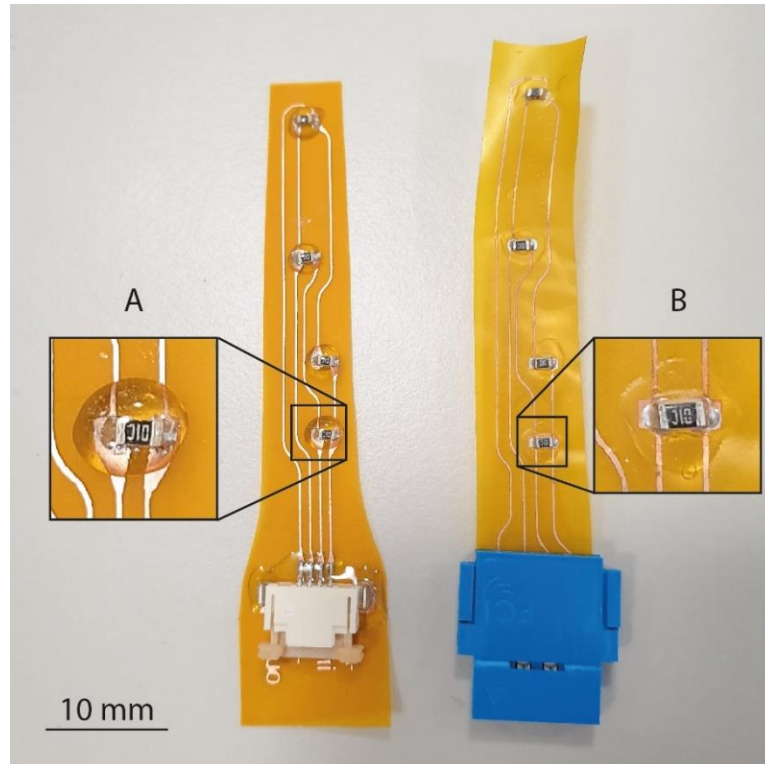
Figure 3-7. Glob top encapsulation of printed and etched flexible circuits.

A) Dymax medical adhesive applied on a resistor on a printed temperature sensor on PI film. The adhesive creates a smooth dome over the component; B) Plasti-Dip encapsulation applied onto the same type of resistor, on an etched temperature sensor on PI film. The Plasti-Dip has cured in an irregular shape, and doesn't maintain a proper 'glob' shape, which should be more domed.

To encapsulate conductive copper or silver tracks, the following methods were used:

- Spray Plasti-dip: an aerosol version of the Plasti-Dip used for glob-top encapsulation, this was sprayed onto conductive tracks.

- Dymax medical adhesive, painted on with a small brush to create a thin layer of encapsulation and UV cured. This was the most used method during this project.

- Coverlay film cut from PI, adhered with Dymax medical adhesive: This was messy, with adhesive spilling out. It also needed to be heat cured, as PI blocks UV light, making UV curing slow and inefficient.

- PI coverlay film, applied with 3M FPC double sided tape: This created an even coverlay, and creates a professional finish, but it can be difficult to achieve an even finish with no air bubbles under the film.

A UV curable dielectric ink was used to encapsulate soldered connections between pin headers and conductive thread in Chapter 5, and is covered in more detail in that chapter.

3.1.5 Attaching components to conductive tracks

Soldering was the main method used to attach components to conductive tracks. Soldering techniques used included:

- Dispensing solder paste using a syringe.
- Dispensing solder paste using the Voltera V-One dispenser printer.
- Stencilling solder paste using vinyl cut PI stencils. Depicted in Figure 3-8, the vinyl cutter was able to cut stencils for components with 1 mm and 0.3 mm pitch.
- Hand soldering using a soldering iron.

Solder paste is a shear thinning fluid, meaning that its viscosity decreases when pressure is applied to it. This means that it can be easily dispensed from a syringe, or squeezed through a stencil, but firms up again after the pressure is removed.

Flexible circuits were adhered to FR4 boards or alumina plates with spray adhesive or PI tape, and heated on a hotplate to solder. For 0603 and larger package components, Type 3 (T3) solder paste was used. For smaller components, T5 solder paste was used. Solder paste consists of solder powder suspended in a liquid flux medium, and the number (3, 4 or 5) refers to the size of the powder particles. Higher numbers correspond to smaller particles. This is shown in Figure 3-8A.

A Fritsch LM 901 manual pick and place machine (Figure 3-8D) was used to place SMD components before soldering, although some components were placed by hand using fine tweezers. The pick and place machine has a vacuum nozzle that allows components to be picked up from their packaging, and then placed on the relevant solder pads. A microscope is fixed next to the nozzle, recording video shown on a monitor, to aid with placement.

Only lead-free solder paste was used. This was for general health and safety reasons, as well as the fact that e-textiles are designed to be in contact with the body, so shouldn't contain lead. In some cases, soldering was performed by hand using a soldering iron instead of using solder paste, particularly when using solderable conductive thread in Chapter 5. Dispensing solder paste using the Voltera V-One was found to be more time consuming than stencilling or applying solder with a syringe, so this was not much used.
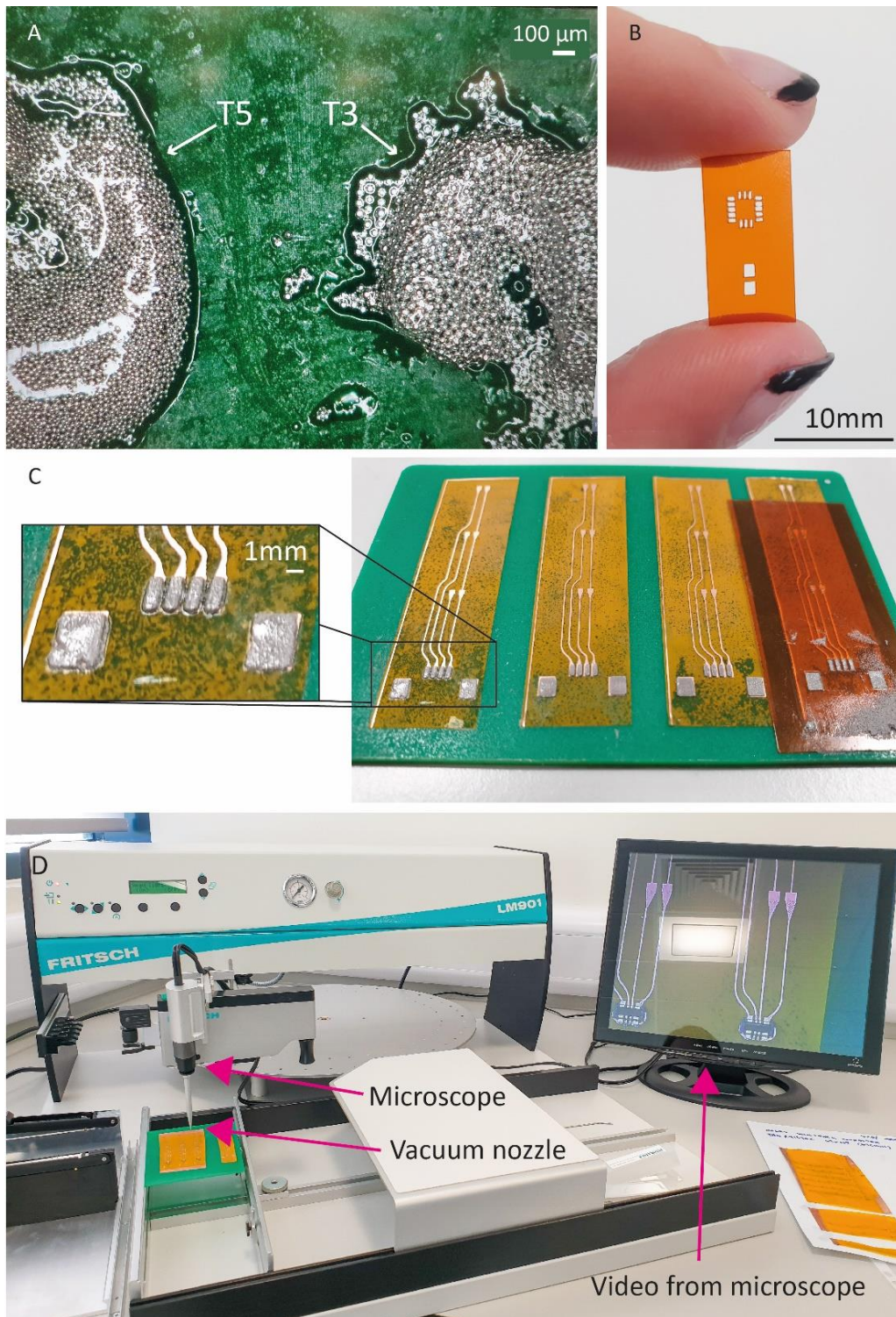
Figure 3-8. Soldering processes, equipment, and materials.

A) Microscope image of T3 and T5 solder paste, showing different sizes of solder balls suspended in the paste. T5, with smaller balls, is more suitable for soldering fine pitch 0402 and 0201 components than T3; B) Solder paste stencil cut from 75 µm thick PI film using the vinyl cutter; C) Solder paste applied to flexible LED circuits using a PI stencil, with inset section showing paste deposited on the solder pads after the stencil is removed; D) Pick and place machine used to place components onto solder pads before soldering.

3.2 Test methods

Several different tests were used in the evaluation of the fabricated e-textile prototypes, to assess their function, as well as their durability.

3.2.1 Mechanical testing

The work presented in this thesis is intended for use in real e-textile garments, and primarily for sports and medical garments, where durability is a core requirement. Therefore, prototypes were subjected to a range of mechanical tests, specifically:

- Tensile tests
- Bending tests
- Twisting tests

All test procedures were based on IPC-9204 Guideline on Flexibility and Stretchability Testing for Printed Electronics [194], as specific standards for e-textile testing are still in development. This standard describes tests for printed electronics on printed and stretchable substrates, including for wearable applications, which makes it a suitable choice for testing stretchable e-textiles. As can be seen in Table 2-4, the tests used to assess stretchable electronics vary significantly, but mostly fall into two categories: strain until failure, and cyclic tensile strain tests. Both of these tests are included in IPC-9204.

Tensile and bending tests in Chapter 5 were performed with a Shimadzu AG-X universal testing machine, with a 1 kN load cell. This had standard metal serrated grips which could grip fabric well, but were not able to hold flexible circuits without causing damage. To address this, laser cut tensile test clamps, and 3D printed fixed plate bending test clamps were fabricated, as shown in Figure 3-9. Later on, a Mecmesin MultiTest-2.5dV, with a 100 N force gauge, was acquired, and this was used for most of the work in Chapter 6. This was used with rubber-coated grips for tensile tests, which are designed for clamping fabric samples.

Two types of test were carried out:

- Stretching or bending until breaking point, to determine the absolute flexibility or stiffness (stretchability) of a prototype.
- Cyclic strain and bending for 1000-3000 cycles, at lower than maximum extension or bending, to mimic the routine bending and stretching e-textile parts would undergo

in a garment. The number of cycles is not set by IPC-9204, but is based on similar work such as that performed by Wicaksono et al [40,].
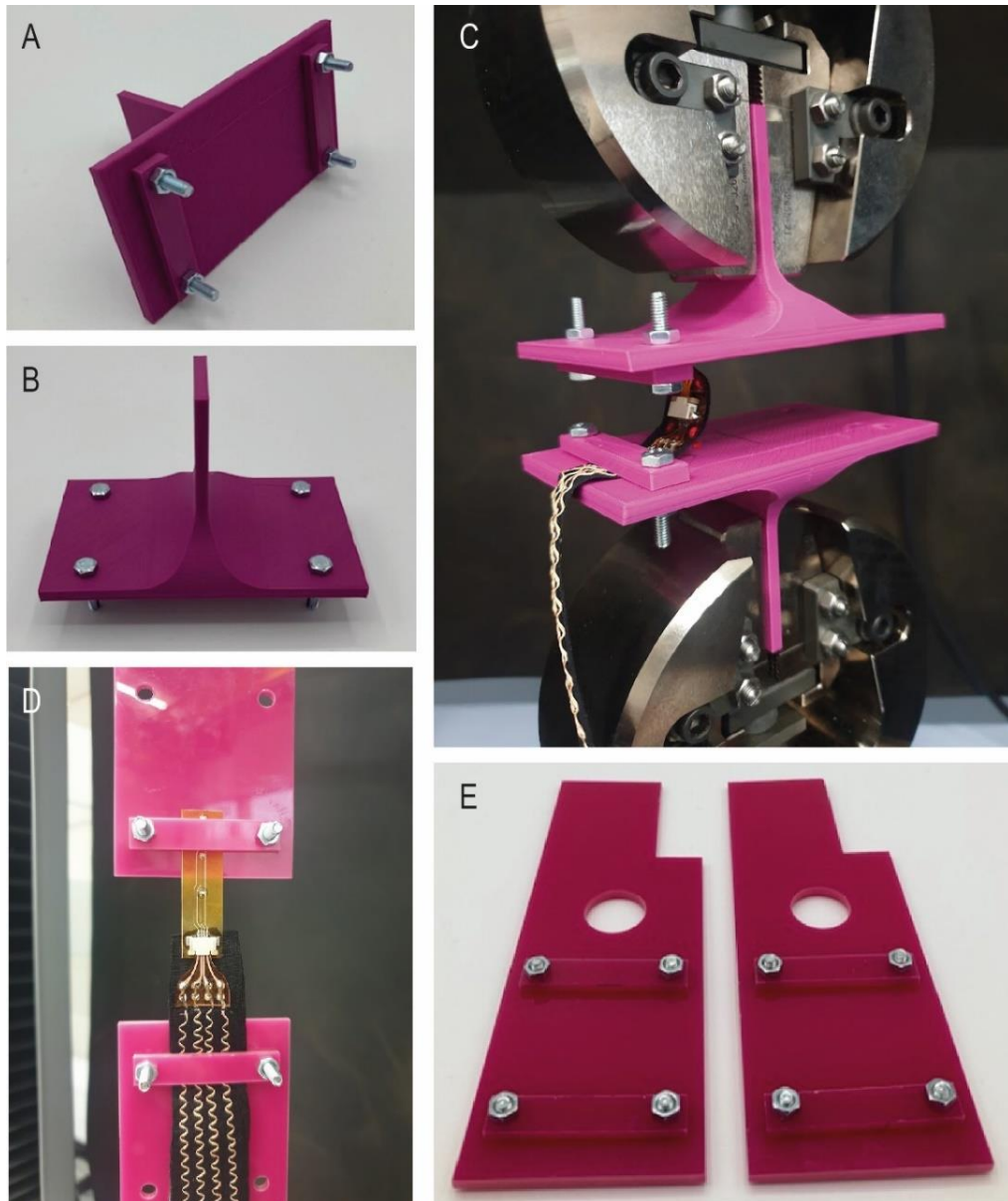
Figure 3-9. Custom clamps for mechanical testing.

A)-B) 3D printed fixed plate bending test clamps; C) Fixed plate bending test clamps in use to test a flexible sensor from Chapter 5. This test is carried out under compression and is designed to change the bending radius; D) laser cut tensile testing clamps clamping a flexible LED strip and stretchable fabric interconnect during a tensile test; E) tensile testing clamps, which have circular cutouts to tidy wires and cables attached to samples under test, and cutout pieces at the top to fit in the jaws of the Shimadzu AG-X metal tensile testing clamps. Images A, B and E were taken by Jasmyn Cliff-Patel.

There is, at the moment, no standard for how many cycles should be performed. 1000-3000 cycles are often reported in the literature, though this should be considered a preliminary evaluation, as e-textile parts can be expected to potentially undergo tens of thousands of cycles, or more even, in a real garment. Thus the mechanical test results presented in this work should be considered preliminary data on durability, with further work required to get a full picture of how well the technology will last in a garment.

A custom twisting jig was fabricated for twisting tests, as shown in Figure 3-10. This consists of two aluminium clamps attached to an aluminium rail, where the distance between clamps is adjustable. One clamp is attached to a stepper motor, which is powered by an Arduino Uno microcontroller. An Arduino sketch controls the maximum twisting angle, rotation speed, and the number of cycles to be performed in a test. The position of the rotating clamp can also be manually adjusted, using physical switches to manually rotate the clamp clockwise or counter-clockwise.

This is a simple device and does not measure torque experienced by a sample during testing, but is useful for carrying out cyclic tests to assess a prototype's ability to withstand repeated twisting.
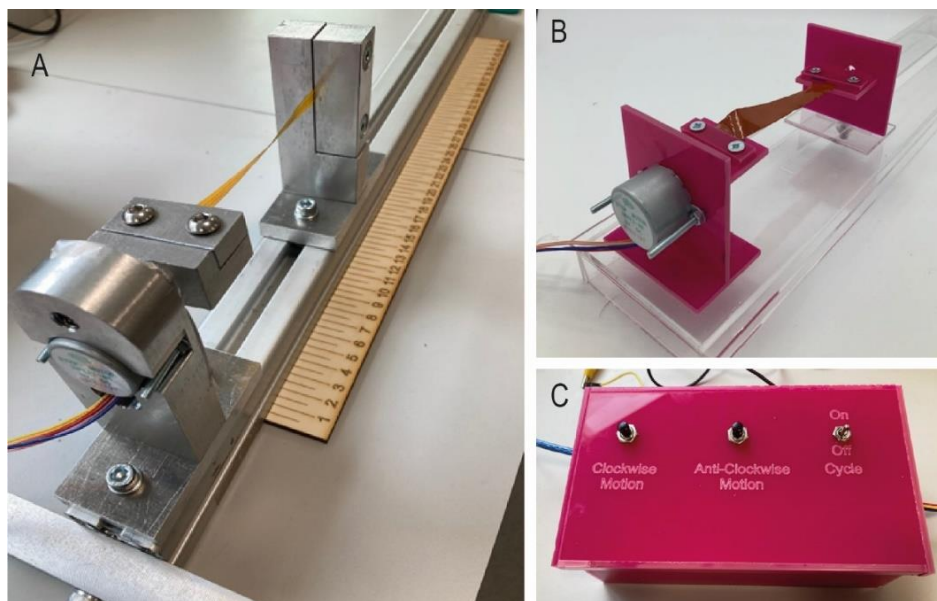
Figure 3-10. Custom twisting jig.

A) The finished twisting jig, featuring aluminium clamps, one of which is rotated by a stepper motor; B) First prototype of the twisting jig, using laser cut acrylic; C) Control unit, which houses an Arduino, and has manual switches to rotate the clamp clockwise or anti-clockwise for calibration, and to start or stop a cyclic test. Images by Jasmyn Cliff-Patel.

3.2.2 Wash testing

Technology for e-textiles needs to be washable, and preferably washable by machine rather than by hand, for user convenience. ISO 6330 standard for domestic washing and drying of textiles was used as a guide for wash tests [195]. As there is not yet a separate wash testing standard for e-textiles, most e-textile research uses some variation of this standard [196].

A makeweight or load ballast was made by assembling 2.2 kg of pieces of polycotton fabric, in accordance with the aforementioned standard. This is intended to simulate a real wash cycle with a full load of washing, instead of washing samples in an otherwise empty washing machine. Wash testing was only performed on helical e-strips covered in Chapter 6. Samples were washed 10 times in a domestic washing machine (Model i-DOS, Bosch GMBH), with a supermarket brand detergent. Samples were weighed before each wash cycle to confirm that they were fully dry, and were air dried in between washes. Samples were washed in a 40 °C, 1400 rpm cycle lasting 2 hours 33 minutes, to replicate a regular domestic wash cycle.

3.2.3 Resistance measurement

Resistance measurement is commonly used to determine the effect of a mechanical test on a sample. Or to check that fabrication has been successful. An increase in resistance during or after testing can indicate cracks in the conductive tracks, or tearing of the flexible / stretchable substrate.

2-wire resistance measurement, using both a handheld multimeter and a Keithley 2110 5 ½ bench multimeter, was used to check continuity, or identify short circuits, after etching, soldering, stitching conductive tracks etc. This was also used to measure the resistance of printed conductive patterns after printing and curing, to assess the quality of the printing. This included the identification of small gaps or cracks in prints, short circuits between layers of multi-layer prints, and unsuccessful curing, as evidenced by a higher than expected resistance measurement. The conductive inks used in this project consist of small silver flakes suspended in a solvent, which enables them to be printable. After printing, heat curing evaporates the solvent, and this increases the conductivity of the printed pattern. A high resistance value after curing indicates that not all of the solvent has been evaporated. As improperly cured ink is also liable to crack, this is also an indicator that the printed pattern will not be durable.

2-wire resistance is a useful technique for quick testing. But for higher accuracy, particularly for measuring resistances of < 100 Ω, 4-wire resistance is a better technique. Figure 3-11 illustrates the wiring configuration for both methods.
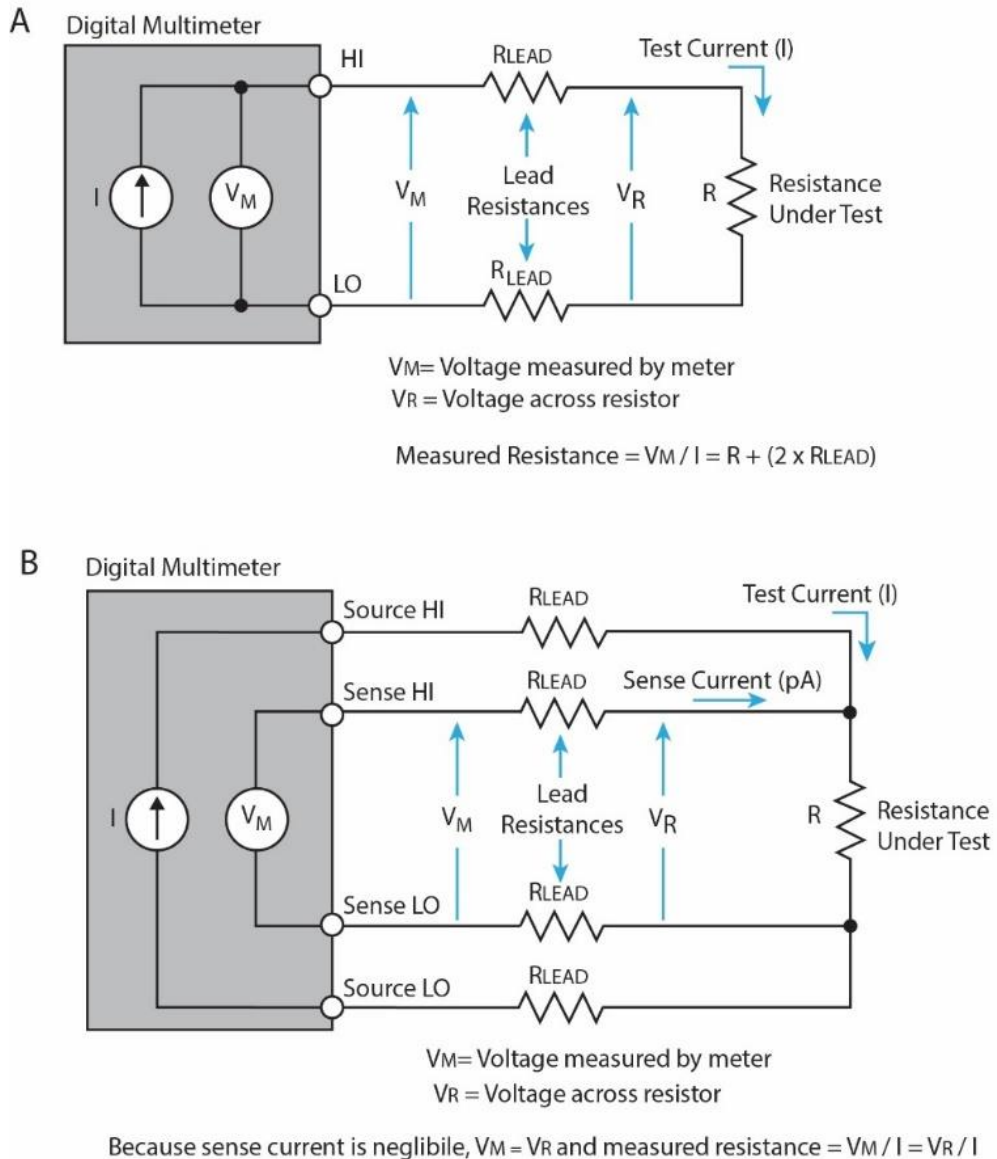
Figure 3-11. Schematics of electrical connections for resistance measurements
A) 2-wire resistance measurement, where one set of test leads supplies the current and measures the voltage across the resistance under test. Here, the resistance of the test leads themselves is included in the measured value of R, which is negligible if R >> R_{LEAD}, but can introduce significant error if R ≈ R_{LEAD}; B) 4-wire resistance measurement, with separate sets of test leads to supply current (source) and measure voltage (sense), resulting in a more accurate measurement. Both figures are re-drawn versions of schematics published by the electronic test equipment manufacturer Keithley Ltd. HI and LO points refer to source voltage and ground.

Resistance is measured by applying a small current between two points, and measuring the resulting voltage drop between those points. However, in a 2-wire measurement, the resistance measured will also include the resistance of the probes used to connect the multimeter (or other measuring device) to the sample under test. These usually have quite low resistance, but as the prototypes tested in this work typically have a resistance of < 1 Ω, including the resistance of the probes introduces error into the measurement. A 4-wire resistance measurement, by comparison, uses one set of probes to supply the current, and another set to measure the voltage drop. This removes the resistance of the probes themselves from the measurement, increasing the accuracy.

First, the previously mentioned bench multimeter was used to measure 4-wire resistance, using two sets of multimeter probes, or Kelvin probes, which are designed for 4-wire measurements. However, these have quite sharp tips, which makes them difficult to use with flexible circuit modules, as they can easily scratch and cause damage to the copper coating on flexible circuits. They also can't be clamped onto the sample and must be held in place. This is fine for one off or intermittent measurements, but continuous measurement is preferable for most mechanical tests. If a sample is being stretched until it breaks, for example, continuously monitoring resistance can provide information about how and when it begins to fail, by detecting increases in resistance. The same applies in cyclic tests.

A few alternative cables were researched to find a solution. To perform continuous measurements, there are two things to consider: a) suitable equipment to measure the resistance, and b) suitable connectors or clamps to connect the sample to the measurement equipment.

Most bench multimeters have companion software that allows resistance to be measured and logged continuously. However, they can usually only measure one sample at a time, and there are some situations where multiple measurements are desirable, for example if a sample has several conductive tracks and all of them need to be measured. An NI-9219 universal analogue input module was purchased to allow continuous 4-wire resistance measurement of up to four samples at a time, at a rate of 2 Hz.

In terms of connectors, a range of cables were purchased, with banana plugs to connect to multimeters. These are shown in Figure 3-12. Alligator clips were ruled out, as they didn't clamp well onto thin flexible circuits. They also tend to have serrated teeth, designed for

clamping onto wire, which is damaging to flexible circuits, but can work well with conductive textiles. Spring hook probes work well to connect to wires, but soldering wires to every sample that needs to be tested is time consuming. An interposer circuit, which is covered in Chapter 5, was designed for connecting flexible circuits to conductive threads, but also turned out to be useful to connect them to wires, to attach spring hook probes to, or to connect to screw or spring terminal connectors on DAQ (data acquisition) devices used to measure resistance or voltage. Using spring hook probes to clamp pins (for sewing) was useful for testing continuity in conductive threads. This has been previously documented by Afroditi Psarra, who used a similar method to test a textile antenna [197].

Helical e-strips covered in Chapters 6 were made with pin header connectors, which allowed them to be connected to a multimeter using banana plug to female pin header probes, or using female jumper cables and pieces of solid core wire to connect to spring terminal connectors on the NI 9219 analogue input DAQ module. Data from the DAQ was recorded in NI LabVIEW.
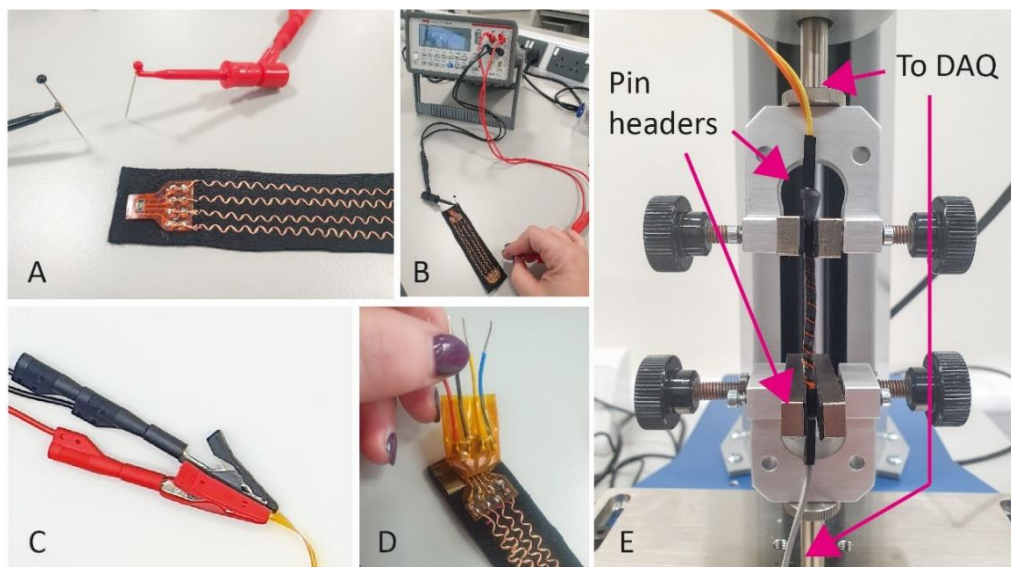
Figure 3-12. Connection methods for resistance measurement.
A) Spring hook probes used to clamp sewing pins to be inserted into conductive textiles; B) Testing continuity of conductive thread module using spring hook connectors and sewing pins; C) Alligator clip multimeter probes; D) Interposer circuit from Chapter 5 to allow spring hook connectors to be attached to wires; E) A helical e-strip from Chapter 6, equipped with male pin header connectors, connected to jumper cables with female pin header connectors, which are in turn connected to spring terminals on a DAQ device.

3.2.4 Microscopy

Visual analysis using a microscope is a useful tool to use in combination with resistance measurement, to characterise failures occurring during fabrication or testing. A Keyence VHX-7000 digital microscope was used to image samples during fabrication, or after failure during mechanical tests. Figure 3-13 shows two examples of this. Scanning electron microscopy was also evaluated, but was not found to be necessary for this work, as most failures could be identified using optical microscopy.
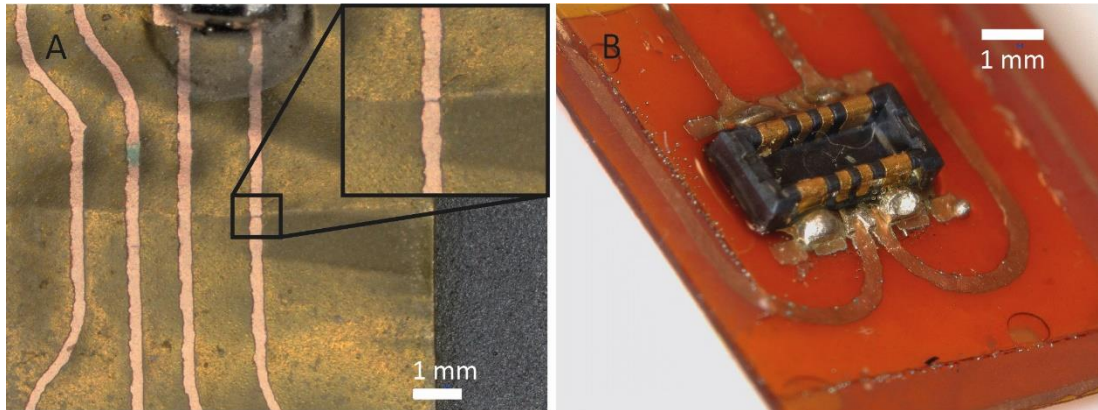
Figure 3-13. Microscope-aided failure analysis.

A) Flexible temperature sensor from Chapter 5, where a crack has formed in a copper track where a fold has been created in the sensor substrate; B) SMD connector on an interposer covered in Chapter 5, showing slight misalignment of the connector on the solder pads, and too much solder.

3.2.5 Sensor characterisation

Several variations on a Wheatstone bridge temperature sensor circuit were produced during this project. Characterisation of these sensors is covered more fully in later chapters, but in brief, temperature sensors were characterised by attaching them to a hotplate and varying the hotplate temperature across the range of normal human skin temperature. Sensor data was recorded using two models of NI USB DAQ – 6008 and 6210 – and NI LabVIEW, where data was plotted in real time and logged to a text file for later analysis. Sensors were also compared against commercial temperature sensors, as will be described in more detail in the methods sections of the chapters documenting this work.

Chapter 4   Evaluation and adaptation of flexible electronics fabrication methods

4.1 Introduction

The previous chapter summarised the fabrication and test methods used in this thesis. This chapter further explores how methods to create conductive tracks on flexible substrates were evaluated, and decisions made for which ones to use in later chapters. It also documents adaptations to these processes for easier prototyping. This is a key point: what works well in an industrial PCB fabrication facility may not suit a smaller research lab. Some of the techniques evaluated here are industry standards proven to work at scale. But for this project and others like it, rapid prototyping is important for quickly iterating and evaluating research prototypes. And this often requires a different approach.

The fabrication of flexible electronic modules involves several elements. To carry out the work documented in later chapters, it was necessary to identify a suitable method for creating conductive tracks on flexible substrates. As discussed in previous chapters, the methods selected from the available options were:

    a.   Dispenser printing
    b.   Etching copper-plated PI film

In previous chapters, it was established that the chosen method should facilitate easy changes to designs. The following criteria were also set:

1. Resolution: what is the minimum pitch (space between tracks) that each method can achieve? Chapter 5 uses small footprint connectors with 300 μm pitch, and Chapter 6 uses 0201 package SMD components requiring features of approximately 100 μm to be etched or printed.

2. Alignment: As discussed in the previous chapter, the ability to accurately align conductive tracks to the outline of the flexible module is critical for proper function.

3. Speed: how many steps does each process involve, and how long does it take to produce prototypes?

This chapter is structured as follows:

First, dispenser printing is evaluated. This included calibrating print settings on a Voltera V-One printer to print with inks other than Voltera's own brand. A printed temperature sensor is also demonstrated. There was also a small investigation into printing on textiles coated with heat transfer vinyl (an adhesive-backed polymer film used in the garment industry to make designs on garments). This was deemed to not be optimal for realising the objectives of this thesis, and is not included here.

The remainder of the chapter covers processes for etching copper-plated PI. This mainly involved evaluating, and developing, methods to make etch masks, which cover selected areas of copper to prevent them from being etched. Two methods were evaluated, one of which was adapted, and one new one was developed, using adhesive vinyl (PVC or PU film with an adhesive backing) and a vinyl cutter to create perfectly aligned etch masks. The chapter closes with a discussion of the various methods and why etching processes are used for the remainder of the thesis.

4.2   Dispenser printing

As explained in Chapter 2, Section 2.1.5.2, dispenser printing is a method for printing electronics by dispensing functional inks onto a substrate. Ink is dispensed out of a nozzle attached to an ink cartridge, which can be moved around the substrate to create the desired pattern. Though it is possible to print many different types of functional ink, this work focuses on printing silver conductive ink, to be used in combination with conventional (rigid SMD) components to make flexible circuits.

Dispenser printed patterns were printed using a Voltera V-One, and were cured using the V-One's heated bed, at 140 °C, for 20 minutes. This was based on the ink manufacturer's recommendation to cure for 15-20 minutes in an oven at 120 °C, plus Voltera's recommendation to increase curing time by 20 °C, accounting for less efficient heat transfer on a heated bed compared to an oven.

4.2.1   Materials and methods

4.2.1.1   *Optimisation of print parameters*
Initially, conductive ink supplied by Voltera (the dispenser printer manufacturer), was used. This ink (product name: 'Conductor') is not designed for use on flexible substrates, and is

susceptible to cracking under bending strain, which makes it unsuitable for e-textiles. While Voltera do have a flexible ink, they are based in Canada and did not have a UK distributor at the time this work was carried out. This meant it was more convenient to use inks obtainable from UK suppliers. Additionally, Voltera inks are sold in small quantities (typically 2 ml), whereas other inks can be purchased in larger, more cost-effective quantities.

To print with CI-1036 ink, it was necessary to calibrate the settings, to make sure that enough, but not too much, ink flows from nozzle to substrate. As there are many settings, rough tests were performed first to assess whether each variable had a noticeable impact on print quality. Settings which appeared to have a significant impact on print quality were varied systematically until the best possible print quality was achieved.

Test patterns (Figure 4-1) were developed to evaluate prints. These are:

- Printed straight lines (Figure 4-1A): These were designed to test print quality. The line widths are standard PCB trace widths. The imperial unit 'mil', being a thousandth of an inch, is shown in the figure as this is the default unit used in PCB design software, including Eagle.
- Printed lines of varying pitch: This assesses the minimum pitch achievable between printed tracks, i.e. how closely tracks can be spaced. Two sets of tracks, where the pitch (spacing between tracks) varies from 150 μm to 1.2 mm. One set has a track width of 800 μm (Figure 4-1B), the other 150 μm (Figure 4-1C). Serpentine lines are included, as curved traces are common in flexible and stretchable electronics.
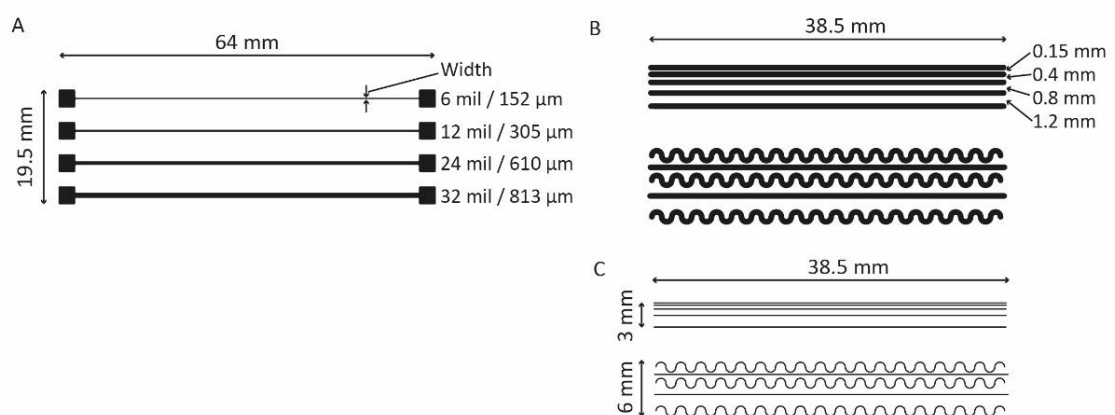
Figure 4-1. Test patterns used to compare printed and etched samples.
A) Straight tracks of varying width; B) 800 μm wide straight and serpentine tracks of varying pitch; C) 150 μm straight and serpentine tracks of varying pitch.

A key component of the dispenser printer is the nozzle through which the ink is dispensed. The V-One uses metal Preci-Tip nozzles and is shipped with black (internal diameter 234 µm) nozzles, which work well for Voltera's own brand inks. However, when printing with CI-1036 ink, there were issues with ink leaking, even after adjusting the print parameters. Several nozzles with smaller diameter were evaluated, to assess whether this could resolve the ink leaking issues. All nozzle details are given in Table 4-1 and pictured in Figure 4-2. This is especially critical for the V-One, as it relies entirely on mechanical pressure to dispense ink. Other printers use pneumatic systems, where vacuum pressure can be applied to hold ink inside the nozzle when it is not actively printing.

Table 4-1. Colours and diameters of nozzles evaluated for dispenser printing.

Nozzle colour	Internal diameter (µm)
Black	234
Blue	159
Orange	108
Yellow	57

Figure 4-2. Preci-Tip dispensing nozzles of different internal diameters evaluated to optimise print quality. The numbers refer to the internal diameter of the nozzle at its tip.

The straight track pattern (Figure 4-1A) was printed with the blue, orange, and yellow nozzles to identify the optimal one for printing CI-1036 ink.

4.2.1.2   Printed temperature sensor

A printed temperature sensor was made to test printing more complex patterns containing components. A Wheatstone bridge temperature sensing circuit was created using an NTC thermistor and three fixed value resistors. This sensor was designed for a project covered in detail in Chapter 5, so further details on its design and choice of components are left until Chapter 5, Section 5.2.4.2. It is included here just as a demonstration of a functional component produced by dispenser printing. Two temperature sensor designs were printed, with different track widths, using the same values as the print patterns in Figure 4-1B and C (800 μm and 150 μm).

After printing and curing, low temperature solder paste (Chip Quik SMD291AX50T3) was dispensed onto solder pads using a syringe, and components were placed and soldered using a pick and place machine and a hotplate (Chapter 3, Section 3.1.5).

4.2.1.3   Evaluation

Prints were assessed by measuring:

1. Continuity, with a digital multimeter. This was used to do an initial quality check on printed samples, as failure of continuity implies that the sample has a crack, a gap in a printed trace, or hasn't been properly cured (Chapter 3, Section 3.2.3).
2. Four wire resistance, measured with a digital multimeter (Chapter 3, Section 3.2.3), with lower resistance values being preferable.
3. General visual inspection, e.g., identification of drips of excess ink, short circuits, and gaps, both with the naked eye and with a digital microscope.

For comparison, the patterns were also created by etching copper-plated PI film, using the toner transfer method described in Chapter 3, Section 3.1.2.2 (as well as in later sections of this chapter).

Printed temperature sensors were also evaluated as described in Chapter 3, Section 3.2.5 by using them to measure the temperature of an Echotherm chilling heating dry bath, which is a calibrated hotplate with 0.2 °C accuracy. This was used to comparing the performance of the printed sensor against a sensor with etched copper tracks. Data was recorded using an NI-6210 USB DAQ and LabVIEW software.

4.2.2 Results

4.2.2.1 Optimisation of print parameters

Initial problems with dispenser printing CI-1036 ink are depicted in Figure 4-4. Excess ink leaked out of the nozzle (Figure 4-4A), and there were issues with too much ink flowing (Figure 4-4B), or inconsistent flow (Figure 4-4C), with alternation between too little flow, with gaps appearing in printed tracks, and excess drops of ink.

In terms of nozzle diameter, the yellow (57 μm) nozzle was ruled out, as several nozzles became clogged, and it is likely that this nozzle is too narrow for the silver particles in the ink to easily pass through. Of the three remaining nozzles, the orange (108 μm) nozzle produced neater prints with less drips and overflowing ink than the blue (159 μm) nozzle. Examples showing these results can be seen in Figure 4-3. The orange nozzle was selected for the remainder of the prints in this section.

| 159 μm nozzle | 108 μm nozzle | 57 μm nozzle |

Figure 4-3. Dispenser prints made using nozzles with different diameters.
108 μm nozzle produces the cleanest prints, the larger nozzle resulting in excess ink drips, and the smaller nozzle becoming clogged with ink.

Calibrated settings are listed in Table 4-2. Two important settings – nozzle height and ink pressure – are not listed. Varying the nozzle height, the distance between the end of the nozzle and the print substrate, was not found to improve print quality, and was left at its default value of 0.1 mm. The only exception to this is when the 57 μm (yellow) nozzle was used. This only produced good quality prints when the height was reduced to 0.8 mm.

Ink pressure is related to kick, which is listed in the table. The kick is the maximum pressure that is applied to the piston to dispense ink. That is, the displacement applied to the piston, compressing the ink in the cartridge and causing ink to flow from the nozzle. Conductive ink

is a shear thinning fluid, meaning that its viscosity decreases temporarily after pressure is applied. A 'kick' of pressure is applied to the piston at regular intervals, causing the ink to flow out of the nozzle. The value of the kick is set before printing starts, but the 'ink pressure' variable allows adjustments to this during printing, if the ink flow is too high or too low. It was found that ink pressure needed to be calibrated at the start of every printing session, and there was no fixed starting value that produced consistently good quality prints.
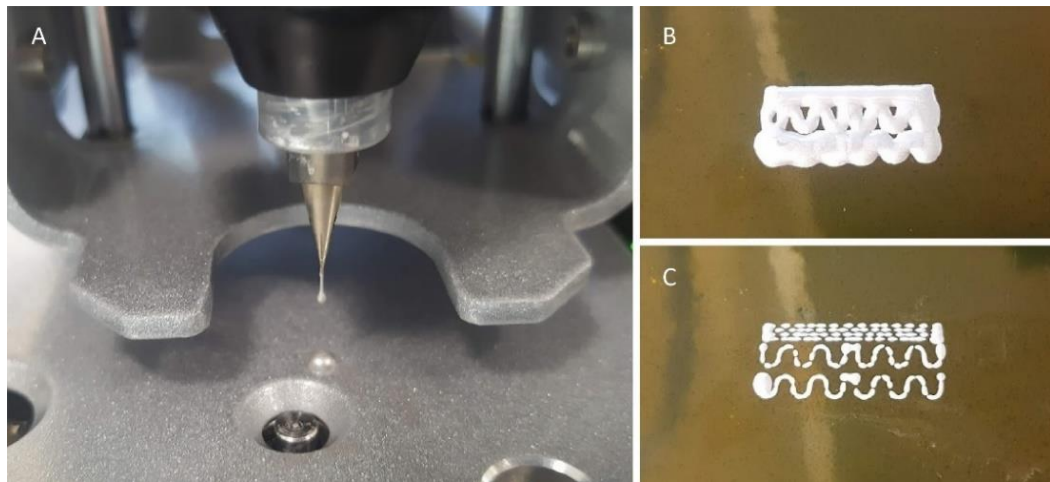
Figure 4-4. Dispenser printing issues.

A) Ink leaking; B) too much ink flow; C) Inconsistent ink flow with areas where there is too little ink flow, with gaps appearing, combined with excess drops of ink in some areas.

Table 4-2. Optimised print settings for CI-1036 silver conductive ink

Property	Initial value	Optimised value	Description
Feed rate	500 mm / min	300 mm / min	The speed at which the ink cartridge and nozzle are moved around the substrate
Trim length	50 mm	80*	The maximum distance travelled before more pressure is applied to the cartridge, i.e. before a 'kick' is applied'
Anti-stringing distance	0.1 mm	0.5 mm	At the end of a track, the print head doubles back before moving to the next point, which helps avoid strings of ink being created
Kick	0.35 mm	0.1 mm	The amount of pressure periodically applied to the piston to dispense more ink, i.e. the displacement applied to compress the ink in the cartridge and cause ink to flow from the nozzle.

* This value is dependent on the pattern being printed, and should be matched to the length of the longest track in the print pattern.

Another example of an improvement in print quality is shown in Figure 4-5, where the trim length is varied. Using the default trim length (Figure 4-5A), the printed tracks contain many drips of excess ink where the printer has paused to apply more pressure, and then continued, with a drip of ink leaking out each time pressure is applied. Increasing the trim length to match the length of the track greatly improves the quality of the print (Figure 4-5B), as the tracks are now printed in one continuous stroke. Some small irregularities remain, for example when the printer pauses before turning a corner (Figure 4-5C), but the quality is much improved. One consequence of increasing the trim length is that the ink pressure has to be increased to print long tracks, so that there is enough ink dispensed to print the track in one motion. But this means that the ink pressure is then too high when printing solder pads and similar features. However, there is an easy solution to this: the V-One allows specific parts of the print to be selected and printed, so it is possible to print different features, requiring different levels of ink pressure, separately.
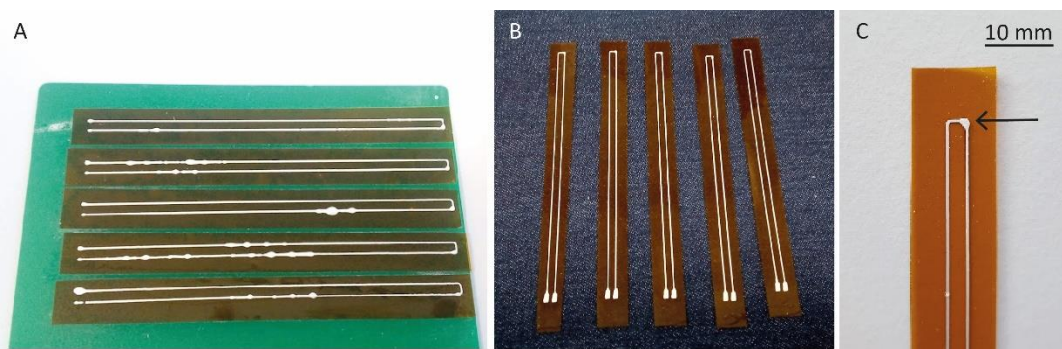
Figure 4-5. Improvement in print quality after increasing the trim length.

A) Print with a short trim length, with many drips of excess ink; B) Print with trim length increased to the length of the pattern, with much fewer drips; C) In the updated pattern, one drip (highlighted by the arrow) remains where the printer reaches the maximum trim length.

4.2.2.2 Minimum achievable pitch

In terms of spacing between tracks (Figure 4-6), dispenser printed patterns spaced 600 μm or 800 μm apart were successfully printed. At 300 μm spacing, narrower (150 μm wide tracks) were printed successfully, but one of the thicker (800 μm) patterns failed. And 150 μm spacing was not achievable with either width of printed track, and was only partially achievable with etching. It is thus recommended that dispenser printed narrow tracks can be spaced as closely as 300 μm apart, but thicker tracks and patterns should allow a clearance of at least 600 μm.
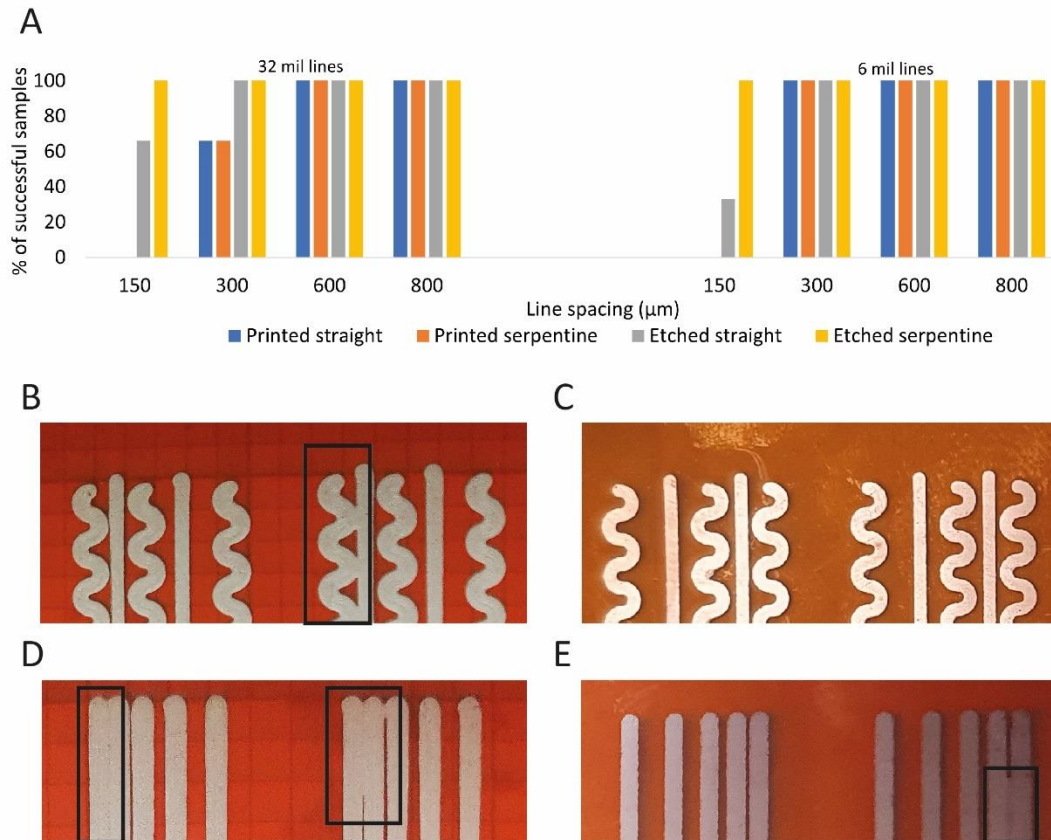
Figure 4-6. Minimum achievable pitch / track spacing with dispenser printing and etching.

A) Graph showing % of samples, printed and etched, of 150 μm and 800 μm track width, were achieved without short circuits; B) 32 mil printed straight and serpentine tracks, with unwanted short circuit highlighted; C) 800 μm etched straight and serpentine tracks, with no failures; D) 800 μm straight tracks, with significant short circuits highlighted; E) 800 μm etched straight tracks, with short circuit highlighted. Note that etched samples are mirrored with respect to printed samples but are otherwise identical.

4.2.2.3   Printed temperature sensor

Figure 4-7 shows images of two iterations of the printed temperature sensor. In the first design, a trace passed too close to a solder pad, and several samples suffered short circuits in this area (ink from the pad flowing over onto the trace). In the second design, adjustments were made to move these closely spaced features further away from each other, which resulted in significantly better print quality. This lines up with the results of the minimum pitch experiment: two narrow (150 μm) traces can be printed close together (approx. 300 μm spacing), but wider features such as solder pads need a larger clearance (at least 600 μm spacing) from other features.
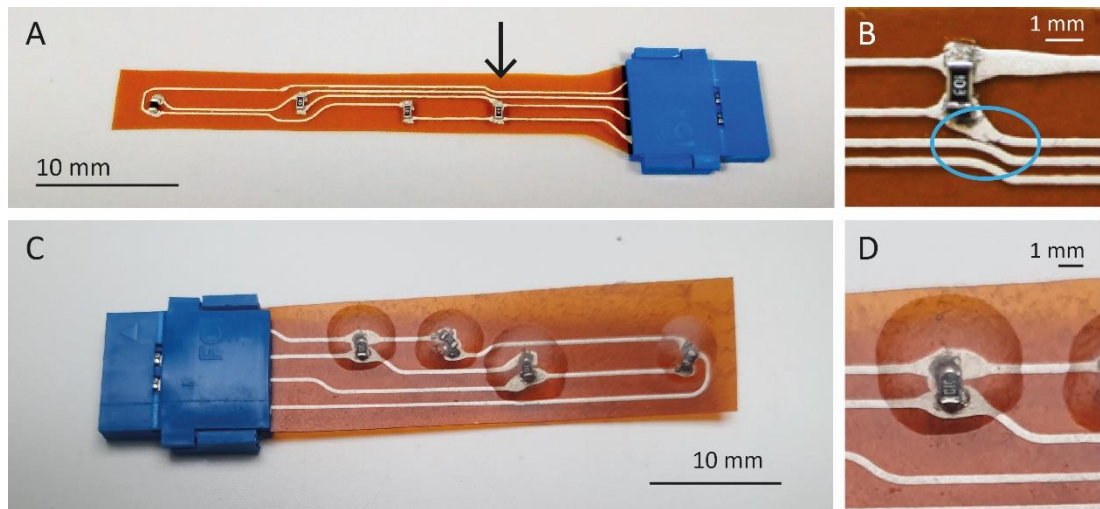
Figure 4-7. Dispenser printed temperature sensor.

A) Version 1 of the temperature sensor, with Amphenol FCI Clincher connector attached, highlighting problematic area; B) Close-up of problematic area, where ink has overflowed from solder pads and is in danger of short-circuiting; C) Updated design, with more space between pads and traces; D) Close-up showing more clearance between traces than previous design.

Resistance values of tracks on both printed and etched temperature sensors are depicted in Figure 4-8A. Resistance values of printed tracks are significantly higher, which is expected as silver conductive ink is inherently less conductive than a sheet of copper, even if the copper sheet is very thin.

However, Figure 4-8 clearly shows that the resistance variations do not have an impact on sensor function, i.e. on the temperature recorded by them. Both printed and etched sensors report very close temperature readings. As the temperature sensor is composed of three 10 kΩ resistors and one 10 kΩ NTC temperature sensor, which decreases 150-200 Ω per increase of 1 °C (in the human skin temperature range), small (<10 Ω) differences in the resistances of tracks on the temperature sensor will have a negligible effect on the sensor's function. It is important to note that this is raw, uncalibrated data from the temperature sensors, and accuracy could be further improved by calibration, comparing each sensor with a known temperature before testing them against each other. The hotplate temperature can vary across its surface by ± 0.3 °C and fluctuates slightly around its set temperature (as seen in Figure 4-8C).
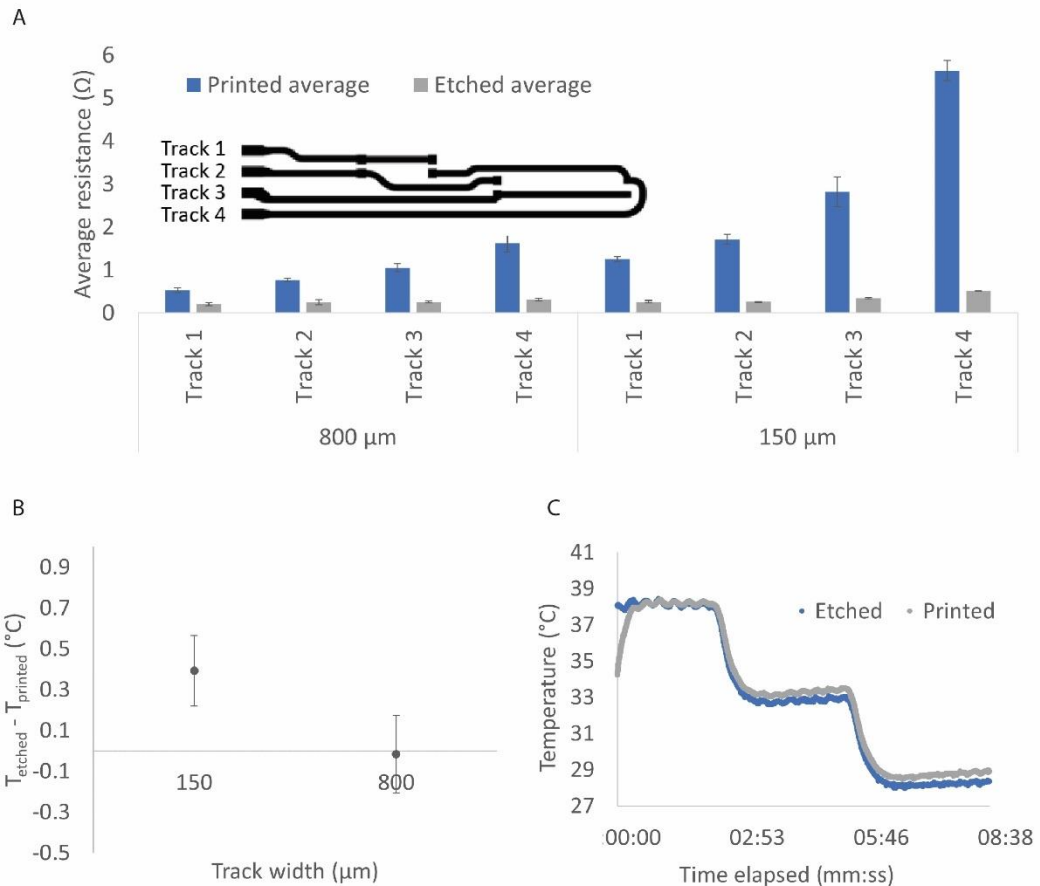
Figure 4-8. Printed and etched temperature sensor results.

A) Resistance of printed and etched temperature sensor tracks, with inset section showing sensor design with labelled tracks; B) Average difference between printed and etched sensors, for sensors of different track widths; C) Raw data from comparison of 150 µm width printed and etched sensors. The large difference in sensor response for the first 1 minute (approximately) is attributed to an experimental error where the sensor wasn't in contact with the hotplate surface for the first minute.

4.2.2.4 Recommended dispenser printing parameters for Cl-1036 and inks with similar rheology

Based on the above data, optimal printing of Cl-1036 and inks with similar viscosity can be optimised by:

- Using the print settings listed in Table 4-2.
- Ensuring a gap of at least 300 µm near solder pads and wide features when designing printing patterns.
- Printing solder pads, or similar features, separately to tracks, and using increased ink pressure to print tracks. The amount by which ink pressure needs to be adjusted will be varied, and should be calibrated at the start of the print session.

- Using a 108 µm nozzle instead of the standard 234 µm.
- Matching the trim length to the length of the longest trace in the design, to avoid excess ink drops appearing mid-track.

4.2.2.5 *Overall performance of dispenser printing*

At the start of the chapter, three criteria established: resolution, alignment, and speed. Dispenser printed samples were compared directly against etched samples to compare the minimum achievable pitch, and dispenser printing performed poorly for closely spaced (< 300 µm) tracks. As this level of resolution was required for a) small footprint connectors in Chapter 5, and narrow circuits with small components and closely spaced tracks in Chapter 6, this made etching copper-plated PI the preferred method. The next section documents the evaluation of several processes used to make masks for etching.

4.3 Evaluation of methods to create masks for etching

Chapter 3, Section 3.1.2 introduced three methods used to create masks to etch circuits from copper-plated PI, all using a bubble etch tank filled with a sodium persulphate solution as described in Section 3.1.2.2. The evaluation of several different methods was motivated by the need to produce increasingly narrow, fine pitch circuits as the project progressed. Initially, a toner transfer process was used, but this wasn't able to reliably produce features less than 0.5 mm in size of spacing. Then, a more professional dry film photolithography process was used. This produced better quality but required many more fabrication steps and a lot of fine tuning, making it difficult to achieve high quality fine pitch circuits. Alignment of mask to substrate was also an issue with both methods. Finally, a mask method suitable for prototyping was developed using adhesive vinyl and a vinyl cutter.

This section documents issues encountered with the first two methods, with evidence, and explains how this led to the development of the vinyl mask method.

4.3.1 Materials and methods

4.3.1.1 *Mask method 1: toner transfer*

This is a low-cost method aimed at hobbyist electronics makers. It uses kits manufactured by PCB Fab-in-a-box Ltd and is shown in Figure 4-9. It is designed for rigid and semi-flexible circuit boards, but was used here to make flexible circuit modules.
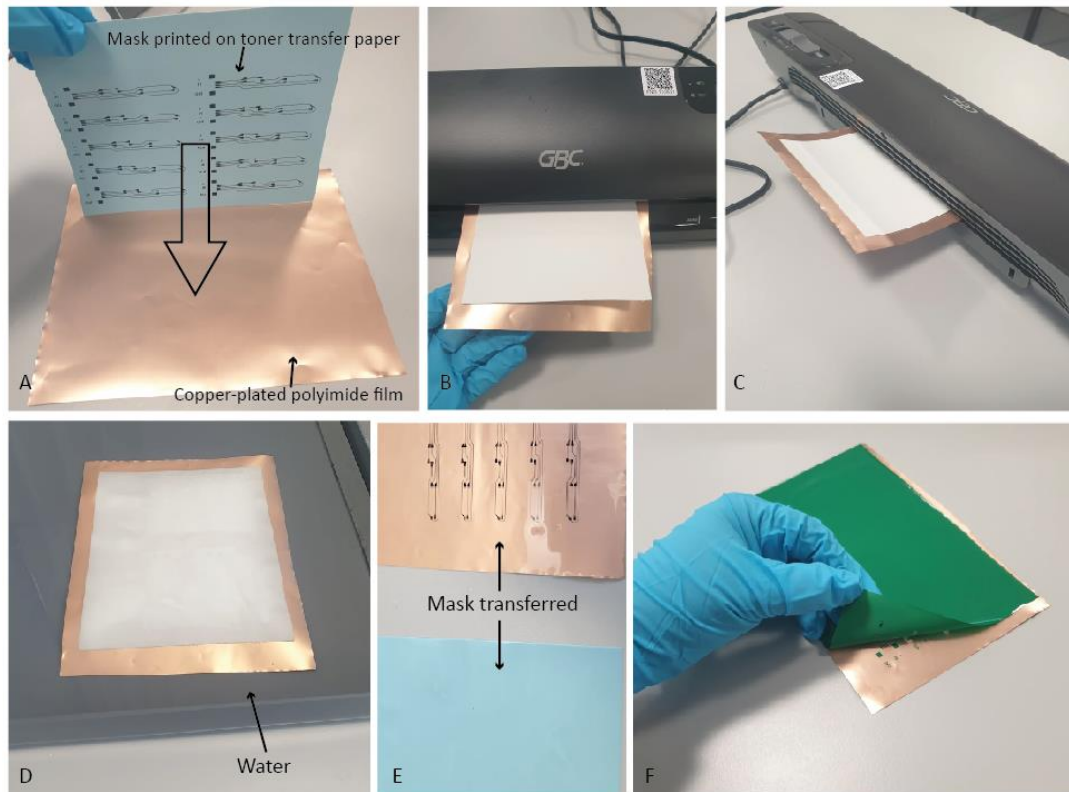
Figure 4-9. Toner transfer etch mask fabrication process.

A) The mask is printed on coated toner transfer paper, and placed on a piece of copper-plated PI film; B) The mask and film are passed through a laminator; C) The heat of the laminator causes the copper-plated PI to warp slightly; D) After laminating, soaking in water releases the paper; E) After soaking, the mask has transferred fully from the paper to the copper; F) A green film is laminated on top to fill in any gaps in the toner, and then peeled off, as shown.

The process includes the following steps:

2. A laser printer was used to print the mask on a special coated paper. The coating prevents the toner ink from sinking into the paper and allows the paper to be soaked in water without dissolving.

3. The mask was applied to the copper-plated film by passing both through a laminator (Figure 4-9A, B and C).

4. The laminated paper and copper-plated PI were then place in a tray of water to soak off the paper, transferring the toner onto the copper (Figure 4-9D and E).

5. An additional green film, which sticks to the printer toner but not the rest of the substrate, was then laminated on to fill in any gaps in the toner (Figure 4-9F). The film is peeled off after lamination.

4.3.1.2   Mask method 2: Dry film photolithography

As the project progressed, circuits with finer pitch (as small as 0.2 mm, as will be seen in later chapters) needed to be fabricated, so a more professional mask fabrication process was set up. Shown in Figure 4-10, the dry film process involves the following steps:

1. The substrate (copper-plated PI film) was cleaned with acetone.
2. Spray adhesive was used to attach the substrate to a piece of FR4. This is to ensure proper lamination, as the substrate alone is below the minimum thickness suitable for the laminator.
3. Photosensitive dry film (Ordyl Alpha, procured from Fortex Engineering Ltd, Lincoln, UK) was placed on top of the substrate, away from direct light. This is ideally carried out in a dark room with UV-safe light, but moderate shade in a normal lab, with blinds down to block light from outside, was found to be sufficient.
4. Both were passed through a laminator together to adhere the dry film to the substrate. After lamination, the laminated substrate was stored in a dark place until it has fully cooled.
5. A negative UV mask was placed on top of the substrate in a UV exposure box, and UV light solidified the mask in the areas where copper is needed for the circuit. A further rest period follows this step.
6. The substrate was agitated in a potassium carbonate developing solution, which washes away any undeveloped photosensitive film. This process was done by hand at first, by shaking a tray of developer, but later on an orbital shaker was procured to automate this step.
7. After development, the mask is complete, and the substrate was ready for etching. Acetone was used after etching to lift the mask off the remaining copper traces.

This process was taken from the instructions provided by the supplier of the dry film. The UV exposure, lamination procedure and development times are dependent on equipment.
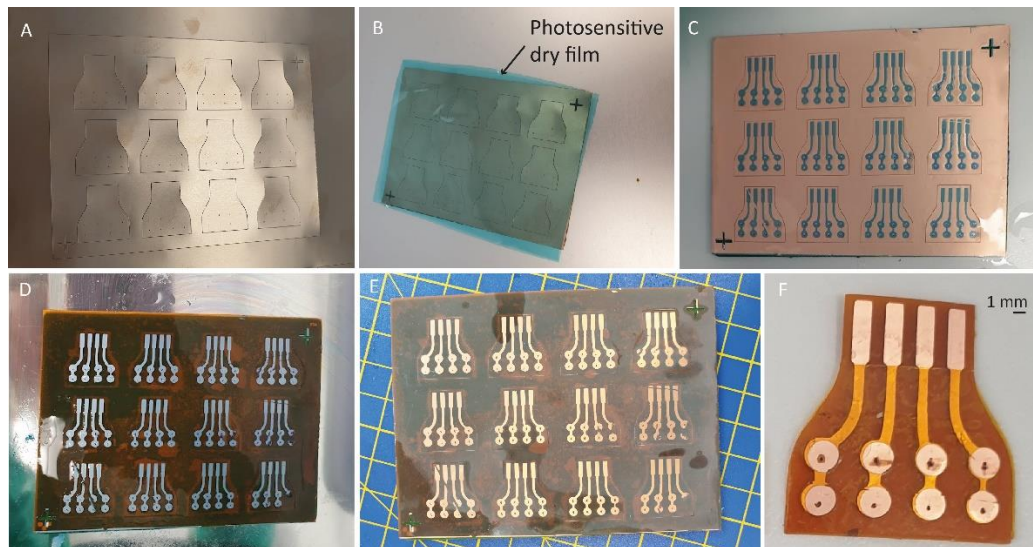
Figure 4-10. Etch mask fabrication using dry film lithography.

A) The outlines of the flexible circuits are cut from copper-plated PI using a vinyl cutter; B) The flexible material is applied to a rigid substrate (not visible) using spray adhesive, and then photosensitive dry film is applied on top using a laminator; C) After UV exposure and developing, the mask is finished and the circuit is ready for etching; D) After etching, all copper except that covered by the mask is removed; E) The mask is removed, using acetone; F) A finished module produced with dry film photolithography, where a PI encapsulation layer has been added, and holes have been punched in the solder pads to allow conductive thread to be stitched to them.

4.3.1.3   Mask method 3: The adhesive vinyl mask

Towards the end of the project, very fine pitch, narrow circuit strips needed to be fabricated to realise some of the helical e-strips documented in Chapter 6. Specifically, helical LED and temperature sensing e-strips with 0201 LEDs and resistors, with pitch as low as 100 µm, and strips as narrow as 1.5 mm. Not only was it difficult to tune the dry film process to realise features this small, it was also challenging to accurately align the mask with the circuit outlines. While it is possible to buy equipment for high accuracy alignment of masks, and it is theoretically possible to tune the dry film mask process to increase the resolution, there was another, simpler option that did not require the purchase of additional equipment.

A novel method was developed, making use of the vinyl cutter already used to cut circuit outlines. By applying adhesive vinyl (used to make stickers and signage) on top of the copper-plated PI before cutting, it is then possible to adjust the cutting force of the vinyl cutter blade, so that it can either a) cut through vinyl only, to form the etch mask, or b) cut through both vinyl and PI, to cut the circuit outlines. This is illustrated in Figure 4-11, where a temperature sensing e-strip with fine pitch and solder pads for 0201 components is made.
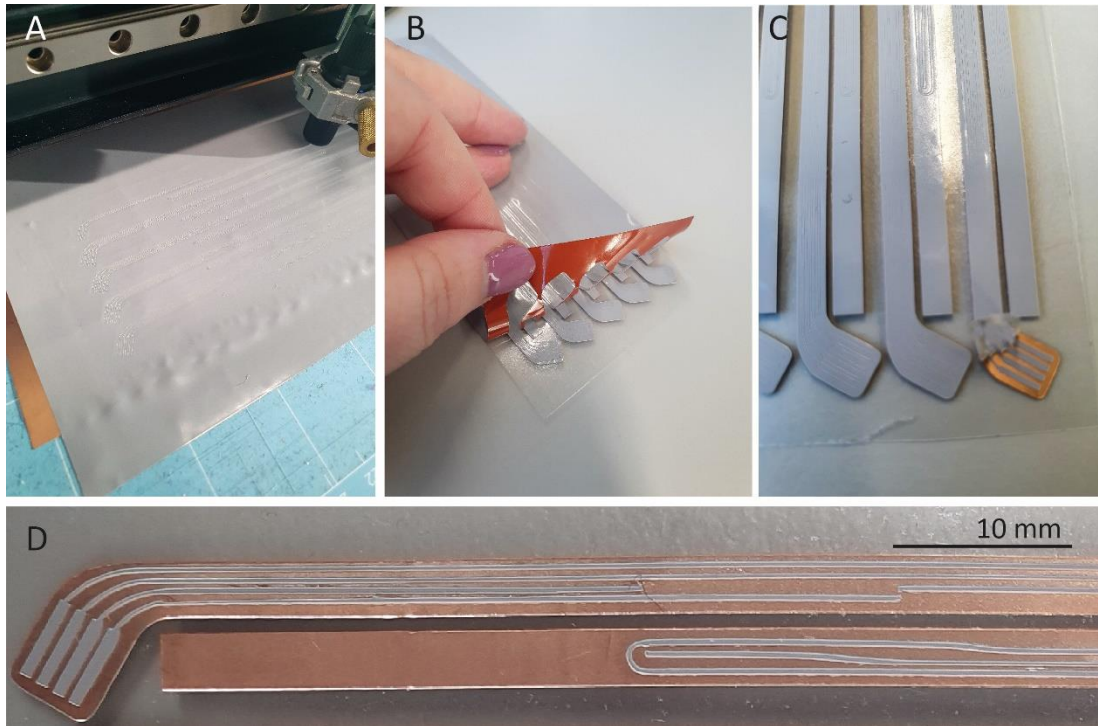
Figure 4-11. The adhesive vinyl etch mask fabrication process.

a) Cutting the vinyl, then the circuit outlines, on the vinyl cutter; B) Peeling away excess copper-plated PI; C) peeling away excess vinyl; D) The finished mask ready for etching.

The process involved the following steps:

1. Copper-plated PI film was applied onto a transfer tape backing.
2. The copper was cleaned by wiping it with an IPA wipe.
3. Vinyl was applied on top of the copper.
4. Circuit traces were cut at low force (~90 gf) to cut through the vinyl layer only.
5. Circuit outlines were cut at medium cutting force (~120 gf) to cut through the copper-plated PI layer.
6. The overall outline of the module was cut at high force (~200 gf) to cut through the transfer tape.
7. Excess vinyl was weeded with tweezers.
8. The circuit was etched in a sodium persulphate bubble etch tank.
9. After etching, the vinyl was peeled off with tweezers, but can also be released with IPA or acetone.

4.3.2 Results

4.3.2.1 Mask method 1: toner transfer

This method was used during the first two years of the project, and used for most of the work covered in Chapter 5. It is easy to perform and produces acceptable results, but has limitations. The following issues were encountered, as shown in Figure 4-12:

- When using very thin flexible substrates, the laminator can cause wrinkling, which deforms the circuit design, leading to gaps in the mask which render the sample unusable.

- With fine pitch circuits, the green film can't be used, because it fills in gaps in between traces.

- Once passed through the laminator, it's difficult to tell if the lamination has worked, until the paper is soaked off, at which point it's too late to fix. Some details can be filled in using a marker, but for circuits with fine details this is challenging.

- If the laminator pressure is too high, the mask can become deformed (i.e., squished) in that the toner spreads out, which can cause short circuits between closely spaced traces.

Overall, this method was quick and easy to set up and use, but had a high rate of failure when using thinner copper-plated PI films of less than 50 μm thickness, and components or traces with pitch of less than 1 mm.

This method was also challenging to use when etch masks needed to be accurately aligned with pre-cut circuit outlines (see Chapter 3, Section 3.1.3 for reasons why outlines were cut before etching).
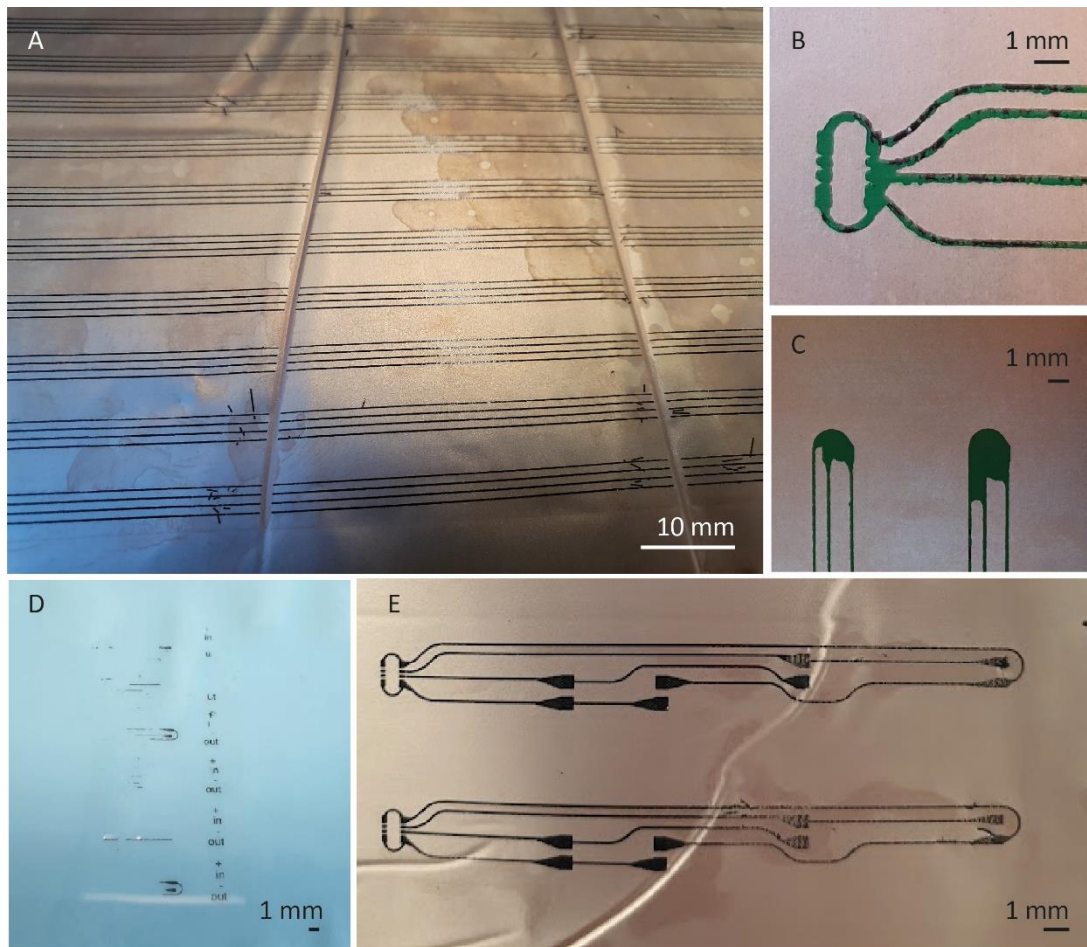
Figure 4-12. Issues encountered with toner transfer etch mask fabrication method.

A) Wrinkling of substrate causing delamination of mask; B)-C) Green film creating unwanted short circuits in fine pitch circuits; D) Toner left on transfer paper due to lamination failure; E) Failed mask where both wrinkling, and lamination failure have occurred.

4.3.2.2 Mask method 2: dry film photolithography

This is a professional method with the ability to create fine pitch, high complexity circuits. However, the process involves many steps (laminating, UV exposure, developing), each with its own calibration process to achieve optimal results, and rest periods in between several of the steps. For prototyping in a research lab with low throughput, it is achievable, but requires a significant investment of time and fine tuning. Issues are shown in Figure 4-13, and included:

- Delamination of the mask during etching, possibly caused by unclean substrate. This was mostly resolved by cleaning with acetone before applying the dry film, but it

was difficult to judge by eye whether a spot had been missed during cleaning (Figure 4-13A, B and C).

- Difficulty aligning the mask to circuit outlines for small scale circuits. As stated in Chapter 3, Section 3.1.3, cutting the outlines before etching proved more successful than etching first and then cutting. But despite trying several different types of registration mark for alignment, and using a microscope to aid alignment, the desired level of accuracy was not achieved (Figure 4-13D).

- This method was able to achieve finer resolution than the toner transfer method, but < 0.5 mm pitch features were still difficult to achieve (Figure 4-13E). This is theoretically possible, as the dry film datasheet states that resolution down to 60 µm is possible. But it is perhaps better suited to a professional photolithography lab, or a lab with high volume of production.
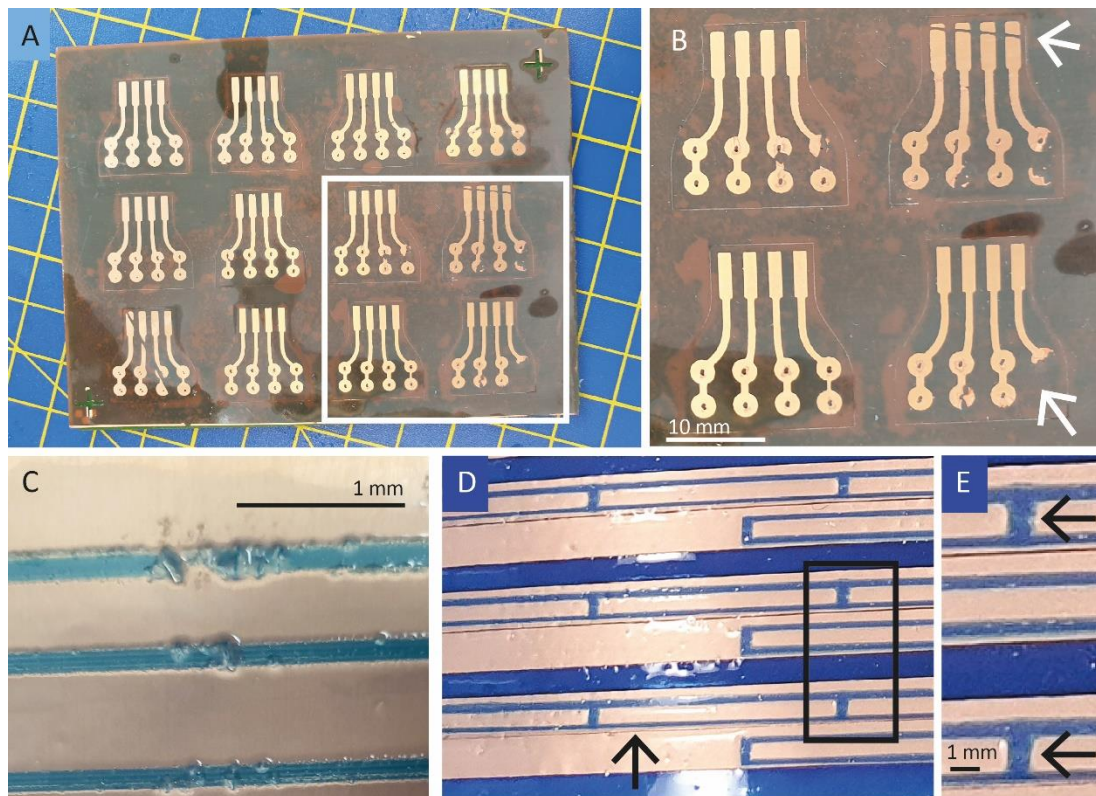
Figure 4-13. Issues encountered with the dry film photolithography etch mask method.

A) A batch of circuit modules, where the highlighted section contains several failures; B) Close-up of the highlighted section, showing over etched areas caused by delamination of the mask; C) Image of mask delaminating; D) A mask for an LED circuit, showing an alignment issue highlighted by the arrow, where a trace is very close to the edge of the module; E) Close-up of the section highlighted by the square in the previous image, where there is supposed to be a gap at the points highlighted by the arrows.

To create the dry film photolithography mask, two methods were evaluated. Initially, the manufacturer's recommendation to print the mask on transparency film with an inkjet printer was used. This worked well for larger circuits (e.g. with > 1 mm pitch and traces > 0.5 mm wide), but two issues were observed:

- The printing was not 100% opaque, and two prints were needed for full opacity. This often resulted in slight misalignment, which is not a problem for larger circuits but an issue for fine pitch.
- The transparency film was slightly stretched by the printer, which resulted in misalignment between etched conductive traces and circuit outlines and PI film applied on top as encapsulation.

An attempt was made to address this by adjusting the mask design to offset the stretching, but another method proved more fruitful: instead of using transparency film, the mask was cut from black heat transfer vinyl (PVC or PU film with a heat activated adhesive backing) (Figure 4-14).The downside of this method is that it requires precise removal of small pieces of vinyl, but it is more accurate compared to printed masks and produced better resolution than the printed UV masks. For clarity, this is specific to masks printed on the inkjet printer and transparency film used in this work. Not all inkjet masks produced on all materials and printers. A professionally manufactured mask would likely have much better accuracy and opacity. But this also comes with increased cost, and increased time delay between iterations of a design. For the prototyping of devices performed in this work, the ability to make masks is much faster and more convenient.
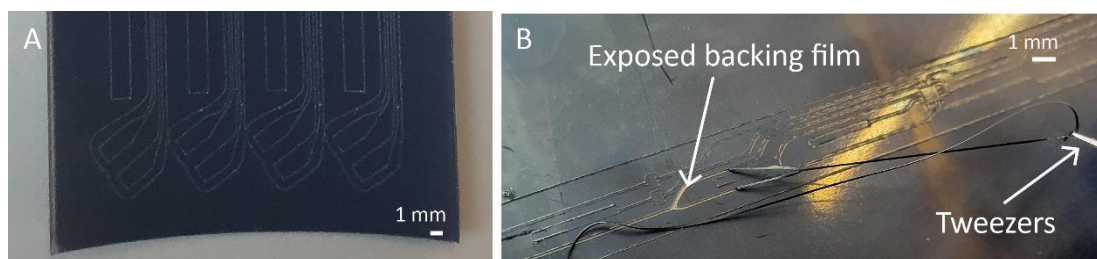
Figure 4-14. The HTV mask for the UV exposure step of the dry film lithography process.
A) Mask after cutting, but before weeding; B) Weeding the excess vinyl with tweezers, exposing the clear backing film in areas where the dry film needs to be exposed to UV light.

4.3.2.3   Mask method 3: adhesive vinyl mask

Figure 4-15 shows issues encountered with the dry film photolithography mask when attempting to etch fine pitch temperature sensor circuits documented in Chapter 6. The mask, after laminating, UV exposure and developing, hasn't achieved the required resolution, and several traces are bridged, which is caused by the mask. Other areas have been over-etched, due to the mask delaminating (Figure 4-15A and B). The vinyl mask, by contrast, has suffered none of these issues, and the circuit has been properly etched (Figure 4-15C and D).
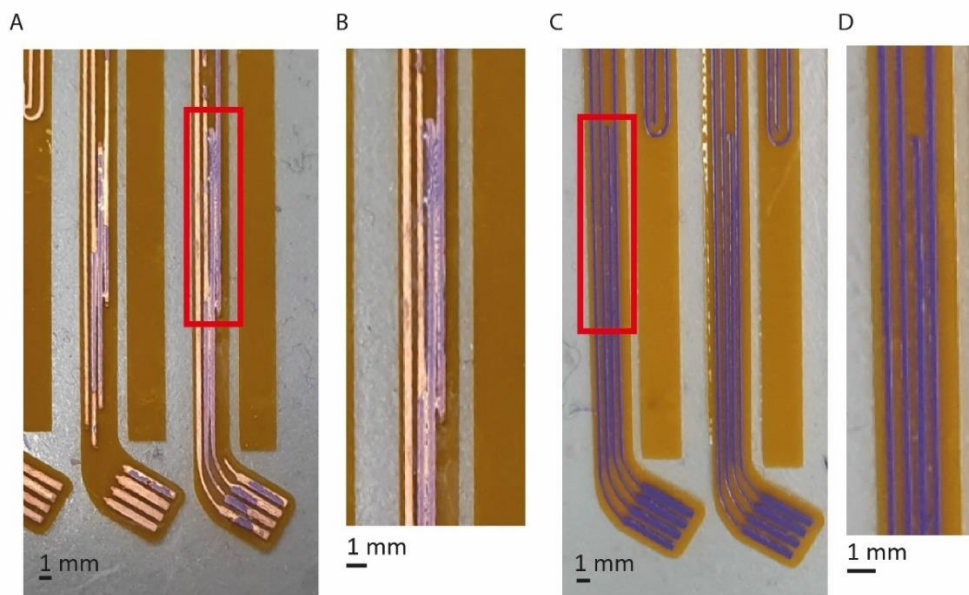
Figure 4-15. Success of vinyl etch mask method compared to dry film photolithography.
A) Circuit etched with dry film photolithography method, with many bridges between traces, and over-etched areas where the mask has delaminated during etching; B) Close-up view of the highlighted section in part A, where it can be seen that the dry film photolithography mask hasn't been successfully created, and is bridging multiple traces; C) The same circuit after etching with the vinyl mask, showing better clear, properly etched traces; D) Close-up of the highlighted section in C, where no bridges between traces can be seen.

The adhesive vinyl mask method addressed the following problems:

- Alignment of mask with substrate: As the vinyl is cut at the same time as the outlines, without removing the substrate from the machine in between, or using different processes and needing to re-align, there are no alignment issues.
- Fine pitch: The Roland GS-24 vinyl cutter has a minimum mechanical resolution of 12.5 µm, which is well below the resolution (approx. 100 µm) required in this work.
- Delamination: the vinyl adheres well to copper but is still repositionable. If it lifts or moves out of place, it can be adjusted or stuck back down.

This method was found to be quicker, and easier to achieve, than the other methods and was the only one where the finest resolution helical e-strip circuits were able to be successfully fabricated. The method does have some limitations, which are:

- It was important not to apply too much force on the vinyl when weeding excess material, or else the mask can stretch and deform.
- Weeding very fine pitch features requires precise use of tweezers but can be made easier with the help of a microscope.
- Vinyl masks, like the other methods, could also delaminate from the surface, but in most cases, it was possible to press the mask back into place.

4.3.3 Discussion of mask methods

Table 4-3 evaluates the three methods against the three criteria set out at the start of the chapter. The adhesive vinyl method is the clear winner, but it is important to note that this does not mean it was the method used for the rest of this work.

As mentioned earlier in the chapter, its development was motivated by the failure to successfully manufacture some circuits with the toner transfer and dry film photolithography methods. And the dry film photolithography method was not available until the third year of the project. This means that all three methods are used at different stages in later chapters.

Table 4-3. Performance of mask methods against criteria established at start of chapter.

Method	Resolution quality	Alignment quality	Speed
Toner transfer	Low – best for > 1mm features	Low – difficult to align pre-cut circuit outlines to toner paper for laminating	Fast – more steps than adhesive vinyl method, but all steps are fast
Dry film photolithography	Medium – was able to achieve features around 500 µm	Medium – was able to achieve 1-2 mm accuracy	Slow – most fabrication steps + rest periods in between steps
Adhesive vinyl	High – most successful method at etching approx. 100 - 200 µm features	High – mask was cut while adhered on top of the substrate, so requires no additional alignment	Fast – least number of steps, most time consuming part is weeding excess vinyl

More generally, for high volume production of complex circuits, the dry film photolithography method is the obvious choice. However, for prototyping, and outside an industrial setup where every process can be tightly controlled and fine-tuned, it is challenging to use successfully. The toner transfer method can produce good results, but for fine details, or with circuits that required precise alignment, it was unsuccessful. In this work, the vinyl mask method was the only method that was able to realise fine pitch circuits. In addition, the vinyl mask method uses fewer hazardous chemicals than the other two methods, fewer pieces of equipment, and more widely available materials. This is summarised in Table 4-4.

Table 4-4. Comparison of etch mask methods.

Category	Toner transfer	Dry film photolithography	Vinyl
Equipment (not including etch tank)	Laser printer Laminator	Inkjet printer Laminator Orbital shaker* UV exposure box	Vinyl cutter
Consumables	Toner transfer paper Green film	Photosensitive dry film Photolithography mask	Adhesive vinyl
Hazardous chemicals (excluding etching solution)	Isopropyl alcohol Acetone	Acetone Developer	Isopropyl alcohol **

The orbital shaker is not essential, but the processing time increases significantly without it

*** It is possible to not use this but it improves adhesion*

To be clear, the vinyl mask is well suited to a) prototyping and b) circuits that are simple and don't contain lots of components. This is because excess vinyl has to be weeded, and for a very complex circuit, or a high volume, this would be time consuming. However, for research or rapid prototyping of flexible electronics, it works very well.

When etching fine pitch electronics, it is sometimes difficult to see if a fine track has etched well, or if there is still a small bit of copper bridging two traces. With toner transfer and dry film photolithography, this must be determined by eye, which can be difficult. Using the vinyl mask, parts of the vinyl can be peeled away to expose the copper and perform a quick continuity test, and then stuck back down if additional etching needs to take place.

Careful weeding is required as the vinyl can stretch, and small pieces can be tricky to work with. Bubbles can also appear, but using a squeegee or roller when placing the vinyl can eliminate this. The other disadvantage of the vinyl mask method is that waste vinyl is discarded after weeding. But the other methods also produce waste, as paper and green film waste are produced in the toner transfer process, and waste dry film is produced in dry film photolithography. Overall, the adhesive vinyl method could be highly beneficial for schools, fablabs and makerspaces, which often have vinyl cutters, but are less likely to have dry film photolithography setups, and might not be in a country where toner transfer kits can easily be purchased. This method could therefore open up flexible electronics fabrication to a broader audience.

4.4 Summary

This chapter has evaluated several methods to create conductive tracks on flexible substrates, to identify a suitable method to be used in this research, to build modular e-textile systems and fabricate stretchable, helical e-strips. Dispenser printing on PI film was evaluated, evaluating print quality, and producing printed temperature sensors.

Three methods for producing masks to etch copper-plated PI film have also been evaluated. Between etching and printing, etching was the process used for the following chapters. This is for two reasons: speed, and resolution. Etching processes proved to be much quicker (for prototyping purposes) than printing. As later chapters demonstrate the fabrication of very narrow flexible circuits with fine detail, the better performance of etching processes at producing fine detail made them a better choice.

Concerning the question of most sustainable process, there isn't a clear winner. In terms of waste material produced, printing has the benefit of being an additive method, meaning that conductive material is added only where needed. With etching processes, by contrast, all the unneeded copper that is etched away is wasted (subtractive method). However, there is inevitably some waste material in printing. When printing with the V-One, it is not possible to squeeze every last drop out of the print cartridge and still print with good quality. With screen printing, there is always excess ink on top of the screen that is washed away after printing. Performing analyses such as a life cycle assessment can be beneficial when developing a product, to identify ways to improve sustainability. This includes many factors, including how materials are sourced, the resources used to manufacture them, how far they

travel to be distributed and sold, and their disposal at end of life. Life cycle assessment has been done in e-textiles [133], but was out of scope for this project.

Ultimately, this chapter has shown how etching processes were chosen over printing processes for e-strip fabrication. And why different etch mask fabrication methods were used at different stages of the project, with the vinyl mask method being developed to produce the most challenging, fine pitch circuits. That is, it may well be possible to produce fine pitch e-strips with other printing processes, different equipment for dispenser printing, or alternative conductive inks. But for this project, etching was the most suitable method for exploring the systems, connections and structures covered in the remaining chapters.

The next chapter moves on to the development of a modular e-textile garment, but it is worth noting the work covered in this chapter took place throughout the project. Much of the work on printing took place before the work discussed in the next chapter, but the evaluation of etch mask fabrication methods continued until almost the end of the entire project, motivated by issues that arose along the way. The toner transfer method was used for the work in the first two sections of Chapter 5. The dry film photolithography method was used with printed photolithography masks for the third part of Chapter 5 and with vinyl photolithography masks in Chapters 6. The adhesive vinyl method was developed at the very end and used in part of Chapter 6.

Chapter 5 Development of a Modular Sensing Garment and E-Textile Interposers for Better Modular Systems

5.1 Introduction

The previous chapter evaluated fabrication methods for flexible electronics, with a focus on making individual circuit modules (such as LED e-strips) and comparing the capabilities of different techniques to produce small circuit modules. This chapter moves on to applying these techniques to building a modular e-textile system. As laid out in Chapter 2, Section 2.2.3, modular systems are built from discrete modules that are assembled to form a full system. This chapter goes into more detail on this topic and investigates a 'more modular' e-textile system than the current convention, where soft or flexible sensors are permanently embedded in a garment, and a rigid control module – containing a power source and microcontroller, or other control electronics – can be connected to these sensors, but is removable.

The overall concept is first explored through the construction of a modular sensing garment to measure skin temperature, which was tested on a human participant. As this work was a collaboration with Dr Katy Griggs and several students in Nottingham Trent University Department of Engineering, the work discussed in this thesis focuses on specific aspects of the project undertaken by the author. Specifically, the design and fabrication of the electronics, assembly of the modular system, and evaluation of what worked well, and what didn't, about the way the garment was constructed.

Later sections of this chapter document the development of a novel interposer to join small electronic components to conductive thread interconnects, motivated by some of the fabrication and reliability issues encountered when creating the modular sensing garment. And finally, an updated prototype of the garment is created, incorporating interposers and additional features such as wireless connectivity.

It's important to note that the work presented in this chapter is largely exploratory, rather than a finished product ready for commercial production. The sensing garment documented in this chapter was in no way robust or comparable to a commercial e-textile garment. But it

was an extremely useful exercise, providing valuable information about constructing modular e-textile garments: how modular parts should be connected, where on the body sensors should be located, and what parts of the system are susceptible to failure. It also provides important background context to the following two sections of this chapter, which are also on modular e-textile systems. The entirety of that work was motivated by lessons learned in this section.

5.2 Development of a modular temperature sensing garment

A modular sensing system was developed to measure skin temperature of cyclists, motivated by a need for reliable and easy methods to monitor athletes' skin temperature. This is both for athletes and trainers looking to optimise performance, and researchers investigating factors affecting athletic performance. As a proof of concept, a prototype modular garment is demonstrated: a temperature sensing cycling suit. The fabrication and evaluation of the garment are presented, and recommendations are made for future work.

5.2.1 Skin temperature effect on physiology and measurement

Both core body temperature and skin temperature has been shown to have a significant impact on athlete performance. Overheating causes fatigue, and high skin temperature measurements can be linked to diminished performance [198]. Elevated skin temperature also increases an athlete's perception of effort, suggesting that monitoring skin temperature can be useful to athletes in setting an appropriate pace for optimal performance [199]. Heat-related illnesses including heat stroke can also affect athletes during high intensity or long duration exercise [200]. And abnormally low temperatures, which can occur when exercising in cold weather, can be a sign of hypothermia or frostbite, requiring urgent medical attention [201]. As an athlete might not be aware that their temperature is rising dangerously high, or falling dangerously low, monitoring skin temperature could also provide data to notify athletes, trainers or event officials when athletes are at risk.

At present, tracking an athlete's skin temperature either requires temperature sensors to be taped to the body [202], which is time consuming, or temperature can be measured with an infrared camera, which is limited to stationary testing, e.g. on a stationary bike, and has been shown to have poor agreement with other temperature sensors [203].

Current standards for skin temperature measurement include the Maxim Integrated iButton, a disc-shaped device which is taped to the skin, with accuracy of 0.5 °C and resolution of

0.125 °C [202]. The iButton has the advantage of being wireless, but data is not available in real time and must be downloaded from the device after use. Measuring average skin temperature requires the use of several iButtons, requiring separate setup and downloading of data for each sensor individually. It is also important to use porous fabric tape to attach iButtons to the skin, as non-breathable tape doesn't allow sweat to evaporate, and this causes error in sensor readings [204].

5.2.2 Skin temperature measurement with e-textiles

Given the limitations of these sensors, there is an opportunity for an e-textile solution for skin temperature measurement. Existing temperature sensing e-textiles have demonstrated potential, but also highlighted several possible issues. Lugoda et al embedded a thermistor inside an 'e-yarn' [205], and related work by Hughes-Riley et al embedded the same e-yarns into a cycling garment [206]. These showed promising results, but require custom machinery for manufacturing, and show that embedding a sensor within a textile reduces its accuracy, and a gap between textile and skin causes further sensor error. E-yarns, at their current level of development, can also not stretch, which limits their applications in sports garments, which are normally made from high stretch fabrics.

Komolafe et al embedded a thermistor on a flexible PI strip in fabric, showing good accuracy but only on woven fabrics, which are also normally not stretchable [207]. The sensor was only tested by placing it in an environmental chamber, which doesn't fully assess its suitability for measuring skin temperature. Skin temperature is normally higher than ambient temperature, and as some temperature sensors are known to drift towards ambient temperature [202], it is important to use a testing setup that mimics these conditions.

Wicaksono et al designed a custom knit garment where sensors are exposed directly to the skin through openings in the fabric [40]. But it is suggested that such a garment should be tailor made for a particular user to ensure sensor accuracy, i.e. it must conform to the body for good contact between sensor and skin. This adds costs for bespoke tailoring and is not currently compatible with clothing production at scale.

5.2.3 Integration of electronics in textiles

Electronic circuitry can be integrated into textiles at different stages in the garment creation process, using a variety of methods, and no method has yet been agreed as standard (See Chapter 2, Section ▢). The approach taken in this work is to insert electronics into channels

or pockets in the garment, using the textile as a carrier for the electronics rather than integrating circuitry into the fabric structure. Electronics can also be woven or knit into the textile structure, or printed or laminated onto textiles, but the approach used here enables a modular design where electronics and textiles are easily separable. It can be achieved by stitching additional fabric channels onto an existing garment, or by incorporating pockets into the design of a fabric or garment while it is being knit or woven.

In this work, long, narrow pockets are added to a triathlon suit by Huub Design, by stitching strips of fabric onto the interior of the suit. This suit is a prototype for the purpose of evaluating the concept, but if developed into a commercial product, these pockets could be integrated into the suit design and incorporated at garment manufacturing stage.

The following criteria were set for the system:

- The electronic circuitry should be able to be disassembled / reconfigured, rather than permanently connected.
- Waste material should be minimised by using rectangular or tessellating designs, for both sensors and textile parts.
- Electronic parts should be integrated in a way that is easy to access for repair, and so that they can be fully removed for recycling at end of life.

5.2.4 Methods

5.2.4.1 Design of the modular system and choice of materials

The cycling suit system is illustrated in Figure 5-1. It consists of:

1. Flexible temperature sensing strips (e-strips)
2. A data acquisition (DAQ) device housed in a pocket in the garment
3. Stretchable interconnect strips that connect the e-strips to the DAQ
4. A laptop connected to the DAQ via USB cable, reading sensor data into LabView
5. A commercial triathlon suit (trisuit) adapted to house the electronics
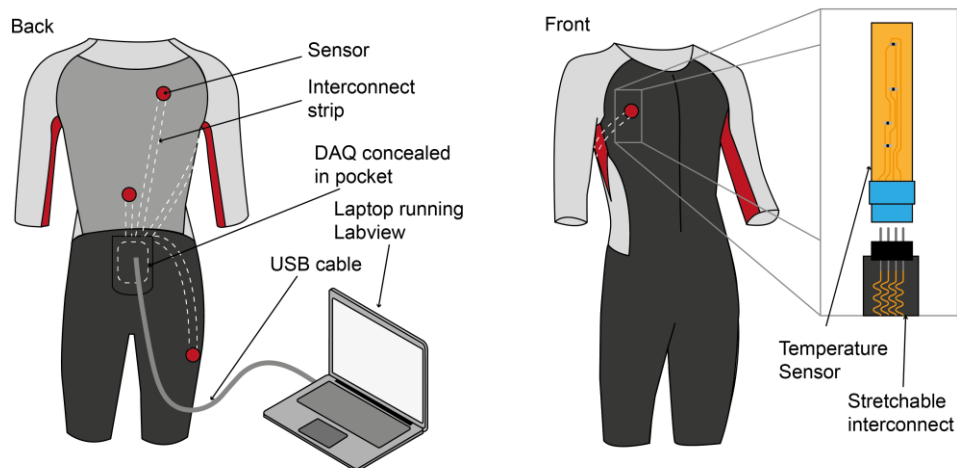
Figure 5-1. Temperature sensing garment: system overview.

The trisuit houses four flexible temperature sensors, each connected to a DAQ via stretchable interconnect strips.

A USB cable enables real-time data readout onto a laptop running LabView.

This is a prototype created to evaluate the concept of placing detachable parts inside the garment. It is suitable for lab-based testing or training on a stationary bike, but would require modifications to realise a wireless system. However, as the work presented in this chapter features only stationary lab-based testing, a wired system is sufficient for this stage of development, and the DAQ's ability to provide high accuracy data is beneficial for assessing the accuracy of the sensors. The DAQ is not designed for wearable use, though it is lightweight and fits inside a pocket in the garment. In a fully developed product this would be replaced by a smaller control module, battery powered and able to transmit data wirelessly.

To reduce waste, the sensor and interconnect are rectangular. This was a conscious choice to minimise fabric and PI waste that would be generated by cutting curved shapes.

5.2.4.2 Design of the temperature sensor

There are many types of temperature sensor, including resistance temperature detectors (RTD), thermocouples, and temperature sensing ICs [208]. For this work, the criteria were:

- Small footprint, so that when embedded in textiles, the sensor is minimally noticeable.
- Good accuracy in the range of human skin temperature (≤ 0.5 °C, to be comparable with other sensors used to measure skin temperature)

As skin temperature varies significantly across the body [209], sensors were placed at multiple locations. Given this variation, it is important to choose a temperature sensor which has good sensitivity across the entire range of skin temperature, rather than the narrower normal range of core body temperature.

A 10 kΩ negative thermal coefficient (NTC) thermistor was chosen. The thermistor's resistance decreases by approximately 150-200 Ω per increase of 1 °C in the range of 15 °C-40 °C range, making it sufficiently sensitive for measuring changes in skin temperature. This thermistor has been used in existing work and has been proven to be a good candidate for e-textile temperature sensing [207,210].

To measure a sensor's resistance, it is necessary to use an interface circuit to convert the resistance into a voltage. This voltage can then be read by an analogue to digital converter in a microcontroller or DAQ, for example. The standard interface circuit is the Wheatstone Bridge (Figure 5-2). Three 10 kΩ fixed resistors complete the bridge circuit. The resistance of the thermistor can be calculated from the voltage across the Wheatstone Bridge, illustrated in Figure 5-2. Resistors $R_1 - R_3$ are all 10 kΩ resistors. When the resistance of the thermistor is exactly 10 kΩ (at 25 °C), the resistance across each side of the bridge (i.e. along both paths from point A to point B) is equal, and the voltage V_{out} is zero. Using Kirchoff's circuit laws, the resistance of the thermistor can be derived (Equation 6-1).
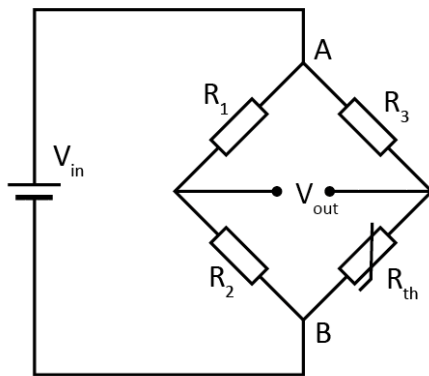
$$R_{th} = \frac{R_2 R_3 - R_3(R_1 + R_2)\frac{V_{out}}{V_{in}}}{R_1 + (R_1 + R_2)\frac{V_{out}}{V_{in}}}$$

(5-1)

Figure 5-2. Wheatstone bridge circuit.

Where R_{th} is the resistance of the thermistor, and V_{out} is the voltage measured between the points shown in Figure 5-2.

The manufacturer's datasheet for the thermistor provided the following version of the Steinhart-Hart Equation (Equation 6-2) for calculating the temperature from the thermistor

resistance and the resistance at the reference temperature, R_{25}, the resistance at 25 °C, which in this case is 10 kΩ.

$$T = \frac{1}{A_1 + B_1 \ln\left(\frac{R_{th}}{R_{25}}\right) + C_1 \ln^2\left(\frac{R_{th}}{R_{25}}\right) + D_1 \ln^3\left(\frac{R_{th}}{R_{25}}\right)}$$

(5-2)

For the thermistor used, the coefficients of the equation given by the manufacturer's datasheet are listed in Table 5-1.

Table 5-1. Coefficients of the Steinhart-Hart Equation for the thermistor used.

A_1	B_1	C_1	D_1
3.35401643468053 x 10⁻³	2.82875 x 10⁻⁴	2.989645 x 10⁻⁶	4.840855 x 10⁻⁸

5.2.4.3 Fabrication of flexible temperature sensing e-strips

Flexible temperature sensors (e-strips) made from copper tracks on a strip of PI film substrate were fabricated, as shown in Figure 5-3. All resistors were 0603 (1608 metric) surface mount. There are smaller component packages, but at 1.6 mm x 0.8 mm, and 0.4 mm (resistors) to 0.8 mm (thermistors) tall, these are small enough to be imperceptible to the wearer in this case, while still being large enough to handle easily during fabrication. Fabrication followed the toner transfer process described in Chapter 3, Section 3.1.2.2, to etch copper-plated PI film (copper thickness: 18 μm; PI thickness: 25 μm). Solder paste was dispensed onto the solder pads using a syringe, and components were placed using a pick and place machine, and then soldered using a hotplate.
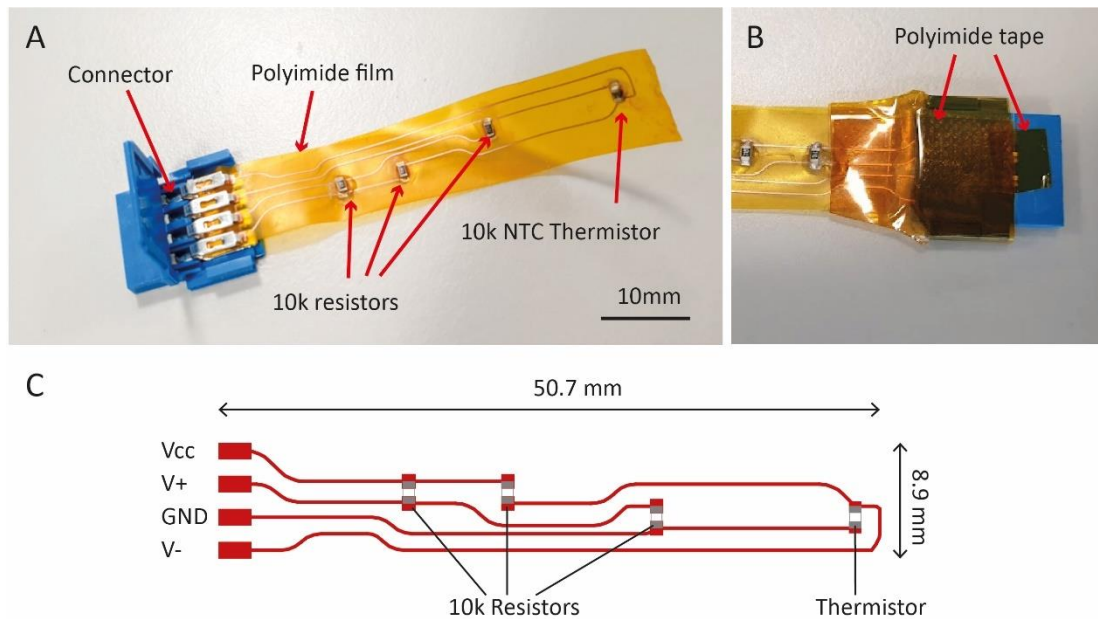
Figure 5-3. Flexible temperature sensor strips (e-strips)

A) E-strip with Amphenol FCI Clincher connector; B) PI tape applied to interface between connector and flexible strip, and exposed metal contacts; C) E-strip design, showing location of components and dimensions.

Encapsulation was applied to the e-strips for structural support and protection from moisture ingress, using Plasti-Dip, a non-toxic liquid rubber coating, as explained in Chapter 3, Section 3.1.4.

Amphenol FCI Clincher connectors were then attached to the e-strips. These create a crimp connection to copper pads on the e- strip and have 2.54 mm pitch, which is compatible with many standard connectors. They have also been used in e-textiles before and have been shown to be washable [83]. PI tape was applied to the Amphenol connectors to cover up any exposed metal and prevent moisture ingress from sweat, shown in Figure 5-3B. This was a suitable solution for prototyping, but a washable encapsulation would be needed for a commercial application.

5.2.4.4 Fabrication of the stretchable interconnect strips

The e-strips are flexible, but not stretchable. The trisuit, like most sports apparel, is made of stretch fabric, and therefore stretchable interconnects are required. By this point in the project, the stretchable helical e-strips documented in Chapter 6 had not yet been developed. Instead, conductive thread was stitched in a zig-zag pattern on strips of stretch fabric. This means that the interconnects mostly consist of textiles, allowing them to drape with the fabric of the suit and making them breathable.

Figure 5-4A shows a microscope image of Sewiy conductive thread used to fabricate the interconnect strips, which is made from six strands of 44 AWG insulated copper wire braided with a Kevlar carrier thread. This thread was chosen because the insulating coating on the wire prevents short-circuits from moisture or accidental touching of threads, and as the conductive elements are made from copper wire, it is solderable. This allows for a more robust electrical connection than just stitching. Stitched connections have been shown to relax over time, which causes resistance to increase, so additional reinforcement is recommended [211]. Table 5-2 compares the properties of Sewiy conductive thread with other popular conductive threads, showing that it is an order of magnitude more conductive than comparable threads.

0.45 mm diameter twisted enamelled copper wire, and fine Litz wire were also investigated as potential interconnects, as these can also be formed into a serpentine shape. Both were found to be considerably stiffer than the stretch fabric used in the trisuit, and when stretched, they remained extended and didn't recover the serpentine shape when relaxed. This would have affected the suit's ability to conform to the body, so these were ruled out.

Table 5-2. Comparison of commercially available conductive threads

Conductive thread	Composition	Resistance (Ω/m)	Solderable	Insulated
Sewiy insulated conductive	Fine copper wires	1.52	Yes	Yes
Adafruit 3-ply stainless steel	Fine stainless steel fibres	32.81	No	No
Light Stitches Madeira HC12	Silver coated nylon	<100	No	No
Shieldex TPU twisted	Silver coated nylon and TPU	<100	No	Yes

A Brother Innovis domestic sewing machine was used to sew the thread onto 25 mm wide strips of 100% polyester scuba jersey fabric. This fabric has a thickness of 0.58 mm (as measured by a micrometer) and was chosen as it has comparable stretch properties to the fabrics used in the cycling suit. It is also thick enough to support the conductive tread traces, as these are thicker than normal thread. But is not bulky, and is widely available. The conductive thread was used as the bottom (bobbin) thread in the sewing machine, as described in Chapter 3, Section 3.1.2.3. A standard cotton thread was used as the top thread, and a zigzag stitch was selected as it has the ability to stretch. A stitch width of 3 mm and length of 3 mm were chosen as this combination exhibited sufficient (approximately 30%) stretch. Interconnects after stitching are shown in Figure 5-4B.
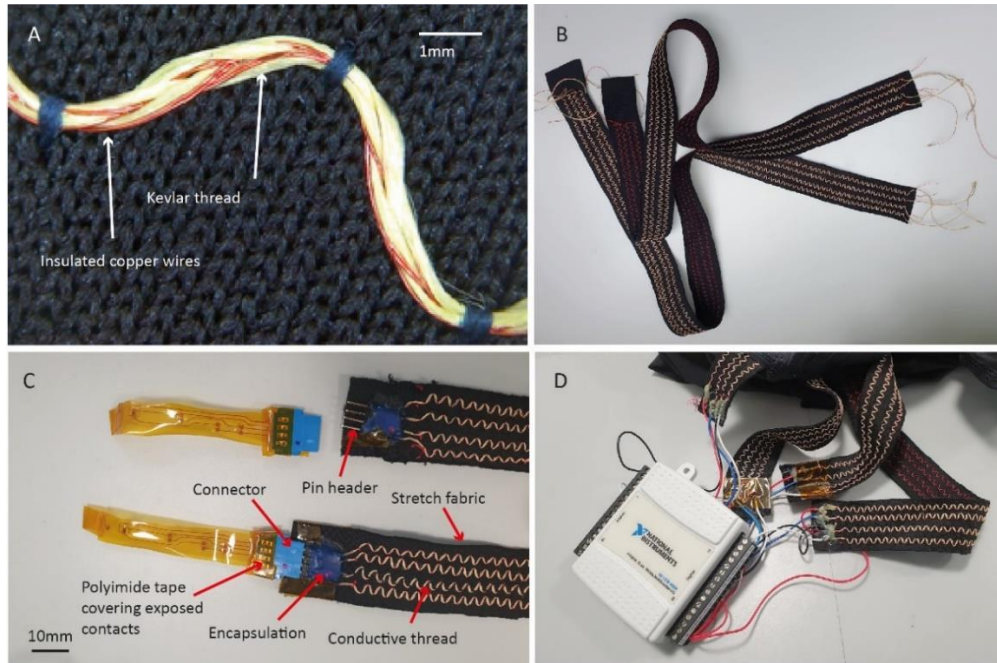
Figure 5-4. Fabrication of the interconnect strips.

A) Microscope image showing the structure of the conductive thread, consisting of enamelled copper wires braided with Kevlar supporting thread; B) Interconnect strips after stitching the conductive thread on stretch fabric; C) connection between e-strips and stretchable interconnects, consisting of conductive thread tracks on fabric with pin headers as connectors; D) Connection between interconnects and DAQ (before encapsulation was added to the conductive thread – wire interfaces on the interconnect strips.

2.54 mm male pin headers were used as connectors to join the interconnect strips to the sensor e-strips, as these are compatible with the Amphenol FCI clincher connectors on the sensing strips (Figure 5-4C). Two methods to solder the conductive threads to the pin headers were evaluated: a) stitching the conductive thread to the pin header, using PI tape to insulate the fabric from the heat of the soldering iron, then soldering; b) burning away the Kevlar carrier thread on the section of thread to be soldered, removing the enamel coating from the copper wires in the process, and then soldering directly to the pin headers. The second method was selected as it proved both easier to achieve and formed a more reliable connection. However, soldering the conductive thread was the most challenging aspect of the fabrication process, and proved to be the least reliable part of the system.

The interconnect strips connect the e-strips to a DAQ, so a further connection method was required for this. Wires were soldered to the conductive threads on the interconnect strips, as this allowed the wires to be screwed into screw terminals on the DAQ (Figure 5-4D). This is not recommended for fully realised application or commercial product, but was sufficient

for this stage of development, as all evaluation was carried out in a lab or on a human participant on a stationary bicycle, rather than on a cyclist in motion.

To protect the solder joints between pin headers and conductive thread, UV curable ink (Ronascreen 1305 B) was applied on top to provide structural support and protect the exposed metal parts from sweat (Figure 5-4C). This was then exposed to UV light for curing until the ink was matt in colour, dry, and not tacky when touched.

5.2.4.5   Integration of electronics into the suit

Long fabric pockets made from the stretch scuba fabric used to make the interconnect strips were stitched onto the interior of the suit using a zigzag stitch. This created channels to house the interconnect strips inside the garment.

To create pockets to house the e-strips, stretch wasn't the only factor to consider. The fabric's thermal conductivity was also important to assess. As this fabric sits between the skin and the e-strip, it must conduct heat well to minimise error in e-strip readings. Five fabrics were evaluated (Figure 5-5A): the stretch scuba fabric used to make and house interconnect strips, a stretch purple jersey fabric, a stretch white polyester and spandex fabric, a stretch denim and a pink polycotton. These fabrics were chosen because they represent a broad range of fabrics commonly used in clothing: both natural (cotton) and synthetic (polyester) fibres, both knit (stretch) and woven (non-stretch) fabrics, and with varying thicknesses.
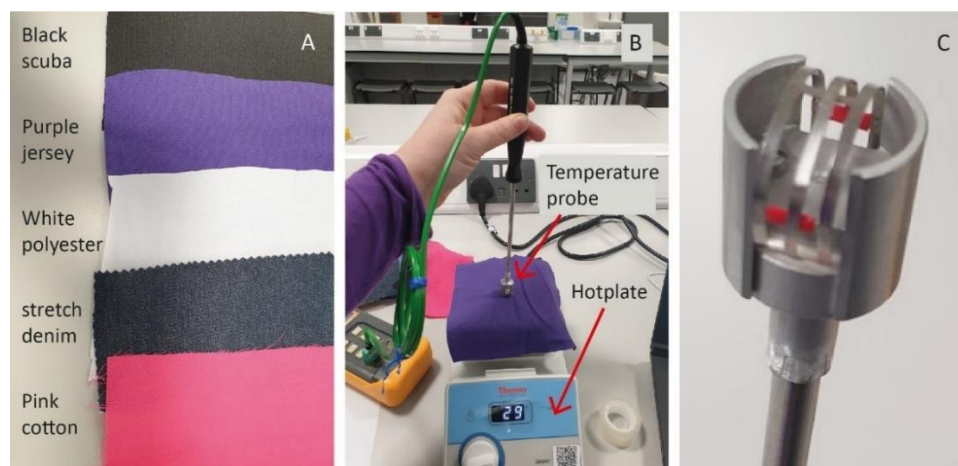
Figure 5-5. Selecting fabric to cover e-strips.
 A) Fabrics evaluated; B) Measuring the temperature offset between hotplate temperature and fabric temperature with a K-type surface temperature probe; C) Close-up of the surface temperature probe, which has spring contacts that press into the surface being measured.

First, each fabric's thickness was measured with a micrometer. Then a thermal conductivity test was performed, using a K-type surface temperature probe attached to a digital thermometer. The protocol was as follows:

1. A Thermo Scientific Cimarec+ hotplate was set to 30 °C (±1 °C approximately, as the hotplate temperature was set using a dial that didn't allow for a fine degree of control over the set temperature). This is a less accurate hotplate than the Echotherm dry bath mentioned in the previous chapter. This is due to different availability of hotplates at different stages during the project.
2. A piece of fabric was placed on top of the hotplate and left for 5 minutes to absorb heat from the hotplate.
3. The surface temperature probe was applied to the centre of the hotplate and the temperature at the surface of the fabric was measured (Figure 5-5).
4. The surface temperature probe was lifted slightly to enable the fabric to be removed, and the temperature of the hotplate surface (without fabric) was immediately measured.
5. The temperature was increased by an interval of 10 °C to 40 °C, and the protocol was repeated. This was then repeated another two times at 50 °C and 60 °C.

The fabric ultimately chosen – 0.32 mm thickness white polyester spandex blend – can be seen in Figure 5-6 and was stitched onto the trisuit the same way as the scuba fabric. A fabric clip attached to a wire was used to guide the interconnect and e-strips into the pockets (partially visible in Figure 5-6B) Small strips of porous tape were used to secure connections between interconnects and e-strips once inserted. This was implemented after the suit was first tried on by a human participant, and it was found that when the garment stretched, e-strips and interconnects could become disconnected. Sensor e-strips and interconnect strips were not glued or stitched in place once inserted, which allowed for easy replacement of sensors or interconnects. This is advantageous for prototyping but would not be robust enough to use in a commercial garment.

Figure 5-6. Integration of electronics into the trisuit.

A) Interior of the trisuit, showing how e-strip and interconnect are housed in pockets; B) Guiding an interconnect into an opening in a pocket with the help of a fabric clip attached to a long wire (not pictured); C) DAQ inserted into a pocket at the rear of the trisuit, with interconnects connected; D) Interior of the trisuit, rear view; E) Close up of fabric pockets stitched onto the interior of the suit; F) Exterior of the trisuit, front view; G) Close up of the exterior of the trisuit, where stitching outlining the interior pockets can be seen.

Another challenge to solve was how to route the electronic parts from the interior of the garment, where the sensors were located, to the exterior, where the pocket that houses the DAQ is located. As can be seen in Figure 5-6B and Figure 5-6C, slits were cut in the fabric of the suit to allow interconnects to pass from the interior of the garment to the exterior. These slits didn't create holes in the suit through which a wearer's skin could be seen, as they were aligned with the long fabric pockets stitched onto the interior of the suit. This arrangement allowed the electronic parts to be fully removable from the trisuit.

Another option for electronics integration would be to stitch conductive thread interconnects directly onto the fabric and attach connectors directly to the fabric instead of to interconnect strips. However, full and easy removal of all electronic parts was a key goal for this prototype garment, which would not have been possible using this method.

5.2.4.6   Data acquisition

An existing pocket located at the lower back of the trisuit was used to house an NI-USB 6008 DAQ (Figure 5-6C). A USB cable connected the DAQ to a laptop running a LabVIEW script, converting the voltages measured from the sensors into temperature readings, and plotting each sensor's temperature reading in real time. Voltages recorded by the DAQ were converted to temperature values in LabVIEW using Equation 6-2. Temperature values were plotted in real time and also logged in a text file for later analysis.

5.2.4.7   Validation of the e-strips

Several experiments were conducted to evaluate the e-strips. The experimental setup is shown in Figure 5-7. This involved placing them on a hotplate and varying the temperature. Sensor readings were then compared against hotplate set temperature, or the temperature recorded by a commercial digital thermometer with a K-type thermocouple probe.

E-strip sensor readings were recorded with a National Instruments USB-6210 DAQ and logged in LabVIEW. As it was found that the hotplate temperature varied across its surface by several degrees, the hotplate set temperature was not relied on for temperature comparisons. And for all measurements involving more than one sensor, sensors were either placed very close together, or a K-type thermocouple was used to identify two spots on the hotplate with similar (within 0.3 °C) temperatures.
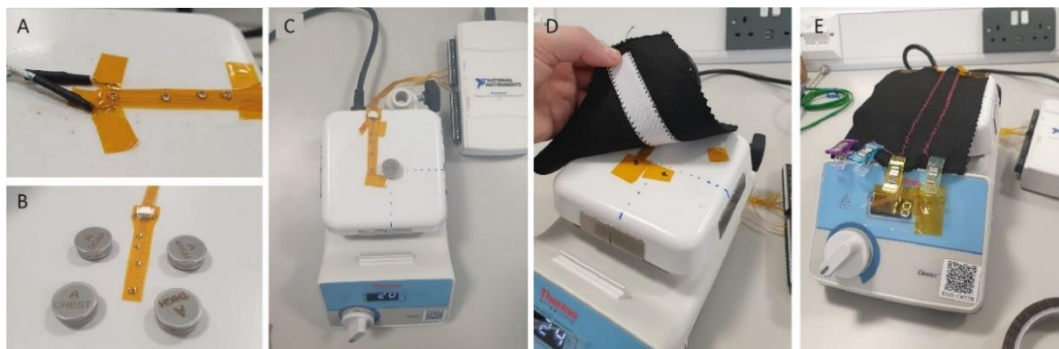
Figure 5-7. E-strip validation.

A) Comparison between e-strip and K-type thermocouple. The original intention was to use two K-type thermocouples, as shown, but one broke during testing; B) Comparing e-strip temperature readings with four Maxim iButtons, at room temperature; C) Comparison between e-strip and iButton, at varying temperature; D) Setup for comparing e-strips directly on the hotplate vs embedded in fabric. The white pocket contains an embedded e-strip; E) Setup for stretching the fabric on the hotplate surface: the fabric is stretched by fabric clips taped to the hotplate.

As can be seen in Figure 5-7, a different connector was used on e-strips used for evaluation, and a flexible cable is used to connect e-strips to a DAQ, rather than using the stretchable interconnects. This was done to isolate the e-strip and evaluate its performance alone, to compare against later tests of the full garment on a human participant.

The following experiments were conducted:

1. Comparison with a k-type thermocouple: the hotplate temperature was raised to 50 degrees, and then turned off. Temperature readings from an e-strip and a k-type thermocouple were both recorded, to compare the e-strip against a commercial sensor.

2. Comparison with a Maxim Integrated iButton: As iButtons are commonly used to measure skin temperature, an iButton and an e-strip were placed on the hotplate. The hotplate temperature was varied from 30 °C to 50 °C in steps of 10 °C, with periods of 10 minutes in between each step. The process was then reversed, returning to 30 °C.

3. Investigation into the impact of fabric between sensor and skin: Two e-strips were placed on the hotplate, one directly on the hotplate surface, and another embedded in a pocket of fabric, as in the sensing garment. The temperature was varied as in the previous experiment. This was done three times, with the fabric relaxed, stretched by 10%, and stretched by 20%. Fabric strain was measured with a steel ruler, using stitches on the fabric as a guide.

In all cases, sensor readings (e-strip and thermocouple, or e-strip and iButton) were taken at the same time. Two statistical tests were used to compare sensor readings. Bland-Altman and correlation plots were generated using a MATLAB toolbox [212].

The correlation between two variables, *x* and *y*, is given by Equation 6-3, where *r* is the correlation value, $\bar{x}$ and $\bar{y}$ are the sample means of the variables *x* and *y*, respectively, and x_i and y_i are corresponding data points belonging to each variable. For example, if *x* denotes an e-strip and *y* an iButton, x_i and y_i would be temperature measurements taken from the e-strip and iButton at the same time.

$$r = \frac{\sum_i (x_i - \bar{x})(y_i - \bar{y})}{\sqrt{\sum_i (x_i - \bar{x})^2 \sum_i (y_i - \bar{y})^2}}$$

(5-3)

A high correlation value indicates that there is a strong relationship between the two variables, but it is not sufficient to determine that the two measurement methods are in agreement, i.e., that one can be replaced by the other.

The Bland-Altman method is a method specifically designed to compare two measurement methods and determine the degree to which they agree. This is done by plotting the difference between two measurements against their mean. That is, $x_i - y_i$ is plotted against $(x_i + y_i)/2$. Good agreement between the two methods means that points on this graph fall between the upper and lower Limits of Agreement, defined as $\bar{d} \pm 2s$, where $\bar{d}$ is the mean of the differences between measurement methods, and s is the standard deviation of $\bar{d}$.

5.2.4.8   Human participant trials

To find out how the prototype garment would survive wear, it was tested on one healthy male participant. Testing on human participants at prototyping stage can provide valuable data on what's working and what needs to be improved. Data from testing on further participants is included in the paper mentioned in the introduction.

Maxim Integrated iButtons were attached to the participant's skin using porous tape, as shown in Figure 5-8. They were placed close to e-strip locations, but without blocking the e-strips' contact with the skin or causing the fabric of the suit to lift up at the location of the e-strips, which would have affected their performance. The iButtons each took separate recordings at a frequency of 0.1 Hz. The cycling trials took place in a humidity and temperature-controlled chamber, on a stationary bike.
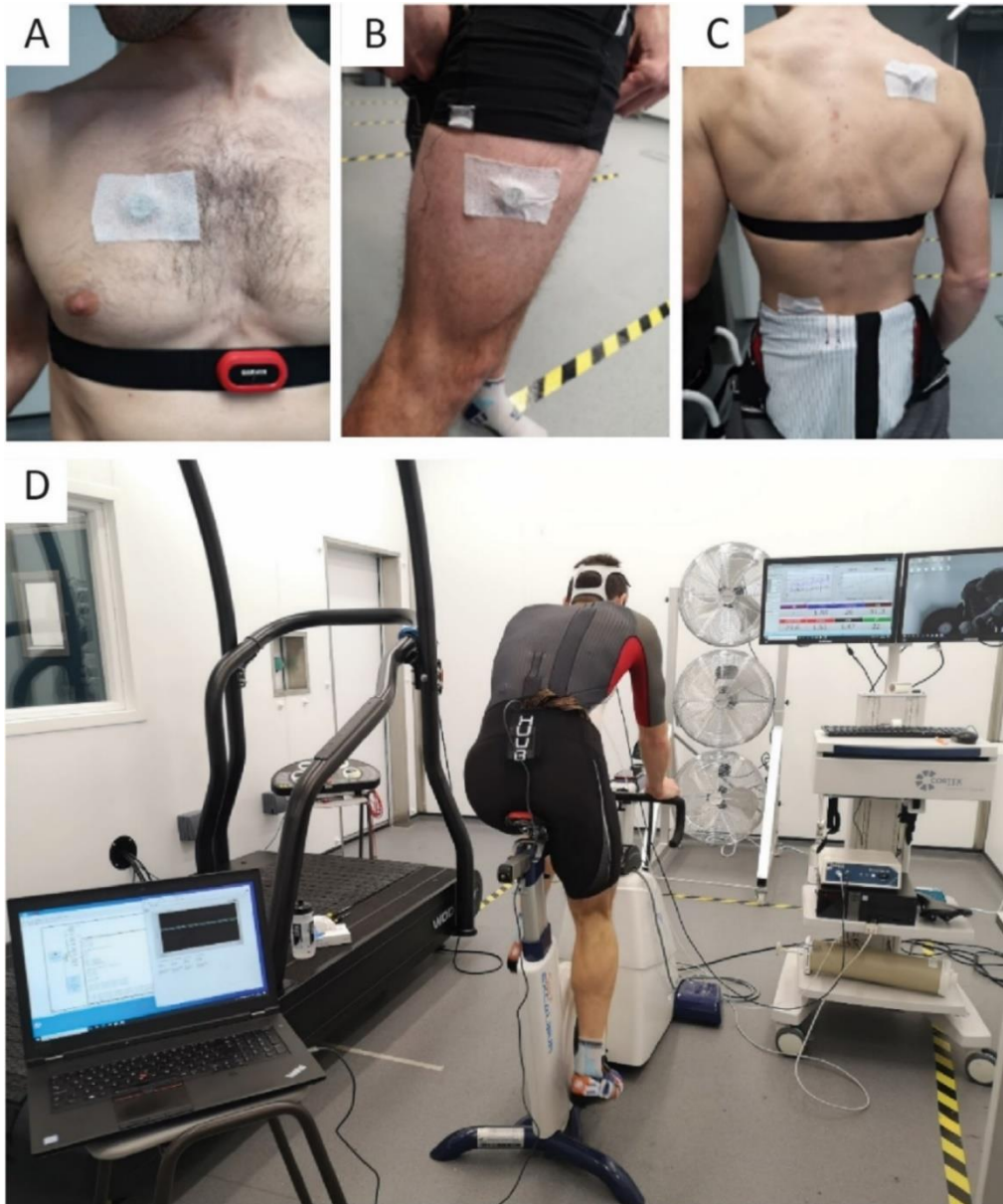
Figure 5-8. Experimental setup for human participant trials.

A) iButton attached to the chest with porous tape; B) iButton attached to the thigh; C) iButtons attached to the scapula and lower back; D) cycling trial in progress, with participant on stationary bike, and laptop recording data into LabVIEW. Photos by Danielle Lawson.

5.2.5   Results

5.2.5.1   Fabric selection

The results of thermal measurements to determine the best fabric for pockets to house the temperature sensors can be seen in Figure 5-9. Fabric thickness isn't the only variable influencing thermal conductivity[213], but in this case, increased thickness approximately corresponds to increased temperature offset (Figure 5-9A), defined as the difference

128

between hotplate temperature, and the temperature measured through the fabric. Thicker fabrics (such as the black scuba fabric) showed a greater temperature offset than thinner fabrics (such as the white polyester and pink cotton). And this effect is amplified at higher temperatures (Figure 5-9B).

The white polyester and pink cotton fabrics showed the lowest error in temperature measurement, and as a stretch fabric was required, the white polyester fabric was selected.
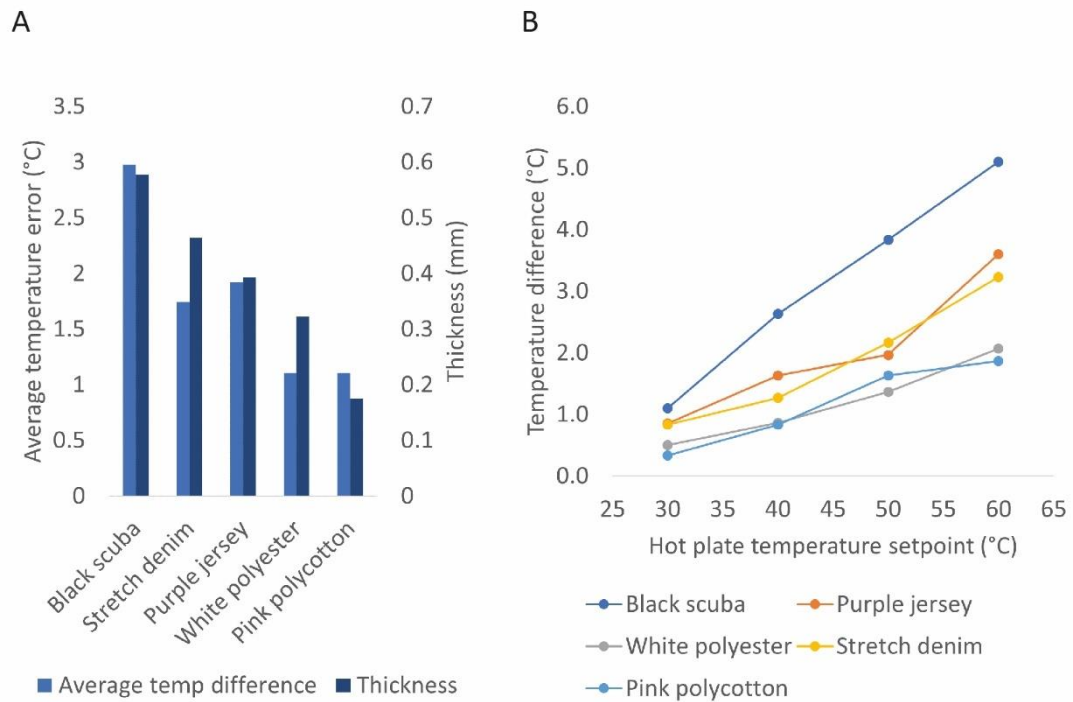
Figure 5-9. Fabric selection.

A) Plot of the thickness of each fabric, and the temperature error at the fabric surface. Thicker fabrics conduct heat less well, as expected; B) Temperature offset at different hotplate setpoints.

5.2.5.2   Validation of the e-strips

Results from the comparison between e-strips and k-type thermocouple are shown in Figure 5-10, showing very close agreement. Only one data point falls outside the limits of agreement in the Bland-Altman plot, and this is at around 50 °C, which is slightly above the top range of human skin temperature and thus not considered to be an issue.
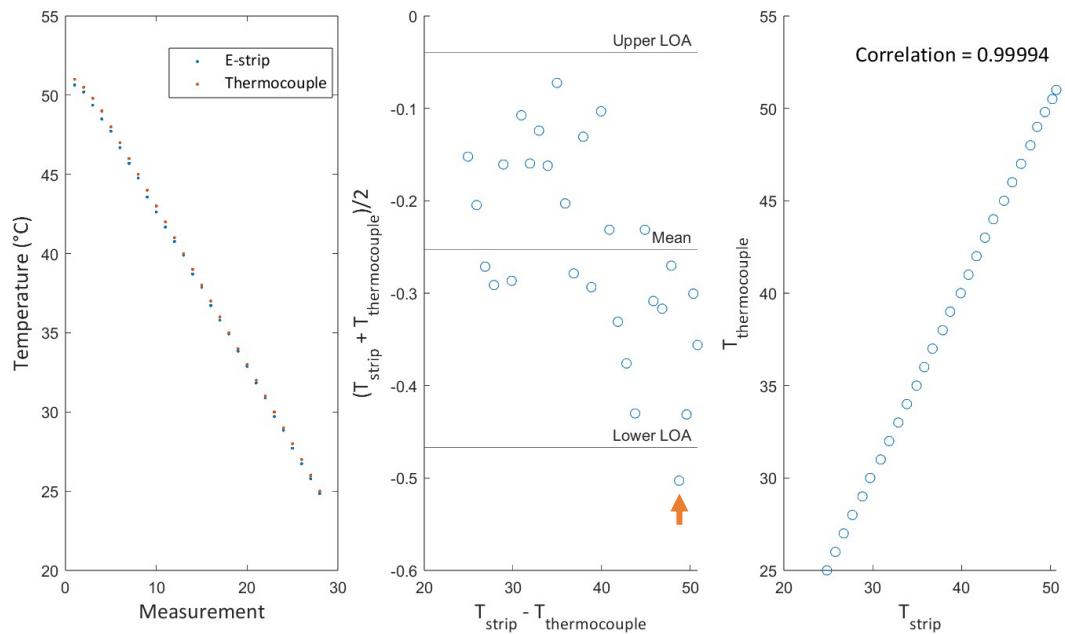
Figure 5-10 Comparison of e- strips to k-type thermocouple, showing close agreement.

Temperature measurements from both sensors are plotted (Left); A Bland-Altman plot (Middle), with arrow

pointing out the one outlier point at 50 °C; Correlation plot (Right)

Comparison between e-strips and iButtons can be seen in Figure 5-11. iButtons respond slower to temperature changes than e-strips, which may be caused by a) the iButton being thicker (5.89 mm) than the e-strip (approximately 50 μm, rising to approximately 1 mm around components). The data from the e-strips is also raw, unprocessed data, whereas it's possible that the iButton is averaging multiple readings, as this is a common technique used in sensor design. Points falling outside the limits of agreement in the Bland-Altman plot, and the wavy shape of the correlation plot, are attributed to this difference in response time. At points where the temperature was maintained constant for several minutes (35, 45 and 55 °C) the sensors are in close agreement. A comparison between four iButtons and one e-strip at room temperature is also shown in Figure 5-11, where it can be seen that there is a variation of approximately 0.3 °C between sensors, including between individual iButtons.
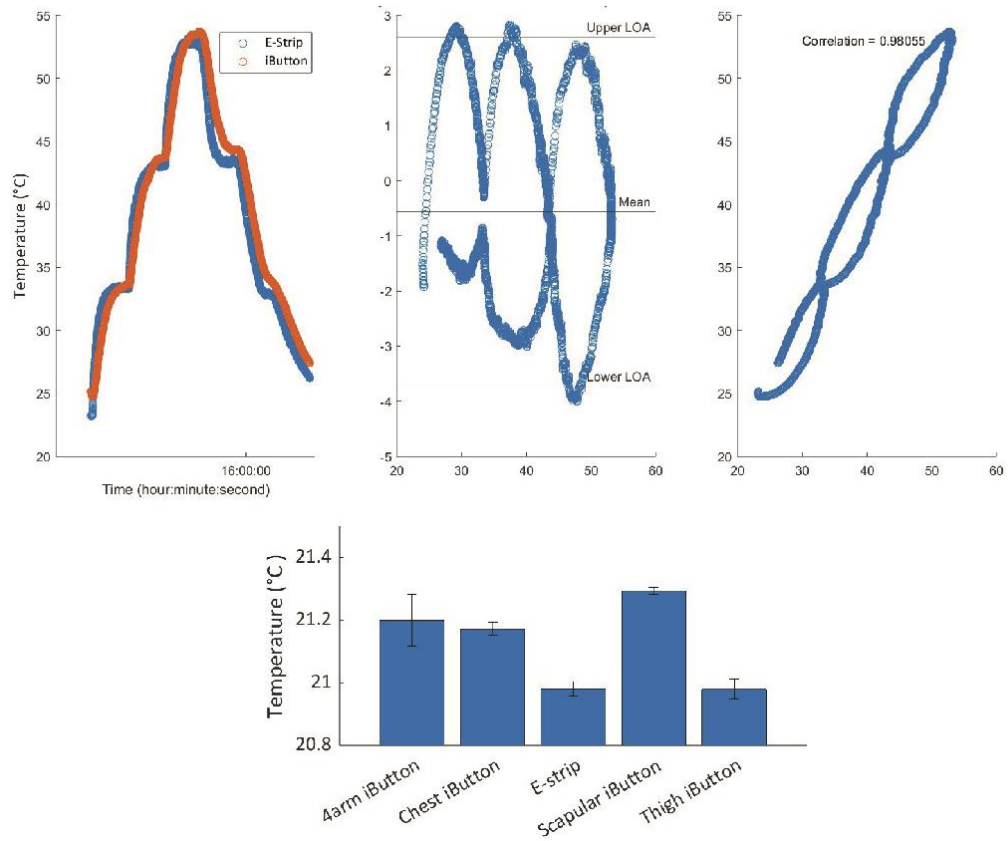
Figure 5-11.E-strip vs iButton results.

E-strip and iButton temperatures plotted (Top Left); Bland-Altman plot of e-strip and iButton temperatures (Top Middle); Correlation plot of e-strip and iButton temperatures (Top Right); Plot of average temperature readings from four iButtons and one e-strip at room temperature (Bottom). iButton labels '4arm', 'Chest', 'Scapular', and 'Thigh' refer to labels written on the iButtons used, not to locations where sensors were placed.

For e-strips embedded in fabric, in Figure 5-12 it can clearly be seen that the fabric has an impact, as does the degree to which the fabric is stretched. Stretching the fabric presses the e-strip and fabric against the hotplate surface, reducing any air gap between sensor and heated surface. The more the fabric is stretched, the closer the agreement between the e-strip embedded in fabric and the one directly on the hotplate. This lines up with previous work demonstrating that good contact between thermistor-based e-textiles and the surface they are measuring is critical for accurate measurements [205,210].
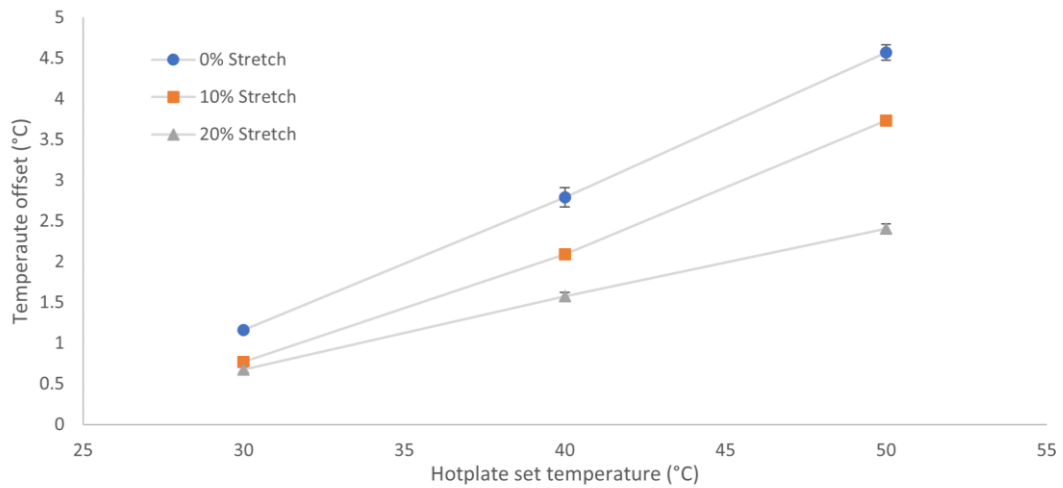
Figure 5-12. Impact of fabric on temperature reading.

The fabric introduces error into e-strip temperature measurement, which decreases as the fabric is stretched, reducing any air gap between e-strip, fabric and hotplate surface. The error is also amplified at increased temperatures. Temperature offset is defined as $T_{bare\ e\text{-}strip}$ - $T_{embedded\ e\text{-}strip}$.

5.2.5.3   Human participant trials

During the human participant trials, a few issues arose. First, when putting on the trisuit, the e-strip at the thigh location became disconnected from the interconnect. This was fixed while the suit was still on the participant, by rolling the leg of the trisuit up, re-connecting the e-strip, and applying a strip of porous tape to hold it in place (Figure 5-13).

Figure 5-13. Using porous tape to prevent e-strip and interconnect from disconnecting.

During the first trial, there were issues with unreliable data from the sensor at the chest location. This was later determined to be caused by a solder joint failure on one of the interconnect strips, where a pin header contact was soldered to a conductive thread. Other than that, data was able to be recorded from all sensor locations throughout the trials.

Overall, the participant described the trisuit as comfortable: embedded electronic parts didn't dig into their skin or restrict movement in any way.

Figure 5-14 shows the results of the human participant trials, averaged over three trials per sensor location. The results show a large difference in temperature measurement except for the thigh sensor, which reports relatively accurate measurements.
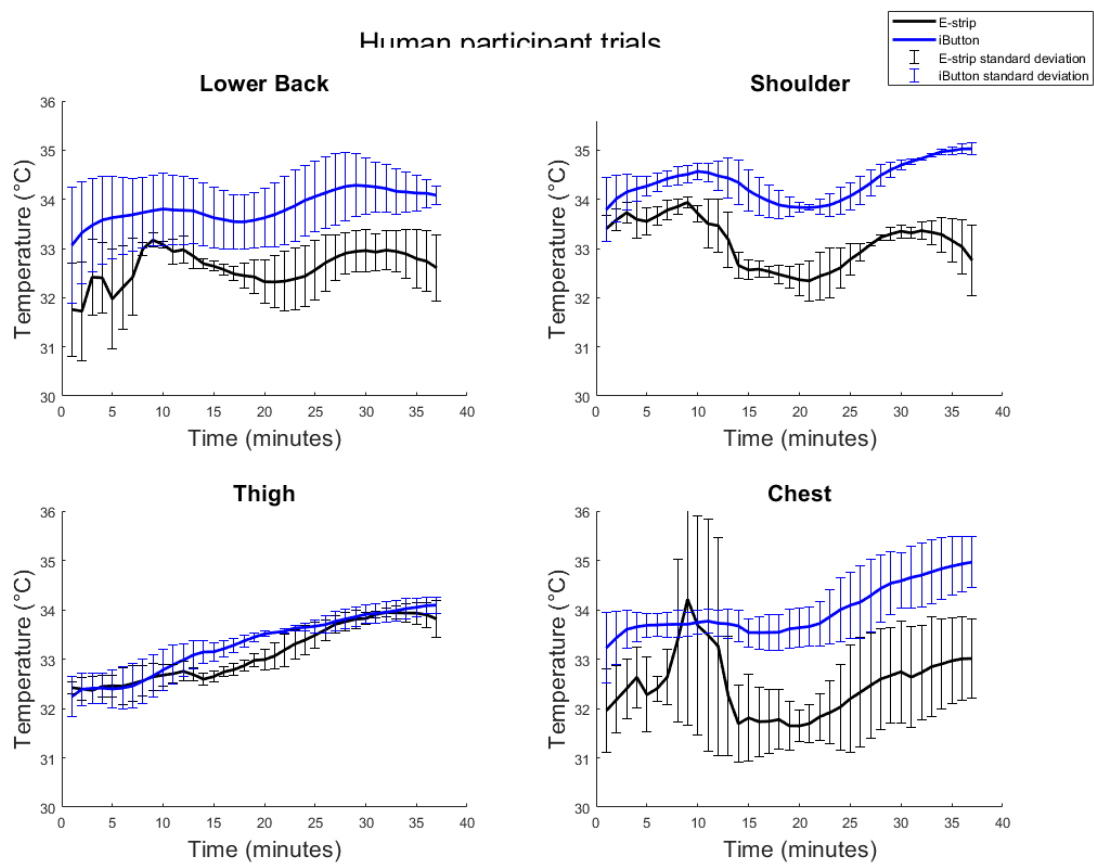
Figure 5-14. Human participant data from e-strips and iButtons.

For each sensor location, data is averaged over 3 identical cycling trials, showing individual sensor data from the four locations. Error bars represent standard deviation.

These trials also provided valuable information about the design of the e-strip. Thin PI film was chosen for the sensor substrate, to maximise flexibility and conformability to the curvature of the body. However, as the e-strips were housed in a pocket in the garment, and not secured in place, this meant that they could also fold easily, or slip out of place, particularly as the garment was being put on. As cycling garments are meant to fit tightly to the body, donning them involves the fabric stretching a lot, particularly when pulling the upper part of the garment up over the shoulders. A broken e-strip can be seen in Figure 5-15. Folds are visible at the bottom of the e-strip, next to where the connector is attached. And a close-up image highlights a small crack that has appeared along a fold line.
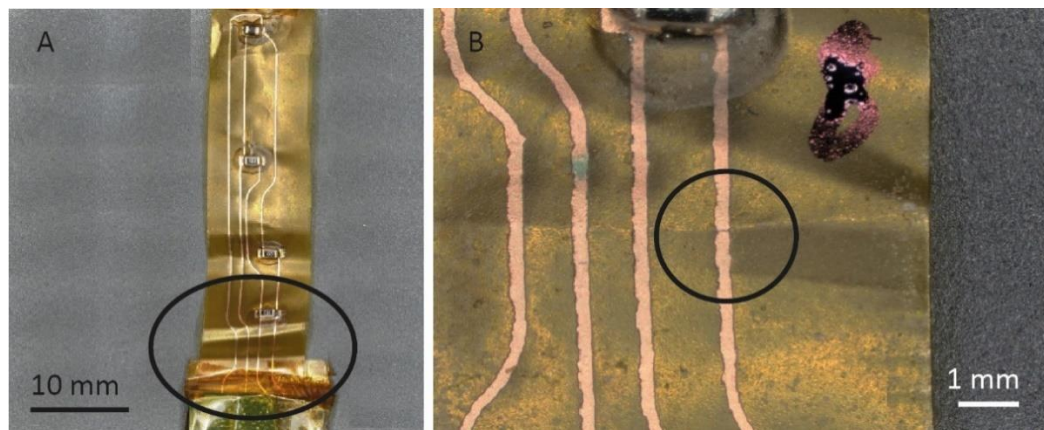
Figure 5-15. E-strip failures caused by folding.

A) Microscope image of full e-strip, highlighting folds that have appeared next to where the connector is attached; B) Close up of the area where the failure is located. A crack in the copper can be seen, located along a fold in the PI film.

5.2.6 Discussion

5.2.6.1 Fabrication of the suit

The modular design of the sensing trisuit proved highly useful for prototyping the garment, as it allowed for changes to be made without taking apart the entire system. For example, after the first human participant trial, an issue was identified with one of the solder joints connecting conductive thread to a pin header contact on one of the interconnects. To fix this, the interconnect just had to be pulled out of the trisuit, the solder joint fixed by removing the encapsulation, re-soldering, and re-encapsulating, and then re-inserted for the next trial. It did not require unpicking of lots of stitching, or significant work to remove and re-insert parts.

That said, reliably connecting the conductive threads to pin headers was difficult. As the thread is copper wire braided with Kevlar thread, much of its surface is Kevlar thread, not copper wire, which makes soldering more challenging than soldering a plain wire, for example. The fact that the thread is insulated is good for sports applications, as it means that sweat from the body won't cause short circuits. However, this also makes it difficult to diagnose issues with interconnects. And it means that each track on an interconnect needs to be stitched with one continuous thread: just stitching two threads together is not enough to make electrical contact between them.

The fact that tape needed to be applied to the interfaces between e-strips and interconnects also highlights the need for connectors in modular e-textile systems to have a latching mechanism, or some other method to keep them connected when the garment stretches, while still allowing parts to be reconfigurable.

5.2.6.2   Sensor location and impact on performance

As seen in Figure 5-14, the thigh e-strip reports the closest agreement to the iButton. At the other locations, there is a larger offset in temperature readings, and overall lower agreement between the two methods. This raises interesting questions about where on the body temperature sensors can be placed, for accurate readings. Once on the body, the thigh sensor isn't subjected to much dynamic bending or stretching, and due to the curvature of the thigh, it is pressed tightly against the skin.

The sensors on the lower back and chest, by contrast, can move around significantly depending on the posture of the body. Figure 5-16 illustrates the case of the lower back: in the cycling position, where the cyclist is bent forward, the convex curvature of the spine stretches the fabric, and brings the sensor in contact with skin. In the standing position, the lower back exhibits concave curvature, and the fabric, and therefore the sensor, is lifted away from the body, which introduces an air gap between the sensor and the skin. This will introduce error into the sensor readings.

A similar effect happens with the chest sensor: when in the cycling position, the cyclist's shoulders round forward, which can cause the fabric in the chest area to wrinkle and lift away from the skin. In the standing position, with arms down by the sides, the sensor will lie more closely against the skin.
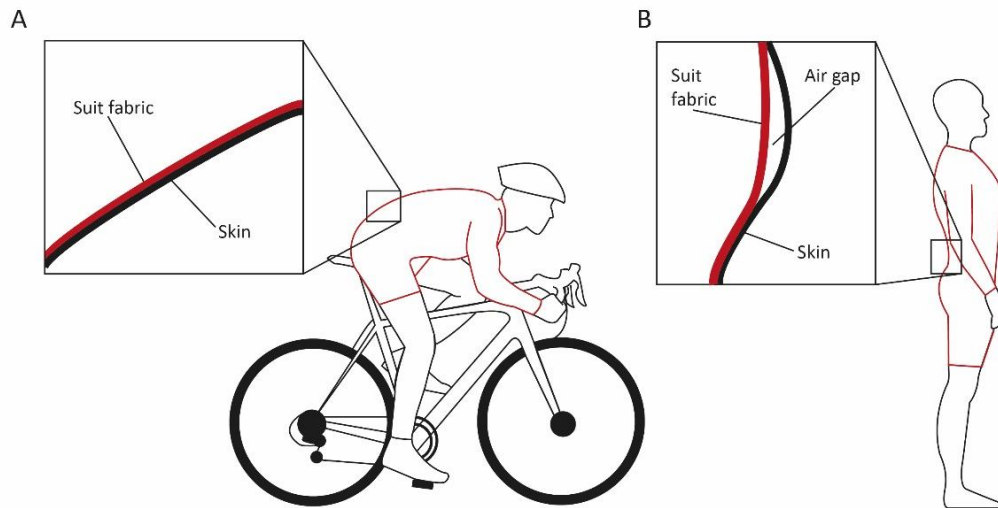
Figure 5-16. Impact of sensor location on accuracy.

A) In the cycling position, the convex curve of the spine brings the sensor on the lower back in contact with the skin B) In a standing position, the concave curvature of the spine, combined with the tight fit of the garment, lifts the fabric, and therefore the sensor, away from the skin. This creates an air gap between sensor and skin, which introduces error into the measurement.

Detailed information on the fit of the trisuit on the participant was not collected, but if it was looser at the waist than on the thigh, this could explain the difference in sensor readings. This provides some evidence that for temperature sensing, the fit of the garment is important. To avoid sensor error, sensors should be placed in locations where the garment will make good contact with the skin, independent of posture (such as the thigh). And unless a garment is tailor made for a specific user, it may need to be calibrated periodically to ensure accuracy, both before the first use, and after any significant change in body shape.

This could be particularly important for products aimed at people who menstruate, as body weight changes during the menstrual cycle due to retention of fluids [214]. This can cause bloating, which can mean that the fit of a garment changes throughout the month. Temperature sensors would need to be carefully placed in locations that are least affected by this, and further research is needed to investigate this.

This is an important factor to consider for temperature sensors, but it's also important to note that it doesn't apply to all sensors that might be embedded in an e-textile garment. Motion sensors, for example, don't need to be directly in contact with the skin. Nor do sensors measuring properties of the environment rather than physiological signals. The

impact of garment fit on temperature sensor accuracy could also be exploited: a sensor placed on the lower back could be used to detect whether a user is standing or bent over, potentially.

5.2.6.3 Is it sustainable?

As stated in the introduction, a major motivation for using modular design in e-textiles is sustainability, as a system made of modular parts should, in theory, be easier to repair, and eventually recycle, than one that is not modular.

In terms of separating electronic and textile parts, as the electronic parts are housed in pockets in the garment, and aren't secured inside it, they can be pulled out in under a minute, leaving the trisuit free to be a) equipped with new electronic parts, b) recycled, or c) used without the electronics as a normal garment, not a smart garment.

This leaves the electronic parts: the e-strips, interconnect strips, and DAQ. As this is a modular system, these can all be quicky disconnected from each other, and if still functioning, can be used to construct a new sensing garment (perhaps in a different size, or a different type of garment). And in terms of repair and recycling, each is different:

- DAQ: This is a commercial, rigid electronic device, which can be recycled using existing Waste Electrical and Electronic Equipment (WEEE) recycling processes. As it is a wired device, it would need to be replaced by a smaller, wireless control module if this system were made into a commercial product. However, this would also be a rigid device so could be reused or recycled in the same way. As there is a well-established repairs industry for rigid electronics, this module is also likely repairable.
- Interconnect strips: This part can be repaired if broken. Broken solder joints can be re-soldered, and damaged threads can be removed and re-stitched. For recycling, some further separation is required:
  - First, both ends need to be cut off, to separate the electronic parts (connectors) from the textiles. These could be further disassembled to try and reuse the connectors, but are more likely to end up as waste as this would be time consuming.
  - This leaves the strip of fabric with conductive thread stitched into it. The recyclability of conductive threads is unclear, but as many textiles contain metal parts, this could be processed through textile recycling. Alternatively,

137

if the threads are intact, they can be unstitched. They could then be reused, or the copper wires harvested for another use.

- E-strips: Repairs are possible if the failure is caused by a solder joint breaking, or a faulty connector. If the failure has involved cracking or delamination of the copper tracks, this is considerably more difficult to repair. If a broken e-strip needs to be recycled, the following steps could be taken:
    - The encapsulation on e-strips can be peeled off, or soaked off with acetone, making the components accessible. This cannot be reused.
    - The resistors soldered to the e-strip could potentially be desoldered and reused in another application.
    - The connector can also be pried off and reused (this is not officially recommended by the manufacturer but was done several times in this project, successfully).
    - This leaves the copper-plated PI substrate. The process for recycling this is unclear: PI can be shredded and reused, but the copper layer would likely need to be delaminated first. Overall, there is lack of end of life solutions for printed and flexible electronics [215], so at the moment, this part would likely become waste.

While reuse of components is not standard, growing interest in developing a circular economy (where resources are reused instead of discarded), as well as the recent semiconductor shortage in electronics, may be enough motivation for processes and infrastructure to be developed to support this.

Overall, there are arguments that can be made against modular systems. One major one is that a modular system has to use connectors, and this means that electronic parts are not concealed fully from the user. However, there is arguably a trade-off between seamless integration and sustainability that must be balanced. Minimisation of connector size would be desirable, but incorporating electronics into textiles to such a degree that they are undetectable creates a garment that cannot be recycled by textile or electronic recycling. And as small rigid elements such as buttons and zippers have been included in garments for centuries, it may not be necessary to remove all rigid elements from e-textiles.

5.3 Development of a novel interposer for modular e-textiles

This section looks for answers to questions and challenges encountered when constructing the modular sensing garment in the previous section. First, a solution for better connections between solderable conductive threads and connectors was explored through the development of an interposer: a circuit module that acts as a bridge between materials or components that are difficult to connect directly. In this case, rather than soldering conductive threads to pin header connectors, a flexible module was created, onto which the connector can be soldered or crimped, and featuring pads onto which the conductive thread is stitched, then soldered. Pin header connectors were also replaced by a smaller footprint connector.

5.3.1 Motivation

In the previous section, interfaces between dissimilar parts proved to be the most troublesome part of the modular sensing garment. That is, joining the solderable conductive threads to electronic connectors was challenging, and unreliable. To improve this, the following problems needed to be solved:

a) Identifying a better way to attach a connector to the conductive thread.
b) Investigating different connectors to join flexible sensors with stretchable interconnects.

A flexible interposer – a bridge between textiles and conventional components – was developed to address the first issue, and two connectors used in flexible electronics were evaluated as replacements for the pin headers. These are not reported in recent e-textile reviews [25,216–218], and are not believed to have been used in e-textiles before.

These connectors are:

a) a 'mezzanine' connector designed for joining flexible or rigid PCBs to rigid PCBs. This consists of two interlocking parts, plug and receptacle. These connect out of plane (i.e. perpendicular to the plane of the circuit boards they are connecting).
b) a zero insertion force (ZIF) connector. This has only one part and has a sliding tab which can be opened and closed. When the tab is open, a flexible circuit can be inserted into the connector. The tab is then closed, locking the flexible circuit in place.
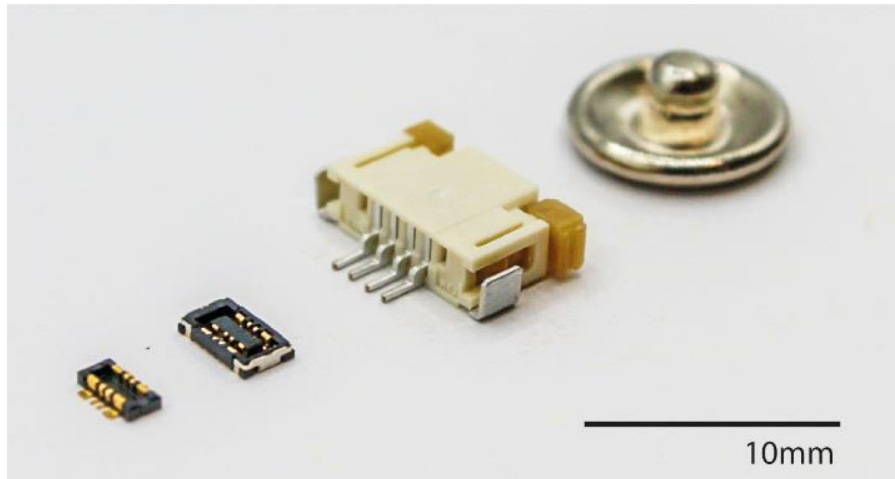
Figure 5-17. Connector comparison.

From left to right: A) Mezzanine plug; B) Mezzanine receptacle; C) ZIF connector; D) snap fastener included for comparison.

Figure 5-17 shows the ZIF and mezzanine connectors alongside a typical snap fastener. Table 5-3 compares their characteristics, highlighting that both have much finer pitch than snap fasteners. As mentioned in Chapter 2, Section 2.2.1.2, snap fasteners are the most common connector used in e-textiles, and they are well suited to applications where repeated connection and disconnection is required, such as attaching a power supply, or a rigid module that needs to be removed for washing, to flexible sensors embedded in a garment. However, as discussed in Chapter 2, Section 2.2.3.4, smaller connectors, such as these ZIF and mezzanine connectors could be used to join sensors to interconnects, to enable a 'more modular' e-textile design.

Table 5-3. Connector comparison.

Characteristic	Mezzanine	ZIF	Snap
Pitch (mm)	0.4	1	>10*
Contacts	8	4	1
Connection direction	Vertical	Horizontal	Vertical
Mating cycles	10	10	>>10*
Width (mm)	3.30	10.15	10*
Length (mm)	2.32	7.60	10*
Height (mm)	0.75	2.75	9.60

ZIF and Mezzanine connector values are from the products' datasheets. Snap fastener values are based on the example shown in Figure 5-17, which is a typical size. Dimensions were measured with a micrometer.

*Snap fasteners are not standard electronic components, and as such do not have standard pitch or maximum mating cycles but are designed for repeated connection and disconnection.

These connectors, with their fine pitch, would be difficult to connect directly to conductive threads. A flexible interposer was developed to bridge this gap. The interposer consists of copper traces on a PI substrate. Soldered to conductive tracks in fabric, it creates a detachable interface which can connect to rigid or flexible PCBs. A detachable interposer with this fine pitch and small footprint has not previously been demonstrated. This allows increased connection density and improves the wearability of an e-textile garment by minimizing rigid parts. The novelty of this work lies in this combination of detachable, flexible, and fine pitch.

Figure 5-18 illustrates interposers using the mezzanine ('the mezzanine interposer") and ZIF ("the ZIF interposer") connectors. A flexible module consisting of copper traces on PI is adhered to a PI stiffener layer. A connector is soldered to the mezzanine interposer, and adhesive encapsulation is applied on top.
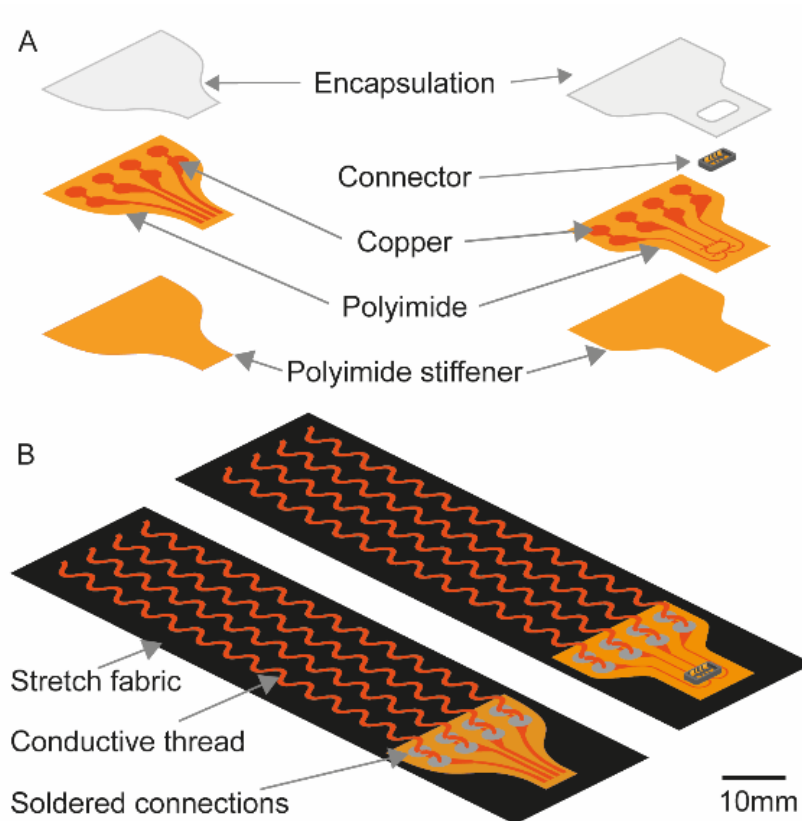
Figure 5-18. Interposer concept.

A) Exploded diagram of interposer parts. Copper traces etched on PI are supported by a PI stiffener. Both interposers are coated with a medical adhesive encapsulation. The mezzanine interposer has a connector soldered on, while the ZIF interposer features a narrow end for insertion into a ZIF connector. B) Integration of the interposers into fabric, via soldered connections to conductive threads.

141

Figure 5-18B shows interposers attached to conductive threads stitched onto fabric. In an e-textile garment this design could connect flexible sensor modules to conductive thread interconnects or interface a textile sensor with a flexible or rigid PCB processing module. As the mezzanine interposer has 8 contacts, and versions of both connectors with higher (and lower) numbers of contacts are available, scaling to more than four is possible, though this would increase overall size.

5.3.2 Fabrication of prototypes

Prototype interposers and flexible LED circuits ("LED e-strips") are shown in Figure 5-19. These prototypes were made to evaluate the interposer concept, but in a fully realized application, interposers and LED e-strips would be covered by a layer of fabric or encapsulation, ensuring that circuitry conforms to the garment.
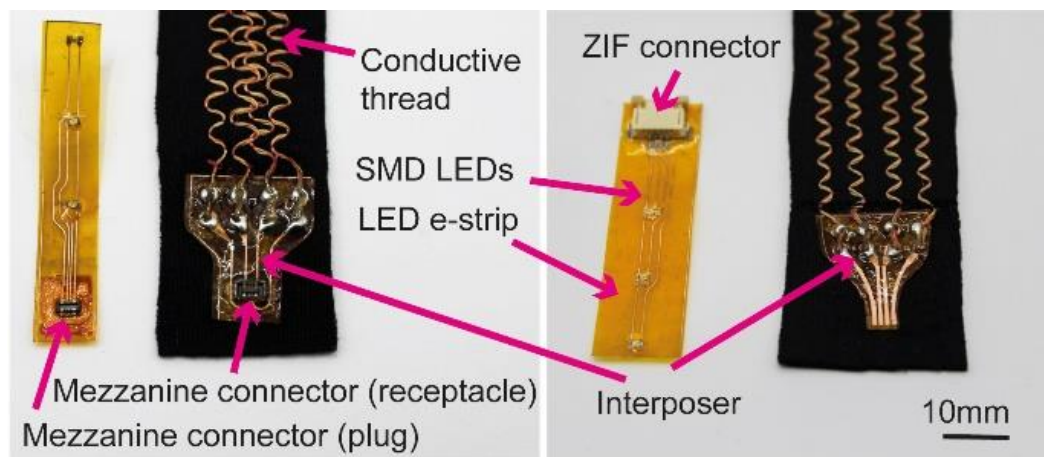
Figure 5-19. Prototype interposers and LED e-strips with corresponding connectors.
ZIF (left) and Mezzanine (right) interposers for interfacing flexible e-strips with conductive textiles. LED e-strips with corresponding connectors are also shown to demonstrate how the interposers may be used with flexible electronic modules. Scale bar applies to both sections of the figure.

5.3.3 Interposer and LED e-strip fabrication

Copper-plated PI film (copper thickness: 18 μm, PI thickness: 25 μm) was etched using the toner transfer process explained in Chapter 3, Section 3.1.2.2. After cleaning with acetone, a Roland CAMM-1 GS-24 vinyl cutter was used to cut out individual interposers, and to fabricate a solder paste stencil from 127 μm thick PI film. The stencil was used to apply solder paste to attach connectors to the mezzanine interposer, and connectors and SMD LEDs to the LED e-strips. Components were placed with a Fritsch LM-901 pick and place machine and soldered using a hot plate.

A 127 μm thick PI stiffener layer was adhered to the bottom of each interposer using a flexible medical adhesive from Dymax (mentioned in Chapter 3, Section 3.1.4), for structural support. Without this, the interposer is too thin and can crease when the fabric bends, causing cracks in copper traces (as seen in Chapter 5, Figure 5-15). However, using a thicker copper-plated PI would remove the need for the stiffener. The adhesive was cured at 150 °C for 45 minutes in an oven. UV curing is also possible with this adhesive, but heat curing was chosen as PI reflects UV light, meaning that UV curing is not effective for adhesive sandwiched between two layers of PI. A small amount of cyanoacrylate adhesive was applied around the mezzanine connectors on interposers and LED e-strips to protect the solder joints and prevent the connectors from breaking off.

5.3.4 Embedding in fabric

Zig-zag tracks of insulated conductive thread were stitched onto 100% polyester scuba jersey fabric as described in Chapter 3, Section 3.1.2.3. The ends of the threads were then hand stitched to copper contact pads on the interposers. Then, a soldering iron was used to solder the threads to the contact pads after stitching. This locally removes the insulation layer on the copper wires in the conductive thread and forms electrical contact between thread and interposer. As PI is a thermal insulator, the fabric underneath the interposer is not damaged by the heat of the soldering process, as long as the soldering is performed quickly. After soldering, a thin layer of the previously mentioned medical adhesive was applied as encapsulation on top of the interposers, though not on top of the connectors, or contact pads to be inserted into connectors. The adhesive was cured on a UV conveyer belt until dry and no longer tacky when touched.

5.3.5 Mechanical testing

Electronics embedded in garments are subjected to mechanical stress as the body moves, and a range of mechanical tests can be used to simulate this movement and assess durability.

5.3.5.1 Cyclic Testing

Two methods for tensile and twist testing from IPC-9204 Guideline on Flexibility and Stretchability Testing for Printed Electronics [194] were used, as described in Chapter 3, Section 3.2.1. These involve repeated stretching or twisting, and four-wire resistance measurements were used to quantify the effects of the tests: resistance increase indicates damage, i.e.

cracks in copper traces, breaks in conductive thread, or broken solder joints. A Keithley 5000 digital multimeter was used for electrical measurements, taking measurements at intervals of 100 test cycles.

A custom jig shown in Figure 5-20B was used for cyclic twisting, as described in Chapter 3, Section 3.2.1. Two aluminium clamps held interposers in place, with one rotated by a stepper motor. Three samples of each interposer type were twisted by 30 degrees in both directions, 2000 times, at a speed of 20 rotations per minute. This twist angle is suggested by Chow et al as a suitable test for e-textiles, as the human back twists on average 30 degrees during normal activity [219]. A Shimadzu AG-X Plus Universal testing machine, with a 1 kN load cell and custom acrylic clamps, was used for cyclic tensile strain tests, as described in Chapter 3, Section 3.2.1. This is shown in Figure 5-20 C.
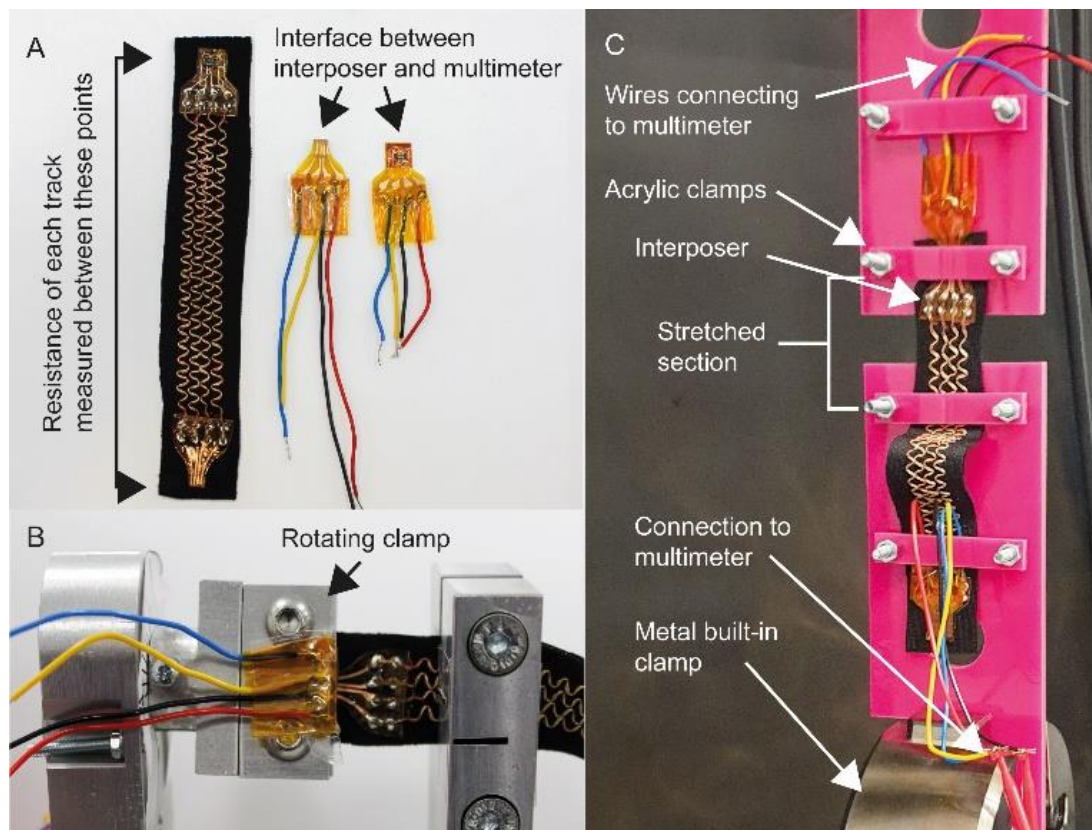
Figure 5-20. Setup for cyclic tests.

A: Illustration of resistance measurement points, and additional interposers with soldered wires used to interface with the multimeter; B: Cyclic twisting using custom jig; C: Cyclic stretching using Shimadzu AG-X Plus.

Three interposers of each type were subjected to 1000 cycles of 20% strain. This figure was determined by stretching the interposer continuously until it appeared to stop stretching, which was at around 20% elongation. This amounted a displacement of 5 mm and an approximate load of 10 N. The gauge length was constant across all samples, and as the interposer itself does not stretch, a 20% elongation over the entire gauge length corresponded to approximately 40% elongation of the fabric part of the sample. Displacement was measured and logged using Shimadzu Trapezium X software. As discussed in Chapter 3, Section 3.2.1, there aren't accepted test parameters for e-textiles, but based on existing literature, 1000 tensile strain cycles can be considered a preliminary evaluation of function and durability.

5.3.5.2   Disconnection Force Test

A further test measured the force required to separate an LED e-strip from each type of interposer. As neither connector is designed specifically for e-textile use, this serves as a preliminary assessment of their suitability. As a garment moves and stretches with the body, tensile strain will be applied to its electronic parts. It is therefore important that these parts are not easily disconnected under low tensile strain.

Figure 5-21 shows the setup for this test, using the same equipment as for cyclic stretching. Two interposers of each type were subjected to three disconnection cycles each, at a constant rate of 1 mm / minute until disconnection, with force and displacement continuously monitored by the testing machine.
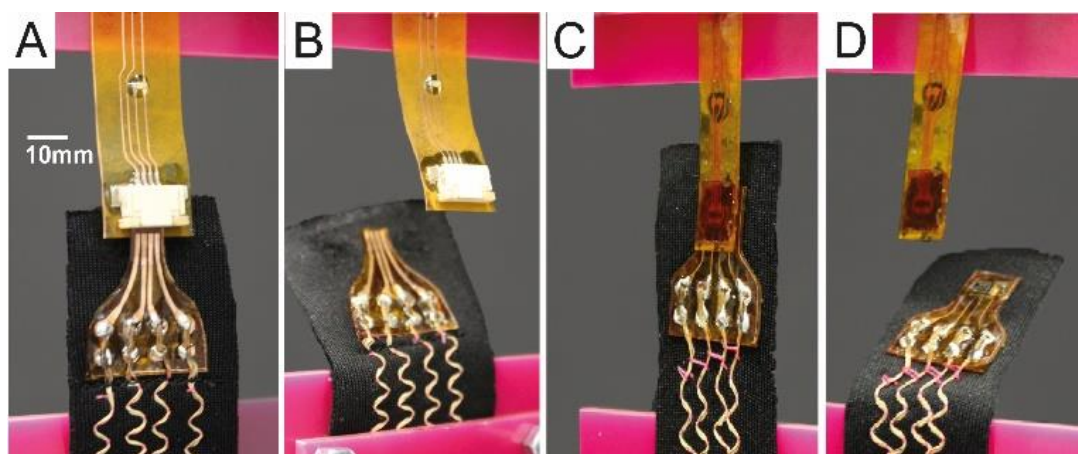
Figure 5-21. Disconnection force test setup.

A: LED e-strip connected to a ZIF interposer. B: After disconnection. C: LED e-strip connected to a mezzanine interposer. D: After disconnection. Scale bar applies to all parts of the figure.

5.3.6 Mechanical testing results

Figure 5-22 shows the results of cyclic stretching and twisting. Neither interposer showed significant change in resistance after stretching or twisting, with the resistance of each track remaining at an average of 0.6 Ω. Error bars in the graph represent standard deviation. It is believed that the variation in R is due to change in contact resistance between the multimeter probe and sample during mechanical measurements, but the magnitude of these variations is at most 0.1 Ω.
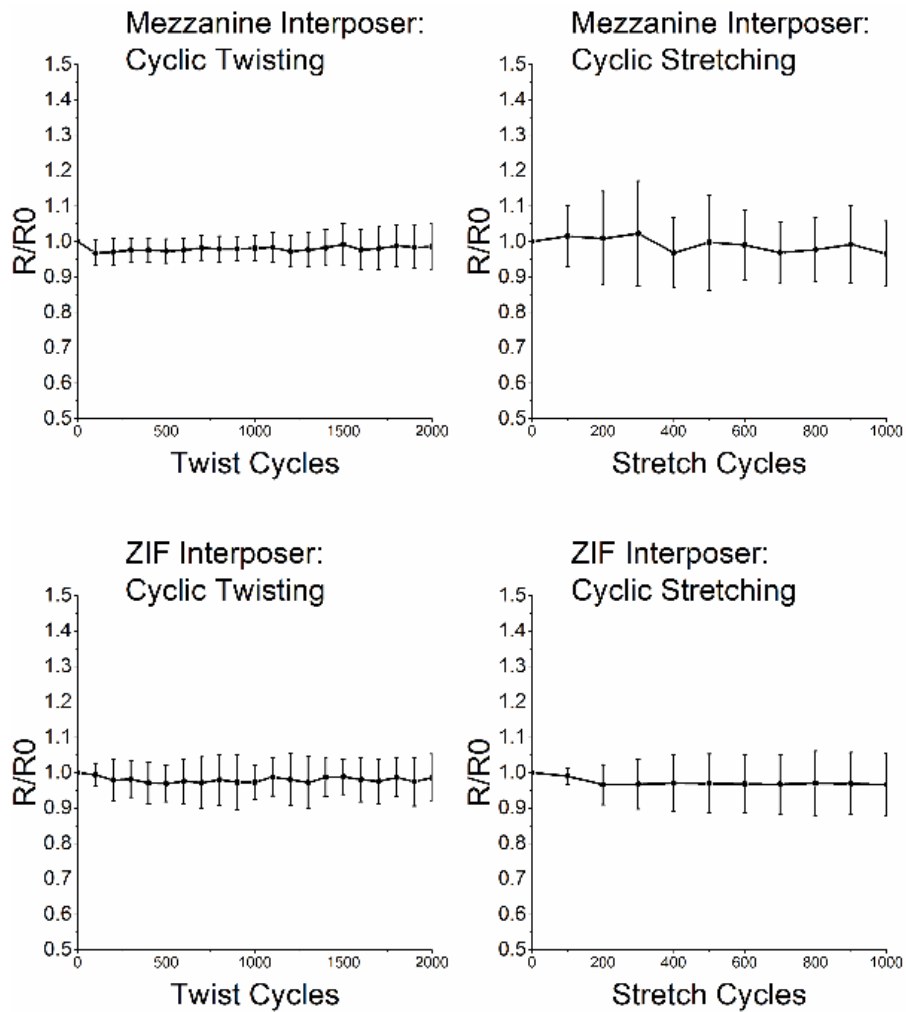
Figure 5-22. Cyclic stretching and twisting results averaged over 12 tracks.
For each interposer type, three interposers were tested, with four tracks each. Neither interposer shows significant change in resistance after 1000 tensile strain cycles or 2000 twist cycles.

In the disconnection force test, mezzanine interposers showed better performance than ZIF interposers. This can be seen in Table 5-4, which lists average disconnection force and distances, along with standard deviation. The mezzanine interposer requires significantly

higher force to disconnect, which is likely because it connects vertically, perpendicular to the direction of tensile force. However, it is expected that interposers embedded in a garment will experience forces greater than 10 N, for example when a garment is being put on, and is stretched a lot to pull it over the arms or legs. Displacement rates higher than 1 mm per minute can also be expected, for example in a sports garment, if an athlete jumps and raises their arms quickly to catch a ball. Therefore, an additional latching or securing mechanism needs to be incorporated to prevent disconnection.

Table 5-4. Disconnection force test results

Interposer	Force (N)	Distance (mm)
ZIF	1.32 ± 0.10	3.77 ± 0.82
Mezzanine	3.65 ± 0.94	4.90 ± 0.34

5.3.7 Failure Modes

Figure 5-23 shows images of mezzanine connectors taken with a Keyence digital microscope, viewed side-on so that the sides of the connector are clearly visible. Two issues are shown: a) broken solder pads between connector and substrate caused by mechanical testing, and b) excess encapsulation around the side of the plug connector, preventing it from fully interlocking with the receptacle.

Both issues can be improved by adjusting the fabrication process, for example by adjusting the amount of adhesive used, or exploring other forms of encapsulation to prevent solder joints from breaking but without excessive amounts of adhesive. No other types of failure were observed, such as undoing of stitches or deformation of interposers or threads. ZIF interposers did not suffer any failures.
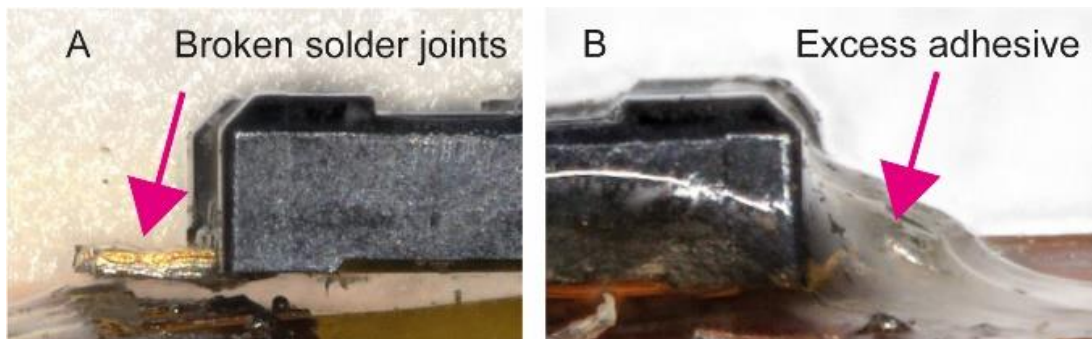
Figure 5-23. Failure modes of mezzanine connectors.
A) Broken solder joints; B) Excess encapsulation preventing plug and receptacle from interlocking.

5.3.8 Summary

Two interposers enabling detachable connection between fabric and flexible electronics have been demonstrated, using two small-scale connectors to enable a modular e-textile platform. Both interposers showed good resistance to preliminary mechanical testing but require modification or additional protection mechanisms to be robust, and washable. Mezzanine interposers have finer pitch, facilitating higher density of connections, and require higher force to disconnect them from a flexible LED e-strip, but ZIF interposers are less susceptible to failure and are easier to handle, as they are larger.

These connectors are not suitable for many connection and disconnection cycles. For such applications, snap fasteners, or electronic connectors such as pogo pins are better options. They are both rated for up to 10 disconnection cycles, though the ZIF connector was found to survive many more than this. This makes them unsuitable for attaching a power source to an e-textile garment, a process that will be performed hundreds of times in the garment's lifetime. But it does not mean that they are entirely unsuitable for e-textiles.

As discussed in Chapter 2, Section 2.2.3.4, there is potential for modular design to be employed inside an e-textile garment, for example to attach a sensing module, or an LED module, to an interconnect. These would be connected when the garment is manufactured and would only need to be detached and reconnected when the garment is being repaired or updated. In this scenario, up to 10 disconnection cycles could be sufficient. This concept can also be extended to interface with different textile tracks, e.g., printed tracks on fabric, and shows potential for the development of robust interfaces between conductive textiles and flexible circuitry.

5.4 Updating and improving the modular sensing garment

Building on the interposer designs, the modular sensing garment from Section 5.2 was revisited, and improved. As with the first prototype, the sensing garment uses four sensors to measure skin temperature at different locations on the body: shoulder, lower back, thigh, and chest. Addition of more sensors is possible, but it is desirable to minimize the number of sensors used in an e-textile garment, to reduce costs and minimize the amount of environmentally harmful materials used.

5.4.1 Overview

The update sensing garment consists of the following components:

a) control module: a PCB and battery in an acrylic enclosure, housed in a pocket on the back of the garment, and transmitting sensor readings via Bluetooth.
b) stretchable conductive thread interconnects, with interposers at each end which route conductive threads to a connector.
c) flexible temperature sensors, using the same components and circuit as in previous sections, but with some changes to materials and dimensions.
d) triathlon suit (trisuit) from Huub Design, onto which long, narrow fabric pockets are added to the interior of the garment to house the electronics.

Additional information on other adaptations to the garment that were prototyped but not ultimately used can be found in Appendix 1.

The re-designed system is depicted in Figure 5-24. The following changes were made to the original design in Section 5.2:

o Replacing the DAQ with a Bluetooth-enabled microcontroller to make the system wireless, moving it closer to a viable e-textile product able to be worn by any cyclist on any bike, not just on a stationary bike in a lab.
o Increasing the thickness of the PI film used to fabricate sensors from 25 μm to 75 μm. 75 μm is still flexible, but not enough to fold when the fabric creases. This is to reduce damage from cracks caused by folding.
o Increasing the width of the copper tracks on the sensor, to increase durability.
o Changing the connector used to interface sensors with interconnects and using an interposer instead of soldering connectors directly to conductive threads, to

149

improve the durability of the interfaces between conductive threads and connectors.

o   Updating the interconnects to make them narrower and use the same fabric as was used to construct the cycling suit itself. The same fabric was used to stitch new pockets onto the suit to house the electronics. This reduces the overall thickness of the suit, and makes the integrated electronics less noticeable.

o   Re-designing the sensor to make it shorter and adding stitching holes to sensors and interposers to secure them to the garment, to prevent sensors from disconnecting from interconnects or becoming displaced within the garment

o   Changing the orientation of the sensors, and adding strategically placed stitches, to prevent sensors disconnecting from interconnects as the fabric stretches.

o   Changing the connectors used on sensors and interconnects to reduce overall bulk and weight added by electronic parts.

Figure 5-24. Updated electronic parts for the sensing garment.

5.4.2 Fabrication

5.4.2.1 Overview

The system is illustrated in Figure 5-25, showing both sides of the garment, and the locations of embedded electronic parts.
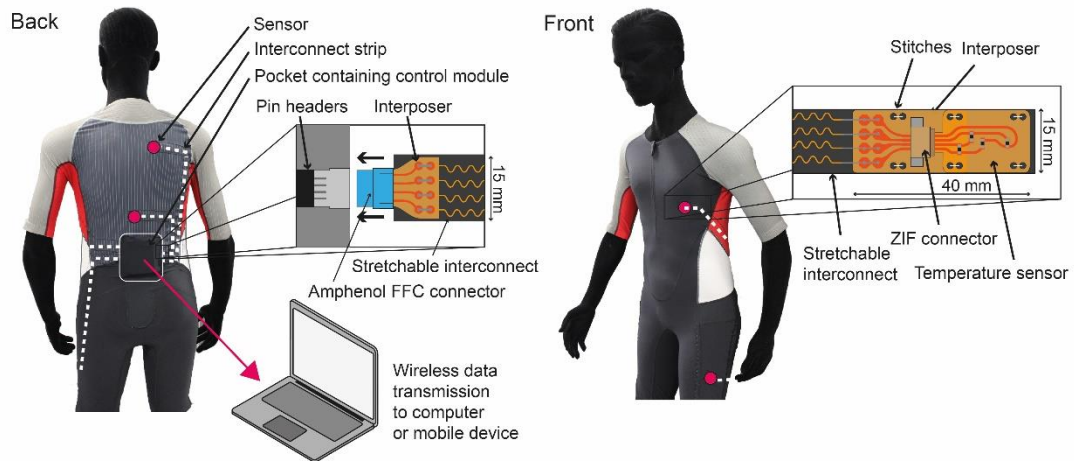
Figure 5-25. System overview, showing parts and layout of system.

5.4.2.2 Control module

Instead of the DAQ used in the previous section, this module consists of an Arduino Nano IoT 33, with an onboard Bluetooth module to enable wireless transmission of data. A custom PCB was created by etching double-sided copper plated FR4, using the dry film photolithography process described in Chapter 3, Section 3.1.2.2. Holes for vias and through hole components were drilled using the drill function on a Voltera V-One dispenser printer, and copper rivets were used to create vias connecting both sides of the PCB.

An enclosure was made for the PCB by laser cutting, stacking, and screwing together several layers of 3 mm acrylic sheet, as illustrated in Figure A-1 in Appendix 1. In a commercial application this case could also be 3D printed or injection moulded.

The control module is relatively bulky (85 mm x 65 mm x 27 mm). It is smaller than the DAQ in the previous iteration of the sensing garment, but could be further reduced in size. However, it sits in a pocket on the lower back, where such a garment will typically have pockets, often packed full of items such as bike tools or snacks. That is, it is normal to carry rigid, bulky items in this area of the garment, so for a cycling garment this is the optimal location for a rigid module.

5.4.2.3   Stretchable interconnects

Conductive thread was stitched in a zigzag pattern on strips of one of the fabrics used to make the trisuit. This fabric is the one of the differences between this and the interconnects in the previous iteration, where a thicker scuba fabric was used. As the new fabric was thinner, a water-soluble backing film was used to help stabilise the fabric during sewing. Otherwise, the conductive threads were stitched using the same method as in the first iteration.

In this version, interposers are also used instead of pin headers and wires to connect interconnects to sensors, and the control module.

5.4.2.4   Interposers and Sensors

Interposers and temperature sensor e-strips were fabricated by etching copper-plated PI (copper thickness: 18 μm; PI thickness 75 μm) using the dry film photolithography process explained in Chapter 3, Section 3.1.2.2. A layer of 25 μm PI film was adhered on top using the same adhesive as in Section 5.3, to insulate the copper traces. Components were soldered in place and additional adhesive was used as glob top encapsulation for components, to provide electrical insulation and protection from mechanical strain. For the interposer connecting interconnects to the control module, Amphenol FCI Clincher connectors were attached by crimping them onto the interposer.

The sensor-interconnect interface and interconnect-control module interface were redesigned in several ways, illustrated and depicted in Figure 5-26:

- Addition of stitch holes (Figure 5-26A): Small holes were cut in the PI, placed to allow sensors and interposers to be stitched to each other after connection, and to the fabric of the interconnect strip. These stitches are easily removable if a part needs to be replaced but are also designed to keep the sensor and interposer connected when the garment stretches and bends.

- Instead of using pin header connectors to join sensors to interconnects, these were used instead to join interconnects to the control module. This is a more wearable solution than the wires used in the first iteration to connect the DAQ to the interconnects. This interface does not feature stitching holes, as the control module should be able to be disconnected from the trisuit for washing.

- Compared to the original interposer design in Section 5.3, the ZIF connector is on the sensor instead of the interposer. The ZIF connector was used instead of the mezzanine connector, as it proved more durable and easier to use in Section 5.3.
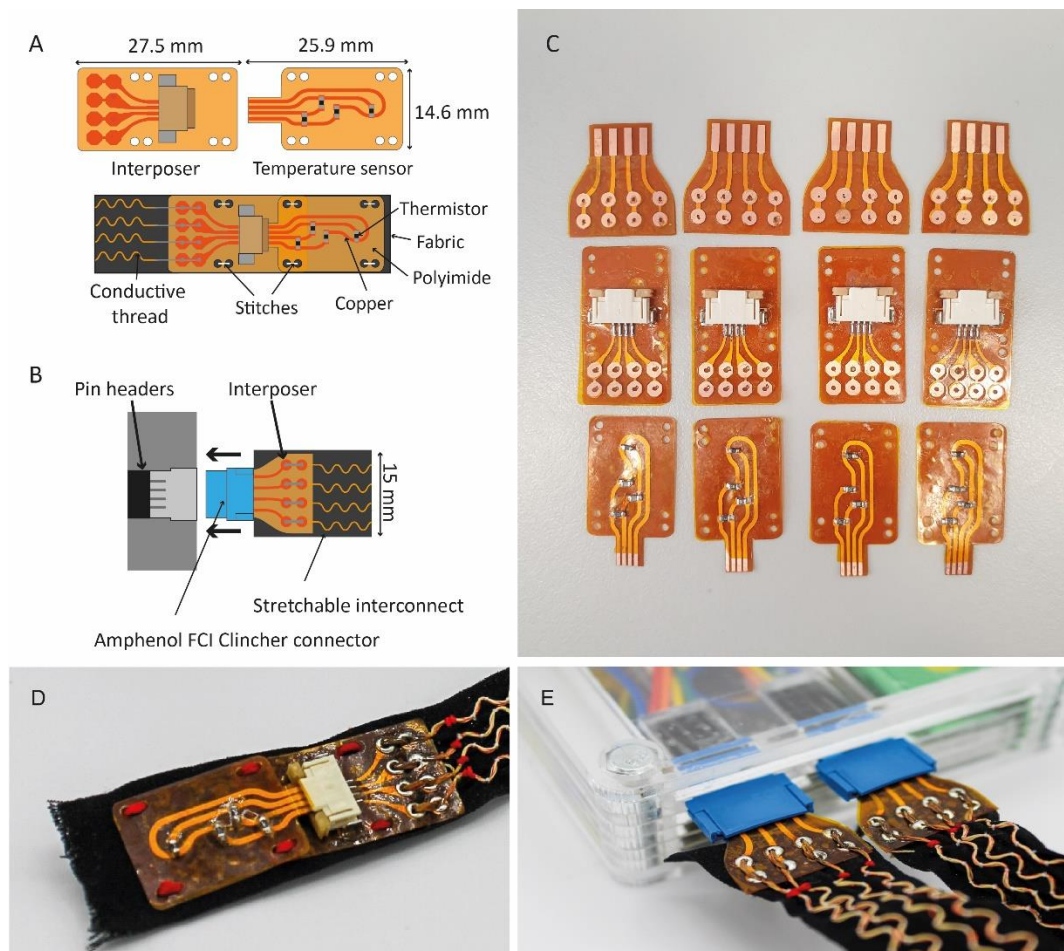
Figure 5-26. Updated sensor and interposer design

A) Illustration of the temperature sensor and its interposer, showing how stitching holes are included in the design; B) Illustration of how the other interposer interfaces with the control module via pin header connectors. Stitching holes are not included in this interposer as the control module should be detachable; C) Image of fabricated interposers and sensors, with all components attached apart from the Amphenol Clincher connectors; D) Assembled sensor and interconnect; E) Other end of the interconnect connected to the control module.

5.4.2.5 System assembly

Long strips of fabric approximately 17 mm wide were stitched onto the trisuit to create channels to conceal interposers and sensors, as in the first iteration, but this time using the same fabric as was used to construct the trisuit. Again, this approach was chosen over stitching the conductive thread directly onto the suit as the conductive threads contain copper wires and may not be compatible with textile recycling.

The layout of the electronic parts is illustrated in Figure 5-27. Interconnects were made in long straight strips and folded to bend around corners. This means they can be cut to size to fit different garments and reduces fabric waste relative to cutting curved shapes. Many sports garments are tight fitting, with significant stretch in the vertical direction as the garment is put on. Interfaces between sensors, interconnects and control module are thus oriented horizontally, to reduce strain on these interfaces and avoid accidental disconnection during the garment donning process (this having happened during human participant trials in the first iteration, with the previous iteration of the garment).

Interconnects and sensors are routed along seams, where possible, as these areas are less stretchy and may therefore provide more structural support.
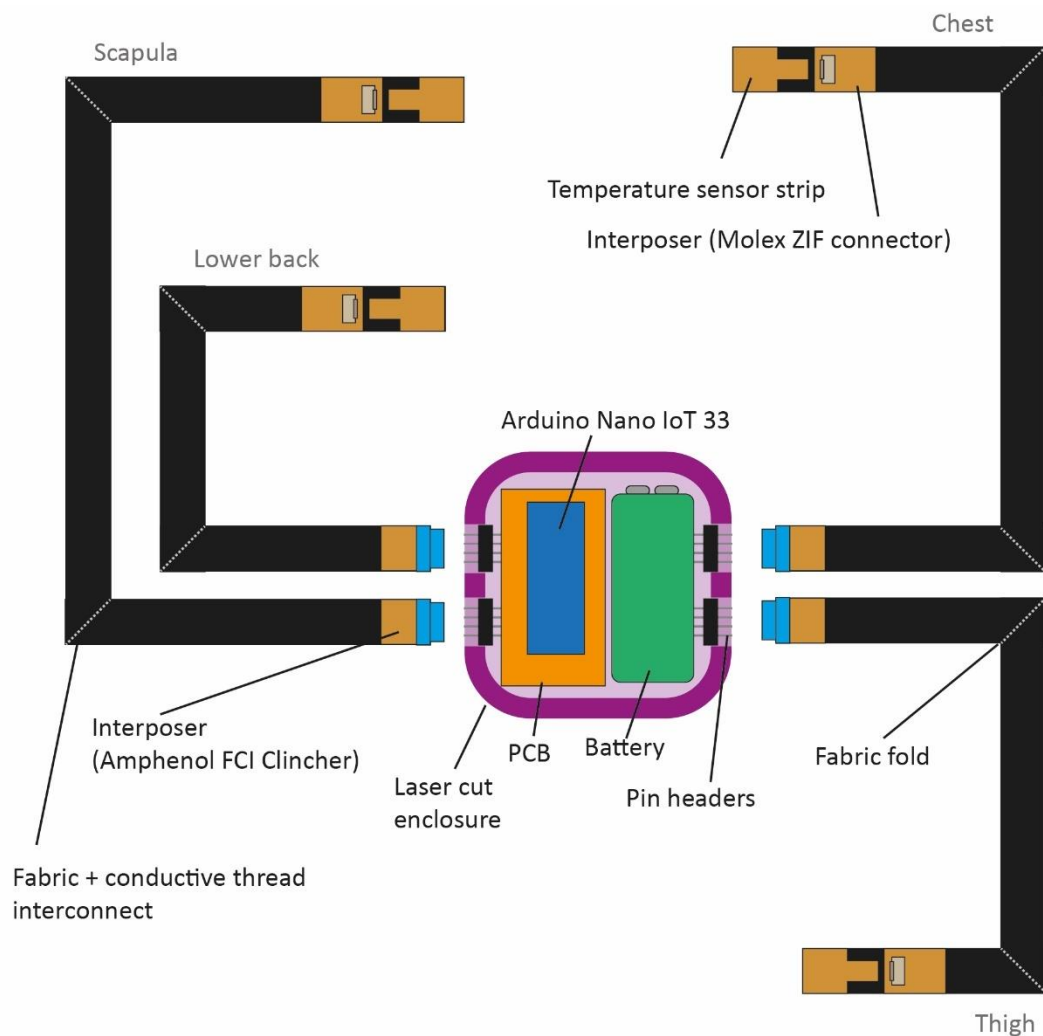
Figure 5-27. Layout of the electronic parts of the system.

Interconnects are folded to form corners, rather than cutting them in angled shapes, to minimise waste material.

The system assembly steps are listed below, with steps 6 to 8 shown in Figure 5-28.

1. Interconnects were cut to size and an interposer stitched to each end.

2. Stitched connections created in Step 1 were soldered.

3. Adhesive encapsulation was added to solder joints and cured using UV light.

4. A temperature sensor was attached to each interconnect.

5. Stitches were added to secure sensor and interposer in place. Hand stitching was used but machine stitching is also possible.

6. Each sensor and interconnect were inserted into a pocket using an elastic guide, a low-cost tool for inserting elastic into textiles.

7. The open end of the fabric pocket by each sensor was stitched shut, concealing the sensor inside the garment, and securing in place by also stitching the end of the interconnect strip onto the garment.

8. The control module was inserted into a pocket on the back of the garment, and the interconnects were connected to it.
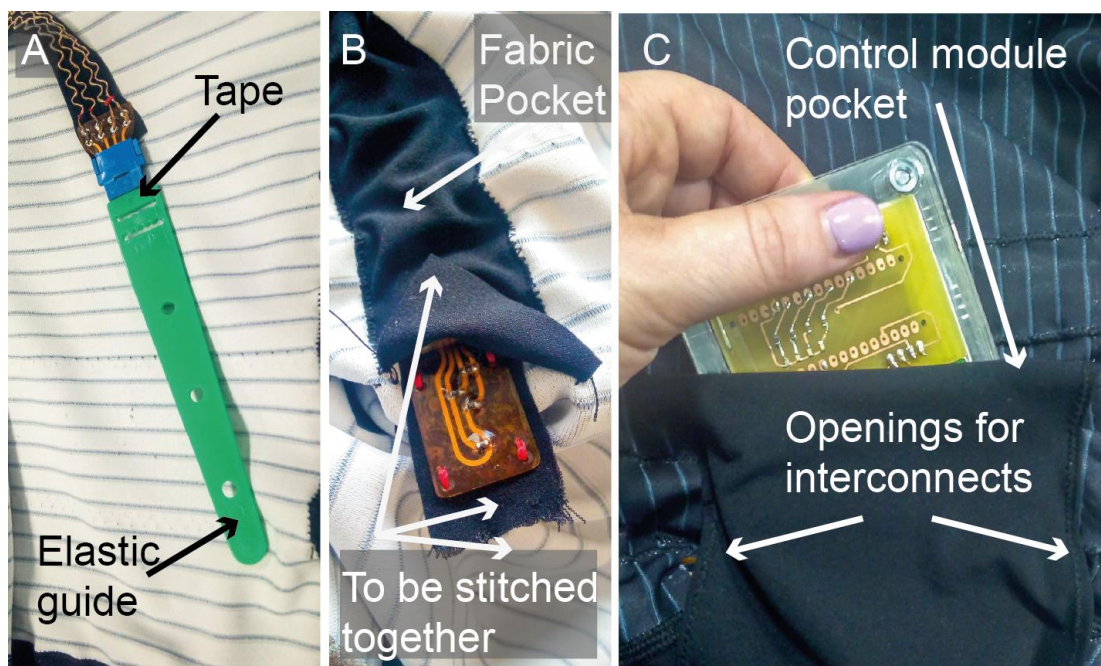
Figure 5-28: Inserting electronics into the garment.

A) Elastic guide taped to an interconnect to guide it into a pocket; B) Sensor in place, showing where fabric will be stitched; C) inserting control module into pocket.

5.4.3 Evaluation methods

5.4.3.1 Mechanical testing

A Shimadzu AG-X universal testing machine was used to carry out two tests, as already covered in Chapter 3, Section 3.2.1. These tests evaluated whether the sensor and interconnect remained connected and functional when subjected to mechanical strain.

1. Stretching an assembled sensor and interconnect up to a load of 10 N, approximately 30% strain. As in Section 5.3.5, the maximum strain amount was determined by stretching an assembled sensor and interconnect up to the point where they stopped extending. This happened at approximately 30% strain.

2. Bending an assembled sensor and interconnect to a bend radius of 17 mm, using custom 3D printed clamps.

1000 cycles of each test were performed, at a speed of 500 mm / min, to assess whether the interposer and sensor can stay connected, and therefore functioning, as the garment moves and stretches. A multimeter measured the resistance between two of the sensor's contacts during testing (effectively measuring the resistance across the Wheatstone Bridge, expected to be approximately 10 kΩ at room temperature), as disconnection or damage will cause an increase in resistance. The mechanical testing setup is shown in Figure 5-29.
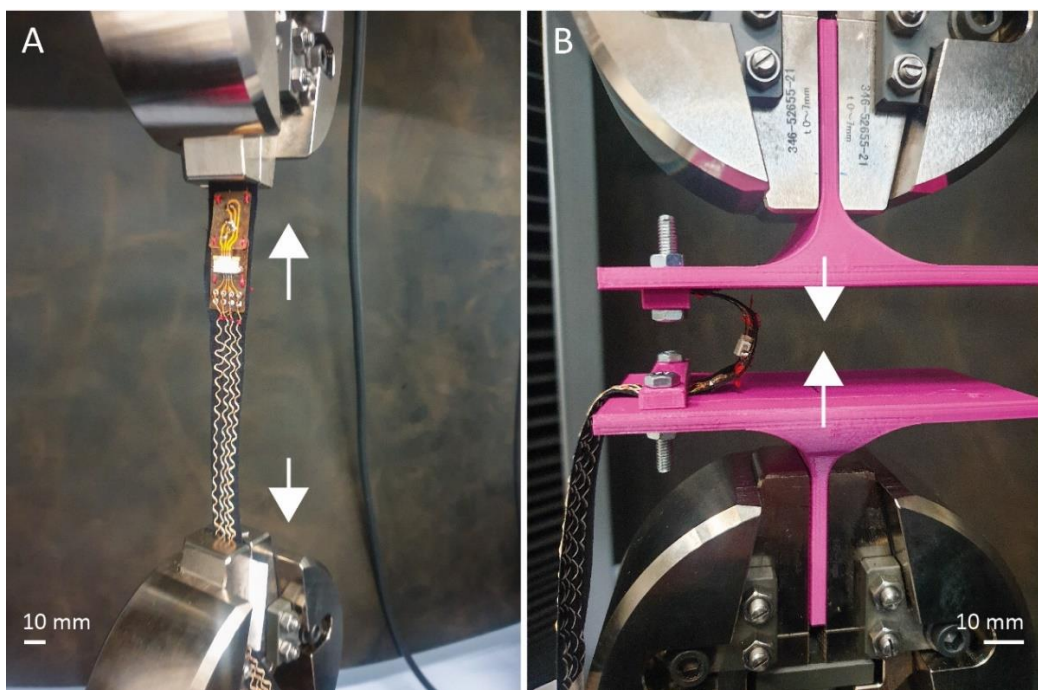
Figure 5-29. Mechanical testing setup for assembled temperature sensors and interconnects.
A) Tensile testing; B) Bend testing with custom 3D printed clamps.

Rather than attaching clamps to the sensor and interposer, one clamp grips the fabric above the sensor, and the other grips the fabric below the interposer. This aims to simulate the scenario of a garment stretching on the body, as the majority of the strain will be applied across the stretch fabric, not by the sensors or interposers.

5.4.3.2   *Validation and calibration of the temperature sensor*

An Echotherm chilling / heating dry bath was used to provide a surface of constant temperature for sensor validation. This is a much more accurate heated surface than the Thermo Scientific hotplate used in the first iteration, with an accuracy of ± 0.2 °C and a maximum difference of ± 0.3 ° C between the edge and the centre of its heated surface. It therefore allows for more accurate measurements than the experimental setup in the first iteration, and the sensors are compared against the hotplate temperature instead of a k-type thermocouple or other sensor.

Temperature was measured from two sensors simultaneously, with one fully embedded in its pocket ('embedded sensor'), and the other pulled out of its pocket so that the sensor made direct contact with the dry bath surface ('exposed sensor'). Dry bath temperature was varied from 27.5 °C to 40 °C in steps of 2.5 °C, covering normal skin temperature range. Sensor readings were recorded for 5 minutes at each step, with a 5 minute acclimatisation period after each increase. An NI USB-6210 DAQ was used for this calibration step, as it has higher accuracy than the Arduino Nano IoT 33. But as a wired system it is not suitable for an e-textile system ultimately intended to be worn while cycling.

5.4.4 Results

5.4.4.1   *Mechanical Testing*

Stitched connections between the interposer and sensor were found to be key in preventing sensors from disconnecting from interconnects: without this, a tensile load of approximately 1 N is enough to cause disconnection (as shown in Table 5-4, in relation to the initial interposer design), which is not sufficiently secure for e-textile applications. With stitches in place, bend and tensile strain testing showed no impact on the sensor's function, and no signs of damage. Resistance measurements stayed constant at 10.2 ± 0.1 kΩ, where the error is attributed to small room temperature fluctuations rather than damage to the sensor.

5.4.4.2 Validation and calibration of the sensor

Figure 5-30 shows the results of the temperature sensor validation. At each temperature interval, the average reading of each sensor is plotted against dry bath temperature. Error bars representing standard deviation are plotted, but not visible due to small magnitude (max. 0.04 °C). Calibrated readings are obtained from a linear fitting of the embedded sensor data, and these deviate by at most 0.16 °C from the dry bath temperature.
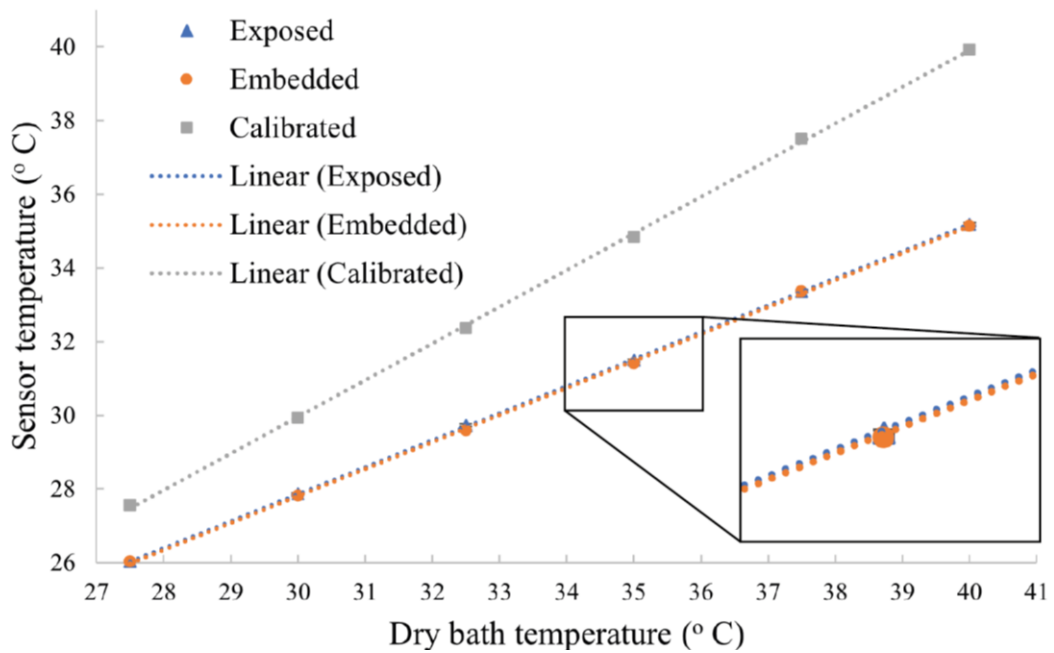
Figure 5-30: Validation of the temperature sensor.

Error bars representing standard deviation are included but invisible due to small magnitude of maximum 0.04 ° C. Inset section shows close agreement between exposed and embedded sensors.

Compared to the initial interposer design in Section 5.3, this configuration is less susceptible to disconnection, with additional (but removable) stitching to prevent accidental disconnection of the sensor from the interconnect. Although this version of the sensing garment was not tested on human participants, it was put on, and taken off, a posable mannequin several times, and the sensors and interconnects remained connected.

5.5 Summary

This chapter has explored modular design in e-textiles, building on the literature review of the subject covered in Chapter 2, and going deeper into what modular design looks like in electronics, textiles, and e-textiles.

To explore whether e-textiles can be made 'more modular' by placing detachable parts inside a garment, a temperature sensing garment for cycling was developed. This was motivated by the need for unobtrusive, real-time temperature monitoring in sports, to monitor and improve performance, and detect early warning signs of temperature-related injury. Embedding sensors in a garment removes the need for rigid temperature sensors to be attached to the body, which is the current standard.

Creating the sensing garment involved modifying an existing triathlon suit (trisuit) by adding additional pockets to it to house electronic parts. The electronic parts consisted of flexible temperature sensing e-strips, stretchable interconnects, and a USB DAQ transmitting data to a computer. These parts were connected using detachable connectors, rather than stitching, soldering, or otherwise permanently joining them.

E-strips were subjected to several tests to evaluate their performance and were shown to perform well compared to two other types of temperature sensor: a K-type thermocouple and a Maxim Integrated iButton. Inserting fabric between the e-strips and the hotplate they were tested on was shown to introduce error into the sensor readings. This error depends on how much the fabric is stretched, and is an important factor to consider when developing temperature sensing e-textiles. The sensing garment was also tested on a human participant.

The modular design of the suit meant that parts could be swapped in and out easily, and quickly. However, the fact that they were not properly secured inside the garment led to failures. So, to answer the question posed at the start of the chapter: yes, detachable parts can be placed inside a garment to make a 'more modular' e-textile garment. But for a durable garment, further investigation was needed into making those detachable connections more robust. And as the prototype sensing garment is wired, i.e. it requires a USB connection to a computer to log data, the development of a wireless version was a critical development step.

This following section documented the development of an interposer, which allows for improved connections between conductive threads and some electronic components. This was motivated by challenges faced during fabrication of the prototype sensing suit, where soldering conductive threads to pin header connectors was found to be difficult and unreliable. The manufacturer of the conductive thread, Sewiy Ltd, advised that the thread solders better when under tension, and this motivated the design of the interposer, where the thread can be stitched tightly onto a copper-plated PI circuit module, and then soldered.

This method did indeed prove easier and more reliable than soldering conductive thread directly to connectors, and allowed connectors with smaller pitch to be used, which wouldn't have been possible to connect directly to the conductive threads.

A further design update, to prevent accidental disconnection of sensors from interconnects, was the introduction of stitching holes, to secure flexible electronic modules to each other, and to the garment. But as stitches are placed in strategic locations (at the interface between sensor and interconnect, and to secure sensors and interposers to interconnect fabric) only, this should allow for electronic parts to be disconnected or separated easily. It isn't necessary to rip out an entire seam, for example, to access and replace parts.

Seamless integration of electronics and textiles is often seen as the goal of e-textiles, where electronic parts are indistinguishable from textiles, but this conflicts with the need to minimize negative environmental impact. If electronic parts are entirely undetectable, it is unclear how they be can removed at the end of the garment's lifetime, or accessed if a part needs to be repaired. A modular design requires – with current technology – slightly different circuit elements including larger components that might be easily detectable by a user. But as stated earlier in this chapter, it is common for clothing to include rigid elements, such as buttons and zippers, so it may not be necessary to remove all rigid parts from e-textiles. While the development of new materials and technologies will enable future e-textiles to be both seamlessly integrated and recyclable, the system proposed here is achievable with current technology, using well established manufacturing techniques in electronics and textile industries, and only requiring specialist e-textile knowledge at the final assembly step.

Chapter 6　Helical E-strips: Stretchable Electronics Enabled by 3D Helical Structure

6.1　Introduction

As set out in Chapter 2, Section 2.3.1, the development of stretchable electronics technology is critical for the commercial success of e-textiles, as many textiles, including those used for sportswear and medical garments, are stretchable. To date, there have been many demonstrations of flexible e-textiles, but very few stretchable. And while there are stretchable electronics technologies – stretchable conductive inks, flexible materials formed into serpentine and zigzag geometries that enable stretch – these have durability limitations.

Another alternative is to use a helical structure, which has been used to create stretchable interconnects or single printed components. In this chapter, a fabrication process is demonstrated to realise fully helical circuits ("helical e-strips"). This was first tested on blank helical e-strips with no components or conductive tracks, to determine design rules for fabrication and optimal geometry. Next, conductive tracks were added to form helical interconnect e-strips and subjected to tensile testing to assess how stretchable they were. The majority of the fabrication steps used standard processes and materials used in flexible electronics manufacturing, in order to minimize the need for custom equipment and materials, enabling an easy transition from low volume fabrication of prototypes to high volume commercial production.

The basic concept is presented in Figure 6-1.
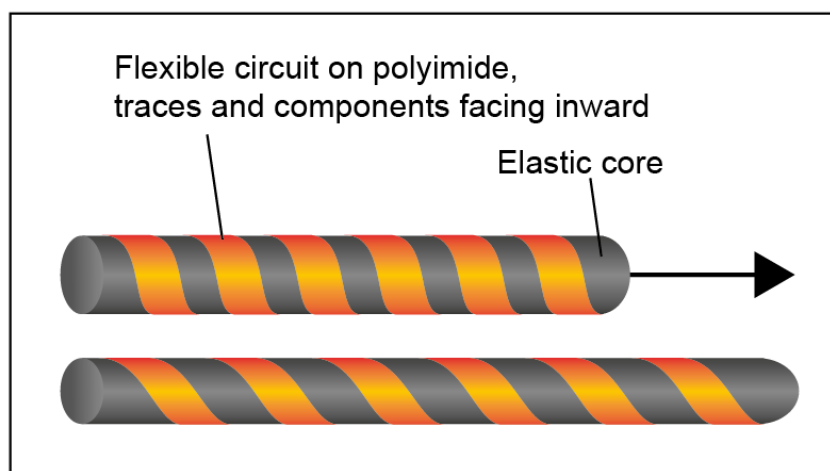
Figure 6-1. Illustration of fundamental helical e-strip concept

In the development of the helical e-strip, the objectives were as follows:

- Develop a fabrication method for helical e-strips, using standard flexible electronics manufacturing processes where possible, or processes that can be easily transferred to high volume, to ensure scalability.

- Demonstrate functionality and assess robustness of stretchable circuits fabricated in this manner, through mechanical and wash testing. These tests mimic the types of physical stresses the helical e-strips will undergo when embedded in a garment: stretching when the garment is being put on, or when the body moves, and being washed between uses.

- Minimize overall e-strip diameter to minimize the visibility of the helical e-strips when embedded in clothing.

- Define design rules for helical e-strips, including the optimal helix angle of the planar e-strip, and how the dimensions of the surface mounted device (SMD) components needed to create a circuit impact the minimum size of the helical e-strip. In principle, any SMD component can be used, but for example, a circuit with a component that is 4 mm x 4 mm won't form a 2 mm diameter helical e-strip.

The helical e-strip concept was then developed further to produce functional demonstrators. First, helical LED e-strips were demonstrated and evaluated through tensile and standard fabric wash-cycle testing. Then, helical temperature sensing e-strips were fabricated, and their performance compared to a planar, flexible temperature sensor.

This technology is designed for integration into channels or narrow pockets in garments, rather than knitting or weaving into the textile at the time of construction. This is the same method as has been used throughout this thesis, particularly in Chapter 5. The only difference here is that planar electronics are replaced with 3D helical electronics.

As mentioned in previous chapters, this approach to electronics integration keeps electronic and textile components of the e-textile garment separate until the garment the final assembly stage of the manufacturing process. This aims to improve sustainability by allowing electronics to be removable for repair or recycling, in line with recommendations for sustainable e-textiles [117,118].

It would also be possible to weave or knit helical e-strips into the fabric itself, or attach them to garments using tailored fibre placement, a technique designed for embroidering wires

onto textiles [220], or laminate them onto textiles using TPU or other polymer films [221]. These integration methods were not explored as the focus was on validation of the helical e-strip concept itself.

6.2 Materials and methods

6.2.1 Materials

6.2.1.1 Choice of planar e-strip substrate

Copper-plated PI film was chosen for the planar e-strip, due to its widespread use in flexible electronics and compatibility with existing manufacturing processes, as discussed in previous chapters. To form circuit traces, etching copper-clad PI film was chosen over alternative methods to fabricate flexible electronics, e.g., screen printing or dispenser printing on PI or other flexible substrates. As already discussed in Chapter 4, etching fabrication processes were chosen so that circuits using components and conductive tracks with < 0.3 mm pitch could be fabricated. As will become clear in later sections, narrow strips of circuitry were needed to form the helical shape, and this means that small footprint components and closely spaced conductive traces were required.

A clear flexible substrate such as PEN film could also have been used. For example, e-strips containing LEDs might benefit from a clear substrate to maximise transmitted light, as e-strip components face the interior of the strip. Or if embedding e-strips in a thin, light-coloured fabric, the amber colour of the PI might be visible through the fabric, and a clear substrate might be preferable. But as the focus of this work was on proving the concept of the helical e-strip, the more easily available PI was used.

Three variants of copper-plated PI film with varying thickness of the PI layer were evaluated: 25 μm, 50 μm and 75 μm. In Chapter 5, 25 μm PI was found to be susceptible to folding and cracking. However, fabricating helical e-strips involves wrapping the PI into a helix around a core, which requires a high degree of flexibility. And as the core supports the helical structure, preventing small angle bending, folding is less of an issue. The copper thickness was 18 μm in all cases. The 25 μm film was selected for use in the helical e-strips, as it is thick enough to support SMD components but was also found to be thin enough to wrap easily around core materials down to 2 mm in diameter. 25 μm PI film with no copper coating was also used to form 'blank' strips fabricated to investigate fundamental helical e-strip geometry.

6.2.1.2   Selection of the core material

The material used as the helical e-strip core needed to satisfy the following requirements:

1. Stiffness, or stretchability: the core must be highly stretchable (at least 50%), so that the finished helical e-strip can stretch.
2. Recovery: it must have good recovery properties, returning quickly to its initial dimensions after stretching.
3. Compressibility: it must be compressible, to allow components facing the interior of the helical e-strip to compress into its surface, maintaining a smooth helical shape, and cushioning the components to provide support.

Rubber foam cord was identified as a good candidate, as it satisfies all of the above requirements. As there are several varieties of rubber foam cord, three of the most widely available options were selected for evaluation: neoprene, silicone, and ethylene propylene diene monomer (EPDM). These are all waterproof.

A tensile test was performed, based on ISO 20932-1:2020+A1:2021[222]. A length of rubber foam cord was clamped such that the length between clamps was 10 mm. The cord was then stretched to 50% extension 5 times, at a rate of 500 mm / minute. The resulting load was measured by the machine throughout the test. The average force at maximum extension was then calculated and used to compare the cords. 3 mm and 5 mm diameter cords of each material were tested. After each test, the sample was removed from the testing machine, and its length was measured at 30 seconds, and again after 30 minutes, to assess recovery after stretching.

A compression test based on ISO 7743:2011 [223] was also carried out. Samples of each cord were placed between circular metal compression plates and compressed by 25% at a rate of 1 mm / minute, in the thickness direction. This was performed 4 times. Both 3 mm and 5 mm diameter samples were tested for each of the three rubber types.

Both tests were performed with a Shimadzu AG-X Universal testing machine, as described in Chapter 3, Section 3.2.1.

6.2.1.3   *Bonding and encapsulation*

Adhesives were used for a) encapsulating components and copper traces, to reduce the likelihood of them breaking off the PI substrate, and b) bonding the planar e-strip to the core. For component encapsulation, flexible medical adhesive (Dymax Ltd, Torrington, CT, USA) was dispensed onto the planar e-strips, as described in Chapter 3, Section 3.1.4.

To bond planar e-strips to the core, several adhesives were tested: silicone adhesive (Wacker Chemie AG, Munich, Germany) and flexible cyanoacrylate (Intertronics, Kidlington, Oxfordshire, UK) were tested after consultation with Intertronics LTD, who are adhesives specialists for the electronics industry. FPC bonding tapes for flexible electronics (3M, Minnesota, USA) were also tested, as these are standard materials used in flexible electronics fabrication. These were assessed both on ease of use in the fabrication process, and their ability to hold the e-strip together when stretched.

Heat shrink (plastic tubing that shrinks when heated) was also used as a kind of encapsulation or strain relief on the interface between connectors and the body of the e-strip. Boundaries between rigid and flexible materials in electronics are known to be susceptible to failures, so the addition of heat shrink aimed to reduce the mechanical strain in this area when the helical e-strips were under strain.

6.2.2   Determining optimal geometry

6.2.2.1   *Composition of the helical e-strip*

The fabrication of the helical e-strip is illustrated in Figure 6-2. A 'strip' is defined here by the length being much greater than the width ("the planar e-strip"). Figure 6-2A shows one end of the e-strip (or both, depending on design) containing solder pads for attaching connectors, and angled so that when the connector is attached, it will be aligned with the core of the helical e-strip. This angle is matched to the desired helix angle of the finished helical e-strip.

Planar e-strips were fabricated in batches on an adhesive tape carrier, using the dry film lithography process to remove copper from selected areas of copper-plated PI. A vinyl cutter was used to cut outlines of planar e-strips. This is illustrated in Figure 6-2B and Figure 6-2C, and more detail on the methods used are reported in Chapter 3, Section 3.1.3 and Chapter 4, Section 4.3. Components and connectors are soldered onto the planar e-strip's copper-plated PI substrate, and a thin layer of adhesive encapsulation is added. Planar e-strips were

then released from their adhesive carrier, and each was wrapped around a rubber core and
bonded in place with adhesive, forming the stretchable structure shown in Figure 6-2D.
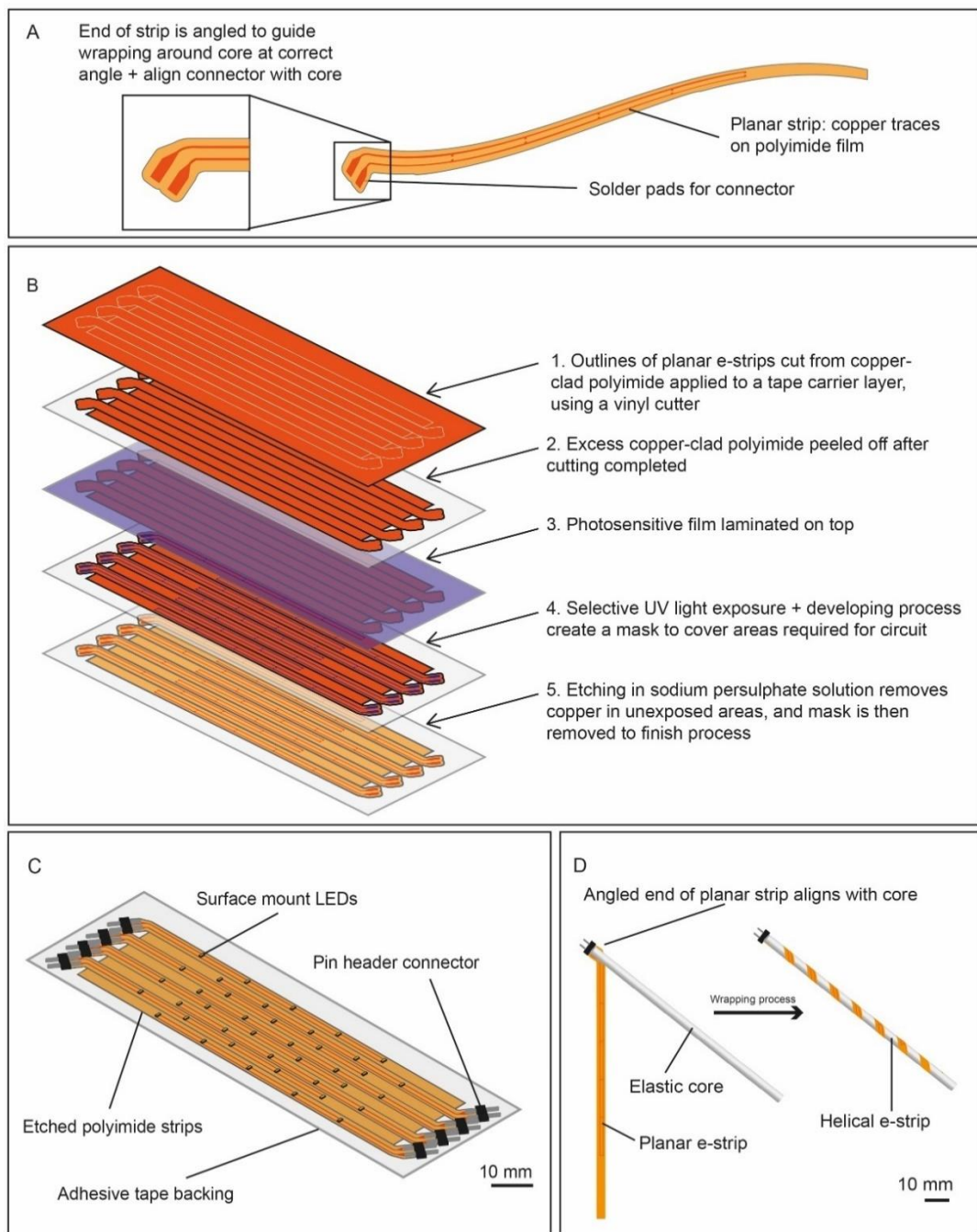
Figure 6-2. Helical e-strip fabrication process.

*A) Design of the planar e-strip, with copper traces etched on PI film, and the e-strip end angled so that an
attached connector aligns with the core; B) Illustration of the fabrication process of a planar LED e-strip; C)
Finished planar e-strips, with components soldered in place and pin header connectors attached; D) Winding
process, where the connector end is bonded first, and then the remainder of the planar e-strip is wound around
the core and bonded to form the helical geometry.*

The process of wrapping the planar e-strip around the core was as follows (Figure 6-3):

1. The planar e-strip was bonded to the core using cyanoacrylate adhesive. First, one end of the planar e-strip was bonded to the core, by applying cyanoacrylate adhesive, then holding both parts together under manual pressure until the adhesive was cured.

2. Then, a printed guide was used to maintain correct helix angle, and silicone paper to prevent any accidental bonding between the helical e-strip and the surface on which it was assembled. Cyanoacrylate adhesive was applied in stages with a syringe, and the helical e-strip was formed by rolling the planar e-strip onto the core.
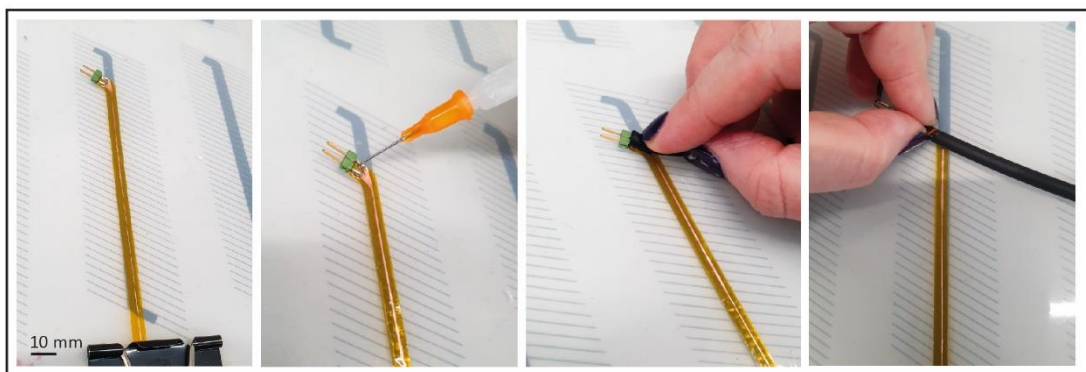
Figure 6-3. Process of forming the helical structure.

The planar e-strip is placed on silicone paper with a printed grid underneath, then cyanoacrylate adhesive is applied, and the core is adhered to the end of the e-strip. The planar e-strip is then rolled along the core (EPDM in this case), adding further adhesive (not pictured) to form the helical structure.

Heat shrink was applied to the interface between the connector and the rest of the e-strip and activated by a hot air gun to make it conform tightly to the e-strip. Small amounts of cyanoacrylate were applied between heat shrink and e-strip using a syringe, to make sure it stayed in place during tensile testing.

6.2.2.2   Evaluation methods

Tensile tests were based on IPC-9204 testing methods for flexible electronics, as described in Chapter 3, Section 3.2.1, and performed with a universal testing machine (Multitest 2.5dV model, Mecmesin / PPT Group UK, Horsham, UK) equipped with a 100 N force gauge and rubber-coated grips. Samples were clamped at each end, and the gauge length was measured with a steel ruler. Mecmesin VectorPro Lite software was used to program tests, and record load and extension data.

Blank e-strips were extended at a rate of 50 mm / minute until a load of 10 N was applied, or until they broke, if that happened sooner. For the remainder of the tensile tests, small strips of fabric were glued on top of the heat shrink on e-strips undergoing tensile testing, to improve grip and prevent the e-strips from slipping out of the universal testing machine's clamps. Mechanical testing of interconnects also included continuous measurement of 4-wire resistance to detect damage to copper tracks. This was measured using an NI-9219 analogue input module (National Instruments Ltd, Texas, USA), connected via USB to a laptop where data was recorded using NI LabVIEW software. Cyclic tests were conducted at a rate of 800 mm / minute.

Tested samples were also assessed by visual inspection, i.e. determining whether a sample had passed or failed a test based on signs of physical damage.

6.2.3 Determining optimal geometry and design rules

In determining optimal geometry, the aims were to a) maximise stretch, for compatibility with highly stretchable fabrics; b) minimize diameter, so that helical e-strips can be embedded in garments without adding noticeable and uncomfortable bulk. To identify the important aspects of the helical geometry, consider a simplified helical e-strip of length, L, and diameter, d (Figure 6-4A). The planar e-strip has a width, w, and the helix angle, ϑ.

If the planar e-strip is wrapped around the core such that successive turns of the helix sit immediately next to each other, with no gap in between, this defines the minimum helix angle, ϑ_{min}, for a given planar e-strip width, w. Figure 6-4A(i) illustrates an unrolled section of the helical e-strip surface to show this, noting that increasing w also increases ϑ_{min}. It also follows that ϑ_{min} is given by Equation 8-1:

$$\theta_{min} = tan^{-1}(\frac{w}{\pi d}) \qquad (8\text{-}1)$$

The upper limit of the helix angle is given by $\vartheta_{max} < 90°$. At 90°, the planar e-strip and the core are parallel, and no helical structure can be formed by wrapping one around the other. It is important to also note that ϑ plays a critical role in the stiffness of the helical structure [224]. As d determines how bulky the helical e-strip will be, this needs to be minimized, and this requirement places constraints on w. The size of components required to build a desired circuit, and the complexity of the circuit, i.e. the number of traces required to interconnect all components, will likewise constrain how narrow the planar e-strip can be.
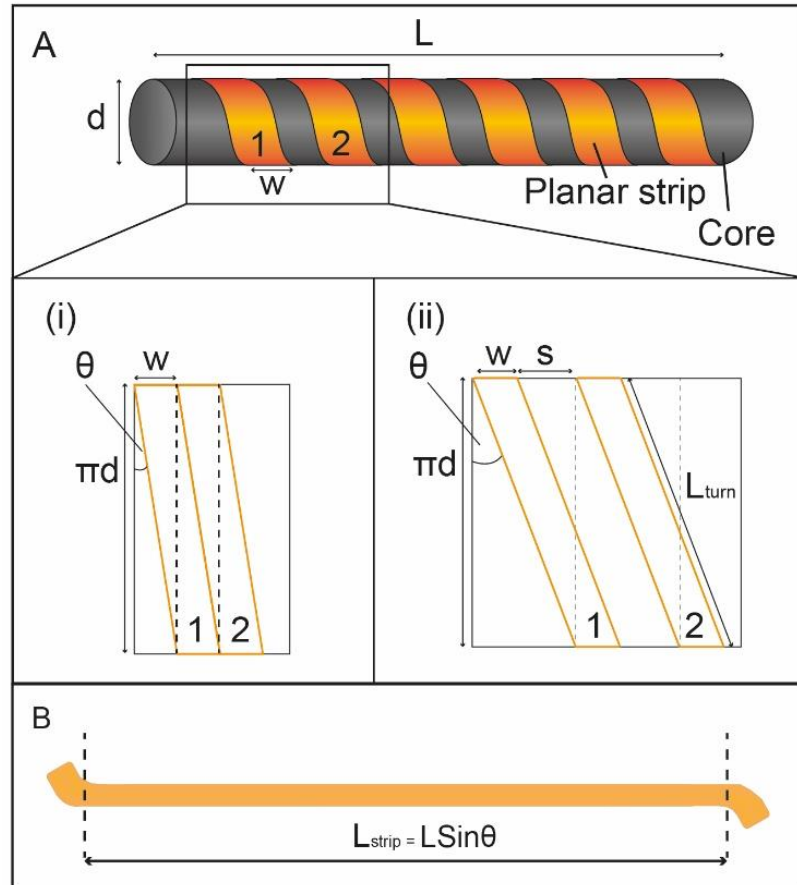
Figure 6-4. Geometric representation of helical e-strips.

A) i) simplified illustration showing helix angle, ϑ, length L, planar e-strip width w; ii) Minimum helix angle, with no gap between turns of the helix; iii) General case where a spacing s exists between helix turns, and L_{strip} is the length of planar e-strip required for each turn; B) Illustration of planar e-strip showing length L_{strip} needed to create a helical e-strip of length L.

Figure 6-4B(ii) shows the general scenario where there is a spacing, s, between turns of the helix. Helices are more commonly characterized by pitch, which is equal to $w+s$ (note that this is a different definition of pitch than the spacing between conductive tracks or contacts). However, in this work they were considered separately, as two helical e-strips with the same pitch, but different ratios of w to s, may exhibit different behaviour when stretched. For a given helix angle, a formula may be derived for the length of planar e-strip, L_{strip}, required to create a helical e-strip of length L. This is useful as it is likely that the desired helical e-strip length will be determined by the design of the garment in which it is to be embedded, rather than the planar e-strip length being fixed before the garment is designed. That is, a designer would know L, and would need to determine the required L_{strip}.

This is given by Equation 8-2:

$$L_{strip} = NL_{turn} = \left(\frac{L}{w+s}\right)L_{turn} = \left(\frac{L}{L_{turn}Sin\theta}\right)L_{turn} = LSin\theta \quad (8\text{-}2)$$

Where N is the number of turns of the helix and can be written in terms of L, w, and s, as $w+s$ is the length of the core covered by each turn of the helix.

Blank and unpopulated helical e-strips were fabricated: strips of PI film wrapped around and bonded to EPDM rubber foam cord. These were used to evaluate the stiffness of helical e-strips with varying geometry. The following experiments were carried out:

1. Helix angle: blank helical e-strips with helix angles varying from 10 ° to 60 °, in steps of 10 °, were subjected to tensile tests, stretching them up to a load of 10 N, or until they broke. Three samples of each were tested, and the core diameter was 4 mm in all cases. For this experiment, d = 4 mm and w = 3 mm were held constant to isolate the impact of ϑ.

2. Width to diameter ratio: blank helical e-strips, with 4 mm diameter, were subjected to the same tensile test as above. The ratio of width to diameter was varied from 0.5 to 1.25, to investigate whether this affected stiffness.

6.2.4 Helical interconnect e-strips

Helical interconnect e-strips were constructed to test the durability of helical e-strips containing conductive tracks. Shown in Figure 6-5A, interconnect e-strips consisted of one 10 mil (0.254 mm) wide copper track, with two pin header connectors soldered at each end. This enabled the four-wire resistance of the helical e-strip to be measured continuously during tensile testing. The testing setup is shown in Figure 6-5B. Interconnect e-strips of 2 mm, 3 mm and 4 mm diameter were fabricated, with w = 0.75d in all cases.

To measure stiffness, three strips of each diameter were stretched until failure. Failure was defined as either the core or the planar e-strip breaking. Then, to achieve a more comprehensive understanding of helical e-strip performance, cyclic tests were also performed, whereby e-strips were repeatedly cycled through stretching and relaxing, stretching up to a maximum extension well below the breaking points identified in the previous experiment. Three strips of each diameter were stretched such that the applied strain was 30%, 50% and 75% for 3000 cycles.
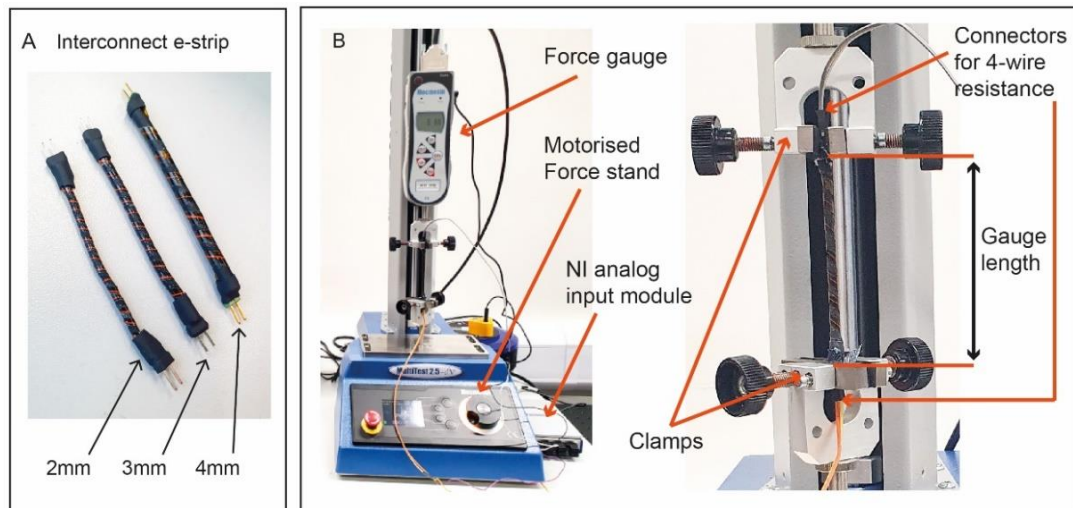
Figure 6-5. Testing setup for interconnect e-strips.

A) Test samples: e-strips of different diameters, with pin header connectors at each end, and all with EODM cores;

B) test setup with Mecmesin MultiTest 2.5dv universal testing machine.

6.2.5 LED and temperature sensing demonstrators

The materials and fabrication methods used to fabricate helical LED and temperature sensing e-strips were largely the same as in the previous section. Planar e-strips were fabricated by etching copper-plated PI, and cyanoacrylate adhesive was used to bond planar e-strips to rubber cord cores.

For temperature sensing e-strips, and the narrowest LED e-strips (2 mm diameter), the dry film photolithography process described in Chapter 3, Section 3.1.2.2 could not be fine-tuned sufficiently to achieve the resolution required for these fine pitch circuits. This motivated the development of the vinyl mask method, covered in the same section, and in Chapter 4, Section 4.3. Other helical e-strips (made with wider planar e-strips) in this chapter were fabricated using the dry film photolithography process.

6.2.6 Components

The helical e-strips in this chapter include components, which were attached using solder paste and a pick and place machine as described in Chapter 3, Section 3.1.5. Components and connectors were encapsulated in the same way as with interconnect e-strips, using UV curable medical adhesive and heat shrink on the connector for extra support.

As discussed in Chapter 6, Section 6.2.3, component size limits the minimum helical e-strip diameter. Helical e-strips were first constructed with 0603 (metric 1608) SMD components,

to validate the concept (as these are easily visible with the naked eye and therefore easy to work with). Further prototypes were fabricated with 0402 and 0201 package components, the smallest standard sizes used in electronics manufacturing, to enable smaller diameter helical e-strips to be made. Microscope assistance was required to accurately place 0402 and 0201 components, and to dispense solder paste onto solder pads.

2.54 mm pin headers were used as connectors for LED e-strips, to enable easy connection to a power supply for testing. In a real garment a latching mechanism would also be needed to prevent disconnection, as discussed in Chapter 5. Ideally, a cylindrical connector would also be used, but the only cylindrical connectors currently on the market are for wires, not flat flexible circuits. A latching mechanism was also not required for this work, as the focus was on the development of individual helical e-strips, not integrating them into a modular system.

For the temperature sensing circuit, a Wheatstone bridge was constructed using a 10 kΩ NTC thermistor and three 10 kΩ resistors (the same as in Chapters 4 and 5, but with different dimensions). Components were soldered to planar e-strips using T5 solder paste (Chipquik Ltd, Ontario, Canada) and a hotplate. With the exception of pin header connectors, which were soldered manually with a soldering iron.

A few other modifications to the materials and designs of helical interconnect e-strips were required to fabricate LED and temperature sensing e-strips, as will be described in detail in the following sections. Table 6-1 summarises the materials and characteristics of helical e-strips covered in this chapter.

Table 6-1. Materials and characteristics of helical e-strips fabricated in this chapter.

E-strip category	Materials (excludes adhesives + solder)	Diameters (mm)	Helix angles (degrees)	Planar e-strip widths (mm)
LED	Copper-plated PI film, EPDM core, pin header connector, SMD LEDs	2, 4	30	1.5, 3.5
Sensing	Copper-plated PI film, EPDM core, SMD thermistor and resistors	3, 4	30	3

6.2.7 Helical LED e-strips

To demonstrate that circuits containing components could be constructed in a helical format, helical LED e-strips ("LED-strips") were fabricated, consisting of 5 LEDs in parallel. This was mainly intended to demonstrate the potential of the technology, but stretchable LED circuits could easily find use in commercial sportswear as an indicator of a sensor recording temperature or heart rate, or for safety purposes including illumination during night-time sporting activities such as running or cycling.

Table 6-2 lists the different LEDs used to create LED-strips. 0603, 0402 and 0201 packages were chosen as they are the three smallest standard sizes that are commercially available. Smaller footprint LEDs are not readily available from electronics suppliers in the UK, where this work was carried out, and are at present not widely used in electronics manufacturing due to their small size [225].

Table 6-2. Dimensions of SMD LED packages used to create helical LED-strips.
The width and length values are standard for all components of the package sizes given, but height is not standardised. The height values listed in the table are for the specific LEDs used in this work.

Package name	Width (mm)	Length (mm)	Height (mm)
0603 (Imperial) / 1608 (Metric)	1.6	0.8	0.2
0402 (Imperial) / 1005 (Metric)	1.0	0.5	0.2
0201 (Imperial) / 0603 (Metric)	0.6	0.3	0.2

For helical LED-strips, a clear core material was needed to transmit the light. EPDM foam cord was not suitable, as it is opaque. Translucent silicone cord and silicone tubing both with a shore hardness of 60 were both evaluated. These are distinct from the silicone foam cord mentioned in earlier parts of this chapter, which is a different material and is opaque. As can be seen in Figure 6-6A, the silicone cord was not compressible enough, preventing components from embedding into the core surface, and resulting in an uneven structure.

Silicone tubing, depicted in Figure 6-6B, resulted in a much smoother surface, and was thus chosen as the LED helical e-strip core material. The inward-facing orientation of the components further allowed the LED lighting to diffuse through the core, as can be seen in Figure 6-7.

An additional fabrication step was required to enable cyanoacrylate adhesive to bond the silicone tubing to the planar e-strips. Loctite silicone primer was brushed onto the silicone tubing and allowed to dry, immediately before bonding. Without this step, the PI planar e-strip did not bond well to the core, and the helical structure was easily destroyed. With the primer, the structure was robust and able to survive many cycles of cyclic stretching.
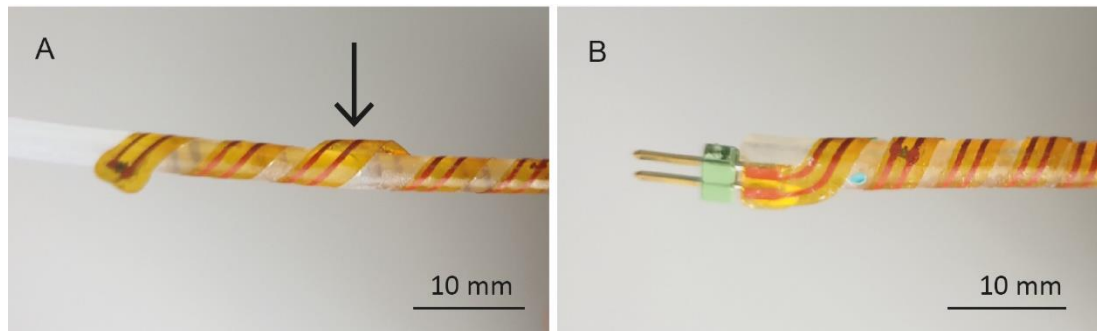
Figure 6-6. Evaluation of core materials for LED helical e-strip.

A) Solid silicone cord: arrows highlight areas the inability of components to compress into the core can be seen, resulting in an uneven surface; B) Silicone tubing core: the surface of this e-strip is much smoother as the higher compressibility of the silicone cord allows components to compress the surface.

LED-strips were first made with 4 mm diameter, using all three package sizes. After the concept had been validated with 4 mm diameter LED-strips, 2 mm diameter LED-strips were fabricated, using 2 mm diameter silicone tubing and 0201 LEDs. These narrower LED-strips are more suitable for integration into textiles, as their smaller diameter would make them less noticeable in the garment. 2 mm LED-strips were only made with 0201 LEDs, as the narrow diameter (both of the core and the planar e-strip) made larger components unsuitable.

The layout of the planar LED-strips is illustrated in Figure 6-7A. The layout of 4 mm LED-strips is illustrated with 0603 components, but the layout and dimensions were the same for LED-strips with 0402 and 0201 components. Fabricated planar and helical LED-strips can be seen in Figure 6-7B, and finished, lit LED-strips of both diameters are depicted in Figure 6-7C.
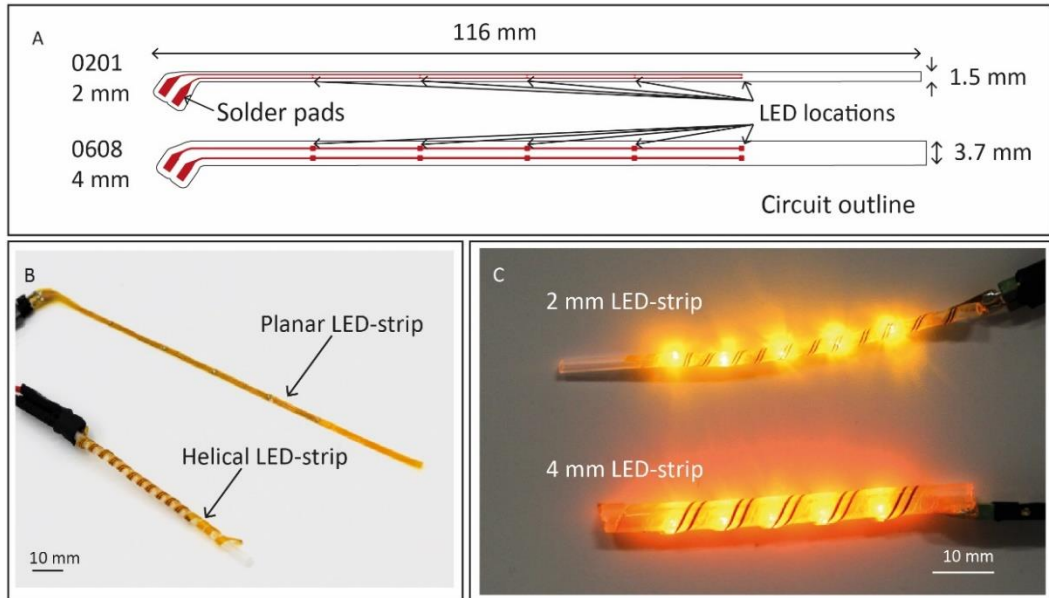
Figure 6-7. Helical LED-strip layout and fabricated samples.

A) Circuit layout for planar LED-strips of 2 mm and 4 mm diameter; B) Planar and helical 2 mm LED-strips, shown side-by-side; C) Lit 2 mm and 4 mm LED-strips with silicone tubing cores.

6.2.7.1 Evaluation methods

6.2.7.1.1 Tensile tests

Tensile testing protocols were the same as earlier in this chapter: a Mecmesin Multitest 2.5dv universal testing machine was used to perform two tensile tests: a) stretching until breaking point; b) cyclic tensile tests.

LED-strips were connected to a bench power supply and stretched while lit, so that damage was indicated by one or more LEDs flickering, dimming, or turning off. LED-strips of 2 mm and 4 mm diameter, and all package sizes, were subjected to the same tests.

6.2.7.1.2 Wash testing

Electronic parts designed for e-textiles need to be washable if embedded in garments, and therefore a series of wash tests were carried out using the 4 mm diameter LED-strips with 0603 LEDs. Wash test samples were created by stitching LED-strips onto a strip of fabric, with each fabric sample containing 3 samples of 4 mm diameter LED-strips. These were then placed in a domestic washing machine (Model i-DOS, Bosch GMBH) and washed on a 40 °C / 1400 rpm cycle with liquid detergent (generic supermarket brand). Each cycle lasted 2 hours 33 minutes, replicating a regular domestic wash cycle. An additional load ballast of 2.2 kg polycotton fabric was added, in accordance with ISO 6330 washing standard [195], as described

in Chapter 3, Section 3.2.2. Samples were air dried in between washes, and weighed on a balance before each wash to ensure that they were fully dry and had not retained any moisture, before the next wash cycle began.

According to a comprehensive study on e-textile wash testing by Rotzler et al [196], this is similar to many other e-textile wash tests in terms of temperature and the use of liquid detergent. However, data on spin cycles used in wash tests are rarely reported. As domestic washing machines typically advertise spin speeds of between 400-1800 rpm, a speed at the higher end of this range was chosen to subject the helical e-strips to maximal stress and identify failure modes quickly. It is expected that using a gentler cycle designed for wool and other delicate fabrics could extend the washing durability. However, subjecting helical e-strips to high stress to identify failure modes was considered more important for this stage of development, to inform future work.

Tested samples were also assessed by visual inspection, i.e., determining whether a sample had passed or failed a test based on signs of physical damage. LED-strips were connected to a bench power supply and stretched while lit, so that damage was indicated by one or more LEDs flickering, dimming, or turning off. A Keyence VHX-7000 microscope was also used for more detailed inspection of failures, such as cracks in copper tracks or solder joint failure.

6.2.8 Helical temperature sensing e-strips

6.2.8.1 *Design and fabrication*

This technology can also be used for sensing physiological signals, and to demonstrate this, temperature sensing helical e-strips ("temp-strips") were fabricated. The temperature sensor design was adapted from the circuit used in Chapters 4 and 5, using 10 kΩ NTC thermistors. 0201 SMD thermistors and 10 kΩ resistors were arranged in a Wheatstone bridge configuration and distributed along the helical e-strip (Figure 6-8A and B).

This circuit has four tracks, requiring a 4-pin connector, so instead of 2.54 mm pitch pin headers, the sensing e-strip terminates with 1 mm pitch flexible contacts. The ZIF interposer developed in Chapter 5, containing a 1 mm pitch zero insertion force (ZIF) connector, was used to connect the e-strip to solid core wire (Figure 6-8A). This wire was then connected to the screw wire terminals on a DAQ device (NI USB-6210, National Instruments Ltd, Texas, USA) to record sensor readings.

3 mm and 4 mm temp-strips were fabricated. The planar temp-strip, having four tracks, needed to be wider than the planar LED-strips. At 3 mm, this made it too wide to make a 2 mm helical e-strip (based on the results of Section 6.2.3As a result, 3 mm diameter was used instead. Two diameters were fabricated, to test the impact of the core on the e-strips function as a temperature sensor.

6.2.8.2   *Temperature sensor characterisation*

Previous work has shown that for skin temperature measurement, good contact between temperature sensor and skin, or at least fabric touching the skin, is key for accurate results [205]. This is also covered in Chapter 5. Other studies have used planar electronics where the orientation and location of the temperature sensor is fixed [40], or where a thermistor was embedded in a yarn that may rotate, but has symmetric structure so that rotation did not impact the distance between thermistor and skin [206]. For helical e-strips, it is expected that orientation is important, as components are not in the centre of the helical e-strip, and should the e-strip rotate, the position of the thermistor relative to the skin may change. A characterization experiment was therefore performed to test the effect of rotation.

Sensing e-strips were characterized using an Echotherm digital chilling/heating dry bath (Torrey-Pines Scientific Inc, CA, USA). During the tests, the planar e-strip was placed flat on the dry bath surface. The helical e-strips were placed such that the thermistor was face down onto the dry bath surface (Face Down condition), at 90 ° (Side On condition) or on the opposite side (Face Up condition), as illustrated in Figure 6-8C. PI tape was used to secure the e-strips to the dry bath surface, taking care not to place tape over the section of the e-strips where the thermistor is located. The experimental setup is shown in Figure 6-8D.

Each test was run twice, once with the temperature decreasing from 40 ° to 30 °, and again with the temperature increasing from 30 ° to 40 °. This range was chosen as it covers the normal range of human skin, and this technology is intended for integration into e-textile garments. After each temperature increment, the sensor readings were allowed to stabilize for 2 minutes, and then data was collected for a further 2 minutes. Data was collected at a rate of 2 Hz.
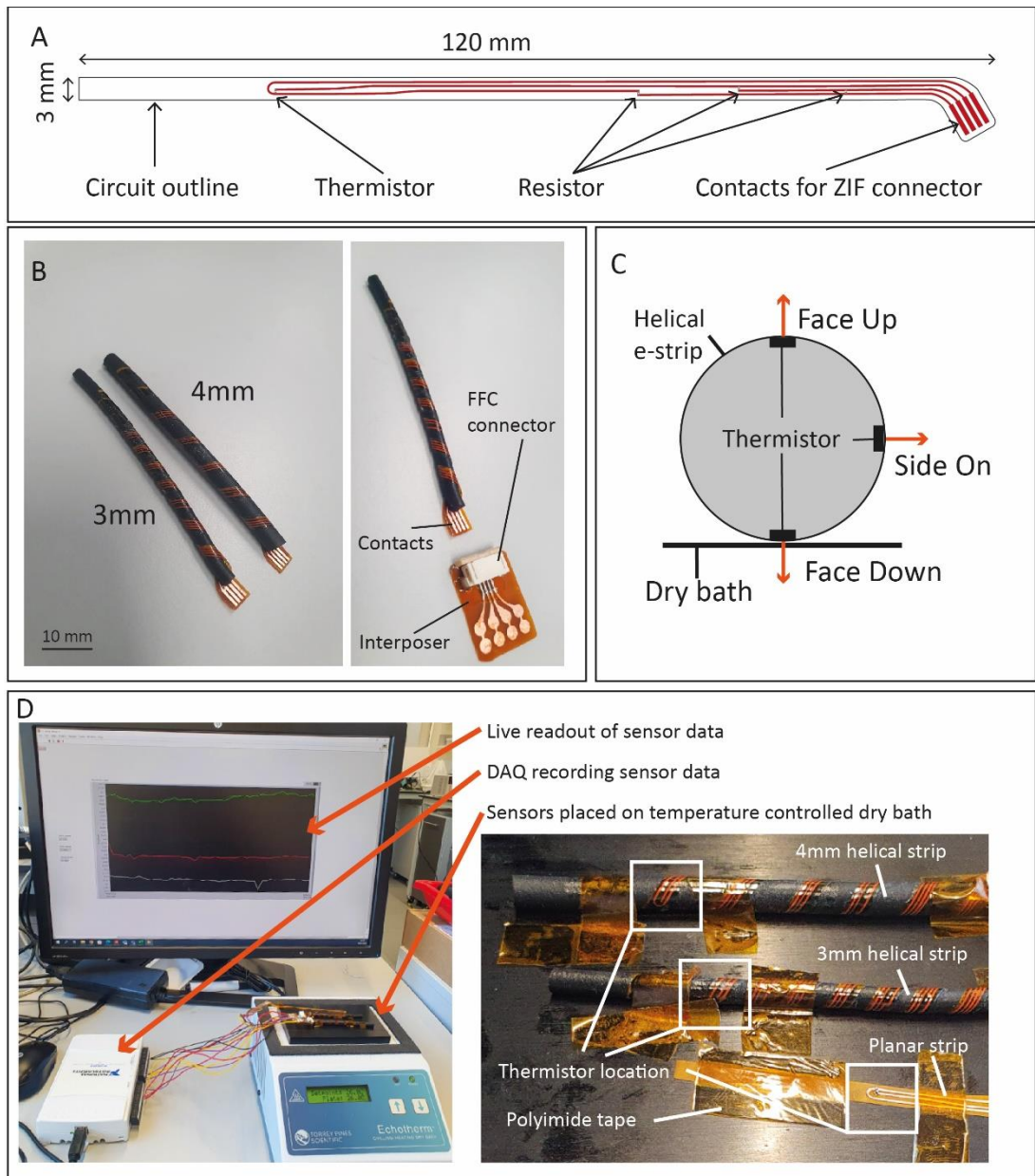
Figure 6-8. Temperature sensing helical e-strips.

A) The planar e-strip used to make temp-strips; B) Image of the temperature sensing e-strip with 4mm and 3mm diameter EPDM cores, and interposer for interfacing with measurement equipment; C) Illustration of experimental conditions, where the thermistor is oriented directly in contact with the heated surface (Face Down), at 90° away from the heated surface (Side On), or 180° away (Face Up); D) Experimental setup of dry bath, temperature sensing helical e-strips, and close-up of sensing e-strips on dry bath surface, with thermistor location highlighted.

6.3   Results

6.3.1   Selection of the core material

Tensile test results are shown in Figure 6-9. Thicker cords of all materials required more force to stretch to 50% strain, as is expected, because thinner pieces of the same material will be inherently less stiff. For 5 mm cords, EPDM was the least stiff, though for 3 mm cords, EPDM and neoprene showed comparably low stiffness.
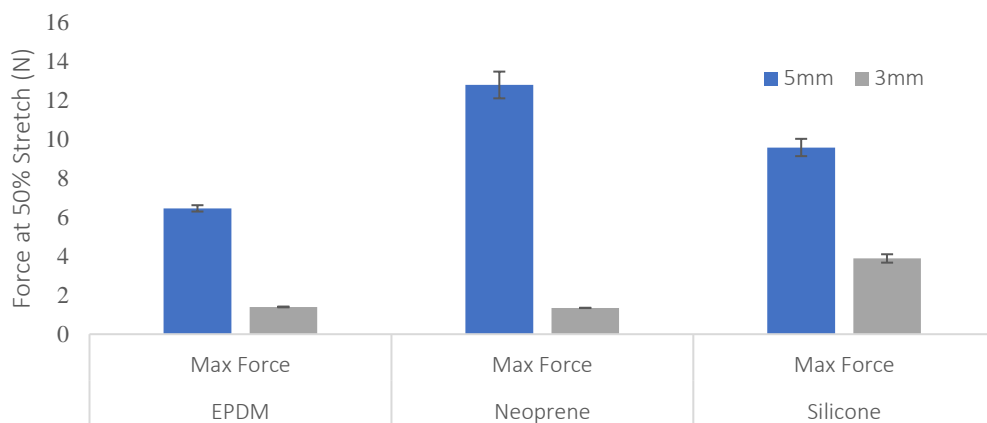
Figure 6-9. Tensile testing of rubber foam cords.

EPDM, neoprene, and silicone rubber foam cords, of both 3 mm and 5 mm diameter, were stretched to 50% strain, 5 times. The average force at maximum strain is shown here, averaged over 5 cycles.

However, recovery results shown in Table 6-3 show that 3 mm neoprene was significantly more deformed than the EPDM and silicone, when measured 30 seconds after the tensile test. All cords, of all diameters, did return to their original length by 30 minutes after the test. But as helical e-strips are designed to be embedded in stretch textiles, quick recovery is important. If a helical e-strip is embedded in a sports garment, the embedded electronics need to conform to the body, and not become temporarily deformed when the athlete kicks or throws a ball, or jumps.

Table 6-3. Recovery properties of rubber foam cords after performing tensile test of 5 cycles of 50% strain
Cord length was measured 30 seconds after tensile testing as described above, % deformation was calculated
relative to cord's initial length. Cords were also measured 30 minutes after testing, to check whether they had
returned to their original length.

Material	Diameter	% Deformation 30 s after test	Recovery to initial length after 30 minutes?
EPDM	3 mm	6.49%	Yes
	5 mm	1.40%	Yes
Neoprene	3 mm	10.32%	Yes
	5 mm	0.00%	Yes
Silicone	3 mm	2.07%	Yes
	5 mm	0.00%	Yes

The results of compression tests are shown in Figure 6-10. Silicone cord of both diameters were the least compressible, and 3 mm EPDM cord was most compressible, with 5 mm EPDM and both diameters of neoprene in between.
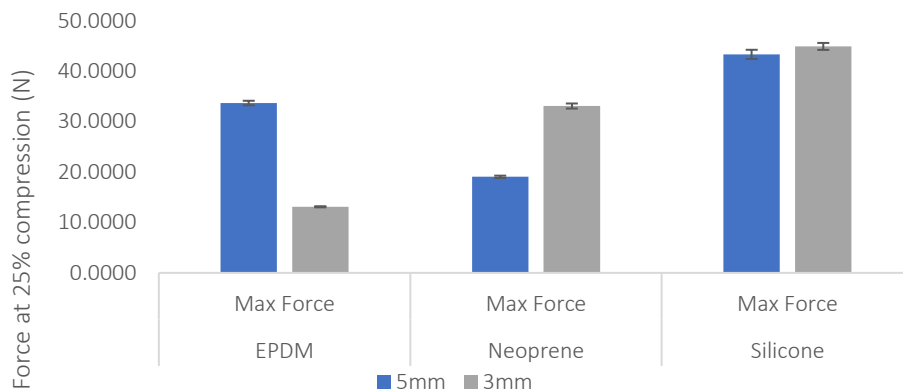
Figure 6-10. Results of compression testing of rubber foam cords: snapshot at 25% strain
3 mm and 5 mm diameter EPDM, neoprene and silicone rubber cords were compressed to 25% at a rate of 1 mm / minute. These results should not be taken to mean that the force/compression relationship is linear.

Other factors were also taken into consideration. The cost of cords was compared, with silicone foam cord being twice as expensive as EPDM and neoprene. All materials are available in medical grade. EPDM and neoprene have high compatibility with adhesives, whereas silicone is much more difficult to bond. Weighing these factors and the mechanical test results, EPDM was chosen as the core material.

6.3.2 Bonding and encapsulation

FPC bonding tape was found to be unsuitable for bonding the planar e-strip to the core, as due to the helical structure of the e-strip, and the compressible core, it was not possible to apply pressure to ensure proper bonding of the tape. Silicone adhesive was also ruled out, as although this created a flexible bond, its 24-hour curing time resulted in some e-strips untwisting after initial bonding, and for this work a quick curing adhesive was needed, to prevent this untwisting from occurring. The flexible cyanoacrylate adhesive was chosen as the preferred bonding method, as its strong bond and fast curing time formed a very secure structure.

6.3.3 Determining optimal geometry and design rules

Blank helical e-strips are depicted in Figure 6-11A. The results of tensile testing to determine their stiffness are shown in Figure 6-11B, where it is demonstrated that stiffness and helix angle are correlated as predicted. Helix angles above 40 ° resulted in a rippling effect when stretched, shown in Figure 6-11(i). As the helical e-strip was stretched, the helix balanced this tensile force by untwisting, as well as compressing in the radial direction towards the core. This is attributed to be the cause of the core rippling deformation observed, which is an undesirable effect as it may cause rippling of the fabric when embedded in a garment.

At the other extreme, helical e-strips with 10 ° and 20 ° helix angle exhibited the lowest stiffness, but also showed signs of damage to the core as shown in Figure 6-11(iii)-(iv). This can be explained by the fact that as the planar e-strip is adhered to the core, sections of the core that lie under the planar e-strip are no longer able to stretch. That is, the sections highlighted by red arrows in Figure 6-11C (iv) are the only parts of the core that remained free to stretch. As ϑ decreases, the amount of core material uncovered by PI also decreases. Thus, at smaller helix angles, stretching can cause the core to tear.

Between these two extremes, a helix angle of 30 ° showed sufficiently low stiffness without any signs of rippling or damage (Figure 6-11C(ii)). 30 ° was therefore chosen as the optimal helix angle. It would be possible to further optimise the helix angle by testing additional angles between 20 ° and 30 °. But without the development of automated machinery to create the helix structure, it is difficult to ensure helix angle accuracy of <10 °, and therefore this was considered out of scope for this stage of development. It is also important to note that these results are specific to helical e-strips with rubber cores, and a smaller helix angle

could be used if the helical geometry was formed without a core. This would increase stretch, but the resulting structure would be unsupported and fragile, and therefore unsuitable for e-textile applications.
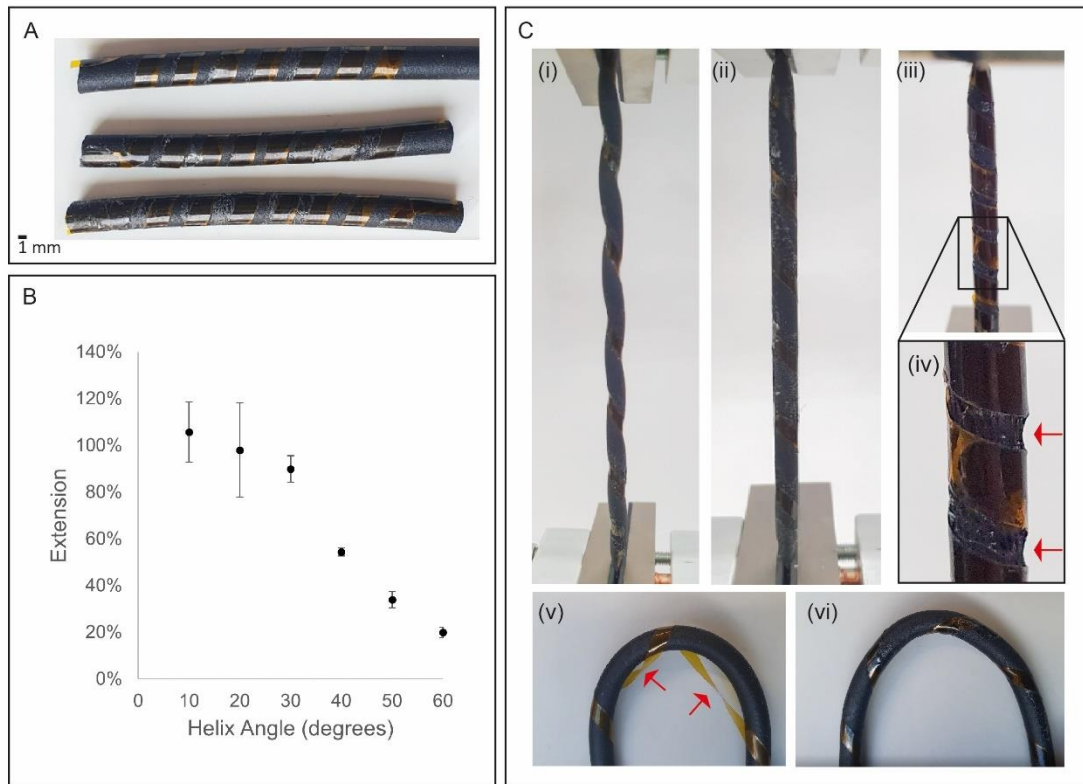
Figure 6-11. *Optimizing geometry.*

A) Image of blank EPDM e-strips with 4 mm diameter; B) Tensile test of blank e-strips of varying helix angle. 3 samples were tested for each data point, and error bars represent standard deviation. One 50° sample and one 60° sample failed before reaching 10N, due to the polyimide strip tearing, and their extension at point of break (rather than at 10N) is recorded. This is consistent with the overall trend of higher helix angle corresponding to higher stiffness; C) Tensile testing images, showing i) undesirable rippling effect for $\vartheta \geq 40°$; ii) 30° e-strip showing no deformation; iii) 10° strip during tensile test; iv) Section of 10° strip showing core damaged occurring at $\vartheta <$ 30°; v) Image of bent blank strip, showing that helical geometry is lost if the planar e-strip is not bonded to the core; vi) An identical blank strip but with the planar e-strip bonded to the core, showing that the helical geometry is maintained. In all cases, d = 4 mm and w = 3 mm.

Jiang et al identified an optimal helix angle of 50.69 ° for printed helical transistors on PEN film wrapped around a PU fibre core [179]. However, they defined their helix angle differently, where the relationship was given by $\vartheta_{\text{Jiang et al}} = 90° - \vartheta$. This means that, while their FEM simulations and these experimental results are similar, there exists a difference of approximately 10 ° which may be due to differences in material properties. It is expected that the optimal helix angle may vary for different core materials or because, in their specific

work, the planar e-strip was wrapped around, but not bonded to the core. As a reminder, this prior work demonstrated a single component – a printed transistor – in helical form, not circuits with multiple components, or SMD components.

Figure 6-11C(v)-(vi) shows why the choice was made to bond the planar e-strip to the core. Without bonding, bending the helical e-strip caused the planar e-strip to lose its helical shape, which could easily result in folding or tearing of the PI film. Bonding the planar e-strip to the core ensures that the helical geometry is maintained throughout the extensive stress and strain cycles expected in e-textile applications.

Figure 6-12A qualitatively illustrates the impact that component size has on minimum w and d: if a component is too wide, or too thick, relative to the core diameter this creates irregularities in the helical geometry which is likely to reduce helical e-strip integrity and reliability. The maximum thickness of a component will depend on the rigidity of the core material. In this work, 0603 LEDs – with a footprint of 1.6 mm x 0.8 mm x 0.2 mm – were sufficiently small that a planar e-strip containing them could be wrapped around a small diameter core (i.e. 2-4 mm) without disrupting the helical geometry. But for larger components, such as temperature sensing or accelerometer ICs, which may have footprints similar to those shown in Figure 6-12A, it was clear that larger diameter cores would be required. This simplified description of the structure also does not factor in solder and/or encapsulation materials applied to these components. Therefore, the minimum diameter for a given component might be slightly larger than shown in the illustration. For this work, only 0603 and smaller components were used, so that 2 mm helical e-strips could be produced. However, future versions of the helical e-strip could use bare die components (semiconductor dies without plastic packaging) instead of standard SMD packages, which would reduce component size and facilitate the realization narrower helical e-strips.

Figure 6-12B shows the results of a tensile test on helical e-strips with constant diameter and ϑ, and varying w. The relationship between the width-to-diameter ratio and stiffness was not entirely linear, which may be attributed to the helical geometry formed by manually winding the planar strip around the core. This led to some small irregularities in the helical geometry. Overall, reducing w, for fixed d and ϑ, resulted in decreased stiffness. Reducing w increased s, the amount of exposed core not bonded under the planar e-strip. This can be seen in the illustrations in Figure 6-12B.

As the planar e-strip contains components and conductive tracks, a helical e-strip of 2 mm diameter and a *w:d* ratio of 0.5 would require *w* = 1 mm, which would be difficult to achieve using conventional SMD components. The smallest commercially available SMD package is the 01005 (metric 0402), with dimensions of 0.4 mm x 0.2 mm, and due to its small size, this package has not seen widespread adoption in the electronics industry [225]. A target ratio of *w* = 0.75*d* was therefore set with the limit that *w* ≤ *d* in all cases.
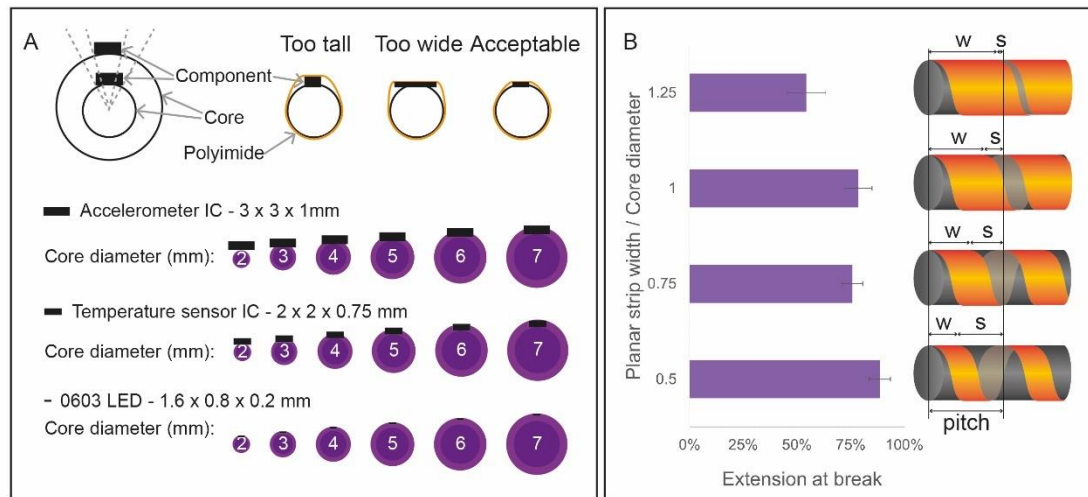
Figure 6-12. Constraints on the width of the planar e-strip.
A) Illustration of the constraints on w and d due to component size; B) Results of tensile tests on 4 mm diameter e-strips investigating relationship between stiffness and width-to-diameter ratio.

6.3.4 Helical interconnect e-strips

The results of the tensile tests until breaking point are shown in Figure 6-13A. Helical e-strips of all diameters were able to extend by 100% before failing. The fact that 3 mm e-strips were able to withstand the highest strain was most likely due to the fact that thinner EPDM cords were less stiff, but also weaker and more susceptible to tearing. Figure 6-13B shows typical behaviour under tensile testing to failure: for 4 mm and 3 mm diameter helical e-strips the planar strip broke first, followed by the core. For 2 mm diameter samples, both tended to break at the same time, or in the opposite order, as illustrated in Figure 6-13C.

As can be seen in Figure 6-13D, only one 4 mm helical e-strip passed the 75% cyclic strain test, with all others failing. Damage to the core was the most common failure mode. Cracks in the core appeared gradually, eventually leading to a tear through the core. In many cases there was additional damage observed on the planar e-strip tracks when the core tore.

At 50% strain, all 4 mm helical e-strips, and 2 out of 3 3 mm helical e-strips, passed, but 2 mm interconnects showed early signs of damage to the core.

At 30%, interconnects of all diameters passed with no signs of physical damage or increases in resistance. From this it was concluded that e-strips with 2 mm – 4 mm EPDM cores can survive 30% strain, but for larger diameters, a thinner and therefore less stiff core is beneficial. And for garments requiring many cycles of high (>50%) stretch, a different core material may be required to ensure longevity.
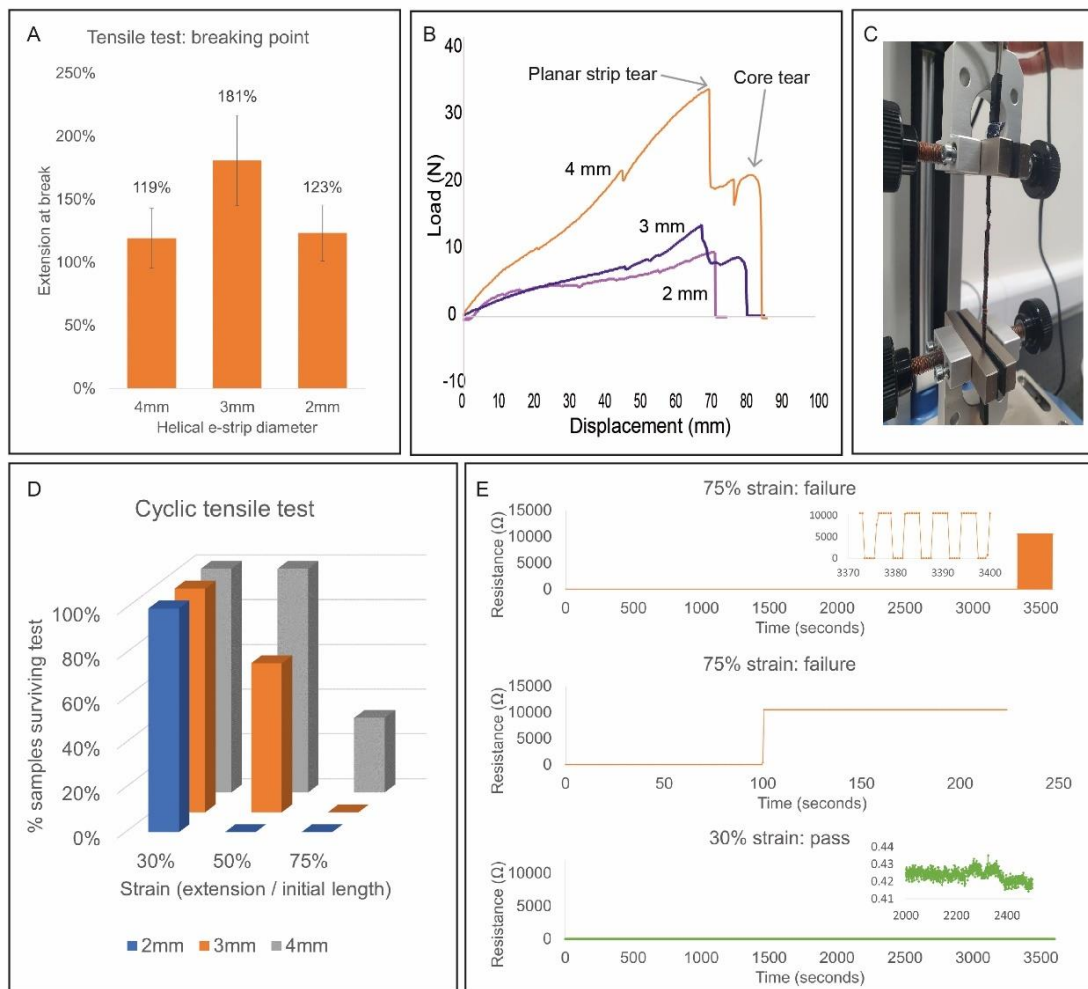
Figure 6-13. Helical interconnect e-strips.

A) results of tensile tests until breaking point. Data points represent the mean of three samples, and error bars represent standard deviation; B) load-extension graph showing stages of failure; C) images of failure modes; D) results of cyclic tensile tests, showing consistent good performance at 30% strain, mixed results at 50% strain, and consistent failure at 75% strain; E) Resistance data from cyclic tests, showing that tearing of the planar e-strip results in either intermittent failure (top figure), abrupt failure (middle figure) , and resistance otherwise remains stable (bottom figure).

Figure 6-13E shows how resistance varied over time during cyclic tests. Helical e-strips tended to remain fully functional, with negligible increase in resistance, followed by a sudden breakage, rather than degrading slowly over time. Breakages occurred at variable points along each e-strip, but often close to the clamps. This variation may be due to the e-strips being assembled by hand and may be reduced in future work through automating the process of winding the e-strips around the core.

6.3.5 Helical LED-strips

Figure 6-14 demonstrates the stretchability and flexibility of successfully fabricated 2 mm helical LED-strips, as well as an example application, where a helical LED-strip has been stitched into fabric to create stretchable, illuminated fabric.
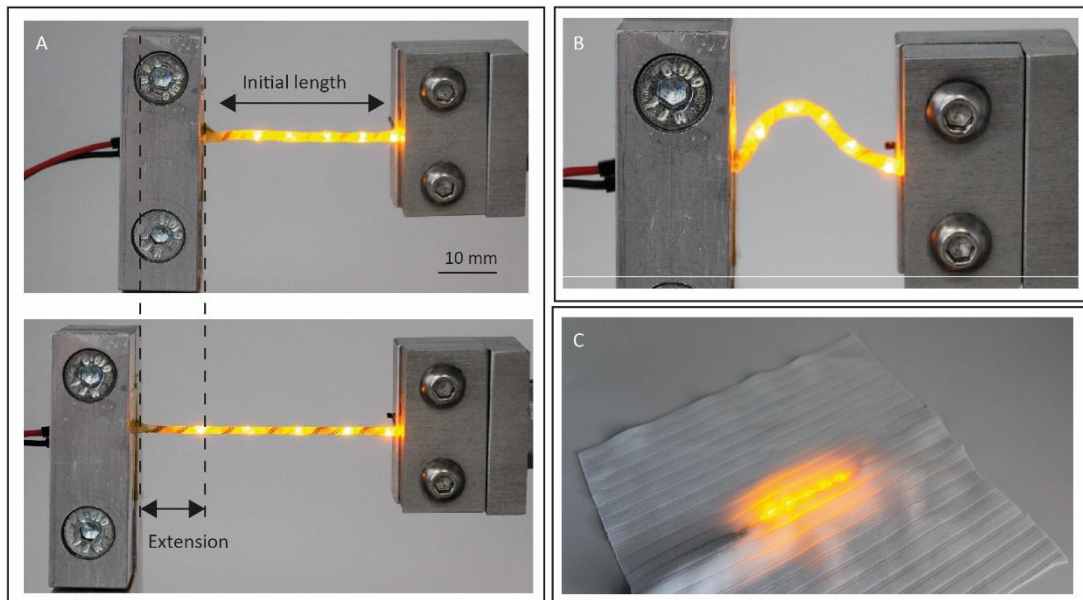
Figure 6-14. 2 mm LED-strips successfully fabricated.

A) Demonstration of stretchability of a helical LED e-strip with silicone tubing core; B) Demonstration of flexibility of helical LED e-strip; C) Example helical e-strip application: stretchable illuminated fabric with a 2 mm LED-strip stitched onto the fabric.

6.3.5.1 Tensile testing

Figure 6-15A shows the results of tensile tests where 4 mm diameter LED-strips, with 0603, 0402 and 0201 LEDs, were stretched to the point of breaking, i.e. until one of more of the LEDs turned off, indicating a crack or tear within the circuit. Three failure modes were observed: in most cases the PI substrate tore near one of the clamps, causing all LEDs to turn off simultaneously (Figure 6-15C). In some cases, the planar strip detached from the core. This failure mode was not observed with interconnect e-strips, which is attributed to

the fact that EPDM is considerably easier to bond than silicone. As the planar e-strips bonded more securely to EPDM, tearing of the core was more likely than delamination of the planar e-strip from the core (for helical interconnect e-strips).
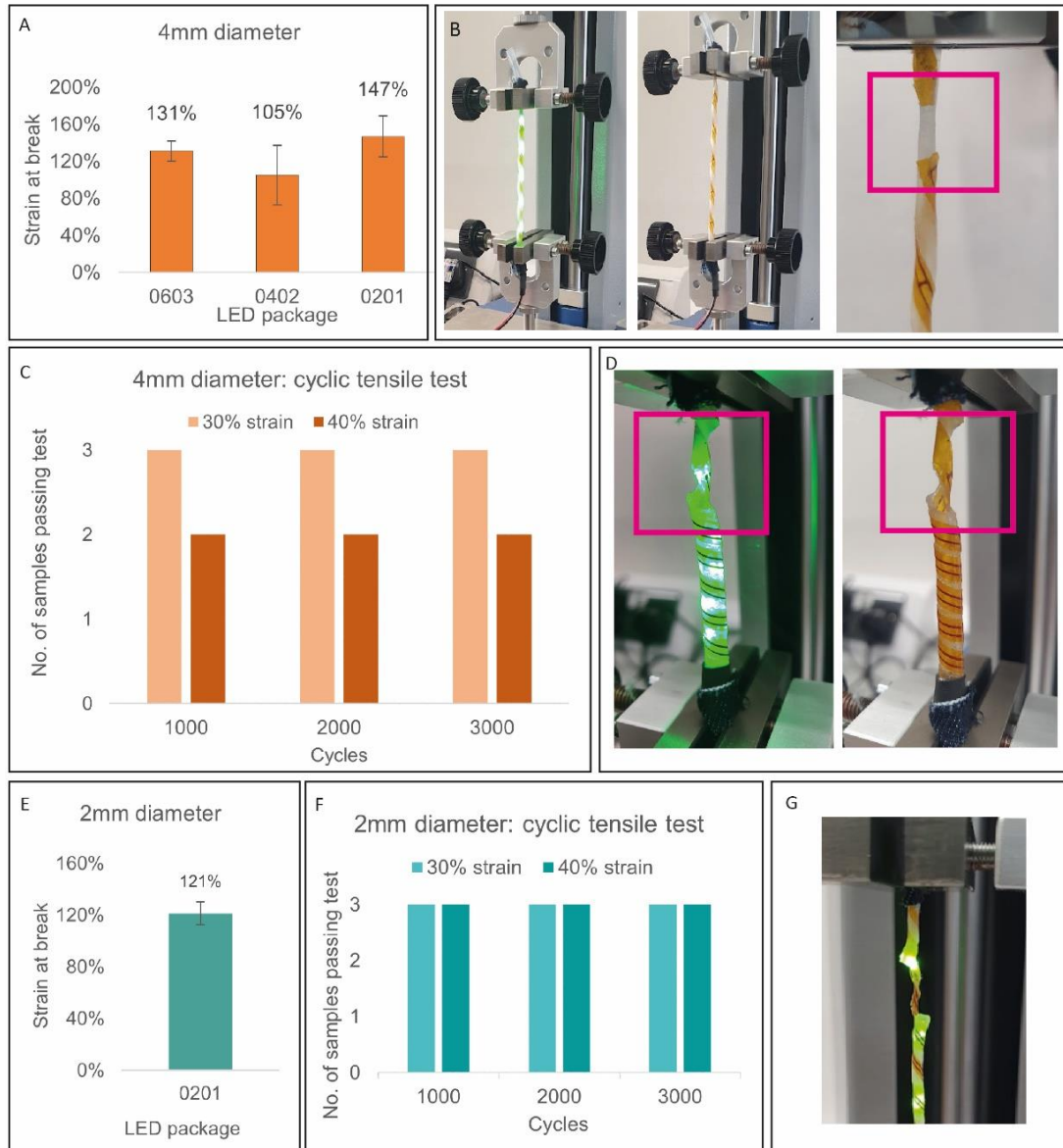
Figure 6-15. Helical LED-strip tensile testing results.

A) LED-strip tensile tests with different LED package sizes to determine stiffness, where error bars represent standard deviation; B) LED strip under strain, lit (left), unlit due to tear in PI (middle), and a close up of the tear (right); C) Results of cyclic tensile tests of 4 mm diameter LED-strips, showing good results at 30% strain but failures at 40% strain; D) Image of one type of failure mode, where the core has torn but the LED circuit is still functional; E) tensile test result for 2 mm diameter LED-strips; F) Cyclic tensile test results for 2 mm LED-strips, showing improved performance relative to 4mm; G) close-up of 2 mm LED-strip failure, where core has torn.

Although e-strips with 0201 LEDs were the least stiff (breaking at approximately 140% extension), there was relatively high standard deviation, and it was not clear that package size significantly impacted stiffness. The main conclusion from these experiments was that all LED-strips were able to withstand >100% strain, and as stretch fabrics may vary from 10-15% stretchable to over 100% stretchable for more specialist fabrics, LED-strips with all LED package sizes can be considered stretchable enough for broad e-textile applications.

Figure 6-15C illustrates the results of cyclic tests on 4 mm LED-strips, showing that samples were able to achieve 30% strain for 3000 cycles with no signs of physical or electrical damage. Increasing the strain to 40% resulted in physical damage to the core of the LED-strips as can be seen in Figure 6-15D, but in all cases, LEDs were still functional after the 3000 cycles test. This indicates that 4 mm LED-strips are suitable for integration into moderate stretch textiles that typically stretch 20-30%, but a less stiff core would be required for more fabrics with higher stretch.

2 mm LED-strips broke at approximately 120% strain (Figure 6-15E), which was not significantly different to the 4 mm LED-strips. However, 2 mm LED-strips demonstrated better performance than 4 mm in the cyclic tensile tests (Figure 6-15F), with all 2 mm LED-strips surviving not only 3000 cycles of 30% strain, but also 3000 cycles of 40% strain. This is attributed to the core being less stiff: both 4 mm and 2 mm silicone tubing were made from the same material, but the 2 mm cores, being thinner, were more elastic. Figure 6-15G shows a 2 mm LED-strip where the core has torn after stretching until breaking point, but where all LEDs are still functional.

6.3.5.2   Wash testing

An image of one of the wash test samples can be seen in Figure 6-16A. The first wash test used 4 mm LED-strips without heat shrink covering the interface between connector and strip.

As seen in Figure 6-16C (Wash Test 1) two of the e-strips in sample 1 failed after 3 washes, both due to tearing of the planar e-strip next to the connector (Figure 6-16B), rendering all 5 LEDs non-functional. The third e-strip survived 9 washes before suffering the same failure. After the final wash test, strips were removed from the fabric, and probing with a multimeter confirmed that all LEDS on the broken e-strips were still functional, and no other damage had been caused.
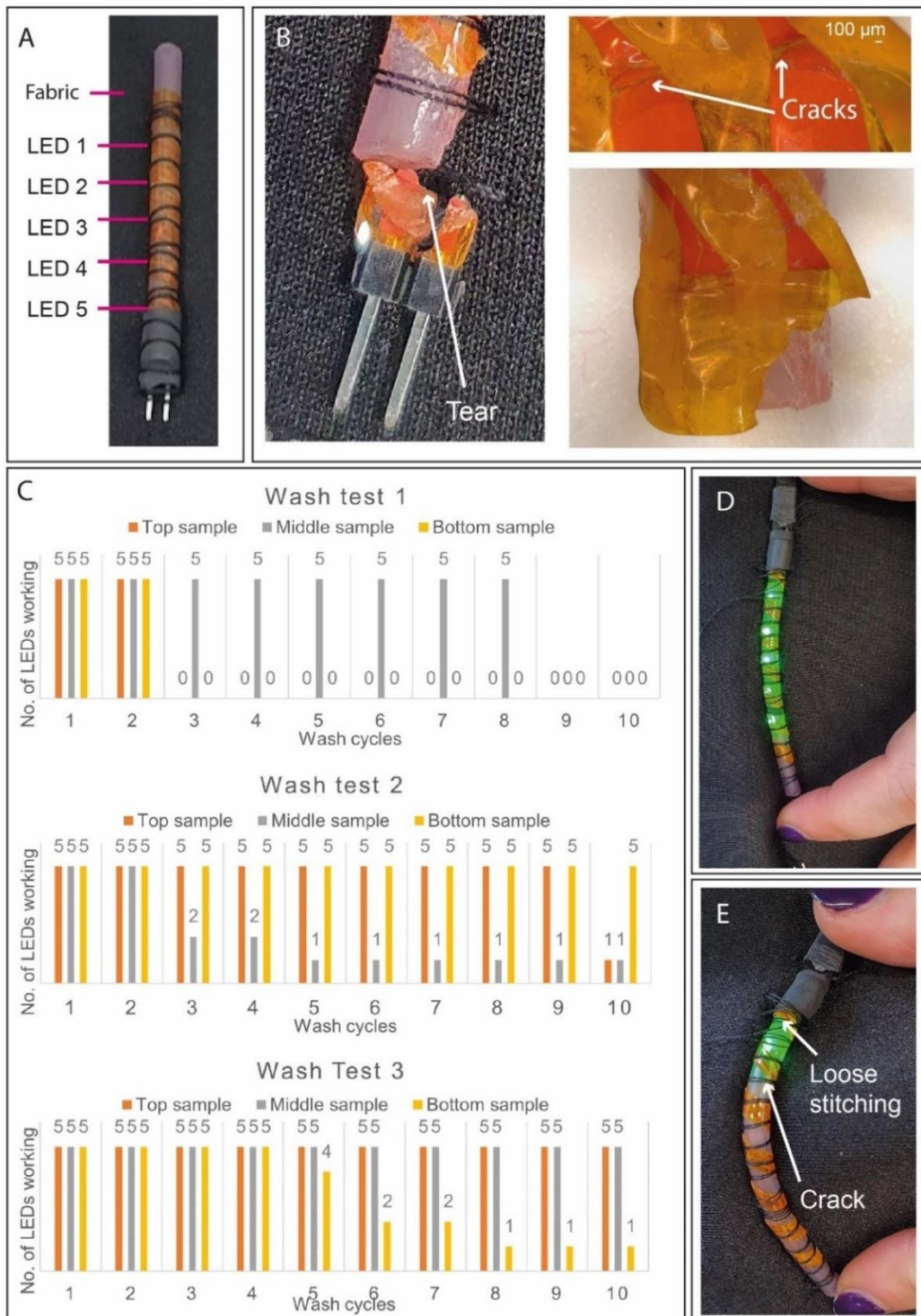
Figure 6-16. Wash testing results for LED helical e-strips.

A) LED-strips stitched onto a piece of fabric for washing; B) Image and microscope image of tear adjacent to connector in sample from first wash test; C) Wash test results, showing that washing durability increased when area adjacent to connector was reinforced with heat shrink, and some samples survived 10 wash cycles; D) Failure mode observed in third wash test, where a crack has formed in the conductive track; E) The same sample, where LEDs turn off when the strip is flexed, opening the crack.

Two further samples were created, this time with heat shrink, one sample with 0603 LEDs and one with 0402 LEDs. Results are shown in Figure 6-16C (Wash Test 2 and 3, respectively). Stitching loosened in one sample, causing an early tear near the connector. Some other LEDs came loose, but otherwise the majority of samples survived 10 washes.

A semi-functional sample is shown in Figure 6-16D and Figure 6-16E. A crack in the strip broke the circuit when the strip was bent, but the LEDs still light when released from bending.

6.3.6 Helical temperature sensing e-strips

The stretchability of helical temp-strips is demonstrated in Figure 6-17A, as well as how temp-strips could be incorporated into textiles, shown in Figure 6-17B and C.
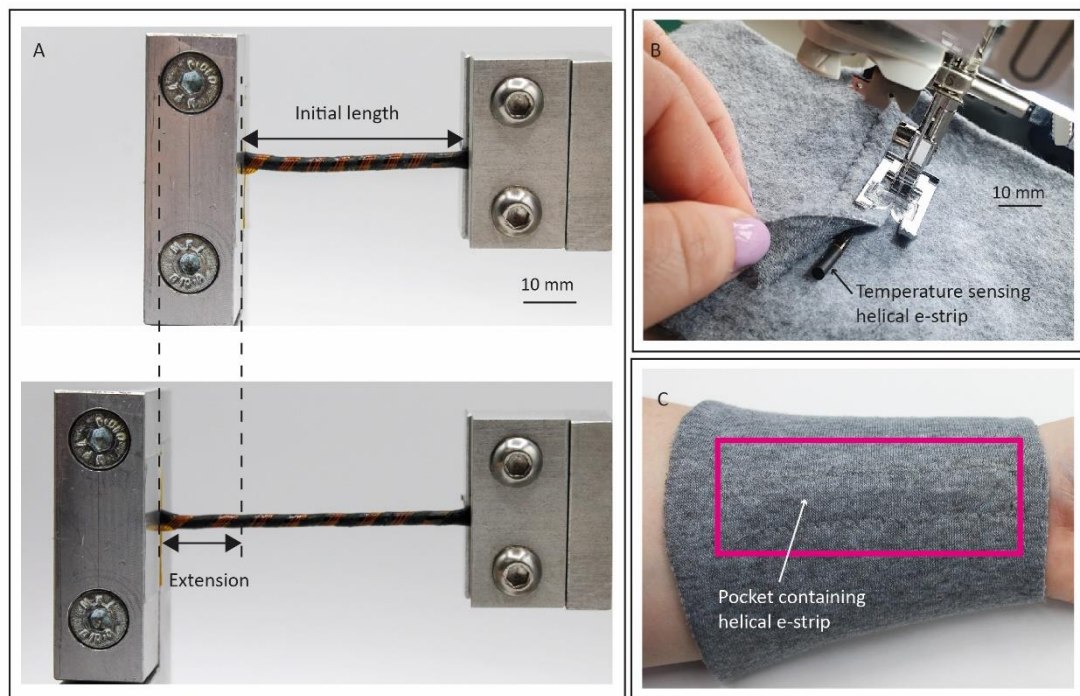
Figure 6-17. Successfully fabricated helical temp-strips.

A) Demonstration of helical sensing e-strip stretchability, with EPDM core; B) Example application: stitching a helical temp-strip into fabric to measure body temperature; C) the helical temp-strip is barely visible in the finished sleeve.

Sensor test results shown in Figure 6-18A show the average temperatures measured by each sensor, and the best results were obtained in the face down condition. In this case, the 4 mm temp-strip obtained more accurate results than the 3 mm temp-strip, which may be because the 4 mm core provides more insulation between the thermistor and the

environment, preventing thermistor readings from drifting towards ambient temperature [202]. In all cases the error was linear, as shown in Figure 6-18B, and could be removed by calibrating the sensor.

In the side on condition, 3 mm and 4 mm temp-strips performed very similarly, both reporting approximately 2-2.5 °C error in temperature measurement. In the face up condition, the 4mm temp-strips performed worse than the 3 mm temp-strips, but both showed increased error and noise in sensor readings relative to the other conditions, with up to 4 °C in measurement error. This is attributed to the core being between the heated surface and the thermistor on the helical temp-strips.
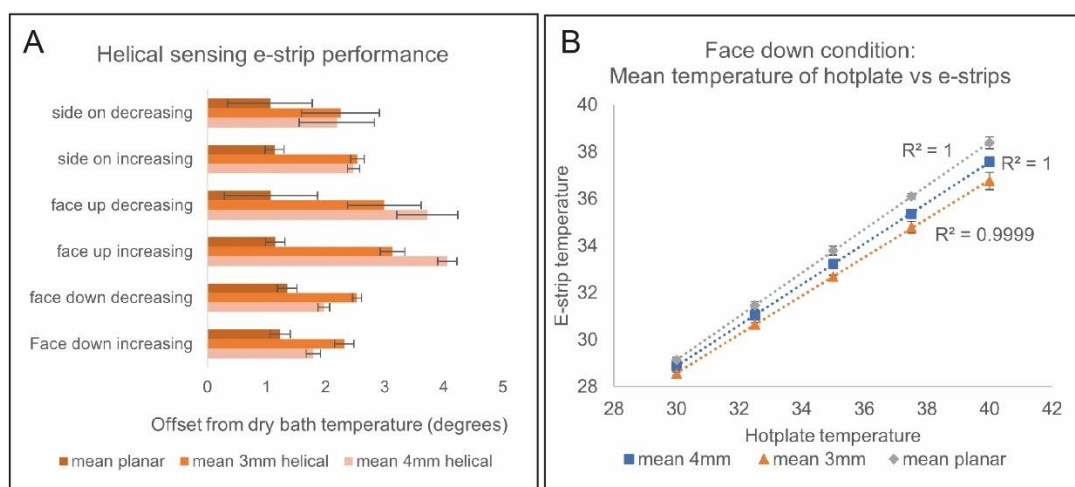
Figure 6-18. Temperature sensing helical e-strips results.

A) Results showing performance of helical e-strips relative to planar e-strip during different conditions; B) Performance of e-strips in Face Down condition across temperature range, showing linear offset in temperature. Data points in graphs represent mean values averaged over 2 minutes of recorded data, and error bars represent standard deviation.

Figure 6-19 shows raw data from temperature sensing e-strips during each of the six test conditions. The planar e-strip data, in all conditions, shows small fluctuations in temperature of approximately 0.5 °C. This is consistent with how the dry bath (hot plate) operates: it maintains a steady temperature, but there are small fluctuations above and below the set temperature. These fluctuations are most accurately recorded by the planar e-strip, but in the face down condition, the helical e-strips are also able to record the fluctuations (though to a lesser degree, approximately 0.2 - 0.3 °C).

In the side on condition, the helical e-strip data is more noisy, with measurement error increasing by approximately 0.5 °C, and no discernible effect of helical e-strip core diameter on the measurement accuracy. And in the face up condition, there is a further increase in noise, with measurement error increasing by a further 1.5 °C and 0.7 °C, respectively, for 4 mm and 3 mm core diameters.
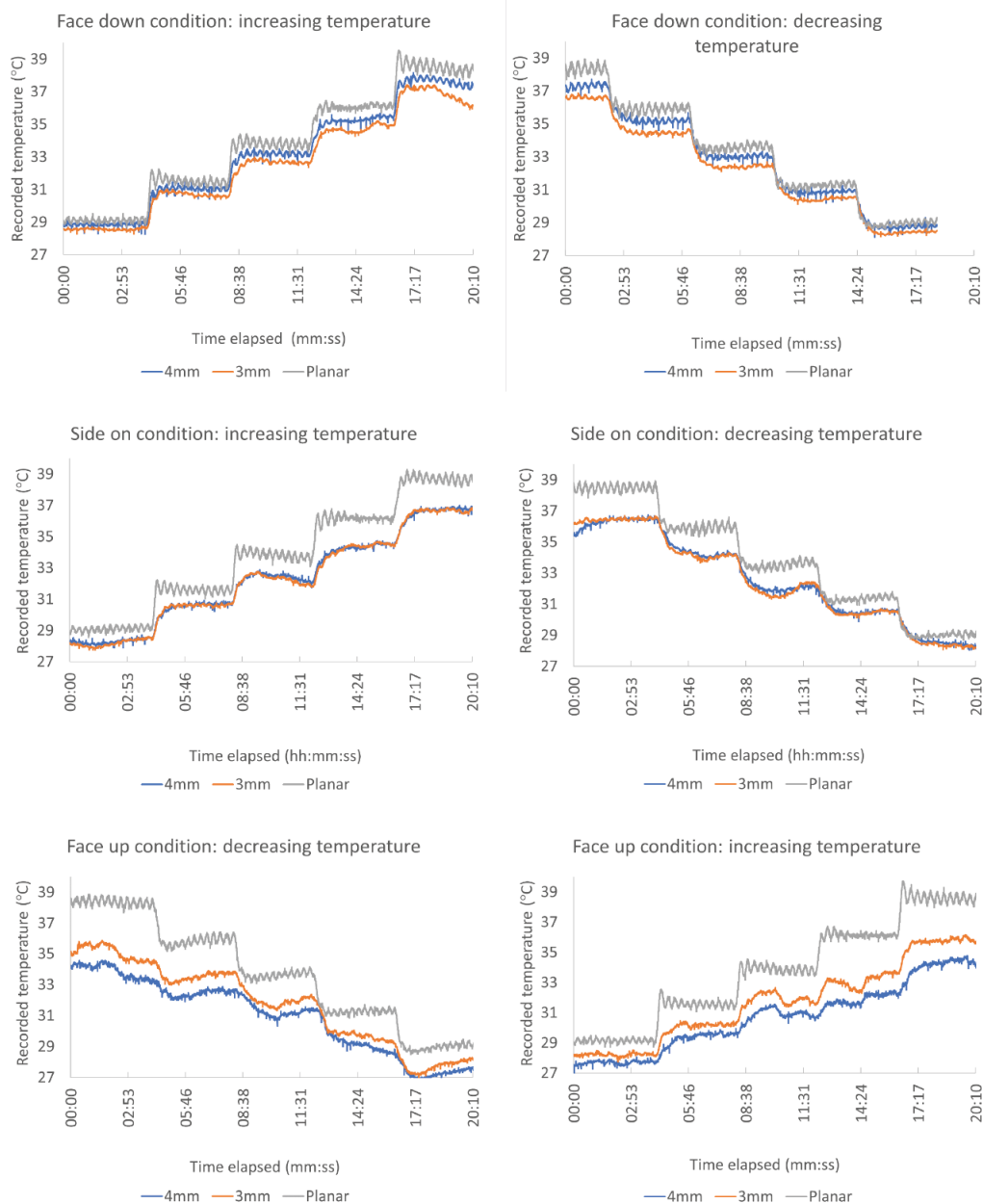
Figure 6-19. Raw data from temperature sensing e-strips.

Helical e-strips in the face down condition are most accurate, showing a slower response to temperature changes than the planar e-strip, but overall recording stable and relatively accurate values. In the side on condition, the diameter of the helical e-strip has no effect on the results, but the sensor readings are less accurate than in the face down condition. And in the face up condition, it is clear that the helical e-strip sensor measurements are the least accurate of all three conditions.

The planar e-strip shows a faster response to the temperature changes, with the helical e-strips lagging behind, particularly in the side on and face up conditions. This is attributed to the core taking time to absorb or release heat. However, in the face down condition, this difference in response time small enough to not be an issue. 3 mm and 4 mm helical e-strips lag behind by less than 1 minute, and as the intended application is e-textiles, detection of rapid fluctuations in temperature are not the main goal. A helical e-strip temperature sensing garment might, for example, monitor the temperature of an athlete during competition, with the aim of detecting early warning signs of heat stroke. Or monitor the temperature of a healing wound, to check for increases in temperature that might indicate the beginning of an infection. But these temperature changes occur gradually, not rapidly.

From this it can be concluded that in a real application it would be important to fix the part with the sensing element so that it is facing the interior of the garment, to prevent rotation and ensure accuracy. For other types of sensors, i.e. motion sensing using accelerometers, contact with the skin is not important, so this would be less of a concern. But as embedding sensors in textiles is known to affect their performance (for example as seen in Chapter 5), additional testing would be required to calibrate temp-strips while embedded in a garment.

6.4 Summary

Helical e-strips can achieve 100-180% elongation before breaking (depending on core material and diameter). This is higher than the 79-88% range achieved with serpentine-shaped PI interconnects encapsulated in TPU, in work aimed at a similar application [40]. Serpentine tracks on elastomer substrates have been shown to achieve 260% strain, but without cyclic testing to properly assess durability [150].

In terms of cyclic testing, helical interconnect e-strips with 4 mm diameter have been shown to withstand up to 50% strain for 3000 cycles. Bossuyt et al suggest that an e-textile sensor with an intended lifetime of a year or longer should survive 10^4 cycles of 5-10% stretch, and 10^6 cycles of 1-3% [188]. But this will depend on the application, and there is currently a lack of data quantifying the mechanical strain e-textile parts undergo when embedded in a garment. 30% strain, for 1000 cycles, has been used to assess similar work [40,156]. And highly stretchable helical interconnects have been shown to survive 500% strain, but only tested for 500 cycles [176]. In this context, the helical e-strip, at this early development stage, performs well against competing technologies.

The results from tensile testing of helical LED-strips have highlighted that the main failure modes were a) tearing of the planar e-strip at the interface between connector and helix; b) tearing of the core material; c) delamination of the planar e-strip from the core, or delamination of components from the planar e-strip. Future work could address these issues by a) applying strain relief to the interface between connector and helix; b) investigating alternative adhesives, and c) applying an additional stretchable encapsulation layer to the exterior of the e-strips. This is discussed further in the next and final chapter.

For helical temp-strips, the orientation of the strip was found to be important. Accurate temperature readings can be recorded by temp-strips of both 3 mm and 4 mm diameter, but if used in a garment, it would be important that the e-strip is secured, and not allowed to freely rotate.

The potential of a 3D helical structure for embedded electronics in e-textiles, with a focus on using standard components and materials compatible with existing manufacturing processes, has been investigated and supported with experimental evidence. To produce the desired structures a process was developed, defining design rules, fabricating prototypes, and performing mechanical testing to validate the concept, and identify key areas for improvement in future iterations.

This chapter has demonstrated functioning helical LED and temperature sensing e-strips, showing successful incorporation of SMD components into helical e-strips. Circuits with 1, 2 and 4 conductive tracks have been successfully fabricated, using 0201, 0402 and 0603 SMD components. 4 mm LED-strips were able to withstand 3000 cycles of 30% strain, and up to 10 wash cycles, using a regular washing program with a 1400 rpm spin cycle. 2 mm LED-strips were shown to withstand at least 3000 cycles of 40% strain. Longer tensile tests, as well as bending and compression tests, were not performed at this early stage of development, because the focus was on validating the helical e-strip concept, rather than comprehensively assessing the durability of an existing technology. Temperature sensing helical e-strips were successfully fabricated and shown to be able to take accurate readings (once calibrated), though it was also found that the orientation of the e-strip – i.e. the location of the thermistor – is critical for accurate readings.

Chapter 7 Conclusion

7.1 Summary

This project began by looking at fabrication methods for flexible electronics, with the goal of incorporating them into e-textiles. This included dispenser printing, and methods to create masks to etch copper-plated PI. Printing was performed on PI film. As etching processes were faster, and more suitable for fine resolution circuits, this was the chosen approach taken for the remainder of the thesis. Two methods to prototype etch masks using a vinyl cutter were developed, to facilitate the fabrication of narrow (down to 1.5 mm) flexible circuits with 100 μm pitch, using 0201 (metric 0402, 0.6 mm x 0.3 mm) SMD components.

These processes were then used to explore modular e-textile systems. A modular temperature sensing cycling garment was constructed, consisting of flexible temperature sensors, stretchable interconnects made from conductive thread stitched onto fabric, and a commercial triathlon suit adapted to house electronic parts. Alongside this, a review of connectors and joining technologies for e-textiles was carried out.

Reliability issues with the initial sensing garment prototype, specifically unreliable connections between conductive threads and electronic connectors, motivated a new development: a novel interposer, which routes conductive threads to a connector, to which a flexible sensor can be attached. Two connectors designed for flexible electronics, not previously used in e-textiles, were used for this. Both are small in size but are only guaranteed to last for 10 mating (connection and disconnection) cycles. Though this makes them unsuitable for some types of connection (e.g. attaching a power supply), it does not render them completely unsuitable for e-textiles. In a modular garment, where some circuit modules only need to be disconnected and re-connected for repair, or to separate parts for recycling, 10 cycles may be more than sufficient.

The sensing garment was updated to incorporate interposer into the design and make the system wireless using a Bluetooth enabled Arduino microcontroller, instead of a wired DAQ which was used in the initial prototype.

Finally, helical e-strips were developed, moving from planar electronics to a 3D stretchable form. This involved the identification of suitable materials, and the development of a fabrication process to produce narrow, fine pitch flexible circuits to wind into a helical

geometry. Where existing examples of helical geometry in electronics have only consisted of helical interconnects, or individual helical (usually printed) components, helical e-strips are fully functional circuits and can contain SMD components.

First, blank helical e-strips, consisting of PI film wrapped around EPDM foam cord, were created. A series of mechanical tests identified an optimal helix angle of 30°, which was found to provide the optimal balance between stiffness and strength. The results from the tests also set a target for the width of helical e-strips to be at most 75% of the diameter, to achieve a trade-off between minimising diameter and maximising stretch. Only 0603 and smaller components were used, to enable helical e-strip diameter to be at most 2 - 4 mm. Helical interconnect e-strips were then fabricated, and 2 mm, 3 mm and 4 mm diameter samples were able to survive 3000 cycles of 30% elongation. At higher levels (50% and 75%) the core material showed signs of tearing by the end of the cyclic tests.

After investigating the basic fabrication and geometry of helical e-strips, two functional demonstrators were produced: light-emitting LED e-strips, and temperature sensing e-strips. LED e-strips, with a silicone tubing core that allows light to be transmitted throughout the structure, were more robust than helical interconnect e-strips with EPDM rubber cores. 2 mm diameter samples survived 3000 cycles of both 30% and 40% stretch. 4 mm helical LED e-strips were also subjected to washing tests, with the majority of samples surviving 10 wash cycles.

Temperature sensing helical e-strips were fabricated using a thermistor arranged in a Wheatstone Bridge circuit. It was found that these could achieve similar accuracy to a planar e-strip using the same circuit, but that the orientation of the e-strip was important: the thermistor needed to be oriented towards the surface it was measuring, i.e. facing the body if embedded in a garment. This has implications for how temperature sensing helical e-strips would be used in a real garment, as they would need to be fixed place in certain areas, to avoid rotation of the thermistor away from the body. Overall, helical e-strips showed promise as a stretchable electronics technology.

7.2   Future work

In general, future work on both modular e-textile systems and helical e-strips should include a) further development of manufacturing processes to enhance durability and enable scaling up of production, and b) additional testing – such as more extensive wash testing, or longer and more complex tensile tests – to simulate real life conditions.

7.2.1   Modular e-textile systems

The future of modular e-textile systems depends heavily on the development of new connectors for e-textiles. The current options are acceptable, but not ideal. This is something of a chicken and egg situation though, as connector development is a multi-faceted endeavour best undertaken by connector manufacturers, who have in-depth knowledge of materials, mechanical engineering, and electrical contact theory. However, the lack of e-textile connectors currently on the market suggests that connector manufacturers are waiting for the e-textile market to grow before investing resources into e-textile connector development. It seems likely that the current practices of adapting electronic or textile connectors to work with e-textiles will continue for a while.

Future development of the interposers developed in this work could include additional mechanical tests, as well as wash testing. On-body human participant trials, and further evaluation of the temperature sensor, are needed to fully assess the reliability of the final version of the modular sensing garment. A user study on assembly and disassembly would also help to assess whether the system can be reconfigured or prepared for recycling easily

7.2.2   Helical e-strips

The viability of the helical e-strip concept has been validated, and future work will improve the reliability of the helical e-strip by refining the fabrication process and choice of core material. For example, in this work the planar e-strip is wound around the core to form the helical structure by hand, which results in small irregularities in the helical geometry. These irregularities will negatively affect performance, particularly lifespan, as irregularities in the structure of the helix are likely to lead to applied strain being unevenly distributed, creating weak points susceptible to failure. This would be improved by automating the winding process, potentially using existing winding equipment used to wind coils of wire, or to wrap textile threads onto spools and bobbins. Apart from the winding stage, all other fabrication

steps used standard processes that can be scaled up for high volume production, and don't require custom equipment or materials.

Prototyping and initial development of the helical e-strip have been covered by this work, but moving forward to manufacturing, a key area for development is sustainability. Cyanoacrylate adhesive was used to bind the planar e-strips to the core, but this is not ideal as it is difficult to disassemble strips for repair, or to separate parts for recycling. However, an advantage of the platform is that it does not rely on any particular material or process. The same structure could be constructed from printed circuitry on a different substrate or using a different elastic core material or adhesives. Potential future development of new types of electronic components – thinner, and therefore more flexible – will also benefit helical e-strip technology, rather than making it redundant.

This work has also only demonstrated helical e-strips with single layer circuitry. Future development of double layer planar e-strips that can be wound into helical form would allow for more complex circuits, and therefore more applications. Some preliminary work on two-layer structures was done during this project but was not completed. A description is included in Appendix 3. This would have been an accelerometer (motion sensing) helical e-strip, using an accelerometer IC. As illustrated in Figure 8-9, a planar e-strip containing this 3 mm x 3 mm x 1 mm component would mean that the helical e-strip would need to be 6 - 7 mm in diameter. This, realistically, is too bulky for most wearable e-textile applications. It is significantly thicker than most fabrics, with the exception of some used for winter outerwear, or footwear.

A thinner accelerometer e-strip could be realised using bare die components, but this was out of the scope of this project, which focused on conventional SMD components. Future work will focus on implementing this and minimizing diameter through the use of printed or bare die components. Another area for future work is increasing the sustainability of the manufacturing process and developing an automated process to create the helical geometry. In summary, this work has explored, and validated, the viability of creating circuits in a helical geometry, and demonstrated that it has potential to be a transformative technology for e-textiles.

Bringing the two main themes of this thesis together, it would also be possible to make a modular helical e-strip system or use interposers to interface helical e-strips with conductive

textiles sensors or printed electrodes, for example. This would require further investigation into connectors for helical e-strips, ideally developing a connector to match the cylindrical geometry of the helical e-strip, and with a latching mechanism to prevent disconnection.

7.3 Conclusion

The aim of this thesis was to investigate new connectors for e-textile garments, and develop stretchable, helical e-strips designed to be embedded inside seams or channels in garments, to realise stretchable sensor circuits, among other applications.

Helical e-strips were successfully fabricated, and evaluated through at set of experiments to determine the factors that affect their stiffness and assess their robustness. Helical interconnect, LED and temperature sensing e-strips were fabricated and tested, with diameters as narrow as 2-3 mm. Helical e-strips were able to survive up to 10 washes in a washing machine, and 3000 cycles of 30%-40% elongation, depending on diameter and materials. Therefore, the objective of developing a helical e-strip fabrication process, and producing helical e-strips able to survive at least 30% strain, was achieved.

Standards for e-textiles are still in development, which means that tests used to evaluate e-textiles vary significantly. The key questions are: a) by how much do e-textile parts need to stretch, and b) how many tensile strain cycles should they be able to survive? The first question depends heavily on the fabrics used in the garment. Different textiles, made with different fibres, using different techniques, vary in how much they can stretch. While some high stretch materials such as spandex can stretch more than 100%, garments made from these materials also contain seams, which are less stretchy, and zippers, which do not stretch at all. Therefore, e-textile circuitry doesn't necessarily need to be as stretchable as spandex, depending on what fabric it is to be embedded in, and where in the garment it needs to be placed. The second question relates to durability, and how a garment is to be used: is it a garment where circuitry will be routed along the elbows or knees, and which will be subjected to a lot of bending and stretching? Or is it a compression garment covering only the forearm, which will be pulled on and then remain at more or less constant elongation while worn?

The point of this is that the helical e-strips demonstrated in this work, which can stretch by 30%-40% repeatedly, may not be able to match the properties of the most stretchy Spandex fabric, but neither can currently available stretchable electronics technologies. And as helical

e-strips are at an early stage of development relative to competing technologies, this suggests that with additional research (as outlined in the previous section) they could be improved to survive repeated cycles of ≥ 75% strain, and be reduced in size to embed unobtrusively in a wide range of fabrics.

Two iterations of a modular temperature sensing garment were created to explore modular e-textile systems and included the development of a modular interposer for e-textiles. The final version of the interposer was able to survive at least 1000 cycles of stretching and relaxing with no damage, and no disconnection. While undertaking this work, printing and etching fabrication processes for flexible electronics were evaluated, and a new prototyping process for flexible electronics, using vinyl and a vinyl cutter, was developed. Overall, several novel contributions were made to the development of better interfaces in e-textiles, and a new format for stretchable electronics to make more stretchable and durable e-textile garments. These developments have been proven to offer improvements to interfaces and to stretchable electronics, which can both contribute to improved e-textile manufacturing.

Given this, why not scrap the entire concept of modular e-textiles entirely? Because, in this writer's view, the benefits for sustainability outweigh the drawbacks. A future for e-textiles that involves seamless integration of electronics into textiles, undetectable by the user, seems completely at odds with the need for sustainable production. Recent semiconductor chip shortages have highlighted the need for the lifetime of electronic devices to be maximised, and this must include e-textiles. Adopting modular design as standard in e-textiles could also benefit the e-textile manufacturing ecosystem. If a garment manufacturer can buy standardised e-textile modules and configure them in a way that fits a particular garment, this could expand e-textile production to a wider range of manufacturers.

In summary, helical e-strips and modular e-textile systems both show promise for driving forward the development of e-textiles, and could help realise a future where essential technologies such as medical devices are reinvented in a comfortable, wearable format.

References

1.   Lovelace, A. A. Sketch of the Analytical Engine invented by Charles Babbage Esq. by L. F. Menabrea, of Turin, Officer of the Military Engineers. [Translated and with notes by A. A. L: Augusta Ada, Countess of Lovelace], Article XXIX. *Taylor's Scientific Memoirs* 3, 687 (1843).

2.   Rosner, D. K., Shorey, S., Craft, B. R. & Remick, H. Making Core Memory: Design inquiry into gendered legacies of engineering and craftwork. *Conference on Human Factors in Computing Systems - Proceedings* 2018-April, (2018).

3.   Gupta, S., Navaraj, W. T., Lorenzelli, L. & Dahiya, R. Ultra-thin chips for high-performance flexible electronics. *npj Flexible Electronics* vol. 2 1–17 Preprint at https://doi.org/10.1038/s41528-018-0021-5 (2018).

4.   Hughes-Riley, T., Dias, T. & Cork, C. A historical review of the development of electronic textiles. *Fibers* 6, (2018).

5.   Kazani, I. *et al. Smart Textiles for Sportswear and Wearables (WG5): State-of-the Art Report. CONTEXT Project*. (2020).

6.   E-Textiles and Smart Clothing Markets 2023-2033: Technologies, Players, and Applications: IDTechEx. https://www.idtechex.com/en/research-report/e-textiles-and-smart-clothing-markets-2023-2033-technologies-players-and-applications/925.

7.   Buechley, L. A. An Investigation of Computational Textiles with Applications to Education and Design. (University of Colorado, 2007).

8.   Buechley, L., Eisenberg, M., Catchen, J. & Crockett, A. The LilyPad Arduino: Using computational textiles to investigate engagement, aesthetics, and diversity in computer science education. *Conference on Human Factors in Computing Systems - Proceedings* 423–432 (2008) doi:10.1145/1357054.1357123.

9.   Sports Bra + HRM - SensoriaFitness. https://store.sensoriafitness.com/sports-bra-hrm/.

10.   Kgatuke, M. *et al.* Exploring the Role of Textile Craft Practice in Interdisciplinary E-Textiles Development through the Design of an Illuminated Safety Cycling Jacket. *Proceedings 2019, Vol. 32, Page 12* 32, 12 (2019).

11.   CUTECIRCUIT | The SoundShirt. https://cutecircuit.com/soundshirt/.

12.   Muhammad Sayem, A. S., Hon Teay, S., Shahariar, H., Luise Fink, P. & Albarbar, A. Review on Smart Electro-Clothing Systems (SeCSs). *Sensors* 20, 587 (2020).

13.   Ankhili, A. *et al.* How to Connect Conductive Flexible Textile Tracks to Skin Electrocardiography Electrodes and Protect Them against Washing. *IEEE Sens J* 19, 11995–12002 (2019).

14.   Wei, Y., Yang, K., Browne, M., Bostan, L. & Worsley, P. Wearable Electrical Stimulation to Improve Lymphatic Function. *IEEE Sens Lett* 3, 1–4 (2019).

15. Yang, K. *et al.* Development of User-Friendly Wearable Electronic Textiles for Healthcare Applications. *Sensors* 18, 2410 (2018).

16. Jacquard by Google - Levi's®. https://atap.google.com/jacquard/products/levi-commuter/.

17. De Vos, M., Torah, R. & Tudor, J. Dispenser printed electroluminescent lamps on textiles for smart fabric applications. *Smart Mater Struct* 25, (2016).

18. Janczak, D. *et al.* Stretchable and washable electroluminescent display screen-printed on textile. *Nanomaterials* 9, (2019).

19. Shi, X. *et al.* Large-area display textiles integrated with functional systems. *Nature* 591, 240–245 (2021).

20. Fang, S., Wang, R., Ni, H., Liu, H. & Liu, L. A review of flexible electric heating element and electric heating garments. *Journal of Industrial Textiles* Preprint at https://doi.org/10.1177/1528083720968278 (2020).

21. Stern, B. & Cooper, T. *Getting Started with Adafruit FLORA: Making Wearables with an Arduino*. (Maker Media Inc, 2015).

22. Packs & Parts — LOOMIA Soft Circuit Systems | E-textiles. https://www.loomia.com/packsparts.

23. HOW TO GET WHAT YOU WANT. https://www.kobakant.at/DIY/.

24. BSI. *Textiles and Textile Products - Smart (Intelligent) Textiles - Definitions, Categorisation, Applications and Standardization Needs (ISO/TR 23383:2020)*. (2020).

25. Castano, L. M. & Flatau, A. B. Smart fabric sensors and e-textile technologies: A review. *Smart Mater Struct* 23, (2014).

26. de Mulatier, S., Nasreldin, M., Delattre, R., Ramuz, M. & Djenizian, T. Electronic Circuits Integration in Textiles for Data Processing in Wearable Technologies. *Adv Mater Technol* 3, 1–26 (2018).

27. Fractal Antennae — Afroditi Psarra. https://afroditipsarra.com/work/fractal-antennae.

28. Lugoda, P. *et al.* Flexible temperature sensor integration into e-textiles using different industrial yarn fabrication processes. *Sensors (Switzerland)* 20, (2020).

29. Zysset, C., Kinkeldei, T. W., Munzenrieder, N., Cherenack, K. & Tröster, G. Integration method for electronics in woven textiles. *IEEE Trans Compon Packaging Manuf Technol* 2, 1107–1117 (2012).

30. Veja, P. An investigation of integrated woven electronic textiles (e-textiles) via design led processes. (2014).

31.   Chen, A., Tan, J., Tao, X., Henry, P. & Bai, Z. Challenges in knitted E-textiles. in *Advances in Intelligent Systems and Computing* vol. 849 129–135 (Springer Verlag, 2019).

32.   Post, E. R., Orth, M., Russo, R. R. & Gershenfeld, N. E-broîdery: Design and fabrication of textile-based computing. *IBM Systems Journal* 39, 840–860 (2000).

33.   Tangsirinaruenart, O. & Stylios, G. A novel textile stitch-based strain sensor for wearable end users. *Materials* 12, (2019).

34.   Liang, A., Stewart, R. & Bryan-Kinns, N. Analysis of Sensitivity, Linearity, Hysteresis, Responsiveness, and Fatigue of Textile Knit Stretch Sensors. *Sensors* 19, 3618 (2019).

35.   Berglund, M. E., Duvall, J., Simon, C. & Dunne, L. E. Surface-mount component attachment for E-textiles. in *ISWC 2015 - Proceedings of the 2015 ACM International Symposium on Wearable Computers* 65–66 (Association for Computing Machinery, Inc, New York, New York, USA, 2015). doi:10.1145/2802083.2808413.

36.   Micus, S., Haupt, M. & Gresser, G. T. Soldering Electronics to Smart Textiles by Pulsed Nd:YAG Laser. *Materials (Basel)* 13, (2020).

37.   ZSK embroidery machines | Smart Textiles. https://www.zsk.de/en/industries-and-applications/technical-embroidery/smart-textiles.php.

38.   Linz, T., von Krshiwoblozki, M., Walter, H. & Foerster, P. Contacting electronics to fabric circuits with nonconductive adhesive bonding. *Journal of the Textile Institute* 103, 1139–1150 (2012).

39.   Rotzler, S. & Schneider-Ramelow, M. Washability of E-Textiles: Failure Modes and Influences on Washing Reliability. *Textiles 2021, Vol. 1, Pages 37-54* 1, 37–54 (2021).

40.   Wicaksono, I. *et al.* A tailored, electronic textile conformable suit for large-scale spatiotemporal physiological sensing in vivo. *npj Flexible Electronics* 4, 5 (2020).

41.   Komolafe, A. *et al.* Integrating Flexible Filament Circuits for E-Textile Applications. *Adv Mater Technol* 4, (2019).

42.   Lugoda, P. *et al.* Flexible Temperature Sensor Integration into E-Textiles Using Different Industrial Yarn Fabrication Processes. *Sensors* 20, 73 (2019).

43.   Kapton® HN. https://www.dupont.com/electronics-industrial/kapton-hn.html.

44.   Zardetto, V., Brown, T. M., Reale, A. & Di Carlo, A. Substrates for flexible electronics: A practical investigation on the electrical, film flexibility, optical, temperature, and solvent resistance properties. *J Polym Sci B Polym Phys* 49, 638–648 (2011).

45.   Ahmad, J., Andersson, H. & Sidén, J. Screen-Printed Piezoresistive Sensors for Monitoring Pressure Distribution in Wheelchair. *IEEE Sens J* 19, 2055–2063 (2019).

46.   Valavan, A., Komolafe, A., Harris, N. R. & Beeby, S. Vacuum Thermoforming for Packaging Flexible Electronics and Sensors in E-Textiles. *IEEE Trans Compon Packaging Manuf Technol* 13, 715–723 (2023).

47.   Varteresian, J. *Fabricating Printed Circuit Boards*. (Newnes, 2002).

48.   Branson, J., Naber, J. & Edelen, G. A simplistic printed circuit board fabrication process for course projects. *IEEE Transactions on Education* 43, 257–261 (2000).

49.   Creating SMD PCB's With Laser Masking Method on a Snapmaker 2.0 : 7 Steps (with Pictures) - Instructables. https://www.instructables.com/Creating-SMD-PCBs-With-Laser-Masking-Method-on-a-S/.

50.   Komolafe, A., Torah, R., Nunes-Matos, H., Tudor, M. & Beeby, S. Integration of temperature sensors in fabrics. in *FLEPS 2019 - IEEE International Conference on Flexible and Printable Sensors and Systems, Proceedings* (Institute of Electrical and Electronics Engineers Inc., 2019). doi:10.1109/FLEPS.2019.8792294.

51.   Inside the Twirkle Shirt | CuteCircuit Twirkle Shirt Teardown | Adafruit Learning System. https://learn.adafruit.com/cutecircuit-twirkle-shirt-teardown/inside-the-twirkle-shirt.

52.   Kajenski, A., Khushrushahi, S., Strack, G. & Akyurtlu, A. Printed Metasurfaces for Wearables. *2022 IEEE International Symposium on Antennas and Propagation and USNC-URSI Radio Science Meeting, AP-S/URSI 2022 - Proceedings* 557–558 (2022) doi:10.1109/AP-S/USNC-URSI47032.2022.9887270.

53.   Yang, K., Torah, R., Wei, Y., Beeby, S. & Tudor, J. Waterproof and durable screen printed silver conductive tracks on textiles. *Textile Research Journal* 83, 2023–2031 (2013).

54.   The making of…. closed loop smart atheleisure fashion « by-wire.net. http://www.by-wire.net/wear-sustain-closed-loop-smart-atheleisure-fashion/.

55.   Smelik, A., Toussaint, L. & Van Dongen, P. Solar fashion: An embodied approach to wearable technology. *International Journal of Fashion Studies* 3, 287–303 (2016).

56.   Hutter, P. C., Rothlander, T., Scheipl, G. & Stadlober, B. All Screen-Printed Logic Gates Based on Organic Electrochemical Transistors. *IEEE Trans Electron Devices* 62, 4231–4236 (2015).

57.   Ostfeld, A. E., Deckman, I., Gaikwad, A. M., Lochner, C. M. & Arias, A. C. Screen printed passive components for flexible power electronics. *Scientific Reports 2015 5:1* 5, 1–11 (2015).

58.   Gupta, S., Navaraj, W. T., Lorenzelli, L. & Dahiya, R. Ultra-thin chips for high-performance flexible electronics. *npj Flexible Electronics* vol. 2 1–17 Preprint at https://doi.org/10.1038/s41528-018-0021-5 (2018).

59.   Levitt, A. *et al.* MXene-Based Fibers, Yarns, and Fabrics for Wearable Energy Storage Devices. *Adv Funct Mater* 30, 2000739 (2020).

60.   Shim, B. S., Chen, W., Doty, C., Xu, C. & Kotov, N. A. Smart electronic yarns and wearable fabrics for human biomonitoring made by carbon nanotube coating with polyelectrolytes. *Nano Lett* 8, 4151–4157 (2008).

61.   Tseghai, G. B., Mengistie, D. A., Malengier, B., Fante, K. A. & Van Langenhove, L. PEDOT:PSS-Based Conductive Textiles and Their Applications. *Sensors 2020, Vol. 20, Page 1881* 20, 1881 (2020).

62.   Khan, S., Lorenzelli, L. & Dahiya, R. S. Technologies for printing sensors and electronics over large flexible substrates: A review. *IEEE Sens J* 15, 3164–3185 (2015).

63.   De Vos, M., Torah, R., Beeby, S. & Tudor, J. Functional electronic screen-printing - Electroluminescent lamps on Fabric. in *Procedia Engineering* vol. 87 1513–1516 (Elsevier Ltd, 2014).

64.   Wei, Y., Wang, X., Torah, R. & Tudor, J. Dispenser printing of electrochromic display on textiles for creative applications. *Electron Lett* 53, 779–781 (2017).

65.   Wagih, M. Direct-Write Dispenser Printing for Rapid Antenna Prototyping on Thin Flexible Substrates. *14th European Conference on Antennas and Propagation, EuCAP 2020* 2–5 (2020) doi:10.23919/EuCAP48036.2020.9135625.

66.   Hu, G. *et al.* Functional inks and printing of two-dimensional materials. *Chem Soc Rev* 47, 3265–3300 (2018).

67.   Matsui, H., Takeda, Y. & Tokito, S. Flexible and printed organic transistors: From materials to integrated circuits. *Org Electron* 75, 105432 (2019).

68.   Linz, T., Simon, E. P. & Walter, H. Modeling embroidered contacts for electronics in textiles. *Journal of the Textile Institute* 103, 644–653 (2012).

69.   Nashed, M. N., Hardy, D. A., Hughes-Riley, T. & Dias, T. A novel method for embedding semiconductor dies within textile yarn to create electronic textiles. *Fibers* 7, (2019).

70.   Rahemtulla, Z. *et al.* The Design and Engineering of a Fall and Near-Fall Detection Electronic Textile. *Materials 2023, Vol. 16, Page 1920* 16, 1920 (2023).

71.   Horowitz, P. & Hill, W. *The Art of Electronics - 3rd Edition*. (2015). doi:10.1119/1.16385.

72.   Linz, T., Kallmayer, C., Aschenbrenner, R. & Reichl, H. Embroidering electrical interconnects with conductive yarn for the integration of flexible electronic modules into fabric. *Proceedings - International Symposium on Wearable Computers, ISWC* 2005, 86–89 (2005).

73.   Simon, E. P., Kallmayer, C., Aschenbrenner, R. & Lang, K. D. Novel approach for integrating electronics into textiles at room temperature using a force-fit interconnection. *EMPC-2011 - 18th European Microelectronics and Packaging Conference, Proceedings* (2011).

74.   von Krshiwoblozki, M., Linz, T., Neudeck, A. & Kallmayer, C. Electronics in Textiles – Adhesive Bonding Technology for Reliably Embedding Electronic Modules into Textile Circuits. *Advances in Science and Technology* 85, 1–10 (2012).

75. Garbacz, K., Stagun, L., Rotzler, S., Semenec, M. & Krshiwoblozki, M. von. Modular E-Textile Toolkit for Prototyping and Manufacturing. *Proc West Mark Ed Assoc Conf* 68, 5 (2021).

76. Mehmann, A., Varga, M., Gönner, K. & Troster, G. A ball-grid-array-like electronics-to-textile pocket connector for wearable electronics. in *ISWC 2015 - Proceedings of the 2015 ACM International Symposium on Wearable Computers* 57–60 (Association for Computing Machinery, Inc, New York, New York, USA, 2015). doi:10.1145/2802083.2802093.

77. Aradhana, R., Mohanty, S. & Nayak, S. K. A review on epoxy-based electrically conductive adhesives. *Int J Adhes Adhes* 99, 102596 (2020).

78. Varga, M., Münzenrieder, N., Vogt, C. & Tröster, G. Programmable e-textile composite Circuit. in *Proceedings - Electronic Components and Technology Conference* vols 2015-July 678–684 (Institute of Electrical and Electronics Engineers Inc., 2015).

79. Jung, S. Y., Hong, H. E. & Paik, K. W. A Study on the Cu-Rod Anisotropic Conductive Films (ACFs) for Flex-on-Fabric (FOF) Interconnections Using an Ultrasonic Bonding Method. *Proceedings - Electronic Components and Technology Conference* 2016-Augus, 2245–2250 (2016).

80. Linz, T., Simon, E. & Walter, H. Fundamental analysis of embroidered contacts for electronics in textiles. in *Electronics System Integration Technology Conference, ESTC 2010 - Proceedings* (2010). doi:10.1109/ESTC.2010.5642823.

81. Muth, J. F. Woven Fabric-Based Electrical Circuits. Part I: Evaluating Interconnect Methods. *Textile Research Journal* 74, 913–919 (2004).

82. Michal, D., Suchy, S., Slauf, J., Reboun, J. & Soukup, R. Resistance Welding in Smart Textile. *Proceedings of the International Spring Seminar on Electronics Technology* 2019-May, 1–6 (2019).

83. Sima, K. *et al.* Washing Resistance of Textile Ribbon Dismountable Interconnections in Smart Textiles. *2021 44th International Spring Seminar on Electronics Technology (ISSE)* 1–5 (2021) doi:10.1109/ISSE51996.2021.9467516.

84. Simon, E. P., Kallmayer, C., Schneider-Ramelow, M. & Lang, K. D. Development of a multi-terminal crimp package for smart textile integration. in *2012 4th Electronic System-Integration Technology Conference, ESTC 2012* (IEEE Computer Society, 2012). doi:10.1109/ESTC.2012.6542057.

85. Lee, S., Kim, B., Roh, T., Hong, S. & Yoo, H. J. Arm-band type textile-MP3 player with multi-layer Planar Fashionable Circuit Board (P-FCB) techniques. *Proceedings - International Symposium on Wearable Computers, ISWC* (2010) doi:10.1109/ISWC.2010.5665879.

86. Buechley, L. & Eisenberg, M. Fabric PCBs, electronic sequins, and socket buttons: Techniques for e-textile craft. *Pers Ubiquitous Comput* 13, 133–150 (2009).

87. Leśnikowski, J. Research on poppers used as electrical connectors in high speed textile transmission lines. *Autex Research Journal* 16, 228–235 (2016).

88. Spring Loaded Contact, Pogo Pin - P70-1000045R | Harwin. https://www.harwin.com/products/P70-1000045R/.

89. Righetti, X. & Thalmann, D. Proposition of a Modular I2C-Based Wearable Architecture. in *Melecon 2010 - 2010 15th IEEE Mediterranean Electrotechnical Conference* 802–805 (2010). doi:10.1109/MELCON.2010.5475965.

90. Hill, C., Schneider, M., Eisenberg, A. & Gross, M. D. The ThreadBoard: Designing an E-Textile Rapid Prototyping Board. *TEI 2021 - Proceedings of the 15th International Conference on Tangible, Embedded, and Embodied Interaction* (2021) doi:10.1145/3430524.3440642.

91. Seager, R. D., Chauraya, A., Zhang, S., Whittow, W. & Vardaxoglou, Y. Flexible radio frequency connectors for textile electronics. *Electron Lett* 49, 1371–1373 (2013).

92. Joo, H. G., Jang, Y. H. & Choi, H. S. Electrical contact resistance for a conductive Velcro system. *Tribol Int* 80, 115–121 (2014).

93. CONDUCTIVE HOOK & LOOP 10CM OR 1 METRE LENGTHS - Light Stitches. https://lightstitches.co.uk/product/conductive-hook-and-loop-10cm/.

94. US5499927A - Zipper-type electrical connector - Google Patents. https://patents.google.com/patent/US5499927A/en.

95. Barnes, K. Zipper Connectors for Flexible Electronic Circuits. *NASA Tech Briefs* 6 Preprint at (2003).

96. Zip and Go® - Genius Objects. https://genius-objects.com/products-and-services/zip-and-go.html.

97. Olsson, T., Gaetano, D., Wiklund, S. & Odhner, J. *Open Softwear: Fashionable Prototyping and Wearable Computing Using the Arduino.* (Blushing Boy Publishing, 2011).

98. Simple E-textile Connector : 8 Steps - Instructables. https://www.instructables.com/Simple-E-textile-Connector/.

99. M20-9773646 | HARWIN M20, 2.54mm Pitch, 36 Way, 1 Row, Straight Pin Header, Through Hole | RS Components. https://uk.rs-online.com/web/p/pcb-headers/5473166/.

100. How to Connect Conductive Thread Ribbon Cable With Flexible Flat Cable (FFC) Connectors : 9 Steps (with Pictures) - Instructables. https://www.instructables.com/How-to-connect-conductive-thread-ribbon-cable-with/.

101. Markvicka, E., Rich, S., Liao, J., Zaini, H. & Majidi, C. Low-cost wearable human-computer interface with conductive fabric for STEAM education. *ISEC 2018 -*

Proceedings of the 8th IEEE Integrated STEM Education Conference 2018-Janua, 161–166 (2018).

102. An E-textile Interface Kit for Persons With Limited Mobility. http://flex-ability.org/.

103. Clincher Flex Connectors | FCI Basics | Industrial Connectors | FFC/FPC. https://www.amphenol-icc.com/product-series/clincher-flex-connectors.html.

104. Heo, E., Choi, K.-Y., Kim, J., Park, J.-H. & Lee, H. A wearable textile antenna for wireless power transfer by magnetic resonance. *Textile Research Journal* 88, 913–921 (2017).

105. Li, Y., Grabham, N., Torah, R., Tudor, J. & Beeby, S. Textile-based flexible coils for wireless inductive power transmission. *Applied Sciences (Switzerland)* 8, (2018).

106. Zhu, D., Grabham, N. J., Clare, L., Stark, B. H. & Beeby, S. P. Inductive power transfer in e-textile applications: Reducing the effects of coil misalignment. *2015 IEEE Wireless Power Transfer Conference, WPTC 2015* 1, 14–17 (2015).

107. Lin, R. *et al.* Wireless battery-free body sensor networks using near-field-enabled clothing. *Nat Commun* 11, 1–10 (2020).

108. Posch, I. & Fitzpatrick, G. The matter of tools: Designing, using and reflecting on new tools for emerging etextile craft practices. *ACM Transactions on Computer-Human Interaction* 28, (2021).

109. Safety Pin Crocodile Clips for ETextiles : 6 Steps (with Pictures) - Instructables. https://www.instructables.com/Safety-Pin-Crocodile-Clips-for-ETextiles/.

110. British Standards Institute. BS 4162:1983 Methods of test for buttons. (1999).

111. Safety Pin Crocodile Clips for ETextiles : 6 Steps (with Pictures) - Instructables.

112. Posch, I., Kurbak, E., Perner-Wilson, H. & Satomi, M. Tools We Want. https://toolswewant.at/about/.

113. Klamka, K., Dachselt, R. & Steimle, J. Rapid Iron-On User Interfaces: Hands-on Fabrication of Interactive Textile Prototypes. in vol. 20 1–14 (Association for Computing Machinery (ACM), 2020).

114. Li, Q., Ran, Z., Ding, X. & Wang, X. Fabric circuit board connecting to flexible sensors or rigid components for wearable applications. *Sensors (Switzerland)* 19, (2019).

115. Köhler, A. R., Hilty, L. M. & Bakker, C. Prospective Impacts of Electronic Textiles on Recycling and Disposal. *J Ind Ecol* 15, 496–511 (2011).

116. Wu, S. & Devendorf, L. Unfabricate: Designing Smart Textiles for Disassembly. doi:10.1145/3313831.3376227.

117. Hardy, D., Wickenden, R. & McLaren, A. Electronic textile reparability. *J Clean Prod* 276, 124328 (2020).

118. Köhler, A. R. Challenges for eco-design of emerging technologies: The case of electronic textiles. *Mater Des* 51, 51–60 (2013).

119. Veske, P. & Ilén, E. Review of the end-of-life solutions in electronics-based smart textiles. *The Journal of The Textile Institute* 1–14 (2020) doi:10.1080/00405000.2020.1825176.

120. Schischke, K., Nissen, N. F. & Schneider-Ramelow, M. Flexible, stretchable, conformal electronics, and smart textiles: Environmental life cycle considerations for emerging applications. *MRS Commun* 10, 69–82 (2020).

121. Niinimäki, K. *et al.* The environmental price of fast fashion. *Nat Rev Earth Environ* 1, 189–200 (2020).

122. Millward-Hopkins, J., Purnell, P. & Baurley, S. A material flow analysis of the UK clothing economy. *J Clean Prod* 407, 137158 (2023).

123. Circular fashion - Loes Bogers. https://class.textile-academy.org/2020/loes.bogers/assignments/week03/.

124. Circular fashion - Maite Sosa Methol. https://class.textile-academy.org/2021/maite.methol/assignments/week03/.

125. os-circular-fashion. https://oscircularfashion.com/.

126. Buechley, L. & Eisenberg, M. The LilyPad Arduino: Toward wearable engineering for everyone. *IEEE Pervasive Comput* 7, 12–15 (2008).

127. Posch, I., Stark, L. & Fitzpatrick, G. eTextiles: Reviewing a Practice through its Tool/Kits. 11 (2019) doi:10.1145/3341163.3347738.

128. Huang, K. *et al.* Delocalizing Strain in Interconnected Joints of On-Skin Interfaces. *Proceedings - International Symposium on Wearable Computers, ISWC* 91–96 (2020) doi:10.1145/3460421.3478812.

129. Ku, P.-S. SkinKit: Construction Kit for On-Skin Interface Prototyping. *Proc. ACM Interact. Mob. Wearable Ubiquitous Technol* 5, 23 (2021).

130. Beemer, M., Dils, C. & Nachtigall, T. Second Skins: Exploring the Challenges and Opportunities for Designing Adaptable Garments Using E-Textile. *Engineering Proceedings 2023, Vol. 30, Page 9* 30, 9 (2023).

131. Jones, L., Nabil, S. & Girouard, A. Swatch-bits: Prototyping e-Textiles with modular swatches. *TEI 2020 - Proceedings of the 14th International Conference on Tangible, Embedded, and Embodied Interaction* 893–897 (2020) doi:10.1145/3374920.3374971.

132. Sensoria Fitness. https://www.sensoriafitness.com/smartsocks/.

133. van der Velden, N. M., Kuusk, K. & Köhler, A. R. Life cycle assessment and eco-design of smart textiles: The importance of material selection demonstrated through e-textile product redesign. *Mater Des* 84, 313–324 (2015).

134. Xiong, Y. & Tao, X. Compression Garments for Medical Therapy and Sports. *Polymers 2018, Vol. 10, Page 663* 10, 663 (2018).

135. Shi, J. *et al.* Smart Textile-Integrated Microelectronic Systems for Wearable Applications. *Advanced Materials* 32, 1–37 (2020).

136. Lipson, S. M., Stewart, S. & Griffiths, S. Athleisure: A qualitative investigation of a multi-billion-dollar clothing trend. *Body Image* 32, 5–13 (2020).

137. Liu, C., Xia, S. & Lang, C. Consumer coping with Covid-19: an exploratory study of clothing consumption shifts and the effect of consumer resilience. doi:10.1108/JFMM-10-2022-0221.

138. Dove, T. Stretch to fit – made to fit†. *International Journal of Fashion Design, Technology and Education* 9, 115–129 (2016).

139. Rogers, J. A., Someya, T. & Huang, Y. Materials and mechanics for stretchable electronics. *Science* vol. 327 1603–1607 Preprint at https://doi.org/10.1126/science.1182383 (2010).

140. Richardson, K. *Designing and Patternmaking for Stretch Fabrics*. (Fairchild Books, 2008).

141. Wicaksono, I. *et al.* A tailored, electronic textile conformable suit for large-scale spatiotemporal physiological sensing in vivo. *npj Flexible Electronics* 4, 5 (2020).

142. Stanley, J. *et al.* Modular E-Textile Platform for Real-Time Sensing. *Proceedings - International Symposium on Wearable Computers, ISWC* 131–135 (2022) doi:10.1145/3544794.3560293.

143. Dong, S. *et al.* Seamlessly knitted stretchable comfortable textile triboelectric nanogenerators for E-textile power sources. *Nano Energy* 78, 105327 (2020).

144. Vogl, A. *et al.* StretchEBand: Enabling Fabric-Based Interactions through Rapid Fabrication of Textile Stretch Sensors. (2017) doi:10.1145/3025453.3025938.

145. Fobelets, K., Thielemans, K., Mathivanan, A. & Pabavassiliou, C. Characterization of knitted coils for e-textiles. *IEEE Sens J* (2019).

146. Kallmayer, C. & Simon, E. Large area sensor integration in textiles. in *International Multi-Conference on Systems, Signals and Devices, SSD 2012 - Summary Proceedings* (2012). doi:10.1109/SSD.2012.6198112.

147. Kim, H., Kim, Y., Kwon, Y.-S & Yoo, H.-J. Embroidering Electrical Interconnects with Conductive Yarn for the Integration of Flexible Electronic Modules into Fabric. *IEEE J. Solid State Circuits* 39, 558–559 (2000).

148. Perner-Wilson, H., Buechley, L. & Satomi, M. Handcrafting textile interfaces from a kit-of-no-parts. *Proceedings of the 5th International Conference on Tangible Embedded and Embodied Interaction, TEI'11* 61–67 (2011) doi:10.1145/1935701.1935715.

149.   Lee, J. C. B., Liu, W., Lo, C. H. & Chen, C. C. Laundering reliability of electrically conductive fabrics for E-textile applications. *Proceedings - Electronic Components and Technology Conference* 2019-May, 1826–1832 (2019).

150.   Biswas, S. *et al.* Integrated multilayer stretchable printed circuit boards paving the way for deformable active matrix. *Nature Communications 2019 10:1* 10, 1–8 (2019).

151.   Vervust, T., Buyle, G., Bossuyt, F. & Vanfleteren, J. Integration of stretchable and washable electronic modules for smart textile applications. *Journal of the Textile Institute* 103, 1127–1138 (2012).

152.   Sliz, R. *et al.* Reliability of R2R-printed, flexible electrodes for e-clothing applications. *npj Flexible Electronics* 4, 1–9 (2020).

153.   Koshi, T., Nomura, K. I. & Yoshida, M. Measurement and analysis on failure lifetime of serpentine interconnects for e-textiles under cyclic large deformation. *Flexible and Printed Electronics* 6, 025003 (2021).

154.   Bossuyt, F. *et al.* Cyclic endurance reliability of stretchable electronic substrates. *Microelectronics Reliability* 51, 628–635 (2011).

155.   Norhidayah, A. A. *et al.* Stress Analysis of a Stretchable Electronic Circuit. *Procedia Eng* 184, 625–630 (2017).

156.   La, T. G. *et al.* Two-Layered and Stretchable e-Textile Patches for Wearable Healthcare Electronics. *Adv Healthc Mater* 7, 1801033 (2018).

157.   Sun, Y., Choi, W. M., Jiang, H., Huang, Y. Y. & Rogers, J. A. Controlled buckling of semiconductor nanoribbons for stretchable electronics. *Nat Nanotechnol* 1, 201–207 (2006).

158.   Li, B. M. *et al.* Kirigami-Inspired Textile Electronics: K.I.T.E. *Adv Mater Technol* 4, 1900511 (2019).

159.   Guan, Y.-S., Zhang, Z., Tang, Y., Yin, J. & Ren, S. Kirigami-Inspired Nanoconfined Polymer Conducting Nanosheets with 2000% Stretchability. *Advanced Materials* 30, 1706390 (2018).

160.   Li, Y., Liu, W., Deng, Y., Hong, W. & Yu, H. Miura-ori enabled stretchable circuit boards. *npj Flexible Electronics 2021 5:1* 5, 1–9 (2021).

161.   Sun, Y., Choi, W. M., Jiang, H., Huang, Y. Y. & Rogers, J. A. Controlled buckling of semiconductor nanoribbons for stretchable electronics. *Nat Nanotechnol* 1, 201–207 (2006).

162.   Guan, Y.-S., Zhang, Z., Tang, Y., Yin, J. & Ren, S. Kirigami-Inspired Nanoconfined Polymer Conducting Nanosheets with 2000% Stretchability. *Advanced Materials* 30, 1706390 (2018).

163.   Dickey, M. D. Stretchable and Soft Electronics using Liquid Metals. *Advanced Materials* 29, 1606425 (2017).

164. Votzke, C., Clocker, K., Mengüç, Y. & Johnston, M. L. Electrical Characterization of Stretchable Printed Liquid Metal Interconnects under Repeated Cyclic Loading. *FLEPS 2019 - IEEE International Conference on Flexible and Printable Sensors and Systems, Proceedings* 2019–2021 (2019) doi:10.1109/FLEPS.2019.8792306.

165. Components | Liquid Wire Inc. https://www.liquidwire.com/components.

166. Suikkola, J. *et al.* Screen-Printing Fabrication and Characterization of Stretchable Electronics. *Scientific Reports 2016 6:1* 6, 1–8 (2016).

167. Harnett, C. K., Zhao, H. & Shepherd, R. F. Stretchable Optical Fibers: Threads for Strain-Sensitive Textiles. *Adv Mater Technol* 2, (2017).

168. Gupta, S., Navaraj, W. T., Lorenzelli, L. & Dahiya, R. Ultra-thin chips for high-performance flexible electronics. *npj Flexible Electronics* vol. 2 1–17 Preprint at https://doi.org/10.1038/s41528-018-0021-5 (2018).

169. Indictor, N. & Blair, C. The Examination of Metal from Historic Indian Textiles Using Scanning Electron Microscope-Energy Dispersive X-Ray Spectrometry. *http://dx.doi.org/10.1179/004049690793711488* 21, 149–163 (2013).

170. Montegut, D., Indictor, N. & Summerfield, J. Technical Examination of Metal Threads in Some Indonesian Textiles of West Sumatra. *http://dx.doi.org/10.1179/004049696793711716* 27, 101–114 (2013).

171. Hacke, A.-M., Carr, C. M. & Brown, A. Characterisation of metal threads in Renaissance tapestries. in *Proceedings of Metal* vol. 592 967 (2004).

172. Post, E. R. & Orth, M. Smart fabric, or `wearable clothing'. *International Symposium on Wearable Computers, Digest of Papers* 167–168 (1997) doi:10.1109/iswc.1997.629937.

173. Sloan, M. R., Wright, J. R. & Evans, K. E. The helical auxetic yarn – A novel structure for composites and textiles; geometry, manufacture and mechanical properties. *Mechanics of Materials* 43, 476–486 (2011).

174. Yang, Z. *et al.* Conductive and Elastic 3D Helical Fibers for Use in Washable and Wearable Electronics. *Advanced Materials* 32, 1907495 (2020).

175. Zhang, W. *et al.* Hierarchically interlocked helical conductive yarn enables ultra-stretchable electronics and smart fabrics. *Chemical Engineering Journal* 462, 142279 (2023).

176. Yun, M. J., Sim, Y. H., Lee, D. Y. & Cha, S. I. Highly stretchable large area woven, knitted and robust braided textile based interconnection for stretchable electronics. *Scientific Reports 2021 11:1* 11, 1–10 (2021).

177. Li, D. *et al.* Lantern-Inspired On-Skin Helical Interconnects for Epidermal Electronic Sensors. *Adv Funct Mater* 33, 2213335 (2023).

178. Smith, M., Cacucciolo, V. & Shea, H. Fiber pumps for wearable fluidic systems. *Science (1979)* 379, (2023).

179. Jiang, C. *et al.* High Stretchability Ultralow-Power All-Printed Thin Film Transistor Amplifier on Strip-Helix-Fiber. in *Technical Digest - International Electron Devices Meeting, IEDM* vols 2021-Decem 16.4.1-16.4.4 (IEEE, 2021).

180. Cuthbert, T. J. *et al.* HACS: Helical Auxetic Yarn Capacitive Strain Sensors with Sensitivity Beyond the Theoretical Limit. *Advanced Materials* 35, 2209321 (2023).

181. Cheng, M. Y., Tsao, C. M., Lai, Y. Z. & Yang, Y. J. The development of a highly twistable tactile sensing array with stretchable helical electrodes. *Sens Actuators A Phys* 166, 226–233 (2011).

182. Yun, M. J., Sim, Y. H., Lee, D. Y. & Cha, S. I. Highly stretchable large area woven, knitted and robust braided textile based interconnection for stretchable electronics. *Scientific Reports 2021 11:1* 11, 1–10 (2021).

183. Dong, L. *et al.* In vivo cardiac power generation enabled by an integrated helical piezoelectric pacemaker lead. *Nano Energy* 66, (2019).

184. Kwon, Y. H. *et al.* Cable-Type Flexible Lithium Ion Battery Based on Hollow Multi-Helix Electrodes. *Advanced Materials* 24, 5192–5197 (2012).

185. Karaylianni, E., Coulston, G. W. & Micka, T. A. EP1931821A1 Energy active composite yarn, methods for making same, and articles incorporating the same. (2008).

186. Cadwell, J. A., Cadwell, J. A. J., Yarger, D. J. & Wallin, C. US2023048642A1 Methods and Systems for Monitoring Circumferential or Linear Displacements to Determine Respiratory Activity. (2023).

187. Olajedi, I. WO2021222326A1 Energy storage device, method of making and method of use. (2021).

188. Bossuyt, F. *et al.* Cyclic endurance reliability of stretchable electronic substrates. *Microelectronics Reliability* 51, 628–635 (2011).

189. Li, B. M. *et al.* Kirigami-Inspired Textile Electronics: K.I.T.E. *Adv Mater Technol* 4, 1900511 (2019).

190. Posch, I., Kurbak, E., Perner-Wilson, H. & Satomi, M. Tools we want: Illustrator meets EAGLE. http://toolswewant.at/tools/software-tools/illustrator-meets-eagle/.

191. Getting Started with your First Print - V-One. https://docs.voltera.io/v-one/getting-started/hello-world-project/3.-getting-started-with-your-first-print.

192. Machine sewing | Conductive Thread | Adafruit Learning System. https://learn.adafruit.com/conductive-thread/machine-sewing.

193. Machine Sewing with SewIY Conductive Thread | SewIY. https://sewiy.com/blogs/guides/machine-sewing-with-sewiy-conductive-thread.

194. IPC. IPC-9204 Guideline on Flexibility and Stretchability Testing for Printed Electronics. *Printed Electronics Test Method Development Validation Subcommitee of the Printed Electronics Commitee of IPC* (2017).

195. British Standards Institute. BS EN ISO 6330:2012 Textiles - Domestic washing and drying procedures for textile testing. (2012).

196. Rotzler, S., Krshiwoblozki, M. von & Schneider-Ramelow, M. Washability of e-textiles: current testing practices and the need for standardization. *https://doi.org/10.1177/0040517521996727* 91, 2401–2417 (2021).

197. Embodied RF Ecologies : Afroditi Psarra. https://afroditipsarra.com/work/embodied-rf-ecologies.

198. Faulkner, S. H., Hupperets, M., Hodder, S. G. & Havenith, G. Conductive and evaporative precooling lowers mean skin temperature and improves time trial performance in the heat. *Scand J Med Sci Sports* 25 Suppl 1, 183–189 (2015).

199. Schlader, Z. J., Simmons, S. E., Stannard, S. R. & Mündel, T. Skin temperature as a thermal controller of exercise intensity. *Eur J Appl Physiol* 111, 1631–1639 (2011).

200. Armstrong, L. E. *et al.* Exertional heat illness during training and competition. *Med Sci Sports Exerc* 39, 556–572 (2007).

201. Fudge, J. Exercise in the Cold: Preventing and Managing Hypothermia and Frostbite Injury. *Sports Health* 8, 133–139 (2016).

202. Harper Smith, A. D., Crabtree, D. R., Bilzon, J. L. J. & Walsh, N. P. The validity of wireless iButtons® and thermistors for human skin temperature measurement Related content. *Physiol Meas* 31, (2009).

203. Bach, A. J. E., Stewart, I. B., Disher, A. E. & Costello, J. T. A comparison between conductive and infrared devices for measuring mean skin temperature at rest, during exercise in the heat, and recovery. *PLoS One* 10, e0117907 (2015).

204. Macrae, B. A., Rossi, R. M., Psikuta, A., Spengler, C. M. & Annaheim, S. Contact skin temperature measurements and associated effects of obstructing local sweat evaporation during mild exercise-induced heat stress. *Physiol Meas* 39, 075003 (2018).

205. Lugoda, P., Hughes-Riley, T., Morris, R. & Dias, T. A wearable textile thermograph. *Sensors (Switzerland)* 18, 1–22 (2018).

206. Hughes-Riley, T., Jobling, P., Dias, T. & Faulkner, S. H. An investigation of temperature-sensing textiles for temperature monitoring during sub-maximal cycling trials. *Textile Research Journal* 004051752093814 (2020) doi:10.1177/0040517520938144.

207. Komolafe, A., Torah, R., Nunes-Matos, H., Tudor, M. & Beeby, S. Integration of temperature sensors in fabrics. *FLEPS 2019 - IEEE International Conference on Flexible and Printable Sensors and Systems, Proceedings* (2019) doi:10.1109/FLEPS.2019.8792294.

208. Horowitz, P. & Hill, W. *The Art of Electronics - 3rd Edition*. (2015). doi:10.1119/1.16385.

209. Lee, C. M., Jin, S. P., Doh, E. J., Lee, D. H. & Chung, J. H. Regional Variation of Human Skin Surface Temperature. *Ann Dermatol* 31, 349–352 (2019).

210. Hughes-Riley, T., Lugoda, P., Dias, T., Trabi, C. L. & Morris, R. H. A Study of Thermistor Performance within a Textile Structure. *Sensors 2017, Vol. 17, Page 1804* 17, 1804 (2017).

211. Linz, T. Analysis of Failure Mechanisms of Machine Embroidered Electrical Contacts and Solutions for Improved Reliability. (Universiteit Gent, 2012).

212. Klein, R. Bland-Altman and Correlation Plot. *MATLAB File Exchange* https://uk.mathworks.com/matlabcentral/fileexchange/45049-bland-altman-and-correlation-plot (2023).

213. Tesinova, P. & Atalie, D. Thermal Comfort Properties of Sport Fabrics with Dependency on Structure Parameters and Maintenance. *Fibers and Polymers* 23, 1150–1160 (2022).

214. Kanellakis, S. *et al.* Changes in body weight and body composition during the menstrual cycle. *American Journal of Human Biology* e23951 (2023) doi:10.1002/AJHB.23951.

215. Keskinen, M. End-of-life options for printed electronics. in *Waste Electrical and Electronic Equipment (WEEE) Handbook* 352–364 (Elsevier Inc., 2012). doi:10.1533/9780857096333.3.352.

216. Mecnika, V., Scheulen, K., Anderson, C. F., Hörr, M. & Breckenfelder, C. Joining technologies for electronic textiles. in *Electronic Textiles: Smart Fabrics and Wearable Technology* 133–153 (2015). doi:10.1016/B978-0-08-100201-8.00008-4.

217. Mehmann, A., Varga, M. & Tröster, G. Reversible Contacting for Smart Textiles. in *Smart Textiles: Fundamentals, Design and Interaction* 185–198 (2017). doi:10.1007/978-3-319-50124-6_9.

218. Simegnaw, A. A., Malengier, B., Rotich, G., Tadesse, M. G. & Van Langenhove, L. Review on the Integration of Microelectronics for E-Textile. *Materials 2021, Vol. 14, Page 5113* 14, 5113 (2021).

219. Chow, J. H., Meth, J. & Sitaraman, S. K. Twist testing for flexible electronics. in *Proceedings - Electronic Components and Technology Conference* vols 2019-May 785–791 (Institute of Electrical and Electronics Engineers Inc., 2019).

220. Mecnika, V., Hoerr, M., Krievins, I., Jockenhoevel, S. & Gries, T. Technical Embroidery for Smart Textiles: Review. *Materials Science. Textile and Clothing Technology* 9, 56–63 (2014).

221. Veske, P., Bossuyt, F. & Vanfleteren, J. Testing for Wearability and Reliability of TPU Lamination Method in E-Textiles. *Sensors 2022, Vol. 22, Page 156* 22, 156 (2021).

222.   International Organization for Standardization. ISO 20932-1:2018/Amd 1:2021 Textiles — Determination of the elasticity of fabrics — Part 1: Strip tests — Amendment 1. Preprint at (2018).

223.   International Organization for Standardization. ISO 7743:2011 - Rubber, vulcanized or thermoplastic - Determination of compression stress-strain properties. Preprint at (2011).

224.   Prévost, L., Lindner, A. & du Roure, O. Pitch controls the flexibility of helical ribbons. *Extreme Mech Lett* 58, 101923 (2023).

225.   Ansys. 0201 and 01005 Adoption in Industry. https://www.ansys.com/resource-center/white-paper/0201-and-01005-adoption-in-industry (2022).

Appendix 1 Additional information the updated modular sensing garment

As mentioned in Chapter 5, Section 5.4.1, there were additional adaptations made to the sensing garment that were not used in the final design. An initial updated design was developed, and is shown in Figure A-1.

Figure A-1. First iteration of the updated electronics for the sensing garment.

The first iteration of the PCB used snap fasteners to connect the interconnects to the PCB. Interconnects featured two interposers: a snap interposer to connect to the PCB (Figure A-2), and an Amphenol FCI Clincher interposer to connect to the sensors (Figure A-2A). The stitching and fabric were otherwise the same as in Section 5.2These were an improvement on the interconnects in Section 5.2, being easier to fabricate, and neater in design. However, there were two issues: first, there was still no latching mechanism to keep sensors and interconnects joined together, which was identified as an issue in Section 5.2 Second, the snap fasteners have a relatively large footprint, which made the PCB quite large and bulky, even without an enclosure. For these reasons, another re-design was carried out, as is documented in Chapter 5.

Figure A-2. The snap interposer.

A) Illustration with dimensions; B) Partially completed snap interposer stitched and soldered to an interconnect, with one snap still to be attached; C) Snap interposers attached to PCB (photo by Oliver Handford).

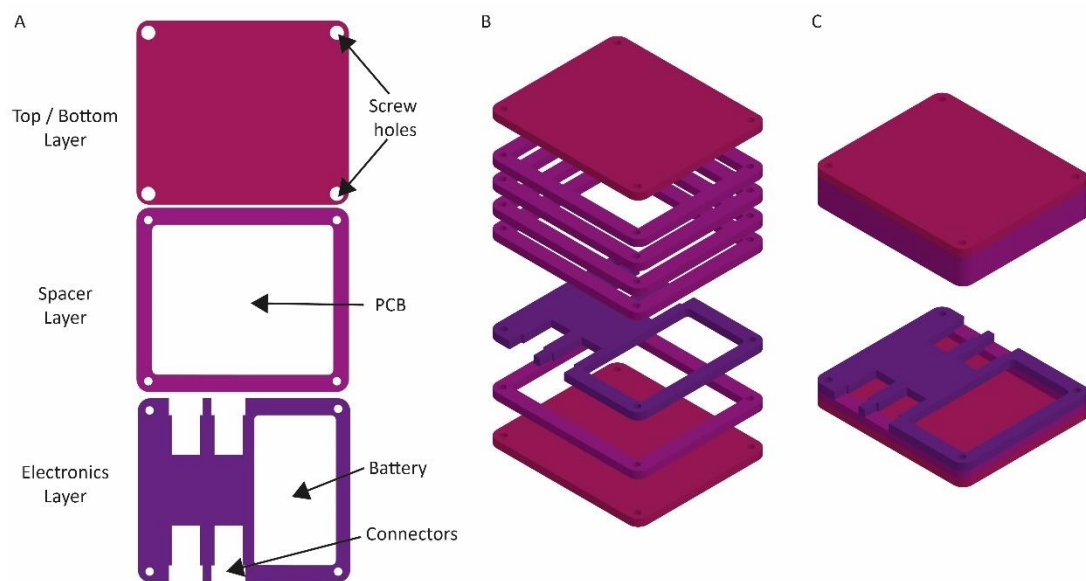Figure A-3 illustrates how the control module enclosure in Section 5.4.2.2 was constructed.

Figure A-3. The control module enclosure.

A) Top-down view of the three different layers used to make the case, showing cutouts for screw holes, space for the PCB, and spaces for the PCB, battery, and connectors to interface with interconnects; B) Exploded view of the entire structure, showing how many of each layer was included; C) illustration of assembled top and bottom modules which are screwed together to make the final case.

Appendix 2 Preliminary research into fabricating two-layer helical e-strips

As mentioned in Chapter 7, Section 7.2.2, some preliminary work was put into developing a two layer helical e-strip, but this was not completed. The motivation for this was to develop an accelerometer helical e-strip for motion sensing. An MMA8452Q accelerometer IC (NXP Semiconductors Ltd) was selected, for its small footprint (3 mm x 3 mm x 1 mm) and as there are open source libraries available to use it with Arduino, so it could potentially be paired with a microcontroller helical e-strip built around an AtTiny or other small footprint IC. This IC required a two layer helical e-strip, as it was not possible to route all the interconnects between components on a single layer.

A two layer design was created, and a couple of methods to create vias between layers were explored. First, copper rivets were evaluated, as these are used to create vias on rigid PCBs, and rivets are also commonly used in clothing. However, copper-plated PI was too thin to properly support the rivets, and they deformed instead of forming a reliable via. Anisotropic conductive adhesive (ACA) tape (3M Ltd) was also evaluated. As explained in Chapter 2, when ACA is sandwiched between two materials, it creates electrical connection in the z-direction (i.e. between layers) but not in the xy-plane. Figure A1 illustrates a concept for two layer helical e-strips using ACA. Long strips of copper are designed to act as vias, with strips of ACA sandwiched between the top and bottom layers. A flexible PCB bonding tape (3M Ltd) was selected to bond layers of the strip outside the via areas.

This work got to the stage of etching the circuits, testing vinyl cutter settings to cut the adhesive tapes, and attempting to align and adhere the two layers, which proved challenging. Work did not proceed further. The decision was made to focus on single layer helical e-strips, though this accelerometer helical e-strip, and other multiple layer structures, will be explored in future work.
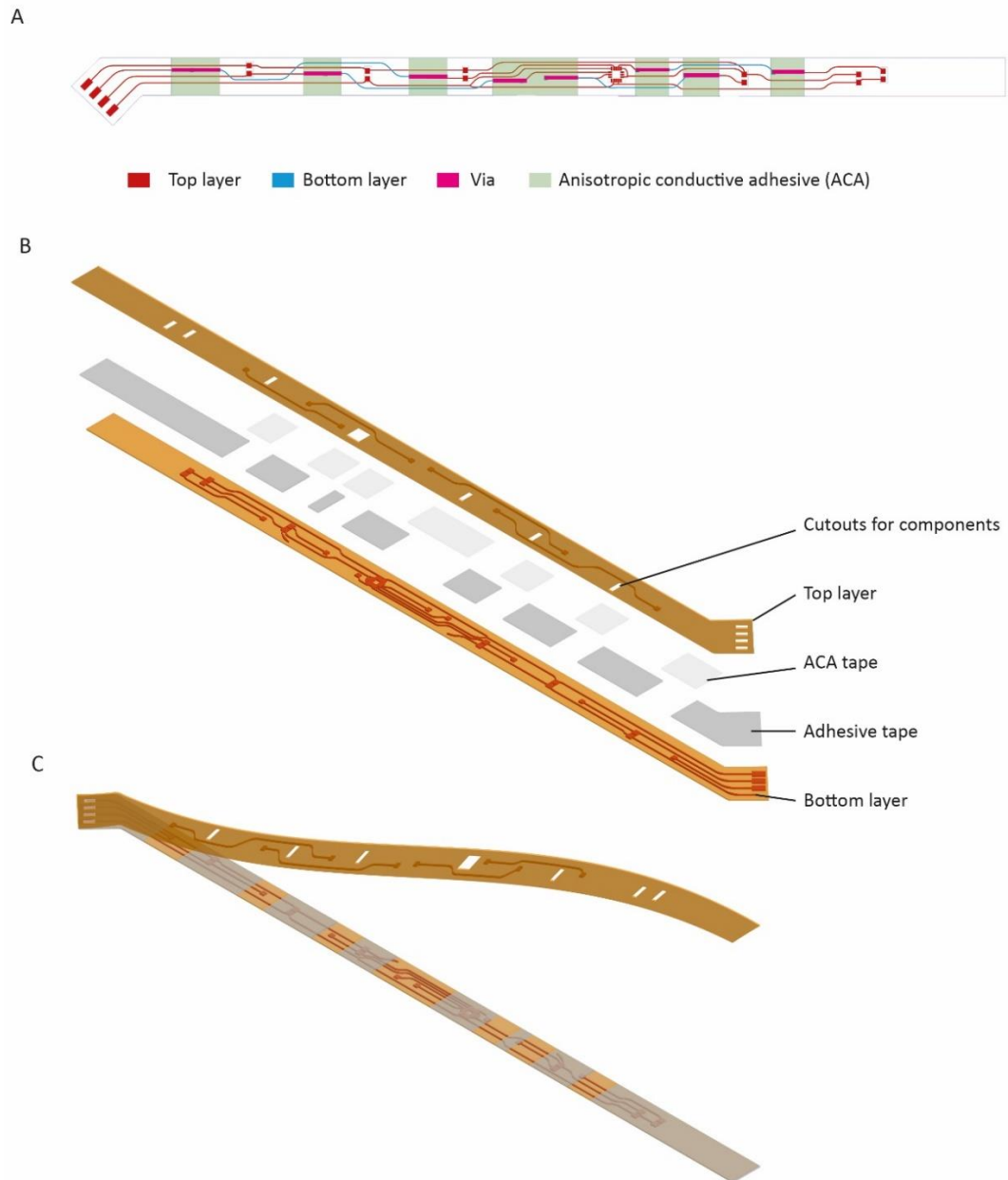
Figure A-4. Preliminary design for a two layer planar e-strip concept for more complex helical e-strips, which was not realised during this project: A) Top-down view of structure, composed of 2 layers of copper tracks on PI film, copper vias, anisotropic conductive adhesive tape, and adhesive tape for flexible electronics; B) isometric exploded view of the structure; C) illustration of the assembled structure with top layer being applied.